

The role of SUMO modification during productive adenovirus
infection and the identification of PIAS4 as a transcriptional
repressor of early adenoviral genes

DISSERTATION

with the aim of achieving a doctoral degree at the Faculty of Mathematics,

Informatics and Natural Sciences

Department of Biology of Universität Hamburg

submitted by

Stewen Krohne from Braunschweig

September 2018 in Hamburg

Tag der Disputation: 23.11.2018

1. Gutachten

Prof. Dr. Thomas Dobner

Abteilung Virale Transformation
Heinrich-Pette-Institut, Leibniz-Institut für Experimentelle Virologie
Martinistraße 52
20251 Hamburg
thomas.dobner@leibniz-hpi.de

2. Gutachten

Prof. Dr. Wolfram Brune

Abteilung Virus-Wirt-Interaktion
Heinrich-Pette-Institut, Leibniz-Institut für Experimentelle Virologie
Martinistraße 52
20251 Hamburg
wolfram.brune@leibniz-hpi.de

Mitglieder der Prüfungskommission:

Prof. Dr. Jörg Ganzhorn (Prüfungsvorsitzender)
Prof. Dr. Thomas Dobner
Prof. Dr. Joachim Hauber
Prof. Dr. Julia Kehr
Dr. Estefania Rodriguez (Fragesteller)
Dr. Niklas Beschorner (Fragesteller)

**HPI**

Heinrich Pette Institute
Leibniz Institute for Experimental Virology

HPI • Martinistraße 52 • D-20251 Hamburg

Christopher Thomas Ford, M. Sc.


Research Unit Virus Immunology

Phone: +49 (0) 40 480 51-322

Email: christopher.ford@leibniz-hpi.de

I confirm that the English language in Steewen Krohne's PhD thesis with the title **The role of SUMO modification during productive adenovirus infection and the identification of PIAS4 as a transcriptional repressor of early adenoviral genes** reads fluently and is well written. I give my support, that the English language is correctly articulated in Steewen Krohne's PhD thesis.

Sincerely,


06/09/18.

Heinrich Pette Institute
Leibniz Institute for
Experimental Virology

Martinistraße 52 · D-20251 Hamburg
Phone: +49 (0) 40 480 51-0
Fax: +49 (0) 40 48051-103
hpi@leibniz-hpi.de

Hamburger Sparkasse
BIC: HASPDEHHXXX
IBAN: DE56200505501001315959
www.hpi-hamburg.de


Leibniz Association

Declaration on oath/ Eidesstattliche Erklärung

I hereby declare on oath that I have written the present dissertation by my own and have not used other than the indicated sources and aids.

Hiermit erkläre ich an Eides statt, dass ich die vorliegende Dissertation selber verfasst habe und dazu keine anderen als die angegebenen Quellen und Hilfsmittel verwendet habe.

Hamburg, 19.09.2018

A handwritten signature in blue ink, appearing to read 'S. Krohne', is written on a light blue rectangular background.

Signature/Unterschrift

Table of contents

Table of contents	I
Abbreviations	VI
Abstract	VIII
Zusammenfassung	X
1 Introduction	1
1.1 Adenoviruses	1
1.1.1 Classification and pathogenesis	1
1.1.2 Adenoviral structure	2
1.1.3 Genome organization	4
1.1.4 Cycle of productive adenoviral infection	4
1.1.5 Role of immediate early gene products during infection	6
1.2 Induction of apoptosis	11
1.3 Posttranslational modification (PTM) with SUMO	14
1.4 Pathogens and the SUMO system	17
1.5 Protein inhibitor of activated STAT (PIAS)	18
1.6 The role of E1B-55K as a viral SUMO E3 ligase during adenovirus infection	21
2 Material	23
2.1 Bacteria, eukaryotic cells, viruses	23
2.1.1 Bacterial strains	23
2.1.2 Eukaryotic cells	23
2.1.3 Viruses	24
2.2 Nucleic acids	24
2.2.1 Oligonucleotides	24
2.2.2 Vectors	26
2.2.3 Recombinant plasmids	27
2.3 Antibodies	31

Table of contents

2.3.1	Primary antibodies	31
2.3.2	Secondary antibodies Western Blot.....	32
2.3.3	Secondary antibodies Immunofluorescence.....	32
2.4	Commercial kits.....	33
2.5	Markers and standards	34
2.6	Chemicals, enzymes, reagents, equipment	34
2.7	Software and databases.....	34
3	Methods	36
3.1	Bacteria	36
3.1.1	Culture and storage.....	36
3.1.2	Chemical transformation	37
3.2	Mammalian cells	37
3.2.1	Maintenance and passaging of cell cultures	37
3.2.2	Storage	38
3.2.3	Transfection of cells	38
3.2.4	Cell harvesting.....	39
3.2.5	Transformation assay of primary baby rat kidney cells (pBRK)	40
3.3	Adenovirus	40
3.3.1	Infection of mammalian cells	40
3.3.2	Propagation and storage of high titer virus stocks	41
3.3.3	Titration of virus stocks.....	41
3.3.4	Determination of virus progeny production	42
3.4	DNA techniques.....	43
3.4.1	Preparation of plasmid DNA from <i>E.coli</i>	43
3.4.2	Determination of nucleic acid concentration	43
3.4.3	Agarose gel electrophoresis.....	44
3.4.4	Polymerase chain reaction (PCR)	45
3.4.5	Site-directed mutagenesis	46

Table of contents

3.5	Cloning of DNA fragments.....	47
3.5.1	Enzymatic DNA restriction	47
3.5.2	Ligation.....	47
3.5.3	DNA sequencing	47
3.6	RNA techniques.....	48
3.6.1	Preparation of total RNA from mammalian cells	48
3.6.2	Reverse transcription of RNA.....	48
3.6.3	Real time PCR (RT-PCR)	48
3.7	Protein techniques	49
3.7.1	Preparation of total cell lysates	49
3.7.2	Determination of protein concentration	50
3.7.3	Ni-NTA pulldown of 6His-tagged SUMO2 modified proteins.....	50
3.7.4	Sodium dodecyl sulfate polyacrylamide gel electrophoresis (SDS-PAGE)	52
3.7.5	Western Blot analysis.....	55
3.7.6	Immunofluorescence analysis.....	56
3.7.7	Subcellular fractionation	57
3.7.8	Reporter gene assay.....	58
4	Results	60
4.1	SUMO2 modification of HAdV-C5 E1B-19K.....	60
4.1.1	Identification of the early protein E1B-19K as a potential SUMO2 substrate during adenovirus infection	60
4.1.2	E1B-19K harbors a highly conserved SUMO consensus motif (SCM) at lysine 44	61
4.1.3	Analysis of E1B-19K SUMO2 modification in different transfection and infection experiments	62
4.1.4	Alternative approaches to confirm E1B-19K SUMO2 modification	67
4.1.5	Nuclear targeting of E1B-19K via Gal4 fusion to enhance its SUMOylation	71
4.2	Characterization of potential E1B-19K SUMO mutants	72
4.2.1	Subcellular localization analysis of E1B-19K SUMO mutants.....	72

Table of contents

4.2.2	Mutation of potential SCM increases the transforming properties of E1B-19K in primary baby rat kidney (pBRK) cells	75
4.2.3	Analysis of the impact of the E1B-19K K44R mutation during viral protein expression and viral growth	76
4.2.4	Analysis of the subcellular localization of the putative E1B-19K SUMO mutant K44R during infection	79
4.3	The role of PIAS4 as a transcriptional regulator of early adenoviral gene products	80
4.3.1	PIAS4 decreases the steady state level concentration of HAdV-C5 E1B-55K in transient transfection	80
4.3.2	PIAS4 specifically represses E1B-55K protein levels	82
4.3.3	E1B-55K is not proteasomal degraded in the presence of overexpressed PIAS4	84
4.3.4	Analysis of E1B-55K subcellular localization in the presence of PIAS4	85
4.3.5	PIAS4-mediated reduction of E1B-55K is not dependent on its direct SUMOylation	87
4.3.6	PIAS4 reduces the activity of the E1B-promoter in a dose-dependent manner	88
4.3.7	PIAS4 represses mRNA and protein expression of several genes encoded within the early E1-transcription unit	91
4.3.8	Overexpression of PIAS4 represses the transforming potential of E1A and E1B-55K in primary baby rat kidney (pBRK) cells	94
4.3.9	Overexpression of PIAS4 shows mild repressive effects on viral protein expression and mRNA transcription during HAdV-C5 wt infection	95
4.3.10	Overexpression of PIAS4 has mild effects on adenovirus progeny production	101
4.3.11	The SUMO E3 ligase function of PIAS4 is partially involved in the transcriptional repression of early adenoviral genes	102
4.3.12	The role of adenovirus capsid and core proteins in counteracting PIAS4-mediated transcriptional repression of adenoviral E1-genes	104
5	Discussion	106
5.1	SUMO2 modification of HAdV-C5 E1B-19K	106
5.1.1	Initial detection and validation of E1B-19K SUMOylation	107
5.1.2	Characterization of E1B-19K SUMO mutants	110
5.2	PIAS4 as an intrinsic anti-viral factor during adenovirus infection	113

Table of contents

5.2.1	PIAS4 during transfection of the E1-gene region.....	114
5.2.2	PIAS4 during adenovirus infection	115
5.2.3	Summary of PIAS4 transcriptional repression of adenoviral early genes.....	117
Literature		120
Acknowledgements		XIII

Abbreviations

aa	amino acid
ab	antibody
Bak	Bcl-2-like protein 7
Bax	Bcl-2-like protein 4
cDNA	complementary DNA
CMV	Cytomegalovirus
Da	dalton
DAPI	4', 6-diamidino-2-phenylindole dihydrochloride
Daxx	death domain associated protein 6
DMSO	dimethylsulfoxide
eGFP	enhanced green fluorescent protein
ffu	<i>focus</i> forming unit
h p. t.	hour post transfection
h p. i.	hour post infection
HA	human influenza hemagglutinin
HAdV	human adenovirus
HEK	human embryonic kidney cells
HPV	human Papillomavirus
HRP	horseradish peroxidase
HSV-1	Herpes Simplex Virus Type 1
IFN	interferon
Ig	immunoglobulin
IgH	immunoglobulin heavy chain
IgL	immunoglobulin light chain
kb	kilobase
kBp	kilobasepair
kDA	kilodalton
MLP	major late promoter
MLTU	major late transcription unit
MOI	multiplicity of infection
NES	nuclear export signal
NLS	nuclear localization signal
NPC	nuclear pore complex

Abbreviations

orf	open reading frame
PBS	phosphate buffered saline
PCR	polymerase chain reaction
PEI	polyethylenimine
PTM	posttranslational modification
qPCR	quantitative PCR
RIPA	radio immunoprecipitation assay buffer
RLU	relative luciferase unit
rpm	round per minute
RT	room temperature
SAE	SUMO activating enzyme
SCM	SUMO consensus motif
SENP	sentrin specific protease
SILAC	stable isotope labelling with amino acids in cell culture
SIM	SUMO interacting motif
SUMO	small ubiquitin related modifier
Tris	tris-(hydroxymethyl)-aminomethane
U	unit
wt	wildtype
PIAS	protein inhibitor of activated STAT
STAT	signal transducer and activator of transcription

Abstract

The human adenovirus type 5 E1B-55K protein is a multifunctional protein that promotes viral replication and E1-mediated transformation of primary cells in cell culture. It has been shown that the functions of E1B-55K are tightly regulated through its posttranslational modification with the *small ubiquitin related modifier* (SUMO). In addition, E1B-55K exploits the host cell SUMO machinery by functioning as a SUMO E3 ligase. In this context, we and others revealed that E1B-55K induces SUMOylation of p53 and probably Sp100A, thereby inactivating these host restriction factors and ensuring a productive infection. In a comprehensive *stable isotope labelling by amino acids in cell culture* (SILAC) analysis we found that adenovirus wildtype infection globally induces the conjugation of SUMO2 proteins. Intriguingly, we identified 78 cellular proteins, which were E1B-55K-dependently SUMOylated during the course of infection, indicating that its SUMO E3 ligase activity is likely not restricted to p53 and Sp100A. Moreover, we found that a considerable number of adenoviral early and late proteins is SUMO modified during infection, among them the adenoviral Bcl-2 homologue E1B-19K. E1B-19K plays an important role in the inhibition of p53-independent induced apoptosis by counteracting the pro-apoptotic mediators Bax and Bak. HAdV-C5 E1B-19K contains two potential SUMO consensus motifs (SCM); one at lysine 44, which is highly conserved among different HAdV species, and a less conserved one at lysine 48. In this work, we aimed to elucidate the biological relevance of SUMOylation for E1B-19K. Therefore, we intended to confirm its posttranslational modification with SUMO in different experimental approaches, and in parallel, functionally characterize plasmid and virus SUMO mutants of E1B-19K. Mutation of E1B-19K SCMs showed no significant phenotype in terms of subcellular localization, protein stability and altered virus growth, but significantly increased the transforming potential of E1B-19K in primary baby rat kidney (pBRK) cells.

In order to investigate cellular factors, which regulate the SUMOylation of E1B-55K, we overexpressed the viral protein with different cellular SUMO E3 ligases of the *protein inhibitor of activated STAT* (PIAS) family. Besides regulating SUMOylation, these proteins are potent transcriptional regulators that interact with a plethora of transcription factors. Here we found for the first time that E1B-55K protein levels are remarkably repressed in the presence of overexpressed PIAS4. We could exclude that the E1B-55K levels were repressed due to enhanced direct SUMOylation. Further, we revealed PIAS4 as a novel host restriction factor of adenoviral infection that putatively acts by repressing the E1B-promoter activity in a dose-dependent manner. This resulted in reduced E1B-55K mRNA and protein levels upon coexpression of the E1-gene region with PIAS4. Interestingly, we could show that the promoter repression is most likely not restricted to the E1B-promoter as E1A mRNA and protein levels were also found to be remarkably reduced. Accordingly, overexpression of PIAS4 led to impaired E1-mediated transformation of

Abstract

pBRK cells. Contrary, high levels of PIAS4 showed rather mild repressive effects on viral mRNA levels and protein expression during HAdV infection without having significant effect on virus progeny production. This implicates a role of an immediately present adenoviral factor during infection in counteracting PIAS4-mediated virus restriction. We showed that this is partially dependent on the SUMO E3 ligase function of PIAS4 which is involved in the repression of viral protein levels. Thus, counteracting PIAS4-mediated SUMOylation might be one mechanism through which adenovirus evades repression of PIAS4.

Zusammenfassung

Das adenovirale Protein E1B-55K trägt durch die Unterdrückung der intrinsischen anti-viralen Immunantwort und dem Aufrechterhalten der Zellproliferation der infizierten Wirtszelle wesentlich zu einer effizienten Infektion bei. Für eine Vielzahl dieser Mechanismen nutzt E1B-55K wirtseigene posttranslationale Modifikationen (PTM) wie z. B. Ubiquitinylierung und SUMOylierung. Dabei wird E1B-55K selbst über SUMO Konjugation reguliert und fungiert zugleich als eine SUMO E3 Ligase. Mit Hilfe von *stable isotope labelling by amino acids in cell culture* (SILAC) konnten wir zeigen, dass E1B-55K einen deutlichen Effekt auf die globale Anzahl der zellulären SUMO2-konjugierten Proteine während der Wildtyp Infektion hat. Zahlreiche zelluläre Proteine, die in Abhängigkeit von E1B-55K höher SUMOyliert wurden, sind an der Reparatur von DNA Schäden, der transkriptionellen Regulation, der Zellzyklus Kontrolle und der RNA Prozessierung beteiligt. Des Weiteren haben wir gezeigt, dass neben E1B-55K eine beachtliche Anzahl weiterer viraler Proteine während der Infektion SUMOyliert wird, darunter das Apoptose-inhibierende E1B-19K Protein. Dieses frühe virale Protein verhindert die Induktion p53-unabhängiger Apoptose, indem es die proapoptotischen Proteine Bax und Bak bindet, und dadurch deren Porenbildung in der mitochondrialen Membran verhindert. Im Rahmen dieser Arbeit haben wir die SUMOylierung von E1B-19K mit verschiedenen Methoden untersucht. Außerdem wurde die biologische Relevanz dieser PTM anhand verschiedener E1B-19K SUMO Mutanten in der Transfektion und Infektion charakterisiert. Dabei konnten wir zeigen, dass die Mutation der Lysine innerhalb der SUMO Konsensus Motive (engl. SCM) das transformierende Potential von E1B-19K in Primärzellen neugeborener Ratten signifikant erhöht, jedoch keine Auswirkung auf die zelluläre Lokalisation und Protein Stabilität von E1B-19K hat und auch das Wachstum einer Virusmutante nicht beeinträchtigt.

Zur genaueren Untersuchung der für die SUMOylierung von E1B-55K zuständigen zellulären SUMO E3 Ligase wurde E1B-55K mit verschiedenen Isoformen der *protein inhibitor of activated STAT* (PIAS) Proteinfamilie koexprimiert. PIAS Proteine regulieren die Transkription zellulärer Gene und besitzen eine SUMO E3 Ligase Funktion. Im Rahmen dieser Arbeit konnten wir erstmalig zeigen, dass ausschließlich humanes und murines PIAS4 die Proteinkonzentration von E1B-55K deutlich reduziert. Des Weiteren geht die Reduktion von E1B-55K nicht mit einer erhöhten SUMOylierung durch PIAS4 einher, sondern die Aktivität des E1B-Promotors wird durch die transkriptionelle Regulation von PIAS4 reprimiert. Dies führt zur Reduktion der E1B-55K mRNA- und Proteinmengen. Neben E1B-55K wird der E1A-Promoter durch eine erhöhte Expression von PIAS4 reprimiert. Dies könnte zur gezeigten erniedrigten Expression der E1-Gene führen, welche das transformierende Potential der E1-Proteine in Primärzellen von neugeborenen Ratten in der Anwesenheit von überexprimiertem PIAS4 stark einschränkt. Während der Infektion hat überexprimiertes PIAS4 nur

einen schwach repressiven Effekt auf die virale Proteinexpression und die Synthese neuer infektiöser Viruspartikel. Die Ergebnisse deuten darauf hin, dass ein viraler Faktor während der initialen Phase der Infektion PIAS4 inaktiviert, wodurch eine produktive Infektion gewährleistet wird. Eine virus-vermittelte Inhibition der SUMO E3 Ligase Aktivität von PIAS4 könnte in diesem Zusammenhang ein möglicher Wirkmechanismus sein, wie Adenoviren der Repression von PIAS4 während der Infektion entgegenwirken, da wir zeigen konnten, dass die enzymatische Aktivität von PIAS4 teilweise in der transkriptionellen Repression der viralen E1-Gene involviert ist.

1 Introduction

1.1 Adenoviruses

1.1.1 Classification and pathogenesis

Adenoviruses were first discovered and isolated from adenoid tissue deriving from patients suffering from respiratory tract infections in 1953 (Rowe et al., 1953). The first adenoviral isolates were named according to their clinical appearance; adenoid degeneration (AD), adenoid-pharyngeal conjunctival (APC) and acute respiratory disease (ARD) agents. In 1956 they were finally summarized due to their shared properties and named as *adenoviruses* based on the origin of the tissue they were discovered in (Enders et al., 1956).

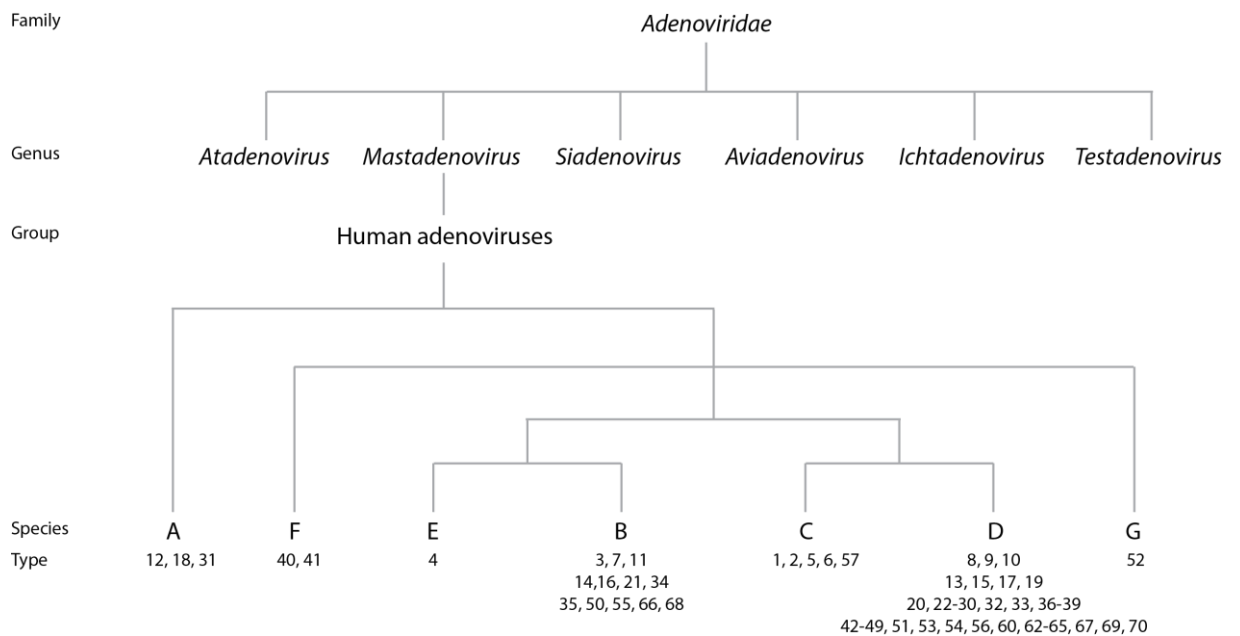


Figure 1: Classification of the family Adenoviridae. The phylogenetic tree shows the taxonomy of *Adenoviridae* with a detailed listing of the human adenoviruses (HAdV) type 1-70. HAdV are classified according to Davison et al. and the international committee on taxonomy of viruses (Davison et al., 2003; Doszpoly et al., 2013; Hage et al., 2015; Harrach et al., 2012).

Today, the family of *Adenoviridae* consists of over 130 known adenovirus types, which are further classified in six distinct genera, depending on their host tropism: Atadenoviruses infect reptiles, Mastadenoviruses infect mammals, Siadenoviruses infect amphibians, Aviadenoviruses infect birds, Ichtadenoviruses infect fish and Testadenovirus infect tortoise (Davison et al., 2003; Doszpoly et al., 2013; Hage et al., 2015; Harrach et al., 2012), shown in Figure 1. The group of human-pathogenic adenoviruses (HAdV), belonging to Mastadenoviruses, comprises seventy known types so far of

which many are highly prevalent among the global human population, see Figure 1 (Hage et al., 2015; Lion, 2014; Mast et al., 2010). HAdV are further sub-classified into seven species (A-G), due to their rate of agglutination of human sera, genomic parameters and their oncogenic potential (Harrach et al., 2012; Rosen, 1960). Since their discovery, adenoviruses were intensively studied leading to a broad understanding of viral-host interplay as well as regulation of various cellular processes. The most important discovery was the description of mRNA splicing in 1977 (Berget et al., 1977; Chow et al., 1977). The oncogenic potential of adenoviruses was first described in 1962 for HAdV type 12, which was shown to induce the formation of tumors when inoculated in newborn hamsters (Trentin et al., 1962). Since then, adenovirus and its oncogenic proteins became a frequently used model system to elucidate the molecular mechanisms of virus-induced oncogenesis in rodents and transformation of primary cells in cell culture. HAdVs primarily infect terminal differentiated epithelial cells which leads to a broad tissue tropism and diverse clinical symptoms (Boyer et al., 1959). In immunocompetent patients, HAdV can be the causative agent for keratoconjunctivitis, diseases of the upper and lower respiratory tract as well as gastroenteritis and infections of the urinary tract (Hilleman, 1957; Jawetz, 1959; Mueller and Klaus, 1993; Shindo K, Kitayama T, Ura T, Matsuya F, Kusaba Y, Kanetake H, 1986; Wood, 1988). These acute infections are usually self-limiting and show a mild clinical progression. However, there are reports of epidemic adenoviral outbreaks in military camps with severe disease progression also for immunocompetent patients (Chmielewicz et al., 2005; McNeill et al., 2000; Vento et al., 2011). In rare cases, mainly affecting immunocompromised patients like AIDS patients or organ transplant recipients, as well as newborns, adenoviral infection can lead to lethal clinical progression and the manifestation of hepatitis, pneumonia and encephalitis (Carmichael et al., 1979; De Ory et al., 2013; Schonland et al., 1976; Straussberg et al., 2001). Until today, a specific anti-adenoviral drug is not available. So far, severe HAdV infections as described above are treated with administration of anti-viral drugs like cidofovir and ribavirin, often associated with strong side-effects for the patient and only modest anti-adenoviral efficacy (Fowler et al., 2010; Gavin and Katz, 2002). This underlines the importance of ongoing research in the field of adenoviral infections to develop specific anti-adenoviral drugs.

1.1.2 Adenoviral structure

HAdVs are non-enveloped virus particles with an icosahedral shaped protein capsid with fiber proteins protruding from each vertex (Figure 2, panel A). An adenoviral particle has a diameter of 90-110 nm and is composed of eleven different structural proteins in total (three *major capsid proteins*: hexon, penton, fiber; four *minor capsid proteins*: protein VI (pVI), protein IIIa, protein VIII,

Introduction

protein IX (pIX); four *core proteins*: terminal protein TP, protein μ (p μ), protein VII (pVII), protein V (pV)). The icosahedral protein capsid, surrounding the DNA containing core, is initially assembled of 240 homotrimeric hexon proteins which form twenty facets, each composed of twelve hexontrimers. The twelve vertices of the icosahedron are composed of twelve pentameric pentons forming a penton base, which is extended by the trimeric fiber polypeptide forming a fiber tail, -shaft and -knob at its end (Figure 2, panel A)(van Oostrum & Burnett, 1985; Berk, 2013). The fiber protein initiates the attachment to the target cell via interaction with the coxsackie B/adenovirus receptor (CAR) or CD46 respectively, followed by interaction of the penton base with integrins located on the cell surface, leading to clathrin-mediated endocytosis of the viral particle into the host cell (Bergelson et al., 1997; Gaggar et al., 2003; Huang et al., 1996; Wu et al., 2003).

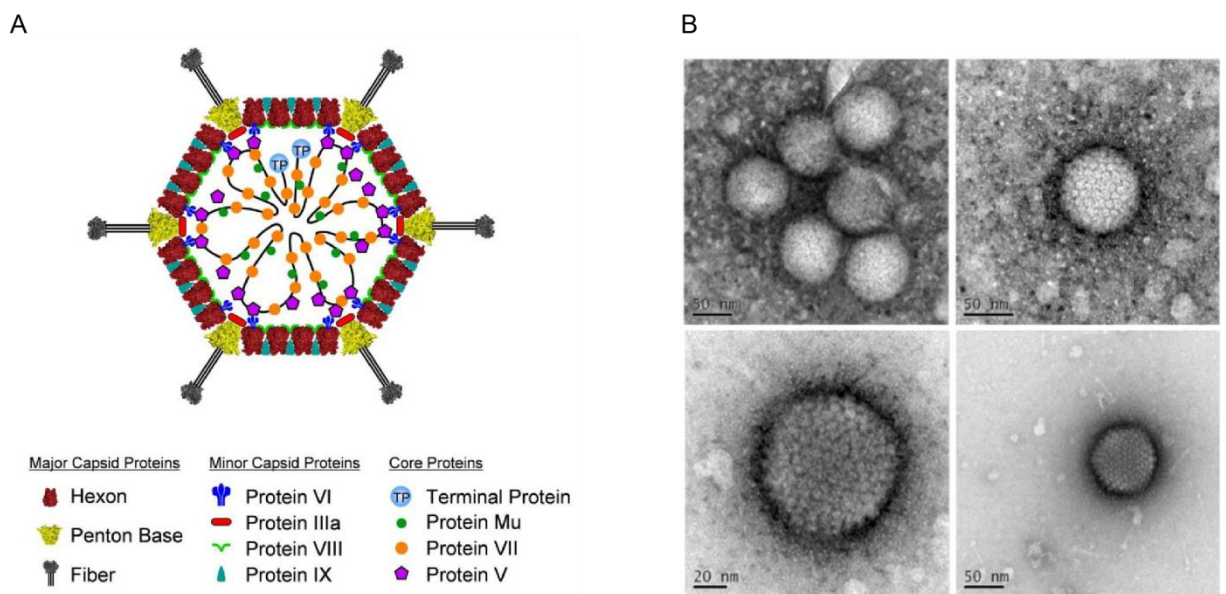


Figure 2: Structure of adenoviral particles. A: schematic cross-section of an adenoviral particle showing the localization of the virion proteins (adopted from Nemerow et al., 2009). The proteins are represented in different colors and shapes, explained below. B: electron microscopic images showing the icosahedral adenoviral particles and their composition of single capsomers (Department of electron microscopy, Heinrich Pette Institute, Leibniz Institute for Experimental Virology).

As shown in Figure 2, the minor capsid proteins (VI, IIIa, VIII, IX) are directly incorporated in the adenoviral protein capsid and described as *capsid cement* stabilizing the interaction of hexontrimers as well as pentons and thus supporting the assembly of viral particles (Liu et al., 2010; Reddy and Nemerow, 2014; Reddy et al., 2010). Apart from this, pVI is described as having a pro-viral function by inhibiting the intrinsic immune response of the host cell early during infection (Schreiner et al., 2012a). The core proteins pVII, pV and p μ bind to the adenoviral genome due to their basic character and thereby promote the formation of a condensed nucleoprotein (Chatterjee et al., 1985). Genome associated pV interacts with pVI at the inner site of the capsid, which links the genome to the capsid and ensures spatial organization of the condensed viral genome within the capsid (Chatterjee et al., 1985; Reddy and Nemerow, 2014). Both 5'-ends of the linear genome

are covalently bound to a terminal protein TP, which serves as an initiation site for viral DNA synthesis during infection (Pronk and van der Vliet, 1993). The core also contains low copy numbers of protein pIVa2 being required for genome packaging into newly synthesized viral particles (Christensen et al., 2008) and of the viral cysteine protease 32, which is needed for maturation of viral particles and the endosomal escape during infection (Weber, 2007).

1.1.3 Genome organization

Adenoviruses have a linear double-stranded DNA genome with a size of 26-45 kbp varying among the species. Each 5'-end is flanked by inverted terminal repeats (ITR) with a size of 36-200 bp serving as an origin of DNA replication (Davison et al., 2003). The adenoviral genome encodes for more than forty regulatory and structural proteins as well as viral associated RNAs (VA-RNA). Sequencing of HAdV genomes revealed a conserved genome structure and encoded gene products among different HAdV species. The viral genome can be divided into nine transcription units: five early units (E1A, E1B, E2A, E3, E4), three intermediate units (E2 late, IVa2, IX) and one late unit (major late unit MLU), whose primary transcript is processed into five late mRNAs (L1-L5) (Figure 3). All adenoviral proteins are expressed from the cellular RNA polymerase II, except the viral associated mRNAs (Weinmann et al., 1974; Berk, 2013).

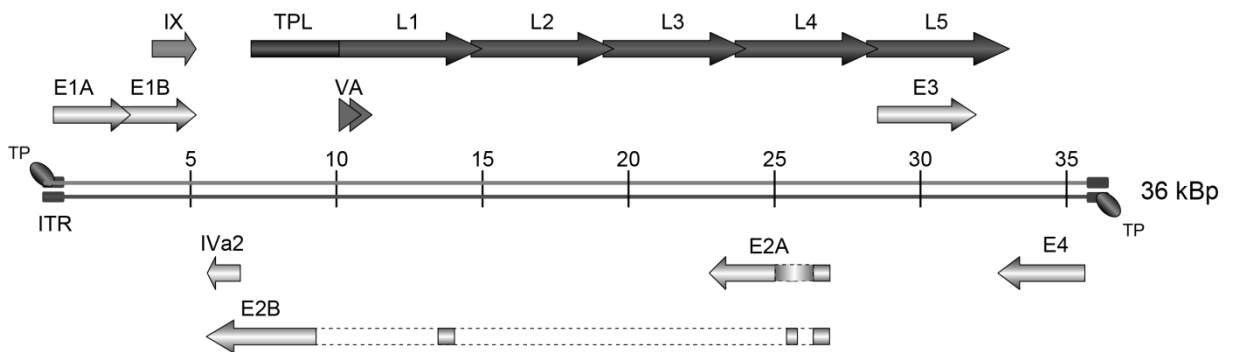


Figure 3: Organization of the HAdV-C5 genome. Schematic overview of an adenoviral genome showing the organization of the transcription units: E-early, L-late, VA- viral associated mRNA. The arrows indicate the orientation of the different gene loci (adopted from Täuber & Dobner, 2001a).

1.1.4 Cycle of productive adenoviral infection

The course of adenoviral infection was intensively studied using HAdV type 2 (HAdV-C2) and 5 (HAdV-C5) due to their ability to infect various tumor cell lines and a certain set of primary cells in cell culture. The productive adenoviral infection starts with the binding of the viral particle to the host cell, followed by the expression of early gene products. The switch from the early to the late phase of the infection is accompanied by the start of viral DNA synthesis. The initial cell attachment

of the virus occurs via high affinity binding of the fiber knob protein to the transmembrane coxsackie B/adenovirus receptor (CAR) expressed on the host cell surface. As a secondary binding event, RGD domains of the penton protein bind to $\alpha\beta3$ and $\alpha\beta5$ integrins located in the cell membrane of the host cell, thus mediating receptor cross-linkage and the formation of a clathrin-coated pit (Meier and Greber, 2003; Nemerow et al., 2009; Wickham, 1993). Subsequently, the virus particle is engulfed by the cell membrane and enters the host cell via clathrin-mediated endocytosis. Alternatively, HAdV infect the cell independent of clathrin pits by binding to CD46 and entering the host cell by macropinocytosis, a process in which large vesicles are taken up by the cell (Kalin et al., 2010). The first partial disassembly of the virion occurs already during virus uptake, whereby the fiber proteins are detached from the penton bases (Nakano et al., 2000). Acidification of the endosome triggers partial disassembly of the viral capsid and finally the lysis of the endosomal membrane by protein pVI (Wiethoff et al., 2005). The partially disassembled viral particles interact immediately with dynein motor proteins within the cytosol and are transported along the host cell microtubule network towards the nuclear microtubule organization center (MTOC) and bind to the nuclear pore complex (NPC) (Dales and Chardonnet, 1973; Leopold et al., 2000; Mabit et al., 2002). Interactions of viral factors, especially hexon, with components of the NPC facilitate the final disassembly of the virus particle and translocation of the genome into the nucleus, whereby it remains associated to protein pVII (Cassany et al., 2015; Chatterjee et al., 1986a; Kremer and Nemerow, 2015; Saphire et al., 2000; Trotman et al., 2001). Six to twelve hours after the initial binding of the virus particle to the cell, the first adenoviral genes are expressed. The first adenoviral gene transcribed by the cellular RNA polymerase II encodes the immediate early E1A protein (Nevins et al., 1979; Berk, 2013). Alternative splicing events generate two major E1A mRNAs encoding for the corresponding E1A isoforms 12S and 13S, respectively (Berk and Sharp, 1978). E1A proteins induce the transcription of the early transcription units E1-E4 by the cellular RNA polymerase II, which leads to the expression of over twenty regulatory proteins due to alternative splicing events (Shenk and Flint, 1991; Winberg and Shenk, 1984). The main function of the early regulatory gene products is the set-up of a pro-viral environment within the infected host cell to ensure a productive infectious cycle. E1A induces cell cycle progression and transition of resting cells into the S-phase, while E1B-gene products E1B-19K and E1B-55K inhibit the onset of apoptosis (Debbas and White, 1993; Gallimore and Turnell, 2001; Rao et al., 1992). The E2-gene locus encodes three different proteins, namely E2A (DNA binding protein; DBP), E2B (viral DNA polymerase) and terminal protein (TP), which are required for viral DNA replication (reviewed in Berk, 2013). The proteins encoded by the E3-region modulate the intrinsic immune response of the host cell e.g. by inhibiting the MHC-I transport to the cell surface and preventing of tumor necrosis factor (TNF) induced cell lysis of infected cells (Andersson et al., 1985; Burgert and Kvist, 1985;

Gooding et al., 1988). The primary mRNA transcript of the E4-region is alternatively spliced which reveals six different E4 proteins, named according to their open reading frame (orf1-4, orf6, orf6/7) (Virtanen et al., 1984). The E4 proteins are mainly involved in DNA repair, transcriptional activation as well as cell cycle control and apoptosis (Boyer et al., 1999a; Carvalho et al., 1995; Täuber and Dobner, 2001b). The late phase of adenoviral infection is initiated by accumulation of DBP, viral DNA polymerase and TP proteins, which stimulates both, the onset of viral DNA replication and the activation of the MLU. The single mRNA transcript with a size of 28 kb is alternatively spliced resulting in the late mRNAs L1-L5, which mainly encode structural proteins as well as regulatory proteins being involved in proper virion assembly and stabilization of the progeny (Nevins and Darnell, 1978). The late mRNAs are equipped with a 5' tripartite leader with a size of around 200 nucleotides, ensuring efficient translation by an alternative translation initiation, called ribosome shunting. Thereby, late viral mRNA can be efficiently translated although the cellular translation initiation factor eIF4F for cap-dependent translation is inhibited. The newly synthesized viral DNA is packed into viral capsids and 24-36 hours after the initial binding, the infected cell is lysed and around 10^4 virus particles are released (Berk, 2013).

1.1.5 Role of immediate early gene products during infection

1.1.5.1 Immediate early protein E1A

After entering the nucleus of the host cell, the adenoviral genome is transcribed whereby the first adenoviral protein, the immediate early protein E1A, is abundantly expressed. The abundance is induced by an enhancer region upstream of the E1A-gene locus (Hearing and Shenk, 1983). The main function of the E1A-gene products is, being an important transactivator of the early adenoviral transcription units E2-E4, to maintain the early phase of infection and to establish a pro-viral environment in the host cell. Furthermore, E1A induces cell cycle progression by driving G_1 or G_0 arrested cells into S-phase (Ghosh and Harter, 2003; Horwitz et al., 2008). However, the E1A driven dysregulation of the cell cycle stabilizes the tumor suppressor p53, leading to the induction of programmed cell death through apoptosis, which is efficiently antagonized by the E1B-encoded proteins during infection (Querido et al., 1997a). Hence, coexpression of the early adenoviral proteins E1A and E1B-55K was shown to be sufficient to transform primary baby rat kidney (pBRK) cells and human mesenchymal stroma cells (hMSC) in cell culture (Endter and Dobner, 2004; Speiseder et al., 2017). The initial E1A mRNA transcript is alternatively spliced resulting in the 13S and 12S E1A proteins (Berk and Sharp, 1978). Both E1A proteins share an identical domain structure with three conserved regions (CR1, CR2, CR4), whereas the large E1A 13S protein encodes

for an additional conserved region (CR3) (Kimelman et al., 1985). It was shown that E1A 13S is the main transcriptional activator of early adenoviral genes, enhancing transcription by 10-(E1B) up to 100-fold (E2 early, E3, E4) via interaction with a broad spectrum of transcription factors (Berk, 2013). CR3 interacts with the MED23 subunit of the human mediator of transcription complex, thus stimulating the assembly of pre-initiation complexes on promoters as well as transcription elongation (Boyer et al., 1999b; Cantin et al., 2003; Stevens et al., 2002). Furthermore, CR3 of E1A 13S binds to the cellular acetyltransferases p300, CBP and PCAF whose recruitment leads to DNA acetylation and thus to enhanced transcriptional activity of the respective promoter (Pelka et al., 2009a, 2009b). E1A 12S and 13S respectively, interact with specific binding motifs of retinoblastoma protein family members (pRb) (Dahiya et al., 2000). These proteins normally bind to E2F-transcription factors thereby suppressing expression of E2F-responsive genes, which comprise proteins tightly associated with DNA synthesis and entry into S-phase. Binding of E1A proteins induces E2F-pRb displacement and enables the expression of E2F-responsive genes like c-myc, N-myc and CDK2, promoting cell growth and S-phase transition of the infected cell (Fattaey et al., 1993; Ferrari et al., 2008; Van Den Heuvel and Dyson, 2008; Liu and Marmorstein, 2007).

1.1.5.2 Immediate early protein E1B-55K

The immediate early E1B-transcription unit is located downstream of the E1A-gene locus. The primary transcript of this gene locus is alternatively spliced into two major transcripts, 13S and 22S, encoding for E1B-19K and E1B-55K, respectively (Berk and Sharp, 1978; Spector et al., 1978). The main function of the two E1B-gene products is to antagonize E1A induced apoptosis and to maintain viability of the infected host cell (Debbas & White, 1993; Rao et al., 1992; Gallimore & Turnell, 2001). The detailed function of E1B-19K is described detailed in the section below. E1B-55K is a multifunctional phosphoprotein consisting of 496 aa and a corresponding molecular weight of 55 kDa. E1B-55K is able to shuttle continuously between cytosol and nucleus, mediated by a nuclear export signal (NES) and a SUMO consensus motif (SCM) at lysine 104 (Endter et al., 2001, 2005; Kindsmüller et al., 2007). E1B-55K directly binds and inactivates the tumor suppressor p53, which is activated upon infection by the abnormal proliferative force of E1A (Martin and Berk, 1998; Querido et al., 1997a) described in 1.1.5.1. Counteraction of growth restricting p53 is the main molecular mechanism of E1B-55Ks transforming potential when cotransfected with E1A. The p53 protein acts as a transcriptional activator and orchestrates the expression of a variety of genes, which encode proteins inducing prolonged cell cycle arrest in G₁, DNA repair as well as cell senescence and apoptosis (Brady and Attardi, 2010; El-Deiry, 1998). Through binding to the amino terminal transactivation domain of p53, the early viral protein effectively counteracts the anti-

proliferative functions of p53 by multiple mechanisms. Shuttling of E1B-55K allows relocalization of bound p53 from the nucleus to the cytoplasm and thereby inactivates its function to induce gene expression (Dobbelstein et al., 1997; Krätzer et al., 2000). In addition E1B-55K alters the PTM profile of p53 through interaction with the cellular acetyltransferase PCAF, thus abrogating its acetylation, which mediates sequence-specific transactivation of p53 (Liu et al., 2000). During the late phase of infection E1B-55K forms an ubiquitin E3 ligase complex in cooperation with E4orf6 and the cellular factors elongin b and c, cullin 5 and RBX1, which plays a key role in counteracting the intrinsic immune response of the host cell. The complex associates with various cellular proteins, followed by attachment of poly-ubiquitin chains, which efficiently target the substrates for proteolytic degradation by the 26S proteasome (Querido et al., 2001). Many of the substrates are components of the DNA damage response, like Mre11, DNA ligase 4 and Bloom helicase, as well as components of the intrinsic antiviral immune defense like ATRX, SPOC1, p53 and integrin alpha 3 (Querido et al., 1997a; Stracker et al., 2002; Schreiner et al., 2012b, 2013a,b). In addition, E1B-55K was shown to function as an adenoviral SUMO E3 ligase for p53 inducing its posttranslational modification with *small ubiquitin related modifier* (SUMO) proteins, which will be explained in detail later in this work (Muller and Dobner, 2008; Pennella et al., 2010). SUMOylation of p53 stimulates the E1B-55K-p53 complex to associate with PML nuclear bodies (PML-NB), prior to its CRM1-dependent nuclear export. Tethering of the complex to PML-NBs limits its nuclear mobility and thereby further decreases the activity of p53 during the early phase of infection (Dobbelstein et al., 1997; Krätzer et al., 2000; Pennella et al., 2010). Recent work of our research unit showed that in addition to direct SUMOylation of p53, E1B-55K further represses p53 activity indirectly through SUMOylation of Sp100A. Sp100A belongs to the intrinsic antiviral immune response of the host cell and activates p53 upon infection. However, SUMO modification inactivates Sp100A by relocalization into the insoluble nuclear matrix fraction. E1B-55K itself is a substrate of SUMOylation with a major SCM at lysine 104. Removal of this SCM by amino acid exchange clearly demonstrates intimate regulation of E1B-55K functions via this particular PTM. SUMO mutants of E1B-55K show impaired nucleocytoplasmic shuttling and accumulate mainly in the cytosol, thus nuclear p53 cannot be inhibited (Endter et al., 2001, 2005; Kindsmüller et al., 2007). Association to PML-NB via isoform-specific binding to PML IV and V is also regulated by E1B-55K SUMOylation and important for p53 repression (Wimmer et al., 2010). Furthermore, the intrinsic SUMO E3 ligase activity of E1B-55K was only observed for E1B-55K wildtype but not for the SUMO mutant, which underlines the importance of this PTM for E1B-55K and its role as a multifunctional regulator during the early phase of infection (Muller and Dobner, 2008).

1.1.5.3 Immediate early protein E1B-19K

The smaller protein expressed from the E1B-gene locus, E1B-19K, consists of 176 aa and is a potent inhibitor of p53-independent induction of apoptosis by functioning as a viral Bcl-2 homologue. This function is crucial to counteract the E1A-induced apoptosis by dysregulation of the host cell cycle in order to establish an appropriate environment for viral DNA synthesis and a productive infection. Therefore, E1B-19K accompanies the p53-dependent anti-apoptotic functions of E1B-55K (Boyd et al., 1994; Rao et al., 1992). As described for E1B-55K, E1B-19K can contribute to the transformation of primary rodent cells in the presence of E1A, due to its anti-apoptotic properties (White and Cipriani, 1990). Bcl-2 is the prototypical member of a well-characterized protein family (Bcl-2 family), which is intimately linked to the regulation of apoptosis and consists of both, pro- and anti-apoptotic regulatory proteins. The family members are further grouped into a Bcl-2 subfamily, which includes all anti-apoptotic molecules, as well as the pro-apoptotic subfamilies Bax and BH3. All members of the Bcl-2 family share a certain degree of homology to the Bcl-2 protein within conserved motifs, so called Bcl-2 homology domains (BH1-4) (Adams and Cory, 1998). Especially the BH3 domain seems to be linked to the pro-apoptotic function of Bcl-2 family members, since it is the only BH domain found in the BH3 subfamily (Chittenden et al., 1995; Conradt and Horvitz, 1998). However, some anti-apoptotic family members contain BH3 domains without stimulating apoptosis. The early adenoviral protein E1B-19K shares limited direct sequence homology to the Bcl-2 protein within a central area of 69 aa (44-113) (Boyd et al., 1994; Chiou et al., 1994a; Rao et al., 1992). Functional analysis of the E1B-19K protein showed, that the part of Bcl-2 homology overlaps with the highly conserved central region of E1B-19K, which is essential for the E1B-19K function as an apoptotic inhibitor (Chiou et al., 1994a; Rao et al., 1992; White et al., 1992). Beside sequence homology, Bcl-2 and E1B-19K are also functional homologues, being able to substitute their anti-apoptotic function for one another through interaction with the same cellular factors (Boyd et al., 1994; Chiou et al., 1994b, 1994a; Debbas and White, 1993; Sabbatini et al., 1995). Thereby, E1B-19K is able to effectively inhibit the onset of apoptosis induced by tumor necrosis factor α (TNF α), Fas ligand and TNF α related apoptosis inducing ligand (TRAIL) as well as E1A, avoiding the immune surveillance of the host cell and ensuring a productive infection (Gooding et al., 1991; Hashimoto et al., 1991; Sundararajan et al., 2001; White, 2001; White et al., 1992). Without inhibition of E1B-19K, immune responses driven by TNF α would result in inflammation as well as degradation of cellular and viral DNA and onset of apoptosis, which would shorten the lifespan of the host cell and decrease virus progeny production (White et al., 1992).

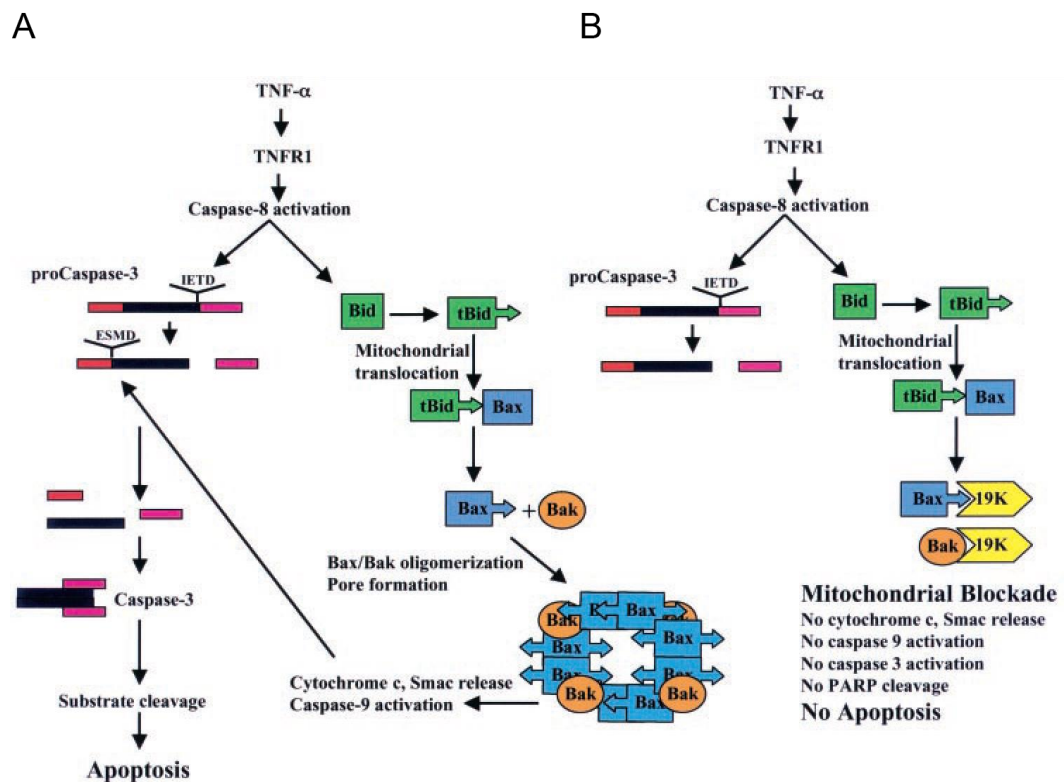


Figure 4: Inhibition of apoptosis by E1B-19K. Simplified illustration of apoptosis inhibition mediated by the early adenoviral protein E1B-19K (yellow) through binding to pro-apoptotic Bax (blue) and Bak (orange) proteins. **A:** The induction of apoptosis by Bax/Bak pore formation which leads to apoptosis through mitochondrial release of pro-apoptotic factors. **B:** Adenoviral E1B-19K efficiently complexes with Bax and Bak and thus abrogates the pore formation and the associated release of cytochrome c and SMAC, which stimulate the cascade of apoptosis. (adopted from White, 2001).

E1B-19K inhibits apoptosis through interactions with the cellular pro-apoptotic Bcl-2 proteins Bax and Bak (Farrow et al., 1995; Han et al., 1996). During early stages of induced apoptosis, Bax proteins experience conformational changes at their N-terminus induced by tBid proteins priorly activated by caspase 8 (Figure 4). The exposed N-terminus of Bax proteins carries a BH3 domain, which was shown to be necessary for E1B-19K binding. In the absence of E1B-19K, TNF α induces further conformational changes at the C-terminus of Bax, which exposes a BH2 domain (Sundararajan and White, 2001). Analogous to some bacterial pore-forming proteins, conformational changes at both termini of Bax are necessary for the exposure of two central helices, allowing Bax oligomerization followed by mitochondrial transmembrane insertion and pore formation (Peraro and Van Der Goot, 2016; Perez and White, 2000). In adenovirus infected cells, E1B-19K binds to Bax after conformational changes of its N-terminus and thereby efficiently blocks further changes at the C-terminus. As a consequence, Bax proteins fail to oligomerize and apoptogenic mediators cytochrome c and SMAC remain inside the mitochondria. Thus the propagation of the apoptotic cascade via caspase 9 activation is blocked by the early adenoviral protein (Figure 4, panel B) (Cuconati and White, 2002; Perez and White, 2000; Sundararajan and White, 2001). E1B-19K also binds to pro-apoptotic Bak proteins, which form oligomers themselves

and are associated to Bax oligomers, in which they are thought to have an activating function for Bax oligomerization and pore formation. Binding of E1B-19K to Bak inhibits Bak oligomerization as well as Bak/Bax binding, which blocks the induction of apoptosis and supports the establishment of a pro-viral environment within the host cell (Sundararajan et al., 2001).

1.2 Induction of apoptosis

Apoptosis is a programmed mode of cell death, which occurs regularly during organismal development, aging and upon maintaining cellular homeostasis. Apoptosis can also function as a response to various cytotoxic stimuli in order to dispose non-functional cells from the organism (J. F. R. Kerr, 1972). As part of the intrinsic antiviral immune response, apoptosis is also induced by various viral infections, thereby destroying the infected host cell and inhibiting viral spread (reviewed in Thomson, 2001). In contrast to necrosis, apoptosis is a controlled and active process, which is ATP consuming and either restricted to individual cells or a small defined cluster of cells (Eguchi et al., 1997). The tightly controlled course of apoptosis allows elimination of cells without the induction of inflammatory immune responses, which is often observed in the passive process of necrosis due to the loss of membrane integrity and release of cytosolic molecules, which activate macrophages, dendritic- and NK cells (Rock and Kono, 2008; Scaffidi et al., 2002). However, both processes share a certain degree of biochemical networks, which enables transition of apoptosis into necrosis under certain circumstances, e.g. decrease of ATP or reduced levels of caspases (Eguchi et al., 1997; Elmore, 2007). The morphological onset of apoptosis is characterized by cell shrinkage and reduced cytosolic volume, leading to compact packaging of cellular organelles. In parallel the nucleus shrinks and the chromatin is irreversibly condensed, leading to fragmentation of the nucleus, which is also called karyorrhexis (Elmore, 2007; Robertson et al., 1978; Wyllie et al., 1980). So called apoptotic bodies are formed at the cell membrane, which are tightly packed with cellular organelles and fragmented nuclear structures. The structures bud at the cell membrane and are efficiently engulfed by phagocytes (J. F. R. Kerr, 1972). Biochemical changes within the apoptotic cell promote the extracellular exposure of phosphatidylserines, which serve as a recognition ligand for phagocytosis (Bratton et al., 1997). A hallmark of apoptosis is the removal of cells without the activation of inflammatory responses. This is achieved through maintenance of cell membrane integrity during the entire process of programmed cell death and immediate uptake of apoptotic bodies by phagocytes before cell rupture occurs (J. F. R. Kerr, 1972). The loss of an intact cellular membrane would trigger the release of cytoplasmic content into the extracellular space and thus induce a massive immune response, as it is described for necrosis. Apoptosis can be activated by three different pathways, which are partially linked between each other and all

converge in the execution pathway, characterized by the activation of executor caspases (Figure 5)(Elmore, 2007). Caspases are key effector molecules during apoptosis and are sub-grouped into initiator- and executor caspases. These proteins are expressed as inactive precursor enzymes (zymogens), which once activated, are able to activate other caspases downstream of the pathway. Activated caspases harbor proteolytic activity and cleave proteins at aspartic residues. A hierarchy between initiator caspases activated early during apoptotic onset, which mainly process and catalytically activate executor caspases exists, whose proteolytic activity leads to the typical morphological changes of apoptotic cells (Stennicke and Salvesen, 1998). The three pathways able to induce apoptosis are illustrated in Figure 5 and described in detail in the following.

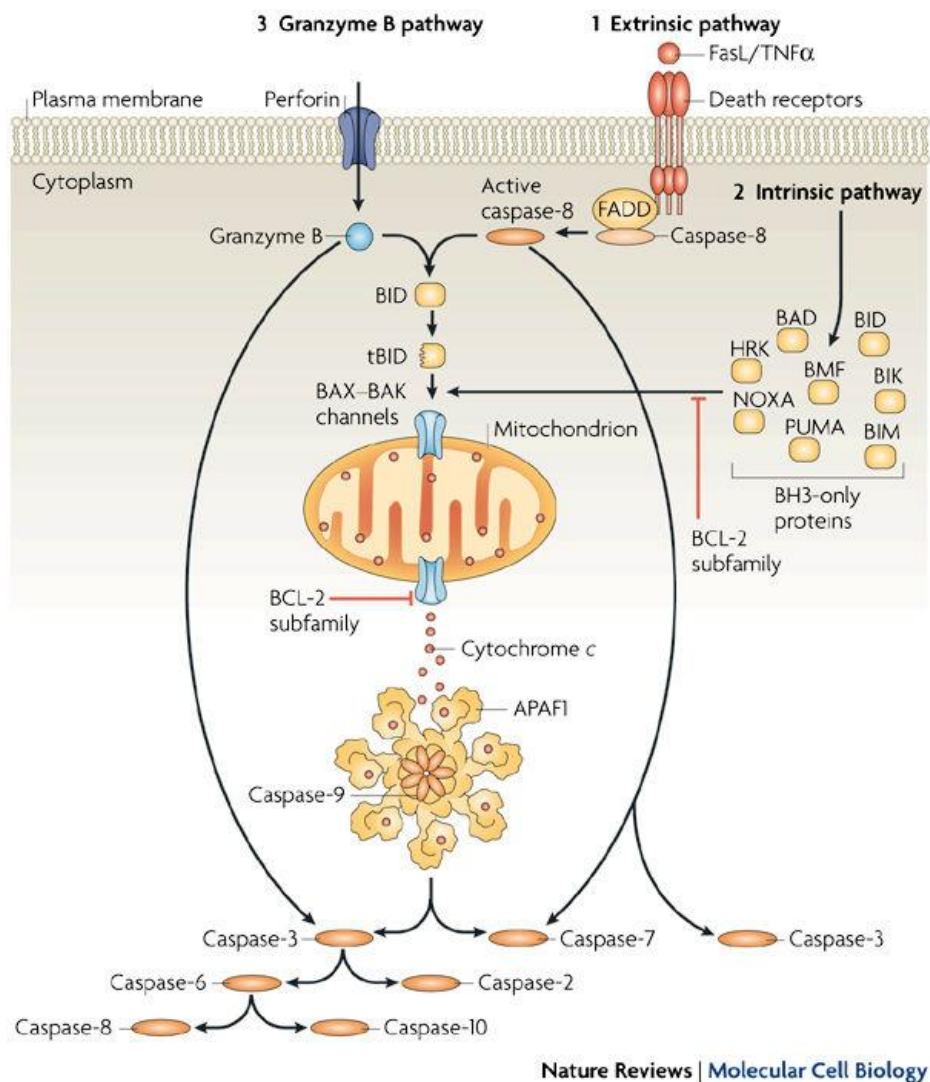


Figure 5: Simplified illustration of pathways inducing the onset of programmed cell death via apoptosis. 1 is showing the extrinsic pathway induced by interaction of cell surface receptors belonging to the TNF superfamily with their distinct ligands leading to the formation the death inducing signaling complex (DISC) composed by FADD and Caspase 8. The DISC activates both executor caspase 3 as well as Bid, which induces the release of cytochrome C from mitochondria. 2 shows the intrinsic pathway, which is induced by cytotoxic stimuli. This pathway is mainly regulated by Bcl-2 family members altering the mitochondrial membrane integrity and thereby inducing the release of pro-apoptotic molecules into the cytosol. Cytochrome c, Apaf-1 and procaspase 9 form a ternary complex, named apoptosome, which induces downstream events in the cascade of apoptosis. 3 shows the granzyme b pathway, which is mediated by cytotoxic t-

Introduction

lymphocytes. Granzyme b mediates both, direct induction of executor caspase 3 as well as activating Bid, leading to mitochondrial cytochrome c release (adopted from Taylor et al., 2008).

The extrinsic pathway of apoptosis is initiated by interaction of cell surface receptors belonging to the tumor necrosis factor (TNF) superfamily with their cognate ligands. The best studied receptors inducing the extrinsic apoptosis cascade are the TNF α receptor as well as the Fas receptor. These transmembrane death receptors contain an extracellular ligand binding domain and an intracellular death domain of around 80 aa in size, which transmits the pro-apoptotic signal from the cell surface into the intracellular space (Itoh and Nagata, 1993; Tartaglia et al., 1993). After binding of Fas ligand to the Fas receptor, the adaptor molecule Fas associated protein with death domain (FADD) is recruited and binds to the receptor via its internal death domain (Scott et al., 2009). Subsequently, FADD provokes the formation of the death inducing signaling complex (DISC) through dimerization with procaspase 8 (Kischkel et al., 1995; Wajant, 2002). Binding to the TNF α receptor results in a similar course of signal transduction, except TRADD binding to the receptor prior to FADD recruitment (Hsu et al., 1995). The DISC enables autocatalytic activation of procaspase 8, which stimulates apoptosis by mainly activating the main executor caspase 3 (Stennicke et al., 1998). Additionally, caspase 8 cleaves the Bcl-2 family member Bid, which in its activated form (tBid) induces pore formation of Bax proteins in the mitochondrial membrane being part of the intrinsic induction of apoptosis (Li et al., 1998). This is one example for the interplay between the different pathways. The intrinsic or mitochondrial pathway is mainly activated by cytotoxic stimuli such as radiation, UV damage, toxins, hypoxia, hyperthermia and oxidative stress. The hallmark of the intrinsic pathway is the alteration of the mitochondrial membrane integrity, which goes along with the efflux of pro-apoptotic factors into the cytosol (Liu et al., 1996; Saelens et al., 2004). Cytochrome c binds and activates the apoptotic protease activating factor 1 (APAF-1) and procaspase 9, which form a ternary complex, called the apoptosome (reviewed in Chinnaiyan, 1999). This protein complex mediates apoptosis by recruiting a vast number of procaspase 9 molecules followed by auto-activation (Zou et al., 1999). SMAC/Diablo and HtrA2 are also released from mitochondria and described as promoting apoptosis by inhibition of anti-apoptotic IAP (Du et al., 2000; Yang et al., 2003). Other pro-apoptotic factors released from mitochondria during the intrinsic pathway are apoptosis inducing factor (AIF), endonuclease G and CAD, which support apoptosis via DNA fragmentation and chromatin condensation (Joza et al., 2001; Saelens et al., 2004). The intrinsic apoptosis pathway is mainly regulated by Bcl-2 proteins, which were already described in section 1.1.5.3. E1B-19K is able to efficiently inhibit both, the intrinsic and extrinsic pathway of apoptosis. Alternatively, apoptosis can be stimulated by the perforin/granzyme pathway. This pathway is induced by CD8⁺ cells and mainly affects tumor- and virus-infected cells. Cytotoxic T-cells are able to secret molecules (perforins), which form pores in

the target cell membrane, prior to introduction of cytotoxic granules (Trapani and Smyth, 2002). These granules contain high numbers of granzyme b, which directly activates caspases and provokes apoptosis through degradation of anti-apoptotic factors like ICAD (Darmon et al., 1995; Sakahira et al., 1998; Shi et al., 1992; Thomas et al., 2000). Granzyme b also cleaves the Bcl-2 protein Bid, whose activated form mediates Bax oligomerization and mitochondrial pore formation, which was already described in 1.1.5.3 (Alimonti et al., 2001). This is another example of overlapping activation between different pathways of apoptosis induction. All three apoptotic pathways converge into the execution pathway, which is characterized by the activation of the major execution caspases 6 and 7 as well as caspase 3, which is activated by all initiator caspases, hence playing a key role in the apoptotic execution pathway. Active executor caspases cleave a vast array of substrates involved in the maintenance of the cytoskeleton, among them actin, filamin and myosin resulting in typical morphologic alterations like rounded shape and membrane blebbing of the apoptotic cell (Taylor et al., 2008). Furthermore, caspases activate a multitude of cellular factors leading to chromosome condensation and karyorrhexis. Finally, budded apoptotic bodies are recognized by phagocytes and internalized without establishing an immune response, which terminates the cascade of apoptosis (Elmore, 2007).

1.3 Posttranslational modification (PTM) with SUMO

The *small ubiquitin like modifier* (SUMO) proteins posttranslationally modify a variety of proteins by covalent linkage. The reversible attachment of SUMO protein causes a broad array of altered protein characteristics and therefore considerably broadens the complexity of the eukaryotic proteome. Posttranslational protein modification with SUMO was initially described in 1996 for the GTPase activating protein RanGAP1, which was found to associate with the NPC upon SUMOylation (Mahajan et al., 1997; Matunis et al., 1996, 1998). SUMO proteins and its homologues are expressed in all eukaryotic cells and have been implicated in the regulation of a variety of biological processes (reviewed in Flotho & Melchior, 2013). In vertebrates, three distinct SUMO paralogs are described, namely SUMO1, SUMO2 and SUMO3, which are expressed in a wide range of tissues and cell types. The SUMO isoforms 2 and 3 are highly related to one another, sharing sequence homology of 95 % and are therefore often referred to SUMO2/3. In contrast SUMO1 shares less than 50 % sequence homology to SUMO2/3. Nearly all SUMO1 molecules are conjugated to its substrates, while large pools of free SUMO2/3 are expressed and conjugated in response to cell stress (Saitoh and Hinchev, 2000). In 2004 SUMO4 was identified in kidney cells, which is probably an intronless, non-expressed pseudogene (Bohren et al., 2004; Su and Li, 2002). Another potential isoform, SUMO5 was recently reported to orchestrate growth and disruption of PML-NBs in human

cells. In contrast to other SUMO isoforms, SUMO5 expression is restricted to testis and peripheral blood cells (Liang et al., 2016). Rapid increase of proteomic research revealed a considerable number of substrates of the SUMOylation machinery and various associated cellular processes, ranging from chromatin remodeling, transcriptional regulation, DNA repair, cell cycle control and telomere maintenance. The functional alteration of SUMOylation for an individual protein is hardly predictable, but generally broadens the profile of protein-protein interaction, regulates the subcellular localization, allows nucleocytoplasmic transport of the target protein and alters its stability (Flotho and Melchior, 2013; Hay, 2005; Kerscher, 2007). Further, SUMOylated proteins can be targeted for degradation through a PTM crosstalk mechanism between SUMO and ubiquitin proteins. *SUMO targeted ubiquitin ligases* (STUbL) interact with SUMOylated proteins and induce their poly-ubiquitination, followed by proteasomal degradation of the protein (Perry et al., 2008; Sriramachandran and Dohmen, 2014). Similar to ubiquitination, SUMO proteins are conjugated to their substrates in a three step enzymatic cascade, involving a SUMO E1 activating enzyme, as well as a SUMO E2 conjugating enzyme and a SUMO E3 ligase (Figure 6). In contrast to the ubiquitin pathway, which employs a set of E2 enzymes in unique combinations with various ubiquitin E3 ligases to ensure substrate specificity, the SUMO machinery consists of only one E2 enzyme, Ubc9, which is sufficient for the transfer of the SUMO protein to the target protein (Hershko and Ciechanover, 1998; Johnson and Blobel, 1997). SUMOylation is initiated by sentrin specific proteases (SENPs), which employ a C-terminal hydrolase activity mediating proteolytic maturation of the SUMO precursor protein. SENP-mediated cleavage reveals a C-terminal di-glycine motif whose carboxyl group forms an isopeptide bond with the ϵ -amino group of a lysine residue of the acceptor protein. Furthermore, SENPs are required for the deconjugation of SUMO proteins from their target proteins (Hay, 2007; Yeh et al., 2000). The SUMO E1 activating enzyme (SAE) is a heterodimer composed of the subunits Aos1 and Uba2. The SAE catalyzes the activation of SUMO proteins via adenylation of their C-terminus under the consumption of ATP, followed by remodeling of the SAE active site and thioester bond formation of SUMO and the SAE complex (Olsen et al., 2010). Upon activation, Uba2 interacts with the SUMO E2 conjugating enzyme Ubc9, resulting in the transfer of SUMO to the E2 via transesterification (Desterro et al., 1997; Hay, 2005; Johnson and Blobel, 1997). Ubc9 directly interacts with SUMO substrates and is able to catalyze the formation of an isopeptide bond between the carboxyl group of the SUMO and the ϵ -amino group of a lysine residue of the acceptor protein. The only substrate, which is efficiently SUMO modified by only E1 and E2 is the Ran-GTPase activating enzyme (RanGAP1) (Bernier-Villamor et al., 2002). For other proteins, SUMOylation with only E1 and E2 is generally very inefficient, clearly indicating the need of SUMO E3 ligases to accelerate the reaction. SUMO E3 ligases are divided into three different classes. The largest class of SUMO E3 ligases is characterized by its SP-ring motif, which is

essential for their function. These enzymes directly bind to their target proteins and Ubc9. An additional SUMO interacting motif (SIM) mediates non-covalent binding to the activated SUMO molecule, thereby orientating substrate and SUMO protein into a favorable position for protein transfer (reviewed in Geiss-Friedlander & Melchior, 2007). A prominent member of SUMO E3 ligases with a SP-ring motif is the family of *protein inhibitors of activated STAT* (PIAS) proteins, which were initially described as transcriptional regulators involved in STAT, p53 and NfκB signaling and comprise five isoforms in mammalian cells (Bischof et al., 2006; Liu et al., 2005; Rytinki et al., 2009). A second class is represented by only a single molecule, the nuclear pore protein RanBP2. In contrast to SUMO E3 ligases with a SP-ring motif, RanBP2 does not directly interfere with the substrate protein, but interacts with the E2-SUMO thioester and stimulates the SUMO transfer to the substrate (Pichler et al., 2002; Tatham et al., 2005). The third class of SUMO E3 ligases encompasses the human polycomb group member Pc2, which induces the SUMOylation of the transcriptional repressor CtBP (Kagey et al., 2003).

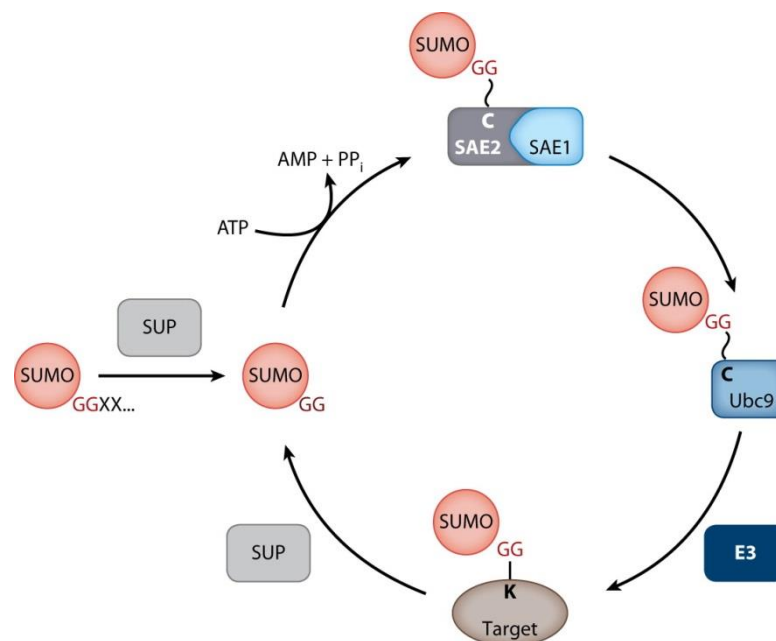


Figure 6: Schematic overview of the SUMOylation cycle. Initially the SUMO precursor is processed by SUMO specific proteases (SUP or SENP) whereby a C-terminal di-glycine motif is exposed (left). The SUMO E1 activating enzyme (SAE) is a heterodimer composed of Aos1 and Uba2 and adenylates the SUMO protein under the consumption of ATP. Conformational changes of the SAE complex allow binding to the SUMO protein via a thioester bond (top). Subsequently, the SUMO protein is transferred to the SUMO E2 conjugating enzyme Ubc9 via transesterification (right). Ubc9 binds to the SUMO consensus motif of the substrate and SUMO E3 ligases, which initiate the formation of an isopeptide bond between the carboxyl group of the SUMO protein and the ϵ -amino group of the lysine residue of the substrate (bottom). Conjugated SUMO can be removed from target proteins by SENPs (adopted from Flotho & Melchior, 2013).

In contrast to ubiquitination, the SUMO modified lysine of the acceptor protein is located within a specific SUMO consensus motif (SCM) ψ KxD/E, wherein ψ designates a large hydrophobic residue and x stands for any aa (Rodriguez et al., 2001). This is based on the presence of a single SUMO E2 conjugating enzyme, whereas ubiquitination is facilitated by an array of different E2 enzymes. The

catalytic pocket of the SUMO E2 conjugating enzyme Ubc9 interacts directly with the lysine residue of the SCM, while the hydrophobic and the acidic residues of the SCM bind the surface of Ubc9 (Bernier-Villamor et al., 2002; Lin et al., 2002; Sampson et al., 2001). However, some proteins are SUMO modified at lysines, which are not embedded in a SCM, while other proteins are not SUMO modified even though they carry a SCM. Interestingly, SUMO2/3 possess internal SCMs, which allow the conjugation of SUMO2/3 chains, while SUMO1 is attached as a monomer to its target proteins (Hay, 2005; Tatham et al., 2001). In addition to the classical SCM, two different extensions have been identified; the phosphorylation-dependent SUMO motif (PDSM, ψ KxD/ExxpSP), which is another example for crosstalk between different PTMs as well as the negatively charged amino acid-dependent SUMO motif (NDSM) carrying clusters of acidic residues downstream of the classical SCM (Hietakangas et al., 2006; Yang et al., 2006).

1.4 Pathogens and the SUMO system

The reversible PTM with SUMO proteins is tightly associated to the regulation of key cellular pathways. Therefore, it is not surprising, that a considerable number of intracellular pathogens evades intrinsic immune responses of the host cell by either manipulating the conserved SUMO machinery or being target of SUMOylation themselves. Exploitation of the hosts SUMO machinery could be shown for different DNA viruses, among them member of *Adenoviridae*, *Herpesviridae*, *Papillomaviridae* and *Poxviridae*, as well as different RNA viruses and bacteria (reviewed in Wimmer et al., 2012; Tavalai & Stamminger, 2008). PML-NBs are closely related to SUMOylation and frequently appear to be target sites of nuclear replicating DNA viruses (Everett, 2001; Tavalai and Stamminger, 2008). These dynamic macromolecular structures can be found as distinct *foci* in the interchromosomal space, where they associate with the nuclear matrix. The main component of PML-NBs is the scaffold forming promyelocytic leukemia protein (PML), which associates with other cellular factors like hDaxx, Sp100, SUMO1 and the Bloom syndrome helicase (Ishov et al., 1999; Negorev and Maul, 2001). So far over 165 additional factors have been reported to be dynamically recruited to PML-NBs, whereas the recruitment at least for some factors depends on the SUMO status or the existence of a SIM (van Damme et al., 2010; Ishov et al., 1999). PML-NBs are implicated in the regulation of various cellular processes e.g. oncogenesis, DNA repair, apoptosis and hence describe a favorable target for viruses to evade intrinsic antiviral immune responses (Dellaire and Bazett-Jones, 2004; Salomoni and Pandolfi, 2002; Takahashi et al., 2004). Even though the detailed biochemical function of PML-NBs is not fully determined yet, they are discussed as catalytic surfaces, serving as hot spots for SUMO modification and thereby orchestrating their regulatory function (van Damme et al., 2010). The importance of SUMOylation

for PML-NBs is underlined by the fact, that PML itself is a substrate of SUMO modification, containing three SCMs and one SIM, which are essential for PML-NB formation and recruitment of hDaxx and other factors (Ishov et al., 1999; Kamitani et al., 1998; Müller et al., 1998; Shen et al., 2006). Research on DNA viruses and their connection to the host cell SUMO machinery showed a strong link between these pathogens with PML-NBs, which are part of the intrinsic immune response and therefore manipulated by viruses to ensure a productive infection. A unique viral strategy to manipulate the host cell SUMO machinery has been shown for the avian adenovirus *Chicken Embryo Lethal Orphan* (CELO) protein Gam-1. This protein dramatically reduces the protein levels of PML and shuts the host cell SUMO machinery by proteasomal degradation of the SAE heterodimer and Ubc9, as well as inhibition of the SAE-SUMO thioester bond formation (Boggio et al., 2004; Chiocca et al., 1997; Colombo et al., 2002). The early adenoviral protein E1A is reported to associate with PML-NBs of the host cell and to interact with both, murine and human SUMO E2 conjugating enzyme Ubc9. However, binding of E1A to Ubc9 does not alter global modification of SUMO substrates (Carvalho et al., 1995; Hateboer et al., 1996; Yousef et al., 2010). The early adenoviral E4orf3 alone is capable to reorganize PML-NBs into nuclear track like structure (Carvalho et al., 1995; Doucas et al., 1996; Ou et al., 2012). Additionally, E4orf3 was shown to function as a SUMO E3 ligase and induces SUMO modification of TIF-1 γ , which is involved in transcriptional regulation and DNA repair (Sohn and Hearing, 2016). The multifunctional regulative protein E1B-55K, described in detail in 1.1.5.2, not only interferes with the SUMO system by functioning as an adenoviral SUMO E3 ligase for p53, but is also intimately regulated by this PTM.

1.5 Protein inhibitor of activated STAT (PIAS)

The term *protein inhibitor of activated STAT* (PIAS) derives from the identification of two family members, PIAS1 and PIAS3, which were initially shown to have inhibitory properties for the function of *signal transducer and activator of transcription* (STAT) protein (Chung et al., 1997; Liu et al., 1998). Further research confirmed that PIAS proteins not only regulate the transcription mediated by STAT, but are also involved in the regulation of an array of different transcription factors (reviewed in Schmidt & Müller, 2003). Overall PIAS proteins are reported to interact with over sixty different transcription factors and are thereby involved in the regulation of a plethora of cellular pathways and molecular processes including PML stability, transcription, DNA damage repair, NF- κ B-mediated signaling, cell cycle progression, innate immunity as well as senescence and apoptosis (Benhamed et al., 2013; Bischof et al., 2006; Galanty et al., 2009; Liu et al., 2004, 2005; Rabellino et al., 2012; Tahk et al., 2007). The regulation is based on different mechanisms, which involve blockade of DNA binding of transcription factors, recruitment of transcriptional

Introduction

coactivators/-repressors and the induction of protein SUMOylation by functioning as SUMO E3 ligases, previously explained in 1.3 (Johnson and Gupta, 2001; Takahashi et al., 2001a). Four different genes *PIAS1*, *PIAS2 (PIASx)*, *PIAS3* and *PIAS4 (PIASy)*, encode for the human PIAS family. Due to alternative splicing of *PIAS2*, *PIAS3* and *PIAS4* seven proteins of the human PIAS family exist (reviewed in Rytinki et al., 2009) (Figure 7). Orthologues of PIAS proteins can be found in a broad set of species, among them non-vertebrate animal species, as well as in plants and yeasts (Hari et al., 2001; Johnson and Gupta, 2001; Miura et al., 2005). Members of the PIAS protein family share a high degree of sequence homology, irrespective of the species. The human PIAS domain structure consists of five domains, which were found in all human PIAS isoforms (Figure 7).

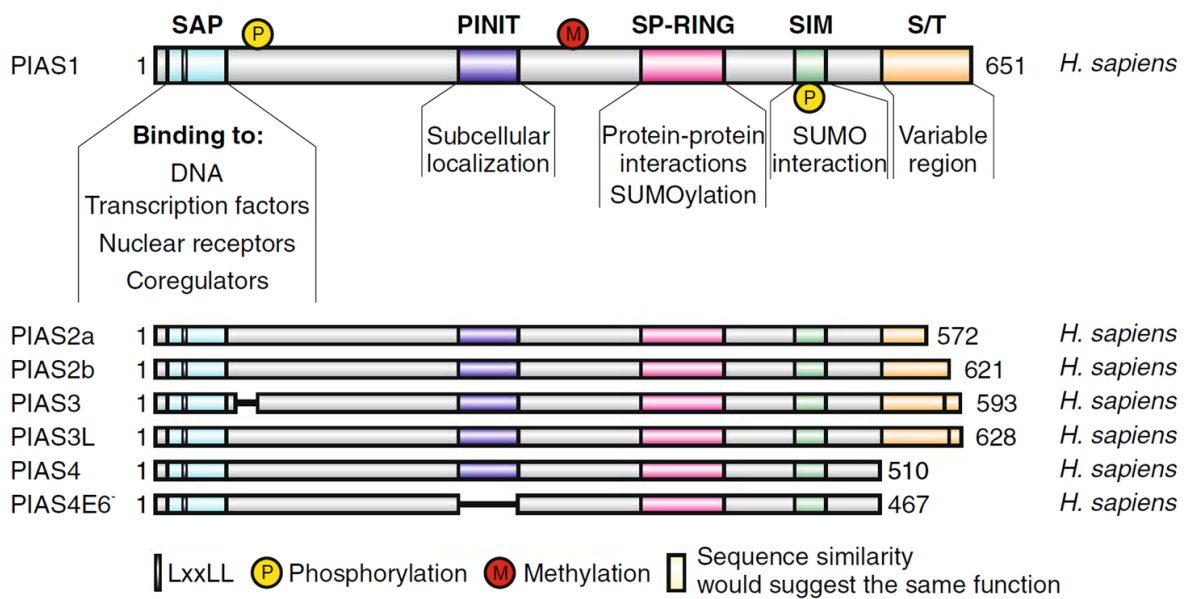


Figure 7: Simplified domain structure of human PIAS proteins. PIAS proteins show a strong sequence homology in their N-terminal region of around 430 aa. The size varies from 510 aa (PIAS4) to 651 aa in the largest PIAS isoform (PIAS1). Splice variants of the isoforms exist for PIAS2, PIAS3 and PIAS4, but not for PIAS1. Generally five different domains are described for PIAS proteins which can be found in human, as well as in other species. The N-terminal scaffold attachment factor-A/B, acinus and PIAS (SAP) domain (cyan) mediates binding to DNA and harbors an internal LxxLL motif, which binds to nuclear receptors. The PINIT domain (purple) is involved in the subcellular localization and seems to play a role for the SUMO E3 ligase function. PIAS4 splice variant E6 is missing the PINIT motif. The central SP-RING domain (pink) was shown to interact with Ubc9 and is essential for the SUMO E3 ligase function of PIAS proteins. The SIM (green) allows binding of PIAS proteins to SUMO and/or SUMO modified proteins and regulates protein-protein interactions. The variable S/T region (orange) of PIAS proteins is the domain with the lowest degree of sequence homology. PIAS proteins functions are, at least in part, regulated through posttranslational protein modifications like phosphorylation (yellow) and methylation (red) at depicted sites (adopted from Rytinki et al., 2009).

The motif with the highest degree of conservation among the human PIAS proteins is the *scaffold attachment factor-A/B, acinus and PIAS motif (SAP)* located at the very N-terminus. SAP domains are often found in chromatin associated proteins where they enable DNA binding (Aravind and Koonin, 2000). The SAP motif is further equipped with an internal LxxLL motif, which is known to be involved in protein-protein interaction during transcriptional regulation and binding to nuclear receptors (Heery et al., 1997; Plevin et al., 2005). PIAS4 mutants lacking the LxxLL motif were

shown to be unable to repress STAT-mediated signaling (Liu et al., 2001). The PINIT domain downstream of the SAP motif was identified to be essential at least for the nuclear retention of the large PIAS3 isoform PIAS3L (Duval et al., 2003). Further, this motif seems to be involved in the SUMO E3 ligase activity and mediates substrate specificity (Reindle et al., 2006; Takahashi and Kikuchi, 2005). The central region of PIAS proteins contains a motif, which shows considerable similarity to the RING finger region found in the largest subfamily of ubiquitin E3 ligases. RING finger domains contain eight cysteine/histidine residues arranged in a Cys-X₂-Cys-X₍₉₋₂₇₎-Cys-X₍₁₋₃₎-His-X₂-Cys-X₂-Cys-X₍₄₋₄₈₎-Cys-X₂-Cys consensus motif, which coordinates two zinc ions. This allows the formation of a globular domain, which alters the protein-protein interaction profile and allows DNA binding as described for classical zinc finger domains (Freemont, 1993; Freemont et al., 1991; Rytinki et al., 2009). However, the RING finger motif itself shows slight differences in the cysteine/histidine spacing and linker regions when compared to the zinc finger domain (Freemont et al., 1991). The RING type domain found in PIAS proteins is suggested to be similar folded as the RING finger domain, but lacks two cysteines within the consensus motif, therefore referred to Siz/PIAS RING (SP-RING) (reviewed in Hochstrasser, 2001). Downstream of the SP-RING domain a SIM is located, which broadens protein-protein interactions via non-covalent binding to SUMO and/or SUMO modified proteins. The SP-RING domain was shown to promote direct interaction with the SUMO E2 conjugating enzyme Ubc9 and is essential for the SUMO E3 ligase function of PIAS proteins *in vivo* and *in vitro* (Takahashi et al., 2001b). Similar to ubiquitin E3 ligases, PIAS proteins are suggested to function as adapters, which stabilize the interaction of SUMO-bound Ubc9 and the substrate protein, hence promoting the transfer of SUMO to its acceptor (Geiss-Friedlander and Melchior, 2007; Rytinki et al., 2009). As described in 1.3, SUMOylation alters protein functions mainly through relocalization and modified protein-protein interactions. The effects of PIAS proteins in transcriptional regulation can, at least in some cases, be linked to their SUMO E3 ligase function. For example PIAS4-mediated induction of cell senescence via p53 activation, which is caused by SUMO modification, or inhibition of p73 through relocalization to the nuclear matrix upon PIAS1 induced SUMOylation (Bischof et al., 2006; Munarriz et al., 2004). Further it was shown, that wildtype PIAS1 and PIAS2 α activate the transcriptional activity of the androgen receptor, while mutants lacking the SUMO E3 ligase function lost this ability (Kotaja et al., 2002). However, in the case of STAT1 and STAT3 regulation, PIAS1 and PIAS3 orchestrate their repressive function independent of SUMOylation by blocking DNA binding of the transcription factors. Nevertheless, the SUMO E3 ligase function is necessary to inhibit STAT1, indicating that its repression relies on SUMO modification of other cellular factors (Chung et al., 1997; Liu et al., 1998, 2007; Rogers et al., 2003; Rytinki et al., 2009). In contrast, PIAS2 and PIAS4 do not affect the DNA binding capacity of STATs, but inhibit STAT1 and STAT4 by recruiting other corepressive factors (Liu

et al., 2001; Shuai, 2006). Due to the regulation of crucial cellular processes like p53 or NF κ B signaling, the role of PIAS proteins in the development of diseases, especially in the context of tumorigenesis, was investigated intensively. In this context, PIAS isoforms 1 and 3 were implicated in tumorigenesis and are often found overexpressed in cancerous tissues. PIAS1-mediated p21 repression increased the proliferation rate in prostate cancer and PIAS1 overexpression is associated with poor prognosis in the course of multiple myeloma (Driscoll et al., 2010; Hoefer et al., 2012; Pühr et al., 2016; Rabellino et al., 2017). Further, PIAS3 is found overexpressed in colorectal cancers (Cerami et al., 2012). As already described in 1.4, viruses are known to exploit the host cell SUMO machinery in order to establish an optimal intracellular milieu, which ensures a productive infection. Thereby, different viruses have been reported to interact with PIAS proteins to modulate their function (reviewed in Lowrey et al., 2017). The early viral oncoprotein E6 of human Papillomavirus (HPV) is described to repress PIAS4-mediated senescence by interfering with its SUMO E3 ligase function (Bischof et al., 2006). The human Cytomegalovirus (CMV) protein IE1 is capable of repressing IFN responsive elements, which are activated during infection. PIAS1-induced SUMOylation of IE1 negatively regulates the viral protein leading to impaired blockage of IFN signaling. However, the viral IE2 protein interacts with PIAS1 and thus inhibits IE1 SUMOylation in order to evade the intrinsic immune response of the host cell (Kim et al., 2014). A novel role for PIAS4 during human Herpes Simplex Virus Type 1 (HSV-1) infection has been recently reported. Knockdown of endogenous PIAS4 levels allowed productive infection with an ICP0 null mutant virus. Under normal conditions, this virus mutant is not able to replicate and is effectively controlled by the intrinsic antiviral immune response, suggesting that PIAS4 has anti-viral functions (Conn et al., 2016). Further, the early adenoviral protein E4orf3 was shown to specifically bind and sequester PIAS3. The outcome of PIAS3 sequestration has to be determined, but likely influences its ability to regulate transcriptional expression (Higginbotham and O'Shea, 2015).

1.6 The role of E1B-55K as a viral SUMO E3 ligase during adenovirus infection

Recently our laboratory performed a comparative SUMO2 proteomic analysis of adenoviral infected HeLa cells and aimed to address the question, if the adenoviral SUMO E3 ligase E1B-55K modulates other cellular factors, besides p53 and Sp100A, through conjugation of SUMO proteins. Therefore a *stable isotope labelling with amino acids in cell culture* (SILAC) screen was performed, comparing the SUMO2 proteome during HAdV wildtype- and Δ E1B-55K mutant virus infection. We could show that adenovirus infection globally increased the SUMO modification of cellular

Introduction

proteins. Intriguingly, the increase of SUMO modification was stronger in the wildtype infection compared to the Δ E1B-55K mutant virus infection. In this context, we found 78 cellular factors exclusively SUMO2 modified in the presence of E1B-55K, indicating that E1B-55K is stimulating the SUMO2 modification of cellular factors. Beside cellular factors, we found that a considerable number of adenoviral proteins is SUMO2 modified during the course of infection, among them the early viral protein E1B-19K. One part of this work was, to confirm SUMO modification of E1B-19K and to investigate the role of this PTM for its function.

2 Material

2.1 Bacteria, eukaryotic cells, viruses

2.1.1 Bacterial strains

Strain	Genotype
DH5 α	<i>supE44, ΔlacU169, (80d lacZΔ M15), hsdR17, recA1, endA1, gyrA96, thi-1, relA1</i> (Hanahan and Meselson, 1983)

2.1.2 Eukaryotic cells

Cell line	Characteristics
A549	human lung carcinoma cell line expressing wildtype p53 (Giard et al., 1973)
H1299	human lung carcinoma cell line, p53-negative (Mitsudomi et al., 1992)
HEK 293	human embryonic kidney cell line, HA Δ V-C5 transformed, expressing E1A and E1B oncoproteins (Graham et al., 1977)
HEK 293T	HEK 293 cell line expressing large T antigen from SV40
HeLa 6his-SUMO2	HeLa cells overexpressing N-terminal 6his-tagged SUMO2 (Tatham et al., 2009)
HeLa parental	human cervix carcinoma cell line (Gey et al., 1952)
HepaRG	human hepatic progenitor cell line expressing stem cell properties, able to undergo complete hepatocyte differentiation (Gripon et al., 2002)
HepaRG 6his-SUMO1	HepaRG cells overexpressing N-terminal 6His-tagged SUMO1
HepaRG 6his-SUMO2	HepaRG cells overexpressing N-terminal 6His-tagged SUMO2 (Sloan et al., 2015)
pBRK	freshly isolated primary baby rat kidney cells

Material

2E2	293 EBNA Tet Cell line. Expression of HAdV-C5 E2A and E4orf6 is inducible via tetracycline (Catalucci et al., 2005)
-----	---

2.1.3 Viruses

Database #	Adenovirus	Characteristics
100	H5pg4100	wildtype HAdV-C5 containing a 1863 bp deletion (nt 28602 – 30465) in the E3 region (Kindsmüller et al., 2007)
149	H4pm4149	HAdV-C5 E1B-55K null mutant containing four stop codons at aa position 3, 8, 86, and 88 within the E1B-55K sequence (Kindsmüller et al., 2007)
154	H5pm4154	HAdV-C5 E4orf6 null mutant containing a stop codon at position 66 within the E4orf6 sequence (Blanchette et al., 2004)
269	Ad5 p15A-cm E1B-19K K44R	HAdV-C5 containing a mutation in the E1B-19K coding region leading to a lysine to arginine substitution at position 44 (K44R), which destroys the potential SUMO conjugating motif around lysine 44.

2.2 Nucleic acids

2.2.1 Oligonucleotides

Database #	Name	Sequence (5'-3')	Application
64	E1Bfw bp 2043 fwd	CGC GGG ATC CAT GGA GCG AAG AAA CCC ATC TGA GC	sequencing
272	pXC 1920fw	CCA GGC GCT TTT CCA AGA GAA GG	sequencing
366	cmv	CCC ACT GCT TAC TGG C	sequencing
636	pcDNA3-rev	GGC ACC TTC CAG GGT CAA G	sequencing

Material

640	E1B-55K PCR-fwd	GGA GCG AAG AAA CCC ATC TGA GCG GGG GGT ACC	RT-PCR
641	E1B-55K-PCR rev	GCC AAG CAC CCC CGG CCA CAT ATT TAT CAT GC	RT-PCR
782	Seq E1-Box fwd 2454 bp	CAA GGA TAA TTG CGC TAA TGA GC	sequencing
1318	E1Bseq978-999	GGC CTC CGA CTG TGG TTG CTT C	sequencing
1421	GAPDH-RT-fwd	ACC ACA GTC CAT GCC ATC AC	RT-PCR
1422	GAPDH-RT-rev	TCC ACC ACC CTG TTG CTG TA	RT-PCR
1686	E1A RT fwd	GTG CCC CAT TAA ACC AGT TG	RT-PCR
1687	E1A RT rev	GGC GTT TAC AGC TCA AGT CC	RT-PCR
2096	E1B-19K + 55K fwd	ATA GGA TCC ATG GAG GCT TGG GAG TGT TTG G	sequencing
2383	LeGO-insert_rev	CGC ACA CCG GCC TTA TTC C	sequencing
2803	E1B-19K rev	ATA CTC GAG TCA TTC CCG AGG GTC CAG GC	sequencing
2820	E1B-19K K44R fwd	GTT AGT CTG CAG AAT TAG GGA GGA TTA CAA GTG G	mutagenesis
2821	E1B-19K K44R rev	CCA CTT GTA ATC CTC CCT AAT TCT GCA GAC TAA C	mutagenesis
2822	E1B-19K K48R fwd	GAA TTA AGG AGG ATT ACA GGT GGG AAT TTG AAG AGC	mutagenesis
2823	E1B-19K K48R rev	GCT CTT CAA ATT CCC ACC TGT AAT CCT CCT TAA TTC	mutagenesis
2824	E1B-19K K44/48R fwd	GTT AGT CTG CAG AAT TAG GGA GGA TTA CAG GTG GGA ATT TGA AGA GC	mutagenesis
2825	E1B-19K K44/48R rev	GCT CTT CAA ATT CCC ACC TGT AAT CCT CCC TAA TTC TGC AGA CTA AC	mutagenesis

Material

3304	Human PIAS4 RT fwd	TGC GCC CAC CTG CAG TGC TTC G	RT-PCR
3305	Human PIAS4 RT rev	GCT GCG CTC CTT TTC GGC GCG GAT	RT-PCR
3353	hPIAS4 W363A fwd	GAA GAA GCC CAC CGC GAT GTG CCC CGT G	mutagenesis
3354	hPIAS4 W363A rev	CAC GGG GCA CAT CGC GGT GGG CTT CTT C	mutagenesis
3355	hPIAS4 fwd	GGC TGA AGA CCA TTG GGG TAA AGC	sequencing
3392	eGFP-RT-fwd	CAG AAG AAC GGC ATC AAG GT	RT-PCR
3393	eGFP-RT-rev	GGT GCT CAG GTA GTG GTT GTC	RT-PCR
3597	BamHI-hPIAS4 fwd	AGA GAG GGA TCC ACT ATG GCG GCG GAG CTG G	cloning
3598	EcoRI-hPIAS4 rev	AGA GAG GAA TTC CAG TCA GCA GGC CGG CAC C	cloning

2.2.2 Vectors

Database #	Name	Application	Reference
136	pcDNA-3	expression vector for mammalian cells, CMV-promoter	InVitrogen
138	pGL3 basic	luciferase assay	Promega
152	pCMX3b-Flag	expression vector for mammalian cells, N-terminal flag tag, CMV-promoter	group database
174	pFA-CMV	expression vector for mammalian cells, N-terminal Gal4 DNA binding motif, CMV-promoter	group database
180	pRenilla-TK	luciferase assay	Promega
196	pcDNA3-Flu	expression vector for mammalian cells, N-terminal HA tag ,CMV-promoter	group database

Material

282	pEGFP-C3	expression vector for mammalian cells, CMV-promoter, N-terminal eGFP tag	Clontech
-----	----------	---	----------

2.2.3 Recombinant plasmids

Database #	Name	Vector	Insert	Reference
608	pXC-15	pXC-15	HAdV-C5 E1 region	group database
737	pE1A	pML	HAdV-C5 E1A	group database
1022	E1B-55K-K104R- pcDNA3	pcDNA3	HAdV-C5 E1B-55K K104R	group database
1319	pcDNA3-E1B-55K	pcDNA3	HAdV-C5 E1B-55K	group database
1664	E4orf6 splice fix	pcDNA3	HAdV-C5 E4orf6	group database
1680	E1-Box 4xS	pPG-S3	HAdV-C5 E1-region carrying four stop codons in the E1B-55K coding region	group database
1968	pCMV-VSV-G	pCMV	core protein G (VSV-G) of SV40	group database
1969	pRSV Rev	pRSV	HIV Rev	group database
1970	pMDLg/pRRE	pMDL	HIV-1 Gag, HIV-1 Pol	group database
2421	pGL3-Prom E1B	pGL3	HAdV-C5 E1B promoter	group database

Material

2476	pcDNA3-HA-E1A genomic	pcDNA3	HAdV-C5 E1A	group database
2738	Flag-pV	pCMX3b	HAdV-C5 pV	group database
2739	HAdV-C5 ppVI	pCMX3b	HAdV-C5 ppVI	group database
2741	Flag-pVII	pCMX3b	HAdV-C5 pVII	group database
2743	Flag-pp μ	pCMX3b	HAdV-C5 pX (pp μ)	group database
2744	E2A pCMX3b	pCMX3-Flag	HAdV-C5 E2A	group database
2866	Ad2 E1B19K	pCMX3-Flag	HAdV-C2 E1B-19K	this work
2867	Ad5 E1B19K	pCMX3-Flag	HAdV-C5 E1B-19K	this work
2869	Ad5 E1B19K	pcDNA3-HA	HAdV-C5 E1B-19K	this work
2870	Ad5 E1B19K	pcDNA3	HAdV-C5 E1B-19K	this work
2874	Ad5 E1B19K K44R	pcDNA3	HAdV-C5 E1B-19K K44R	this work
2875	Ad5 E1B19K K48R	pcDNA3	HAdV-C5 E1B-19K K48R	this work
2876	Ad5 E1B19K K44/48R	pcDNA3	HAdV-C5 E1B-19K K44/48R	this work

Material

2877	Ad5 Flag-E1B19K K44R	pCMX3b-Flag	HAdV-C5 E1B-19K K44R	this work
2878	Ad5 Flag-E1B19K K48R	pCMX3b-Flag	HAdV-C5 E1B-19K K48R	this work
2879	Ad5 Flag-E1B19K K44/48R	pCMX3b-Flag	HAdV-C5 E1B-19K K44/48R	this work
3019	human Ubc9	pcDNA3	human Ubc9	group database
3020	HA-mPias1	pKW2T	mouse PIAS1	group database
3021	HA-mPIAS γ	pKW2T	mouse PIAS γ	group database
3021	HA-mPIAS γ	pKW2T	mouse PIAS4	group database
3022	Flag-hPIAS α	pCMV-Flag	human PIAS α	group database
3023	Flag-Piasxbeta	pCMV-Flag	human PIAS2 β	group database
3024	Flag-hPIAS γ	pCMV-Flag	human PIAS γ	group database
3072	E1-Box pPG-S3_E1B-19K K44R	pPG-S3	HAdV-C5 E1 region expressing E1B-19K with K44R mutation	this work
3073	E1-Box pPG-S3_E1B-19K K48R	pPG-S3	HAdV-C5 E1 region expressing E1B-19K with K48R mutation	this work
3074	E1-Box pPG-S3_E1B-19K K44_48R	pPG-S3	HAdV-C5 E1 region expressing E1B-19K with K44/48R mutation	this work

Material

3075	E1-Box 4xS_E1B-19K K44R	pPG-S3	HAdV-C5 E1 region expressing E1B-19K with K44R mutation	this work
3076	E1-Box 4xS_E1B-19K K48R	pPG-S3	HAdV-C5 E1 region expressing E1B-19K with K48R mutation	this work
3077	E1-Box 4xS_E1B-19K K44_48R	pPG-S3	HAdV-C5 E1 region expressing E1B-19K with K44/48R mutation	this work
3084	pFA-CMV-HAdV-5 E1B-19K Gal4	pFA-CMV	HAdV-5 E1B-19K	this work
3110	His-SUMO2 pcDNA3	pcDNA3	human SUMO2	group database
3275	Flag-hPiasy W363A	pCMV-Flag	human Piasy with a W363A point mutation	this work
3382	piLenti-siRNA-scramble-GFP	piLenti-siRNA-GFP	siRNA scramble	Applied Biological Materials, Inc. Cat. No. LV015-G
3383	piLenti-siRNA-PIAS4 A-GFP	piLenti-siRNA-GFP	siRNA anti PIAS4	Applied Biological Materials, Inc. Cat. No. i017280
3384	piLenti-siRNA-PIAS4 B-GFP	piLenti-siRNA-GFP	siRNA anti PIAS4	Applied Biological Materials, Inc. Cat. No. i017280
3385	piLenti-siRNA-PIAS4 C-GFP	piLenti-siRNA-GFP	siRNA anti PIAS4	Applied Biological Materials, Inc. Cat. No. i017280
3386	piLenti-siRNA-PIAS4 D-GFP	piLenti-siRNA-GFP	siRNA anti PIAS4	Applied Biological Materials, Inc. Cat. No. i017280

2.3 Antibodies

2.3.1 Primary antibodies

Database #	Name	Characteristics	Source
1	2A6	monoclonal mouse ab binding the N-terminus of HAdV-C5 E1B-55K (Sarnow et al., 1982)	group database
57	α -Ubc9	monoclonal mouse ab (IgG2a) binding the human Ubc9 protein (aa. 26-156)	BD Transduction Cat. No. 610749
62	DO-1	monoclonal mouse ab (IgG2a) binding the N-terminal aa 11-25 of human p53 (Vojtěšek et al., 1992)	Santa Cruz Cat. No. sc-126
88	AC-15	monoclonal mouse ab (IgG1) binding β -actin	Sigma Aldrich, Inc. Cat. No. A-5441
94	RSA3	monoclonal mouse ab binding the N-terminus of HAdV-C5 E4orf6 and E4orf6/7 (Marton et al., 1990)	group database
113	B6-8	monoclonal mouse ab binding the HAdV-C5 E2A protein (Reich et al., 1983)	group database
131	M73	monoclonal mouse ab binding the HAdV-C5 E1A proteins 12S and 13S (Harlow et al., 1985)	group database
196	M2	monoclonal mouse ab (IgG1) binding the Flag epitope (DYKDDDDK)	Sigma Aldrich, Inc. Cat. No. F3165
275	α -L4-100K	monoclonal rat IgG binding the HAdV-C5 L4-100K protein (Kzhyshkowska et al., 2004)	group database
369	4E8	monoclonal rat ab binding the central region (aa 94-110) of HAdV-C5 E1B-55K (Kindsmüller et al., 2009)	group database
452	α -Capsid	polyclonal rabbit ab binding the HAdV-C5 capsid proteins	group database
477	α -MRE11	polyclonal rabbit ab binding the human Mre11 protein	NOVUS Biologicals Cat. No. NB100-142
490	α -E1B-19K	polyclonal rabbit ab binding the C-terminus of HAdV-C5 E1B-19K (Lomonosova et al., 2005)	group database

Material

551	α -His	monoclonal mouse ab (IgG2a) binding the His-tag	Clontech Cat. No. 631212
566	α -PML	polyclonal rabbit ab binding the human PML protein	NOVUS Biologicals Cat. No. NB 100-59787
622	α -GFP	polyclonal rabbit ab binding the green fluorescent protein GFP	Abcam Cat. No. ab 290
629	3F10	monoclonal rat ab (IgG1) binding aa 98-106 of influenza HA protein	Roche Cat. No. 11867423001
633	α -PIAS4	polyclonal rabbit ab binding the N-terminus of human PIAS4	LifeSpan Biosciences, Inc Cat. No. LS-C108719

2.3.2 Secondary antibodies Western Blot

Product	Characteristics	Source
HRP α -mouse	polyclonal horseradish peroxidase (HRP) coupled goat F(ab') ₂ against mouse IgG (H+L)	Jackson ImmunoResearch Laboratories, Inc. Cat. No. 115-036-003
HRP α -rabbit	polyclonal horseradish peroxidase (HRP) coupled goat F(ab') ₂ against rabbit IgG (H+L)	Jackson ImmunoResearch Laboratories, Inc. Cat. No. 111-036-003
HRP α -rat	polyclonal horseradish peroxidase (HRP) coupled goat F(ab') ₂ against rat IgG (H+L)	Jackson ImmunoResearch Laboratories, Inc. Cat. No. 112-036-003

2.3.3 Secondary antibodies Immunofluorescence

Product	Characteristics	Source
Alexa Fluor™ 488 α -mouse	polyclonal Alexa Fluor™ 488 coupled goat F(ab') ₂ against mouse IgG (H+L)	ThermoFisher Scientific Cat. No. A 11017
Alexa Fluor™ 488 α -rabbit	polyclonal Alexa Fluor™ 488 coupled goat ab against rabbit IgG (H+L)	ThermoFisher Scientific Cat. No. A 11008

Material

Alexa Fluor™ 488 α-rat	polyclonal Alexa Fluor™ 488 coupled goat ab against rat IgM (H+L)	ThermoFisher Scientific Cat. No. A 21212
FITC α-mouse	polyclonal fluorescein (FITC) coupled donkey F(ab') ₂ against mouse IgG (H+L)	Jackson ImmunoResearch Laboratories, Inc. Cat. No. 715-096-151
FITC α-rabbit	polyclonal fluorescein (FITC) coupled donkey F(ab') ₂ against rabbit IgG (H+L)	Jackson ImmunoResearch Laboratories, Inc. Cat. No. 711-096-152
FITC α-rat	polyclonal fluorescein (FITC) coupled donkey F(ab') ₂ against rat IgG (H+L)	Jackson ImmunoResearch Laboratories, Inc. Cat. No. 712-095-153
Texas Red α-mouse	polyclonal Texas Red® dye conjugated donkey F(ab') ₂ fragment against mouse IgG (H+L)	Jackson ImmunoResearch Laboratories, Inc. Cat. No. 715-076-151
Texas Red α-rabbit	polyclonal Texas Red® dye conjugated donkey F(ab') ₂ fragment against rabbit IgG (H+L)	Jackson ImmunoResearch Laboratories, Inc. Cat. No. 711-075-152
Texas Red α-rat	polyclonal Texas Red® dye conjugated donkey F(ab') ₂ fragment against rabbit IgG (H+L)	Jackson ImmunoResearch Laboratories, Inc. Cat. No. 712-075-153

2.4 Commercial kits

Product	Source
Dual-Luciferase® Assay System	Promega
High Capacity cDNA Reverse Transcription Kit	Thermo Scientific
Lipofectamin®2000	Invitrogen
Plasmid purification Mini, Midi and Maxi Kit	QIAGEN
ProFection® Mammalian Transfection System	Promega
Protein Assay	BioRad
QIAquick® Gel Extraction Kit	QIAGEN
QIAquick® PCR Purification Kit	QIAGEN
QIAshredder 250	QIAGEN

Material

RNeasy Plus Mini Kit	QIAGEN
SensiMix® SYBR Hi-Rox	Bioline
SuperSignal® West Pico Chemiluminescent Substrate	Pierce

2.5 Markers and standards

Product	Source
100 bp DNA ladder	NEB
1 kb DNA ladder	NEB
PageRuler™ Plus Prestained Protein Ladder	Pierce

2.6 Chemicals, enzymes, reagents, equipment

Chemicals, enzymes and reagents used in this study were obtained from Agilent, Applichem, Biomol, Merck, New England Biolabs, Roche and Sigma Aldrich. Cell culture materials, general plastic material as well as equipment were supplied by BioRad, Biozym, Brand, Engelbrecht, Eppendorf GmbH, Falcon, Gibco BRL, Greiner, Hartenstein, Hellma, Nunc, PAN-Biotech, Sarstedt, Protean, Schleicher & Schuell, VWR and Whatman.

2.7 Software and databases

Product	Application	Source
Acrobat X Pro	PDF data processing	Adobe
CLC Main Workbench 7.9.1	sequence data processing	CLC bio
Fiji	image processing	(Schindelin et al., 2012)
Filemaker Pro 11	database management	Thomson
Gene tools	documentation of agarose gel electrophoresis	Syngene

Material

GraphPad Prism 5	data processing and biostatistics	Statcon
Illustrator CS6	layout processing	Adobe
Leica Application Suite X	immunofluorescence analysis	Leica
Mendeley Desktop	reference management	Mendeley
Office 2010	text processing	Microsoft
Photoshop CS6	image processing	Adobe
Pubmed	literature database, open sequence analysis software	open software provided by NCBI
Rotor-Gene Q2.3.1	RT-PCR data processing	QIAGEN

3 Methods

3.1 Bacteria

3.1.1 Culture and storage

Liquid bacterial cultures (*E.coli*) were inoculated with a single colony and cultured in sterile LB-medium containing the corresponding antibiotic (100 µg/ml ampicillin; 25 µg/ml kanamycin) at 30-37 °C and 200 rpm in an *Innova 4000 Incubator* (New Brunswick) for 16-24 h. For solid cultures, bacterial cells were plated on plastic dishes containing LB media with 15 g/l agar and the corresponding antibiotic (100 µg/ml ampicillin; 25 µg/ml kanamycin). After incubation overnight at 30-37 °C single colonies can be picked and cultivated as described above. If needed, the bacterial concentration was determined by measuring the optical density at 600 nm (*Smart Spec Plus*, Biorad). Sealed with *Parafilm* (Pechiney Plastic Packaging), the dishes containing solid bacterial colonies can be stored at 4 °C for several weeks. For long term storage, 5 ml of liquid cultures were centrifuged at 4000 rpm for 5 min (*Megafuge 1.0*, Heraeus) and resuspended in LB-medium supplemented with glycerol (1:1, v/v), transferred to *CryoTubes™* (Sarstedt) and stored at -80 °C.

LB-medium	10 g/l	tryptone
	5 g/l	yeast extract
	5 g/l	NaCl
		*autoclave
antibiotic solution	100 mg/ml	ampicillin
	25 mg/ml	kanamycin
		*sterile filtered
		*stored at -20 °C

3.1.2 Chemical transformation

100 µl chemical competent *E.coli* DH5α were gently thawed on ice. The desired plasmid DNA (~200 ng) was transferred into a polypropylene round bottom tube (14 ml, Falcon) and mixed with the bacteria by pipetting up and down carefully. The mixture is incubated on ice for 30 min, followed by a heat shock at 42 °C for 30 sec in a water bath. After cooling down the probe on ice for 2 min, 1 ml LB-medium (without antibiotics) was added and the bacteria were incubated at 37 °C and 200 rpm in an *Innova 4000 Incubator* (New Brunswick) for 45 min. Finally, different volumes of the bacteria suspension (10, 100 µl) were plated on LB-medium plates containing the corresponding antibiotic and grown overnight at 30-37 °C.

3.2 Mammalian cells

3.2.1 Maintenance and passaging of cell cultures

Adherent cells were grown in monolayers on polystyrene cell culture dishes (12-well/ 6-well, 100mm/ 150 mm tissue dishes, Sarstedt/Falcon) in *Dulbeccos Modified Eagle Medium* (DMEM, Gibco) containing 0.11 g/l sodium pyruvate. DMEM was supplemented with 10 % FCS (PAN-Biotech) and 1 % penicillin/streptomycin solution (10000 U/ml penicillin; 10 mg/ml streptomycin in 0.9 % NaCl, PAN-Biotech). All cells were cultured in Hera Safe 6220 incubators (Heraeus) at 37 °C and 5 % CO₂ to a confluency of 90 %. To passage the cells, the medium was aspirated, the cells were washed with sterile PBS and subsequently incubated for 5 min at 37 °C in an appropriate volume of trypsin/EDTA (0.05 % in PBS, PAN-Biotech). The enzymatic activity of trypsin was blocked by DMEM medium containing 10 % FCS and the detached cells were transferred into 15 ml/ 50 ml reaction tubes (Sarstedt) and pelleted via centrifugation (*Multifuge 3S-R*, Heraeus) at 2000 rpm for 3 min. After discarding the supernatant, the cells were resuspended in fresh cell culture medium and diluted (1:5-1:20) for further propagation. Cells designated for experimental approaches were counted using a hemocytometer (*Neubauer cell counter*, Carl Roth) prior to seeding. Cells were diluted in trypan blue solution (1:1, v/v) to distinguish between viable and dead cells. 10 µl of the cell suspension was pipetted onto the cell counter and the cells were analyzed under a light microscope (DMIL, Leica). The following formula was used to determine the total number of viable cells:

$$cell\ number\ \left[\frac{cell}{ml} \right] = number\ of\ cells * dilution\ factor * 10^4$$

PBS (pH 7.3)	140 mM	NaCl
	3 mM	KCl
	4 mM	Na ₂ HPO ₄
	1.5 mM	KH ₂ PO ₄
		*autoclave
trypan blue solution	0.15 % (w/v)	trypan blue
	0.85 % (w/v)	NaCl in H ₂ O

3.2.2 Storage

For long term storage cells were washed, detached and pelleted as described in 3.2.1. An appropriate amount of cells was taken up in 1 ml pure FCS containing 10 % DMSO (v/v), transferred into a *CryoTube*[™] (Sarstedt) and gradually frozen down to -80 °C using a freezing container (*Mr. Frosty*, Nalgene Labware) before storing them in liquid nitrogen. For recultivation, cells were thawed quickly at 37 °C and immediately transferred into 10 ml culture medium containing 10 % FCS. After pelleting and resuspending, the cells were seeded onto tissue culture dishes and cultured as described before in 3.2.1.

3.2.3 Transfection of cells

3.2.3.1 Transfection with polyethylenimine (PEI)

Mammalian cells were transiently transfected with PEI (Polysciences) dissolved in ddH₂O with a concentration of 1 mg/ml, pH 7.2 (adjusted with 0.1 M HCl) sterile filtered (0.22 µm pore size), aliquoted and stored at -80 °C. The cells were seeded 24 h before transfection on either 6-well or 100 mm dishes. Desired amounts of plasmid DNA was transferred into 1.5 ml reaction tubes (Sarstedt). 800 µl prewarmed DMEM medium without supplements was added to the DNA and incubated for 10 min. Afterwards, prewarmed PEI solution was added in a ratio of 1:10 (DNA:PEI, v/v) and the mixture was incubated for 20 min at room temperature (RT). In the meantime, the medium of the cells to be transfected was changed to DMEM medium without additives. The

transfection mixture was centrifuged shortly (*Biofuge 13*, Heraeus) and then added dropwise onto the cells. After 4 h of incubation at 37 °C and 5 % CO₂, the medium was exchanged to standard cell culture medium to avoid toxic effects of PEI and the cells were cultured at 37 °C and 5 % CO₂ before harvesting. PEI transfection was the standard transfection method in this study, if not specified further.

3.2.3.2 Transfection with calcium phosphate

Calcium phosphate transfection was performed with the *ProFection® Mammalian Transfection System* (Promega). All reagents were thawed at RT. The desired plasmids were diluted in sterile ddH₂O to a total volume of 437.5 µl and slightly mixed by vortexing before adding 62.5 µl of CaCl₂ solution (2 M). 500 µl of 2x HBS were transferred into a 15 ml reaction tube (Sarstedt) and the transfection mixture was added dropwise, while blowing air into the solution using a pasteur pipette, and afterwards incubated for 30 min at RT. Meanwhile, the cell culture medium was replaced by fresh prewarmed cell culture medium with additives. The transfection mixture was mixed and added dropwise to the cells and incubated for 6-8 h at 37 °C and 5 % CO₂, before fresh cell culture medium was added to the cells to propagate them further.

3.2.3.3 Transfection of linearized viral genomes with lipofectamin

8 µg of *PacI/SwaI* digested viral genomes were diluted in DMEM without additives to a total volume of 500 µl in a 1.5 ml reaction tube (Sarstedt) and mixed gently. The DNA solution was gently mixed with 500 µl DMEM without additives containing 4 % lipofectamin (v/v) and incubated for 20 min at RT. In the meantime, the cell culture medium of the cells (2E2 cells on 60 mm cell culture dishes) to transfect was replaced by DMEM without additives and the transfection mixture was carefully added to the cells. The cells were incubated for 6-8 h at 37 °C and 5 % CO₂ and slewed hourly. Afterwards fresh cell culture medium was added and the cells were propagated further.

3.2.4 Cell harvesting

Adherent transfected and infected mammalian cells were detached using a cell scraper (Sarstedt). The cell culture medium containing the cells was transferred into appropriate reaction tubes (15/50 ml, Sarstedt) and centrifuged at 2000 rpm for 3 min (*Multifuge 3S-R*, Heraeus). The supernatant was discarded and the pelleted cells were washed with PBS, pelleted again and frozen at -20 °C for further analysis.

For determination of virus progeny production experiments (3.3.4), the infected cells were resuspended in an appropriate volume of DMEM without additives and stored at -20 °C. For RNA extraction (3.6.1), the cells were lysed in RLT⁺ buffer (*RNeasy Plus Mini Kit*, QIAGEN) containing 1 % β -mercaptoethanol (v/v) prior to freezing at -80 °C.

3.2.5 Transformation assay of primary baby rat kidney cells (pBRK)

3×10^6 freshly isolated pBRK cells were seeded 24 h prior to transfection onto 100 mm cell culture dishes (Sarstedt) and propagated in cell culture medium at 37 °C and 5 % CO₂. pBRK cells were transfected with adenoviral oncogenes using calcium phosphate (3.2.3.2). Two days post transfection, the cells were washed once with PBS and detached with trypsin. Subsequently equal proportions of the cells were seeded onto three 100 mm cell culture dishes and cultured in standard cell culture medium for 4-8 weeks, while the medium was renewed twice a week. After visible colony formation of transformed cells growing in multilayers, the cell culture medium was removed and the cells were fixed and stained using an aqueous solution crystal violet solution for visualization and statistical analysis.

crystal violet solution

1 % crystal violet (w/v)

25 % methanol

*in ddH₂O

3.3 Adenovirus

3.3.1 Infection of mammalian cells

Cells were seeded 24 h prior to infection as described before in section 3.2.1. For infection the culture medium was removed, cells were washed with PBS and prewarmed DMEM without additives was added to the cells. The desired amount of adenoviral particles was diluted in an appropriate volume of prewarmed DMEM without additives and applied to the cells. For calculation of a specific amount of viral particles per cell, the following formula was used, wherein MOI stands for *multiplicity of infection* and ffu for *fluorescent forming units*:

$$\text{volume virus stock solution } [\mu\text{l}] = \text{cell number} * \frac{\text{MOI}[\text{ffu}]}{\text{virus titer } [\text{ffu}/\text{cell}]}$$

After incubation of 2 h at 37 °C and 5 % CO₂ the medium was replaced by fresh cell culture medium and the cells were propagated and harvested at indicated time points (8 h-72 h)(3.2.4).

3.3.2 Propagation and storage of high titer virus stocks

For the generation of high titer virus stocks H1299 cells were grown on 150 mm cell culture dishes (Sarstedt) to a confluency of 80 % and infected with a MOI of 20-50 (3.3.1). The cells were harvested (3.2.4) 4-6 day post infection and resuspended in 1 ml DMEM without additives per 150 mm dish. To release the viral particles, the cells were disrupted by three cycles of freeze (liquid nitrogen) and thaw (37 °C water bath, GFL, Gesellschaft für Labortechnik) followed by centrifugation at 4500 rpm for 15 min (*Multifuge 3S-R*, Heraeus) to pellet the cell debris. The supernatant was supplemented with 10 % glycerol (v/v) and stored at -80 °C. Cells transfected with linearized viral genomes (3.2.3.3) were harvested 4-6 days post infection in their culture medium and without washing, to avoid loss of cells. After cell rupture by freeze and thaw (see above) two 150 mm cell culture dishes with 80-90 % confluent H1299 cells were reinfected with 2 ml supernatant to generate high viral titers.

3.3.3 Titration of virus stocks

The virus titers were determined based on ffu of reinfected HEK 293 cells stained for the adenoviral protein E2A/DBP. Therefore, 1×10^6 HEK 293 cells/well were seeded into 6-well cell culture dishes (Sarstedt) and infected with different dilutions of the virus stock ranging from $10^{-1} - 10^{-5}$ (3.3.1). 24 hours post infection the cells were washed with 1 ml/well sterile PBS and fixed with 1 ml ice-cold methanol/well for 20 min at -20 °C. Afterwards the methanol was removed and the cells were air-dried at RT prior to further analysis or storage at -20 °C. To reduce unspecific binding of the antibodies, each well was incubated with 1 ml/well TBS-BG for 1 h at RT. Afterwards, 1 ml/well primary antibody solution containing the E2A specific antibody B6-8 (1:10 v/v in TBS-BG) was added to the fixed cells and incubated for 2 h at RT. The cells were washed three times with 1 ml/well TBS-BG for 10 min prior to incubation with the secondary Alexa™ 488 coupled antibody (1:1000 v/v in TBS-BG) for 2 h at RT and exclusion of light. The cells were washed again as described above and finally overlaid with 1 ml/well sterile PBS. Under this conditions cells can either be directly analyzed with the fluorescence microscope (Leica DMIL) or stored at 4 °C for 48 h. The number of ffu in at least three different visual fields with uniform cell density was counted and

averaged afterwards. For the calculation of the total number of infectious particles [ffu/ μ l] the number of infected cells as well as the dilution factor and the magnification of the used microscope objectives have to be taken into account.

TBS-BG	137 mM	NaCl
	3 mM	KCl
	20mM	Tris/HCl (pH 7.6)
	1.5 mM	MgCl ₂
	0.05 % (v/v)	tween20
	0.05 % (w/v))	NaN ₃
	5 % (w/v)	glycine
	5 % (w/v)	BSA

3.3.4 Determination of virus progeny production

To determine the virus progeny production, 4×10^5 cells of an appropriate cell line were seeded into 6-well cell culture dishes one day prior to infection with a MOI of 20 (3.3.1). The infected cells were harvested at desired time points, generally 24, 48, and 72 hours post infection as described in 3.2.4, resuspended in 300-500 μ l DMEM without additives and stored at -20 °C. After lysis of the cells by repeated freeze and thaw cycles, the supernatant was diluted in DMEM without additives by factors ranging from 10^{-1} to 10^{-5} and H1299 or A549 cells were reinfected to determine the viral titers as described above in 3.3.3. The numbers of virus progeny per cell [ffu/cell] can be calculated by taken into account the number of seeded cells as well as the dilution factor of the generated virus suspensions.

3.4 DNA techniques

3.4.1 Preparation of plasmid DNA from *E.coli*

For the preparation of large scale plasmid DNA, liquid *E.coli* cultures were used. 500 ml sterile LB-medium were either directly inoculated with a single bacterial colony picked from a LB-agar plate or with appropriate volume of a liquid preculture, depending on the growth rate of the desired bacterial stocks. The bacterial culture was supplemented with the appropriate antibiotic and incubated at 30-37 °C and 200 rpm for 16-24 h in an *Innova 4000 Incubator* (New Brunswick). The bacteria were sedimented at 6000 rpm for 15 min and the supernatant was discarded. The plasmid DNA was extracted following the manufacturers protocol (*Plasmid purification Mini, Midi and Maxi Kit*, QIAGEN). The isolated DNA was resuspended in appropriate volumes of 10 mM Tris/HCl (pH 8) and adjusted to a final concentration of 1 µg/µl. The DNA solution was stored at 4 °C or -20 C for long term storage.

For the analysis of newly generated plasmid DNA, 5 ml LB-medium containing the appropriate antibiotic was inoculated with a single colony and cultured at 30-37 °C and 200 rpm for 16-24 h. 1 ml of the bacterial suspension was transferred into a 1.5 ml reaction tube (Sarstedt) and the bacteria was pelleted at 3000 rpm for 3 min (*Centrifuge 5417 R*, Eppendorf). The supernatant was discarded and the bacteria resuspended in 300 µl buffer P1 (QIAGEN). The cells were lysed by adding 300 µl alkaline buffer P2 (QIAGEN) prior to neutralization with 300 µl buffer P3 (QIAGEN). The debris was removed by centrifugation at 14000 rpm for 15 min at RT (*Centrifuge 5417 R*, Eppendorf). 750 µl of the supernatant were transferred into a fresh 1.5 ml reaction tube (Sarstedt) equipped with 600 µl isopropanol to precipitate the DNA. The DNA was sedimented by centrifugation at 14000 rpm for 12 min (*Centrifuge 5417 R*, Eppendorf), the supernatant was discarded and the DNA washed with 500 µl 75 % ethanol, and air-dried after an additional centrifugation step. The DNA was dissolved in 20 µl 10 mM Tris/HCl pH 8.

3.4.2 Determination of nucleic acid concentration

The concentration of nucleic acids was determined with a spectrophotometer (*NanoDrop1000*, Peqlab) at a wavelength of 260 nm. DNA purity was assessed by the ratio of OD₂₆₀/OD₂₈₀, whereupon values of 1.8 indicate high grade of purity for DNA. Pure RNA refers to OD₂₆₀/OD₂₈₀ values of 2.0.

3.4.3 Agarose gel electrophoresis

A desired amount of agarose (analytic gels: GENAXXON bioscience, preparative gels: SeaKem® Lonza) was dissolved in TBE buffer using a microwave (AFK) and supplemented with 0.5 µg/ml ethidiumbromide (Roth) for the detection of DNA. Additionally, preparative gels contained 1 mM guanosine to minimize UV radiation damage. The usual agarose concentration used in this study varied between 0.6-1.2 % (w/v). After boiling, the suspension was cooled down to 40-50 °C and poured into a suitable gel tray (*PerfectBlue™ Gel system*, PeqLab). The DNA samples were mixed with 6x loading dye (NEB) prior to loading into preformed gel pockets. Appropriate markers (100 bp and 1 kb ladder, NEB) were used as size references and the samples were separated using a constant voltage of 5-10 V/cm in TBE buffer.

Analytical gels were documented at a wavelength of 312 nm with an UV transilluminator (*G-box system*, Syngene) using *gene tools* software. Preparative gels were analyzed using a UV table and desired DNA bands were excised using a clean scalpel. DNA gel extraction was performed by centrifugation or by using the QIAquick® Gel Extraction Kit (QIAGEN)(3.4.3.1).

5x TBE buffer	450 mM	Tris/HCl pH 8
	450 mM	B(OH) ₃
	10 mM	EDTA
		*pH 7.8
6x loading dye	0.25 % (w/v))	bromphenol blue
	0.25 % (w/v)	xylene cyanol
	50 % (v/v)	glycerol
	2 % (v/v)	50 x TAE (tris acetate)

3.4.3.1 DNA isolation from agarose gels

To isolate desired DNA fragments, the excised gel pieces (3.4.3) were transferred into sterile water and centrifuged at 20000 rpm for 90 min (*RC 5B Plus*, Sorvall). The DNA containing supernatant was transferred into a 1.5 ml reaction tube (Sarstedt) and the DNA was precipitated by adding 10 % (v/v) sodium acetate (3M) and 90 % (v/v) isopropanol. The precipitated DNA was sedimented by centrifugation at 14000 rpm for 15 min (*Centrifuge 5417*, Eppendorf), washed with 500 µl 75 % ethanol and air-dried at RT. The DNA was rehydrated in 50 µl 10 mM Tris/HCl pH 8 and used for further approaches. Alternatively, the nucleic acids were isolated with the *QIAquick® Gel Extraction Kit* (QIAGEN) according to the manufactures protocol.

3.4.4 Polymerase chain reaction (PCR)

PCR is a method to amplify specific DNA fragments *in vitro* (Saiki et al., 1988). In this study PCR was performed in a total reaction volume of 50 µl in sterile 0.2 ml reaction tubes (Sarstedt), containing 25 ng DNA template to be amplified, 125 ng of a forward primer, 125 ng of a reverse primer, 1 µl dNTPs (1 mM each, NEB), 5 µl of PCR reaction buffer (10x) and 1 µl of a suitable DNA polymerase. In this work, either *DreamTaq* DNA Polymerase (5 U/µl, ThermoFisher) or *Pfu Ultra II* DNA Polymerase (5 U/µl, Stratagene) have been used. Sterile water was added to a total volume of 50 µl and the following PCR program was performed in a *MJ Mini™ Personal Thermo Cycler* (BioRad).

step	temperature	duration	
initial denaturation	95 °C	2 min	
denaturation	95 °C	1 min	27-35 cycles
annealing	55-70 °C	45 sec	
elongation	72 °C	1 min/kb	
final elongation	72 °C	10 min	
storage	4 °C	∞	

The success of a PCR was determined by loading 5 μ l of the reaction mix on an analytical agarose gel (3.4.3). Size and yield of the amplified DNA fragments were analyzed using a UV transilluminator (*G-box system, Syngene*).

3.4.5 Site-directed mutagenesis

Plasmid DNA with site-directed point mutations was generated by quick change PCR (QC-PCR). The reaction mix was of the same composition as described in 3.4.4., primers carried a desired nucleotide exchange, which is introduced into the DNA template and *Pfu Ultra II* DNA Polymerase (5 U/ μ l, Stratagene) was used for QC-PCR. The standard reaction program shown in 3.4.4 was modified depending on primer annealing temperature and template size, see table below:

step	temperature	duration	
initial denaturation	98 °C	2 min	
denaturation	95 °C	1 min	12-16 cycles
annealing	55-70 °C	45 sec	
elongation	68 °C	1 min/kb	
final elongation	72 °C	10 min	
storage	4 °C	∞	

To determine the efficiency of the QC-PCR, 5 μ l of the reaction mix were analyzed on an analytical agarose gel (3.4.3). The remaining 45 μ l were incubated with 1 μ l *DpnI* (NEB) for 2 h at 37 °C in a *thermomixer comfort* (Eppendorf) to remove methylated template DNA. 10 μ l of the PCR reaction were transformed into chemical competent *E.coli* DH5 α (3.1.2). Single colonies were picked and cultured in 5 ml sterile LB medium (3.1.1) and extracted DNA (3.4.1) was analyzed via sanger sequencing (3.5.3).

3.5 Cloning of DNA fragments

3.5.1 Enzymatic DNA restriction

1-10 µg of DNA were incubated with 20 U of an appropriate restriction endonuclease (NEB) and its designated reaction buffer (supplied by the manufacturer NEB) in a total volume of 50 µl at 37 °C for 2-16 h in a *thermomixer comfort* (Eppendorf) using sterile 1.5 ml reaction tubes (Sarstedt). If needed, consecutive restriction digests were carried out using different restriction endonucleases, while the DNA was precipitated with isopropanol between the enzymatic reactions. To isolate the desired DNA fragments, the DNA was separated using a preparative agarose gel (3.4.3) and extracted either via centrifugation or with the *QIAquick® Gel Extraction Kit* (QIAGEN)(3.4.3.1).

Enzymatic DNA restriction was also used for analytical approaches to validate the success of DNA cloning on the basis of its fragmentation pattern. 1 µg DNA was incubated with 3-10 U of an appropriate restriction endonuclease and its designated reaction buffer in a total volume of 20 µl for 90 min-3 h at 37 °C in a *thermomixer comfort* (Eppendorf). The DNA fragments were visualized on an analytical agarose gel (3.4.3).

3.5.2 Ligation

Prior to ligation, DNA fragments were enzymatically restricted and purified, as described in 3.5.1. In this study, the *Rapid DNA Ligation Kit* (Roche) was used according to the manufacturers protocol to ligate desired DNA fragments. 20-50 ng backbone DNA were incubated with a 5-fold excess of the DNA fragment to be inserted in a total reaction volume of 20 µl containing 2 µl DNA dilution buffer (10x), 10 µl T4 ligase buffer (2x) and 5 U T4 ligase at RT for 90 min. Afterwards, the ligation product was transformed into chemical competent *E.coli* DH5α (3.1.2) and 5 ml LB-cultures were inoculated with single colonies (3.1.1). The transformed plasmid DNA was extracted (3.4.1) and verified via sanger sequencing (3.5.3).

3.5.3 DNA sequencing

For DNA sequencing, 1.2 µg purified DNA was supplemented with 30 pmol of a suitable sequencing primer, mixed with sterile water to a total volume of 15 µl and send to Microsynth Seqlab, Göttingen.

3.6 RNA techniques

3.6.1 Preparation of total RNA from mammalian cells

Preparation of total RNA from mammalian cells was performed with the *RNeasy Plus Mini Kit* (QIAGEN). The cells were harvested as described in 3.2.4. and the dried pellet was lysed in 600 μ l RLT⁺ buffer (QIAGEN) supplemented with 1 % β -mercaptoethanol (v/v) by pipetting up and down. The cell lysate was transferred onto a *QIAshredder* spin column (QIAGEN) and centrifuged for 1 min at 14000 rpm (*centrifuge 5417 R*, Eppendorf) to completely homogenize the probe. Afterwards, the RNA was extracted from the flow through following the manufacturers protocol. An optional on column DNaseI digest was performed to remove contaminations of genomic DNA in the probe. The purified RNA was eluted in 30 μ l RNase free water into sterile 1.5 ml reaction tubes (Sarstedt) followed by determination of the RNA concentration with a spectrophotometer (*NanoDrop1000*, Peqlab), as described in 3.4.2., and adjusted to a final concentration of 1 μ g/ μ l by the addition of RNase free water. The extracted RNA was either stored at -80 C or directly reverse transcribed into complementary DNA (cDNA) (3.6.2).

3.6.2 Reverse transcription of RNA

The reverse transcription of 1 μ g purified RNA (3.6.1) into cDNA was done with the *High Capacity cDNA Reverse Transcription Kit* (Thermo Scientific) according to the manufacturers protocol using a *MJ Mini™ Personal Thermo Cycler* (BioRad). The cDNA was stored temporarily at 4 °C or at -20 °C for long term storage.

3.6.3 Real time PCR (RT-PCR)

Semi-quantitative RT-PCR experiments were performed to compare the cDNA content in different samples relative to each other. A total reaction volume of 10 μ l contained 25 ng cDNA (3.6.2), 5 μ l *2x SensiMix™SYBR-Green* (Bioline) and 5 pmol of each primer. The used primer sets amplify fragments of 100-200 bp within the DNA coding region of the desired gene. Each sample was measured in technical replicates to determine the average threshold cycle (CT), which was subsequently normalized with CT values of the housekeeping gene GAPDH. The RT-PCR was performed in sterile 0.1 ml STRIP tubes (LTF-Labortechnik) using a *Rotor-Gene 6000* (Corbett Life Sciences) machine with the following program:

step	temperature	duration	
initial denaturation	95 °C	10 min	
denaturation	95 °C	30 sec	40 cycles
annealing	63 °C	30 sec	
elongation	72 °C	30 sec	

3.7 Protein techniques

3.7.1 Preparation of total cell lysates

To prevent degradation of proteins, all steps were performed at low temperature levels to reduce the proteolytic activity of proteases. Dry cell pellets (3.2.4) were thawed on ice and lysed in an appropriate volume of ice-cold radio-immunoprecipitation assay (RIPA) buffer for 30 min (vortex every 10 min). RIPA buffer was freshly supplemented with PMSF (phenylmethylsulfonyl fluoride, 0.2 mM, Sigma), aprotinin (5 mg/ml, Sigma), pepstatin A (1 mg/ml, Sigma) and leupeptin (10 mg/ml, Sigma) to inhibit proteases. Subsequently, each probe was sonicated in a precooled *Branson Sonifier 450* (Branson) by applying 30 cycles per probe (output 0.8; 0.8 pulses/s). The cell debris was pelleted by centrifugation at 11000 rpm for 5 min at 4 °C (*centrifuge 5417 R*, Eppendorf) and the supernatant was transferred into sterile 1.5 ml reaction tubes (Sarstedt). Protein concentrations were determined using a Bradford assay, as described in 3.7.2.

All probes were adjusted to the same protein concentration by adding sterile water. The proteins were denaturated in appropriate volumes of 5x SDS loading buffer, freshly supplemented with 200 mM β -mercaptoethanol, and incubated at 95 °C for 5 min in a *thermomixer comfort* (Eppendorf). Protein lysates were either directly separated by SDS-PAGE (3.7.4) or stored at -20 °C.

RIPA lysis buffer		
	50 mM	Tris/HCl pH 8
	150 mM	NaCl
	5 mM	EDTA

	1 % (v/v)	nonidet P-40
	0.1 % (w/v)	SDS
	0.5 % (v/v)	sodium desoxycholate
5x SDS loading buffer	100 mM	Tris/HCl (pH 6.8)
	200 mM	DTT
	10 % (w/v)	SDS
	0.2 % (w/v)	bromphenol blue

3.7.2 Determination of protein concentration

Protein concentrations were determined using *Protein Assay Dye Reagent Concentrate* (BioRad) bradford reagent, which shifts its absorbance maximum from 470 nm to 595 nm once it is complexed with proteins. The increased absorbance at 595 nm is proportional to the protein concentration in the probe and can be interpolated from a standard curve (Bradford, 1976). 1 μ l of protein solution (3.7.1) was mixed with 800 μ l sterile water in a semi-micro cuvette (Sarstedt) and supplemented with 200 μ l bradford reagent. The probe was mixed and incubated for 5 min at RT prior to measure the absorbance at 595 nm in a *SmartSpec™ Plus* photospectrometer (BioRad). Finally, the protein concentration of the probe was determined by interpolation from a freshly measured standard curve, ranging from 1 μ g-16 μ g protein concentration (BSA, NEB).

3.7.3 Ni-NTA pulldown of 6His-tagged SUMO2 modified proteins

4x10⁶ parental HeLa cells or HeLa cells overexpressing 6His-tagged SUMO2 (HeLa SUMO2) were seeded onto 10 mm cell culture dishes (Sarstedt). The following day, the cells were either transfected (3.2.3.1) and harvested after 48 h or infected (3.3.1) and harvested at desired time points. The cells were gently scraped off the plates using a cell scraper (Sarstedt) and quickly transferred into sterile 15 ml reaction tubes (Sarstedt). The cells were pelleted by centrifugation at 2000 rpm for 3 min (*Multifuge 3S-R*, Heraeus), the supernatant was aspirated and cells were resuspended in 5 ml sterile PBS. 20 % (v/v) of the volume was transferred into sterile 1.5 ml reaction tubes (Sarstedt) and processed as already described for the preparation of total cell

Methods

lysates (3.7.1-3.7.2). The remaining cells were sedimented at 2000 rpm for 3 min (*Multifuge 3S-R*, Heraeus), the supernatant was discarded and the cells were lysed in 10 ml freshly prepared ice-cold GuHCl lysis buffer and sonicated in a precooled *Branson Sonifier 450* (Branson) by applying 30 cycles per probe (output 0.8; 0.8 pulses/s). 60 µl/pulldown Ni-nitrilotriacetic acid (Ni-NTA) agarose (*HisPur™ NiNTA Resin*, ThermoFisher) was prewashed three times with lysis buffer, pelleted at 900x g and 4 °C for 2 min (*centrifuge 5417 R*, Eppendorf) and equally distributed among the probes. After incubation for 16 h at 4 °C on a *rotator 3025* (GFL, Gesellschaft für Labortechnik) the Ni-NTA agarose was sedimented at 4000 rpm and 4 °C for 5 min (*Megafuge 1.0*, Heraeus), resuspended in 750 µl lysis buffer and transferred into sterile 1.5 ml reaction tubes (Sarstedt). The probe was centrifuged (900x g, 4 °C, 2 min, *centrifuge 5417 R*, Eppendorf) followed by removal of the supernatant and two consecutive washing steps with 1000 µl freshly prepared washing buffer A and B. The bound proteins were eluted in 60 µl elution buffer and incubated at 95 °C for 3 min in a *thermomixer comfort* (Eppendorf). Afterwards, the proteins were either stored at -20 °C or directly separated by SDS-PAGE (3.7.4) and visualized via immunoblotting (3.7.5).

The GuHCl lysis buffer, washing buffer A and washing buffer B were freshly supplemented with the protease inhibitors prior to usage: (phenylmethylsulfonyl fluoride 0.2 mM, aprotinin 5 mg/ml, pepstatin A 1 mg/ml, leupeptin 10 mg/ml, 25 mM iodoacetamide, 25 mM N-ethylmaleimide; all from Sigma).

GuHCl lysis buffer	6 M	guanidinium hydrochloride
	0.1 M	Na ₂ HPO ₄
	0.1 M	NaH ₂ PO ₄
	10 mM	Tris/HCl pH 8
	20 mM	imidazole
	5 mM	β-mercaptoethanol
wash buffer A	8 M	urea
	0.1 M	Na ₂ HPO ₄

	0.1 M	NaH ₂ PO ₄
	10 mM	Tris/HCl pH 8
	20 mM	imidazole
	5 mM	β-mercaptoethanol
wash buffer B	8 M	urea
	0.1 M	Na ₂ HPO ₄
	0.1 M	NaH ₂ PO ₄
	10 mM	Tris/HCl pH 6.3
	20 mM	imidazole
	5 mM	β-mercaptoethanol
elution buffer	150 mM	Tris/HCl pH 6.7
	5 % (w/v)	SDS
	200 mM	imidazole
	30 % (v/v)	glycerol
	720 mM	β-mercaptoethanol
	0.01 % (w/v)	bromphenol blue

3.7.4 Sodium dodecyl sulfate polyacrylamide gel electrophoresis (SDS-PAGE)

Denatured proteins (3.7.1 and 3.7.3) were separated by SDS-PAGE according to their molecular weight. Negatively charged SDS accumulates on denatured proteins with constant weight ratios leading to compensation of their positive charge and thereby to electrophoretic mobility

Methods

depending exclusively on their molecular weight. The separation of proteins is further optimized by the use of a discontinuous stacking gel (Laemmli, 1970). The proteins were first concentrated in a 5 % stacking gel (pH 6.8) prior to migration into the separation gel (pH 8.8). In this study separation SDS gels were prepared using a 30 % acrylamide/bisacrylamide stock solution (*37.5:1 Rotiphorese Gel 30*, Roth) diluted to concentrations ranging from 6-15 %. SDS-PAGE was run at 20 mA/gel in TGS buffer using a *Multigel SDS-PAGE system* (Biometra) and a *PowerPac™ Basic* (Biorad) power supply. As a reference for protein sizes, the *Page Ruler™ Plus Prestained Protein Ladder* (ThermoFisher) standard was used.

5 % stacking gel	17 % (v/v)	acrylamide/ bisacrylamide stock solution (30 %)
	120 mM	Tris/HCl pH 6.8
	0.1 % (w/v)	SDS
	0.1 % (w/v)	APS
	0.1 % (v/v)	TEMED
	0.01 % (w/v)	bromphenol blue
6 % separation gel	20 % (v/v)	acrylamide/ bisacrylamide stock solution (30 %)
	250 mM	Tris/HCl pH 6.8
	0.1 % (w/v)	SDS
	0.1 % (w/v)	APS
	0.04 % (v/v)	TEMED
8 % separation gel	27 % (v/v)	acrylamide/ bisacrylamide stock solution (30 %)
	250 mM	Tris/HCl pH 6.8
	0.1 % (w/v)	SDS

Methods

	0.1 % (w/v)	APS
	0.04 % (v/v)	TEMED
10 % separation gel	34 % (v/v)	acrylamide/ bisacrylamide stock solution (30 %)
	250 mM	Tris/HCl pH 6.8
	0.1 % (w/v)	SDS
	0.1 % (w/v)	APS
	0.04 % (v/v)	TEMED
12 % separation gel	40 % (v/v)	acrylamide/ bisacrylamide stock solution (30 %)
	250 mM	Tris/HCl pH 6.8
	0.1 % (w/v)	SDS
	0.1 % (w/v)	APS
	0.04 % (v/v)	TEMED
15 % separation gel	50 % (v/v)	acrylamide/ bisacrylamide stock solution (30 %)
	250 mM	Tris/HCl pH 6.8
	0.1 % (w/v)	SDS
	0.1 % (w/v)	APS
	0.04 % (v/v)	TEMED

TGS buffer	25 mM	Tris
	200 mM	glycine
	0.1 % (w/v)	SDS

3.7.5 Western Blot analysis

Proteins separated by SDS-PAGE (3.7.4) were transferred onto *Amersham™ Protran™ 0.45 μm NC* nitrocellulose (GE healthcare) membranes and thereby immobilized for immunodetection. In this study, a wet-blotting procedure was performed using a *Trans-Blot Electrophoretic Transfer Cell* (Biorad) in towbin buffer. A blotting cassette (Biorad) contained a stack composed of a blotting pad (Biorad), two layers of blotting paper (Whatman), SDS gel with proteins to be blotted, nitrocellulose membrane, two layers of blotting paper (Whatman) and a blotting pad (Biorad). Blotting pads, blotting paper and the nitrocellulose membrane were soaked in towbin buffer prior to assembly of the stack. Air bubbles between SDS gel and nitrocellulose membrane were removed carefully and the cassette was closed. The blotting of the proteins was performed at a continuous current of 400 mA/per blotting tank for 90 min using a *PowerPac™HC* (Biorad) power supply.

To saturate unspecific protein binding sites on the nitrocellulose, the membranes were incubated in 5 % (w/v) non-fat milk (Frema) in PBS for at least 2 h at 4 °C on orbital shaking platform (3016, GFL). The blocking solution was removed by three consecutive washing steps with PBS-T buffer (10 min at RT) and subsequently incubated with the primary antibody for 2 h at 4 °C on an orbital shaking platform (3016, GFL). All primary antibodies used in this study were diluted in PBS-T individually depending on their signal strength. After incubation, the primary antibody solution was removed and the membranes were washed as described above to remove residual antibodies. Suitable horseradish peroxidase coupled (HRP) secondary antibodies (Jackson Immune Research) were diluted 1:10000 in PBS-T supplemented with 3 % (w/v) non-fat milk (Frema) and incubated for 2 h at 4 °C on an orbital shaking platform (3016, GFL). The membranes were washed as described above and the protein bands were visualized by chemiluminescence using a *SuperSignal® West Pico Chemiluminescent Substrate* (ThermoFisher) following the manufacturers protocol. The protein signals were detected with *medical X-ray screen film blue sensitive* (CEA) at suitable exposure times and developed with a *GX Developer* (Kodak). The developed X-ray films were scanned with an *EPSON perfection 4490 Photo* (EPSON) scanner and further processed with *Photoshop CS6* and *Illustrator CS6* (Adobe).

towbin buffer	25 mM	Tris/HCl pH 8.3
	200 mM	glycine
	0.5 % (w/v)	SDS
	20 % (v/v)	methanol
PBS-T buffer	0.05 % (v/v)	tween20 in PBS

3.7.6 Immunofluorescence analysis

For immunofluorescence analysis 3×10^5 cells were seeded onto sterile 6-well plates (Sarstedt), which were equipped with glass cover slips (18x18 mm, VWR). Depending on the experimental set-up, the cells were either transfected (3.2.3.1) or infected (3.3.1) and cultured for the desired period. The medium was removed, the cells were washed with sterile PBS and fixed with 1 ml/well 4 % paraformaldehyde (v/v) in PBS for 20 min at 4 °C. The fixed cells were washed with sterile PBS and permeabilized by incubation in PBS-triton X-100 (0.5 % v/v) for 10 min at RT. Unspecific protein binding sites were saturated with 1 ml TBS-BG for 30 min at RT. 50 µl of PBS containing the desired primary antibodies was transferred onto the dry coverslip and incubated for 1 h at RT. Primary antibody dilutions were established in the lab dependent on their signal strength. The cells were washed three times with TBS-BG prior to incubation with the secondary fluorophore-coupled antibodies. All secondary antibodies were diluted 1:200, DAPI (Sigma) was diluted 1:8000 (v/v) in PBS. 50 µl of the antibody/DAPI suspension were transferred onto the dry coverslip and incubated for 1 h at RT and exclusion of light. The cells were washed twice with TBS-BG to remove unbound antibodies. Finally the cells were washed once with PBS, and the coverslip was mounted onto a glass slide (Menzel) with 50 µl/cover slip *glow* mounting medium (EnerGene) and incubated at 4 °C overnight. The immunofluorescence samples were analyzed using a *DMI 6000B fluorescence microscope* (Leica) using Leica Application Suite X software and images were further processed with *Photoshop CS6* and *Illustrator CS6* (Adobe) software.

PBS-triton X-100	0.5 % (v/v)	triton X-100 in PBS
TBS-BG buffer	100 mM	Tris/HCl pH 7.6
	685 mM	NaCl
	15 mM	KCl
	7.7 mM	MgCl ₂
	0.25 %	tween20
	0.25 %	sodium azide
	25 mg/ml	BSA fraction IV
	25 mg/ml	glycine

3.7.7 Subcellular fractionation

4x10⁶ cells were seeded onto sterile 10 mm cell culture dishes (Sarstedt) and either infected (3.3.1) or transfected (3.2.3.1) depending on the experimental approach. Cells were harvested in a sterile 50 ml reaction tube (Sarstedt) and transferred into fresh 1.5 ml reaction tubes (Sarstedt) after washing with sterile PBS. For subcellular fractionation, all incubation steps were performed on ice and the used centrifuge was precooled to 4 °C. The cells were pelleted (2000 rpm, 3 min, *centrifuge 5417 R*, Eppendorf) and lysed in 250 µl isotonic buffer IB containing 16.6 µl 10 % NP-40 for 5 min. The cell nuclei were pelleted by centrifugation at 1000 rpm for 4 min and the supernatant was transferred into a fresh 1.5 ml reaction tube (Sarstedt), as cytoplasmic fraction (F1). Afterwards the pellet was resuspended again in 250 µl isotonic buffer IB containing 8.3 µl 10 % NP-40 and 4.15 µl 10 % SDC and pelleted at 1000 rpm for 4 min. The supernatant was transferred into a fresh 1.5 ml reaction tube (Sarstedt) as the nuclear membrane fraction (F2). The pellet was resuspended in 200 µl RSB buffer supplemented with 3.33 µl DNase I (2.7 KUnits/µl; QIAGEN) and incubated for 30 min. The probe was centrifuged at 1200 rpm for 4 min and the supernatant was transferred into a fresh 1.5 ml reaction tube as the soluble nuclear fraction (F3). The remaining pellet was solubilized in 200 µl RSP buffer supplemented with 25 µl 5 M NaCl and incubated for 5 min to remove the chromatin from the nuclei. The probe was centrifuged at 2000 rpm for 6 min and the

Methods

supernatant was transferred into a fresh 1.5 ml reaction tube (Sarstedt) as the chromatin fraction (F4). Finally, the residual nuclei were resuspended in 250 μ l isotonic buffer IB supplemented with 0.2 % SDS (v/v) and 10 mM EDTA to isolate the insoluble nuclear matrix fraction (F5) (Van Eekelen and Van Venrooij, 1981; Hodge et al., 1977; Long et al., 1979).

isotonic buffer IB	10 mM	Tris/HCl pH 7.5
	150 mM	NaCl
RSB buffer	10 mM	Tris/HCl pH 7.5
	10 mM	NaCl
	3 mM	MgCl ₂
F5 buffer	10 mM	EDTA
	0.2 % (w/v)	SDS
		*in isotonic buffer IB

3.7.8 Reporter gene assay

For the quantification of promoter activities a *Dual Luciferase Reporter Assay System* (Promega) was used in this study, according to the manufacturers protocol. 2×10^5 H1299 cells were seeded onto sterile 12-well plates (Sarstedt) one day prior to transfection. The cells were transfected (3.2.3.1) with pGL-3 (Promega) vector (0.5 μ g), which encodes the reporter gene *firefly* luciferase (*photinus pyralis*) under the control of the promoter of interest. The expression of the *firefly* luciferase can be quantified by chemiluminescence and was subsequently normalized to the activity of a *renilla* luciferase (*renilla reniformis*) under the control of a thymidine kinase promoter, which was cotransfected (0.5 μ g) in every sample. 24 h post transfection, the cells were washed in sterile PBS and lysed in 100 μ l/well *passive lysis buffer* (Promega) on an orbital shaker (3016, GFL) at RT for 15 min. 10 μ l of each lysate were transferred into 5 ml round bottom plastic tubes

Methods

(Sarstedt) equipped with 20 μl *firefly luciferase substrate* and the *firefly luciferase* activity was measured for 10 s in a *Lumat LB 9507 luminometer* (Berthold Technologies). 20 μl 1:50 (v/v) diluted *stop and glow* solution was added into the tube, followed by measurement of the *renilla luciferase* activity for 10 s.

4 Results

4.1 SUMO2 modification of HAdV-C5 E1B-19K

4.1.1 Identification of the early protein E1B-19K as a potential SUMO2 substrate during adenovirus infection

In an initial attempt to test whether E1B-55K, one of the key regulatory viral proteins, induces SUMO modification of so far unknown cellular- and viral factors, a comprehensive proteomic analysis based on *stable isotope labelling with amino acids in cell culture* (SILAC) was performed. This method relies on the incorporation of isotopically labelled amino acids into newly synthesized proteins, allowing the relative quantification of specific changes within a bulk of proteins. HeLa cells, which stably overexpress 6His-tagged SUMO2 (HeLa SUMO2), were infected with either HAdV-C5 wildtype (wt) or Δ E1B-55K mutant virus to determine the effect of this early viral protein on the viral and cellular SUMO2 proteome. Adenoviral infection in general led to a global increase of SUMO2 modification of proteins (unpublished results from our research unit). However, the wt infection showed, compared to Δ E1B-55K mutant virus, a stronger increase of SUMO2 conjugates, suggesting that E1B-55K plays a role in SUMO modification of various host cell proteins. In this context, we could identify 78 cellular proteins with a significant E1B-55K-dependent increase of SUMO2 modification during infection. Furthermore, twenty adenoviral proteins were identified as being SUMO2 modified during infection, among them both, early and late adenoviral proteins (Figure 8). As expected, E1B-55K was only detected in wt infection, but not in the Δ E1B-55K mutant virus infection. Interestingly, E4orf6, E4orf6/7 and pVI showed E1B-55K-dependent SUMOylation and could not be found SUMOylated in its absence (Figure 8).

The early HAdV-C5 E1B-19K protein (from here on referred to as E1B-19K) was detected as being SUMO2 modified, which has not been described before. Its SUMOylation could be measured in wt and Δ E1B-55K mutant virus infection, indicating that E1B-19K SUMO2 modification occurs independently of E1B-55K (Figure 8, red asterisk).

Results

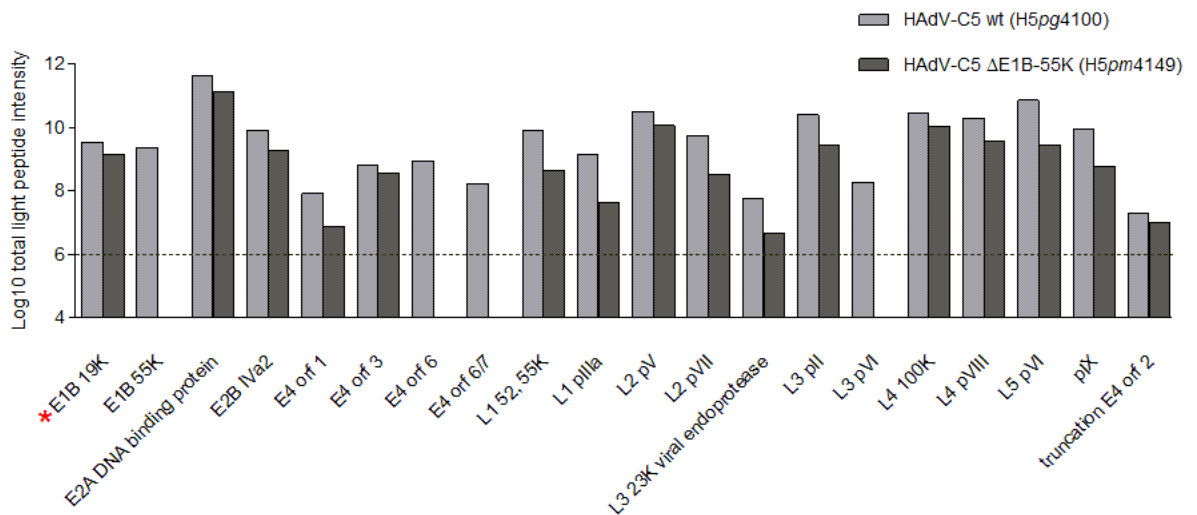


Figure 8: Overview of SUMO2 modified adenoviral proteins detected in the SILAC screening. Parental HeLa and HeLa SUMO2 cells were infected with either HAdV-C5 wt (H5pg4100) or HAdV-C5 ΔE1B-55K mutant virus (H5pm4149) and the abundance of SUMOylated viral proteins was determined (light grey: wt infection; dark grey: ΔE1B-55K mutant virus infection). E1B-19K shows a similar degree of SUMOylation in both infections, labelled with a red asterisk.

4.1.2 E1B-19K harbors a highly conserved SUMO consensus motif (SCM) at lysine 44

In order to confirm E1B-19K SUMO2 modification, we first performed an *in silico* analysis of the E1B-19K protein sequence to look for conserved SUMO consensus motifs (SCM). SCMs (ψ KxD/E) contain the lysine (K) where SUMO proteins will be conjugated, surrounded by a large hydrophobic aa residue (ψ) and an acidic aa residue (D/E) (Rodriguez et al., 2001). *In silico* analysis of the HAdV-C5 E1B-19K protein sequence revealed two potential SCMs in close proximity to each other; one at lysine 44 (IKED), and the other one at lysine 48 (YKWE) (Figure 9). Interestingly, the SCM at lysine 44 is highly conserved among the different HAdV species. Figure 9 illustrates an alignment of the first fifty aa of the E1B-19K protein from HAdV species A-G, with one representative virus type per species. Even though the composition of the SCM differs between the virus types, they all contain the entire motif following the consensus sequence ψ KxD/E. The second SCM at lysine 48 is less conserved and can only be found in HAdV-C5, HAdV-B2 34, and HAdV-D9. However, the high degree of conservation of the SCM at lysine 44 strengthens the hypothesis that E1B-19K is SUMO modified and that SUMOylation might be intimately involved in its functional regulation.

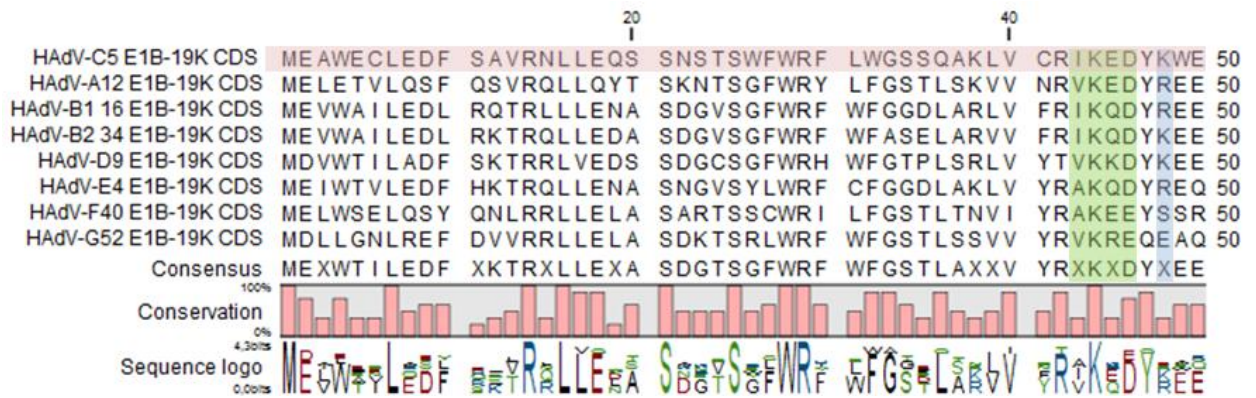


Figure 9: Amino acid alignment of E1B-19K from HAdV species A-G. Each HAdV species (A-G) is represented by one virus type (12, 16, 34, 5, 9, 4, 40, 52). The HAdV-C5 sequence is shown on top and is highlighted in pink. The SCM at lysine 44 shows a high degree of conservation among all virus types (green). The motif sequence differs between the virus types, but they all contain a complete SCM, which follows the consensus sequence ψ KxD/E. HAdV-C5 contains an additional SCM at lysine 48, which can also be found in type 34 and 9, however the lysine is not conserved among the other virus types (blue).

4.1.3 Analysis of E1B-19K SUMO2 modification in different transfection and infection experiments

To verify the initial observation of the SILAC experiment regarding E1B-19K SUMOylation, transfection and infection experiments were carried out in parental HeLa cells as well as HeLa SUMO2 cells (Tatham et al., 2009). Different plasmids encoding either untagged, N-terminally HA- or Flag-tagged E1B-19K were initially transfected in both HeLa cell lines to determine the most suitable antibody for Western Blot detection in further experiments (Figure 10).

Staining of untagged E1B-19K with an E1B-19K antibody showed a strong signal for the viral protein in the input probes as well as in the Ni^{2+} -NTA purifications (Figure 10, lanes 1-4). Staining of Flag-tagged E1B-19K with the Flag antibody (Figure 10, lanes 7 and 8) was comparable to the staining of untagged E1B-19K, while the HA-tagged protein detected with the HA antibody showed a very weak signal (Figure 10, lane 5 and 6). The His staining in the Ni^{2+} -NTA purifications confirmed the overexpression of 6His-tagged SUMO2 with a molecular weight of around 12 kDa in the HeLa SUMO2 cells, which was not detectable in the control parental HeLa cells, as expected. In the Ni^{2+} -NTA purifications, staining of E1B-19K revealed a single band (Figure 10, lanes 3, 4, 5, 7, 8) with a size corresponding to unmodified E1B-19K, which suggests that E1B-19K bound to the Ni^{2+} -NTA beads in a unspecific manner. Moreover, slower migrating bands, which would denote SUMOylated forms of E1B-19K, could not be detected in these experiments. The staining with the anti E1B-19K antibody (#490) allowed a stronger and more specific signal than the tag-specific antibodies, therefore it was chosen for the rest of the experiments in this work.

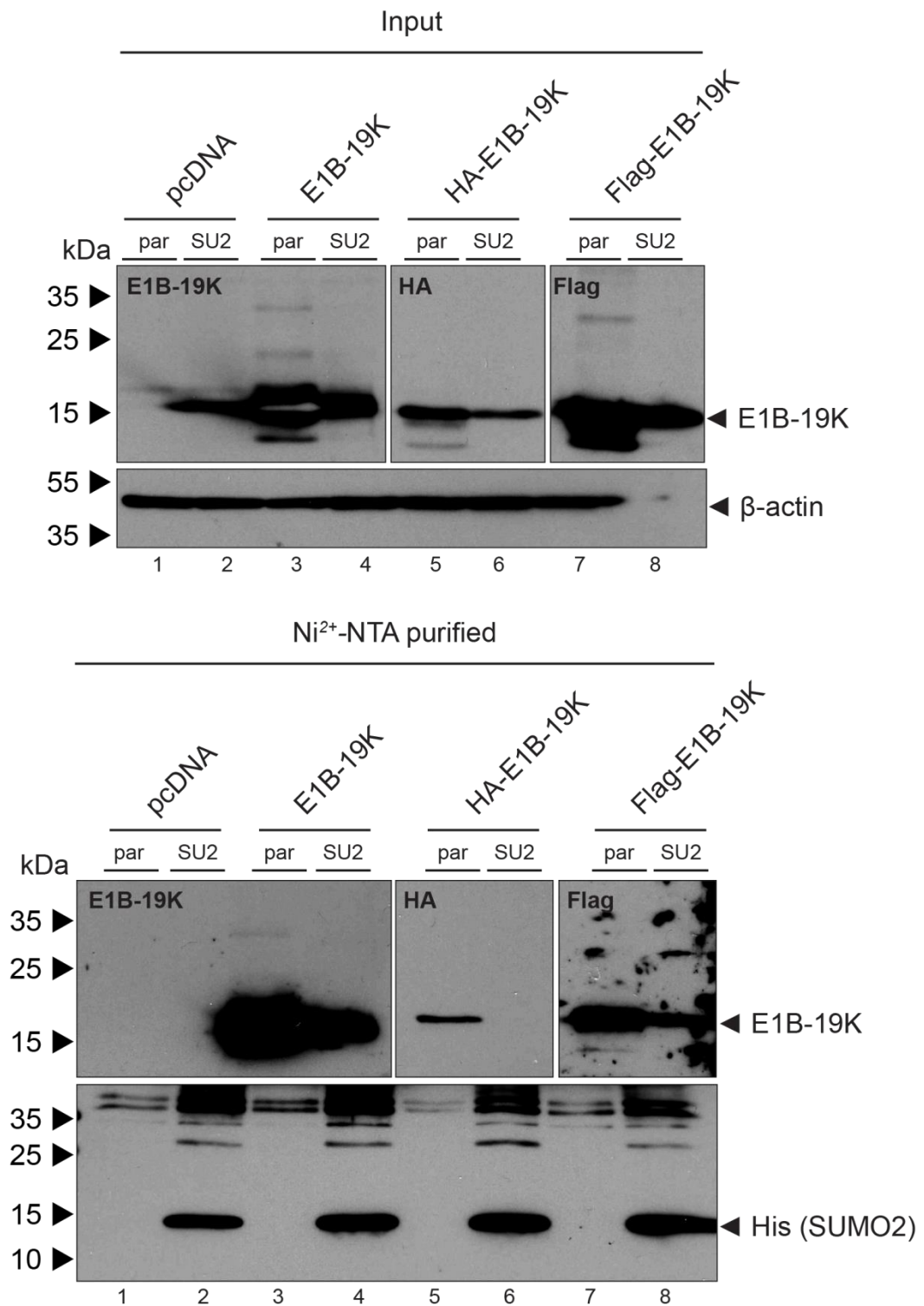


Figure 10: Analysis of HAdV-C5 E1B-19K SUMO2 modification during transient transfection. Subconfluent HeLa parental (par) and HeLa SUMO2 (SU2) cells were transiently transfected with 5 μ g of plasmids encoding either untagged E1B-19K (#2870), HA-tagged E1B-19K (#2869) or Flag-tagged E1B-19K (#2867) and harvested 48 h p. t. SUMOylated proteins were enriched by Ni²⁺-NTA purification, while the input probes were lysed in RIPA buffer. The proteins were resolved by SDS-PAGE and visualized via immunoblotting, using antibodies specific for E1B-19K (#490), HA-tag (#629), Flag-tag (#196), β -actin (#88) and His-tag (#551).

In addition to transfection experiments shown in Figure 10, parental HeLa cells as well as HeLa SUMO2 cells were infected with HAdV-C5 wt virus prior to protein analysis via immunoblotting

Results

(Figure 11). The infection with HAdV-C5 in this approach aimed to determine if other viral factors were needed for the SUMO2 modification of E1B-19K. In these experiments, E1B-19K could be detected in both, the input and the Ni²⁺-NTA purification, with an intense band corresponding to unmodified E1B-19K (Figure 11, lane 2 and 4). Unfortunately, slower migrating bands in the Ni²⁺-NTA purified HeLa SUMO2 cells could not be detected, which would have been indicative for SUMOylated forms of E1B-19K (Figure 11, lane 4).

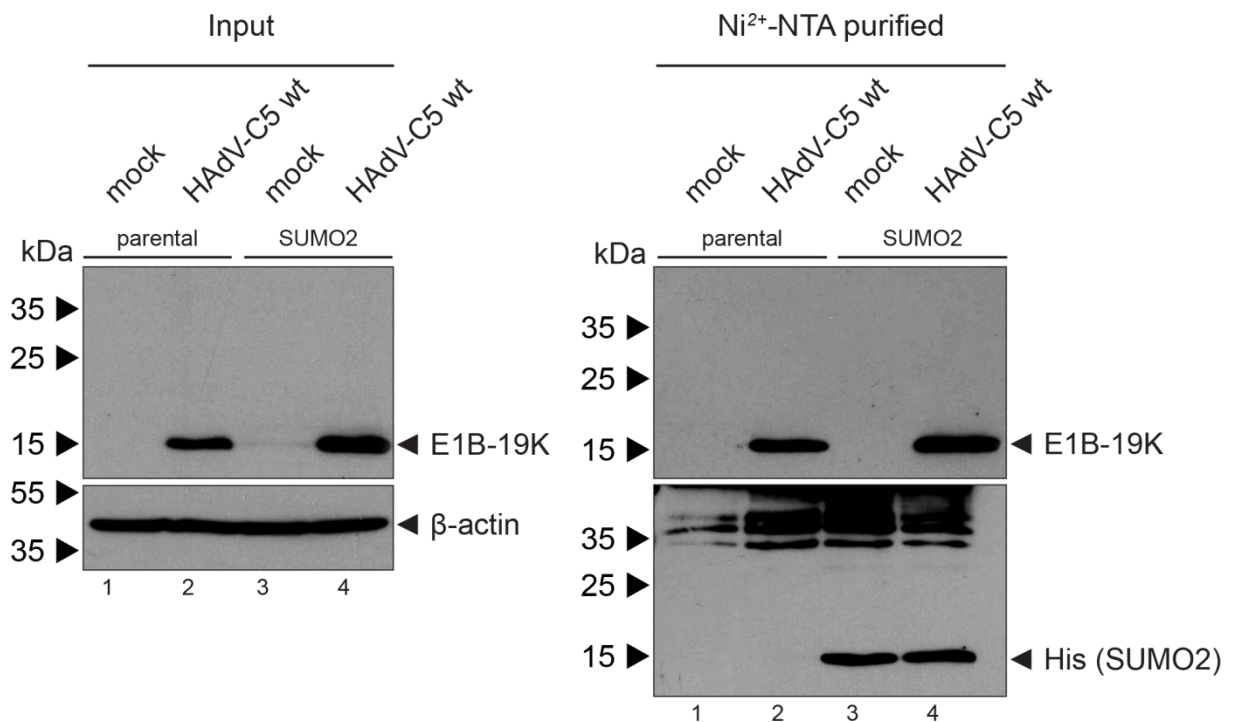


Figure 11: Analysis of HAdV-C5 E1B-19K SUMO2 modification during infection (48 h p. i.). Subconfluent HeLa parental and HeLa SUMO2 cells were infected with HAdV-C5 wt virus with an MOI of 10. At 48 h p. i., cells were harvested and SUMOylated proteins were enriched by Ni²⁺-NTA purification, while the input probes were lysed in RIPA buffer. The proteins were resolved by SDS-PAGE and visualized via immunoblotting using antibodies specific for E1B-19K (#490), β -actin (#88) and His-tag (#551).

Although the infection experiment was performed in similar conditions to the SILAC screening, no E1B-19K SUMOylation could be confirmed in neither transfection nor infection experiments. In order to rule out the possibility, that SUMOylation of E1B-19K was not detectable at that particular time point of infection, a time course experiment was performed with the aim to determine E1B-19K SUMOylation at different time points (Figure 12). Parental HeLa cells and HeLa SUMO2 cells were infected with HAdV-C5 wt virus and harvested at indicated time points, followed by protein analysis via immunoblotting. Increasing amounts of E1B-19K could be detected in the input of both cell lines, starting at 24 h p. i. in parental cells and 16 h p. i. in HeLa SUMO2 cells (Figure 12, lanes 5-7 and 9-12). In the Ni²⁺-NTA purified probes, E1B-19K was also detected in increasing amounts in both cell lines, but with the absence of slowly migrating bands corresponding to SUMOylated forms of E1B-19K, as observed in previous experiments (Figure 12, lanes 3-5 and 8-10).

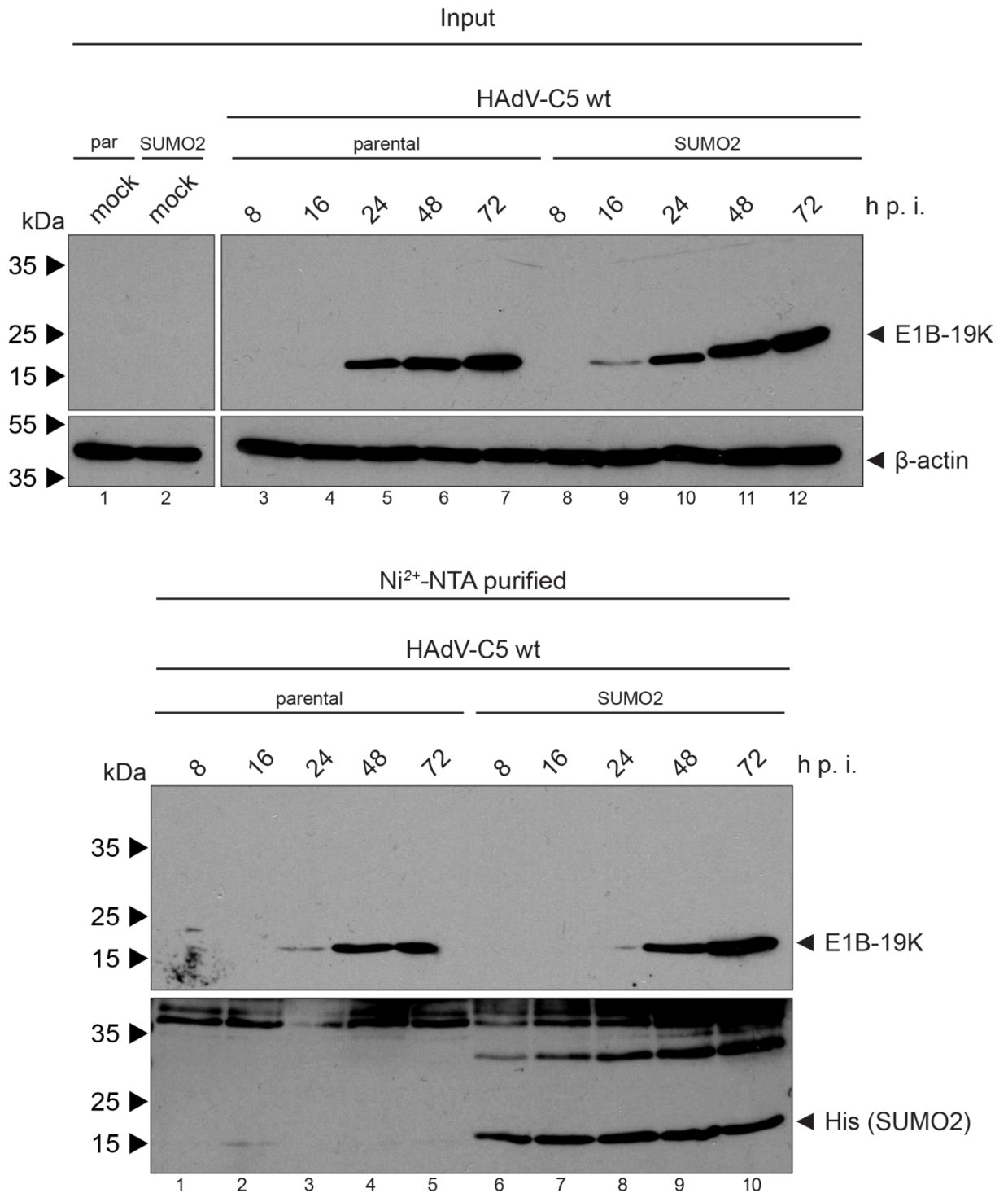


Figure 12: Time course analysis of E1B-19K SUMO2 modification during HAdV-C5 wt infection. Subconfluent HeLa parental (par) and HeLa SUMO2 cells were infected with HAdV-C5 wt virus with an MOI of 10. Cells were harvested at indicated time points (8, 16, 24, 48, 72 h p. i.) and SUMOylated proteins were enriched by Ni²⁺-NTA purification, while the input probes were lysed in RIPA buffer. The proteins were resolved by SDS-PAGE and visualized via immunoblotting, using antibodies specific for E1B-19K (#490), β-actin (#88) and His-tag (#551).

In order to exclude an influence of the utilized cell lines on the obtained results, we used HepaRG cells as an alternative cell line to confirm E1B-19K SUMOylation. HepaRG cells are derived from a hepatic carcinoma and have a pseudodiploid karyotype containing only two main chromosomal abnormalities (Gripon et al., 2002). Parental HepaRG cells, as well as HepaRG cells overexpressing

Results

6His-tagged SUMO1 or 2 (HepaRG SUMO1 or 2) were infected with HAdV-C5 wt virus and analyzed at 48 h p. i., comparable to the experiment shown in Figure 11. The adenoviral proteins E1B-19K and E2A could be detected with comparable signal strength among the different cell lines in the infected input probes (Figure 13, lanes 4-6). The His staining revealed free SUMO2 protein (Figure 13, lanes 3 and 6), but free SUMO1 was not detectable (Figure 13, lanes 2 and 5). This might be due to the fact, that in contrast to SUMO2/3 which can be found in large pools of unconjugated protein, free SUMO1 is hardly expressed (Golebiowski et al., 2009; Saitoh and Hinchev, 2000). Nevertheless, Ni²⁺-NTA purifications showed SUMO1 and SUMO2 modification of the adenoviral protein E2A, which served as a positive control. The infected parental HepaRGs showed a single band of around 70 kDa, which corresponds to unmodified E2A (Figure 13, lane 4). In contrast, infected HepaRG SUMO1 and SUMO2 showed slower migrating bands, which correspond to SUMO modified E2A (Figure 13, lanes 5 and 6). In this context, the presence of overexpressed 6His-tagged SUMO1 could be assumed even though it was not detectable in the input probes. Staining of E1B-19K in the Ni²⁺-NTA purifications resulted in a single band of around 15 kDa representing unmodified E1B-19K, as observed in previous experiments (Figure 13, lanes 4-6).

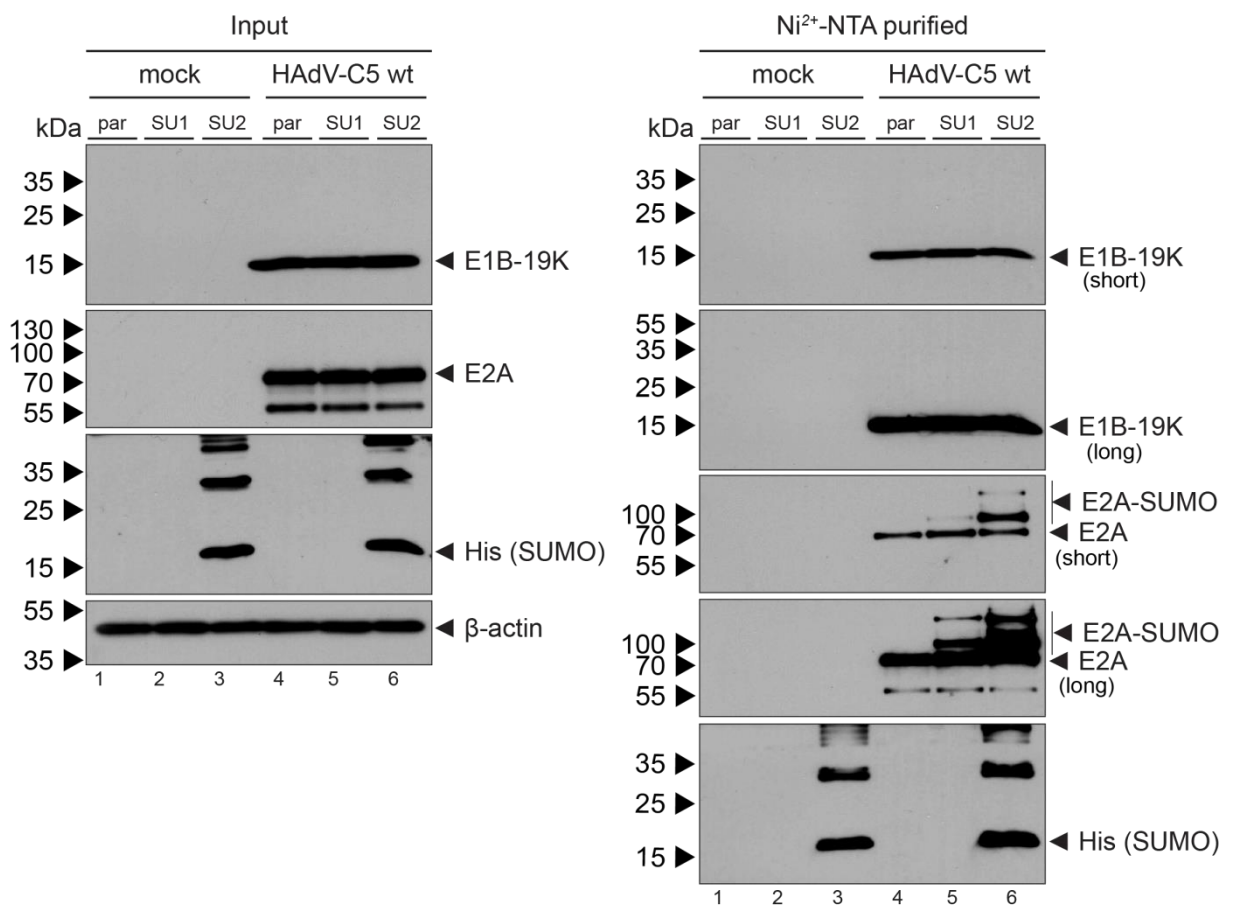


Figure 13: Analysis of E1B-19K SUMO modification in HepaRG SUMO1 and SUMO2. Subconfluent HepaRG parental (par) and HepaRG SUMO1 (SU1) or SUMO2 (SU2) cells were infected with HAdV-C5 wt virus with an MOI of 60. The cells were harvested at 48 h p. i. and SUMOylated proteins were enriched by Ni²⁺-NTA purification, while the input probes were

lysed in RIPA buffer. The proteins were resolved by SDS-PAGE and visualized via immunoblotting, using antibodies specific for E1B-19K (#490), β -actin (#88), His-tag (#551) and E2A (#113).

4.1.4 Alternative approaches to confirm E1B-19K SUMO2 modification

To rule out the possibility, that immunoblotting after enrichment of SUMO2 modified E1B-19K was not sensitive enough to detect its SUMO modification, experiments to increase the global SUMO conjugation of proteins, like overexpression of the SUMO E2 conjugating enzyme Ubc9 or induction of cellular stress via heat shock treatment, were performed. Ubc9 is the only known SUMO E2 conjugating enzyme and described to directly interact with SUMO substrates and various SUMO E3 ligases, hence catalyzing the formation of the isopeptide bond between the SUMO protein and the lysine residue of the acceptor protein (Geiss-Friedlander and Melchior, 2007; Hershko and Ciechanover, 1998; Johnson and Blobel, 1997; Rytinki et al., 2009). In order to increase SUMOylation of E1B-19K, plasmids encoding E1B-19K and Ubc9 were cotransfected in parental HeLa cells and HeLa SUMO2 cells. Overexpressed E1B-19K was detected in the input probes following transfection (Figure 14, lanes 2, 4, 6 and 8). Lanes 3, 4, 7 and 8 in Figure 14 showed high protein levels of overexpressed Ubc9, in contrast to weaker endogenous Ubc9 signals (Figure 14, lanes 1, 2, 5 and 6). However, even though Ubc9 was overexpressed in this experimental set-up, SUMO2 modified E1B-19K could not be detected in Ni^{2+} -NTA purified probes. Due to the weak E1B-19K signal in the purified fraction (Figure 14, lanes 6 and 8), the experiment was repeated but also increasing expression level of E1B-19K in the presence of overexpressed Ubc9 allowed no detection of SUMOylation.

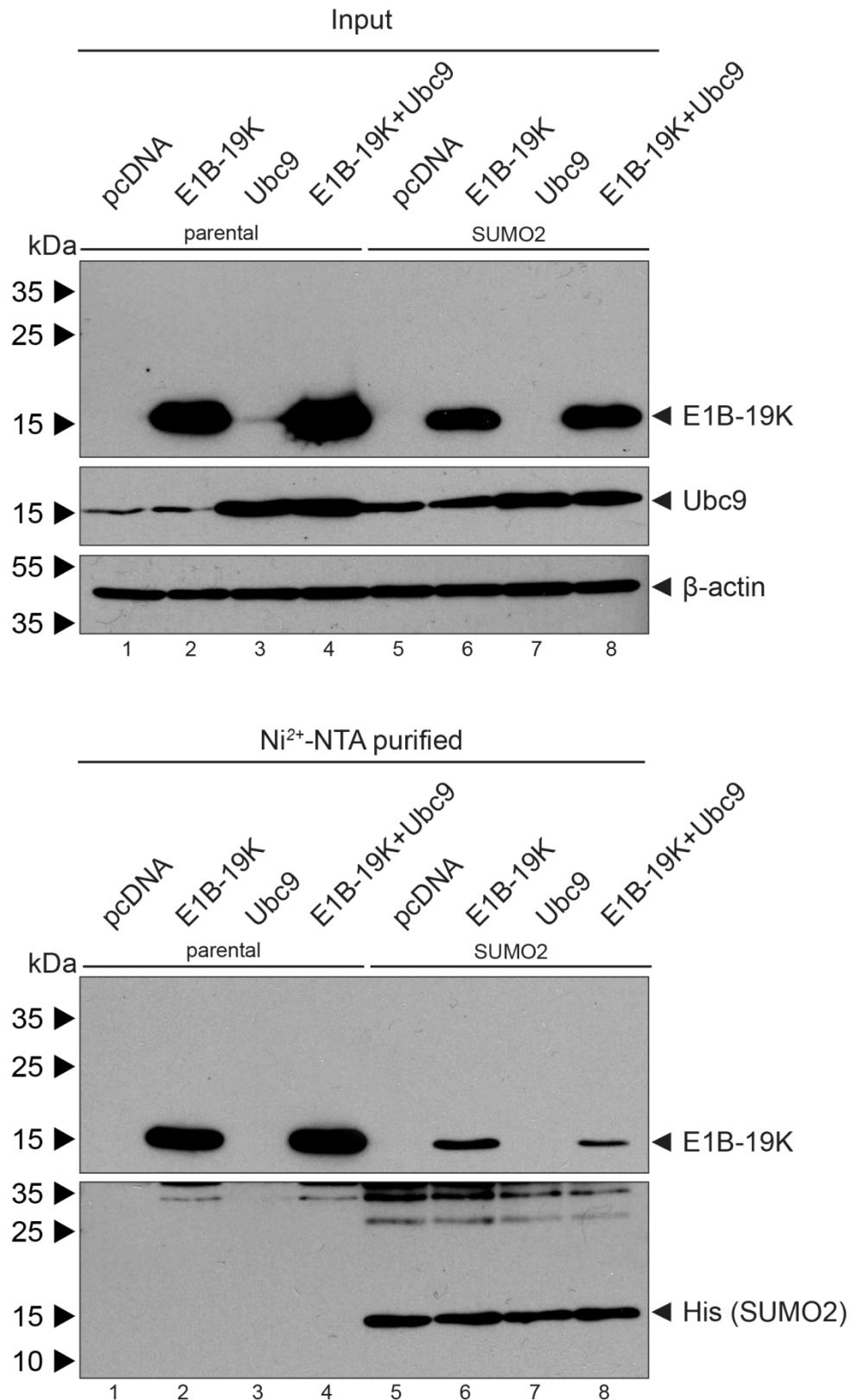


Figure 14: Analysis of E1B-19K SUMO2 modification in the presence overexpressed SUMO E2 conjugating enzyme Ubc9 during transient transfection. Subconfluent HeLa parental and HeLa SUMO2 cells were transiently transfected with 2 μ g of plasmid encoding for E1B-19K (#2870) and Ubc9 (#3019). The cells were harvested 48 h p. t. and SUMOylated proteins were enriched by Ni²⁺-NTA purification, while the input probes were lysed in RIPA buffer. The proteins were resolved by SDS-PAGE and visualized via immunoblotting, using antibodies specific for E1B-19K (#490), β -actin (#88), Ubc9 (#57) and His-tag (#551).

Results

In contrast to SUMO1, the SUMO isoforms 2 and 3 can be found in large free pools of unconjugated protein and have been shown to be intensively conjugated upon cell stress stimuli like temperature fluctuations or heat shock (Golebiowski et al., 2009; Saitoh and Hinchev, 2000). In order to induce SUMOylation of E1B-19K, parental HeLa cells and HeLa SUMO2 cells were infected with HAdV-C5 wt virus and heat shocked for 30 min at 42 °C prior to cell harvesting. Further, the infected cells were harvested 72 h p. i. in order to enrich the concentration of viral proteins. Staining of E1B-19K and E2A in the input probes showed strong expression of the viral proteins (Figure 15, lane 2 and 4). In the Ni²⁺-NTA purified probes slower migrating bands could be detected for E2A, indicating SUMO2 modification of E2A (Figure 15, lane 4). However, only unmodified E1B-19K could be stained with a band of around 15 kDa, hence, heat shock treatment did not increase the SUMOylation status of E1B-19K during infection (Figure 15, lane 2 and 4).

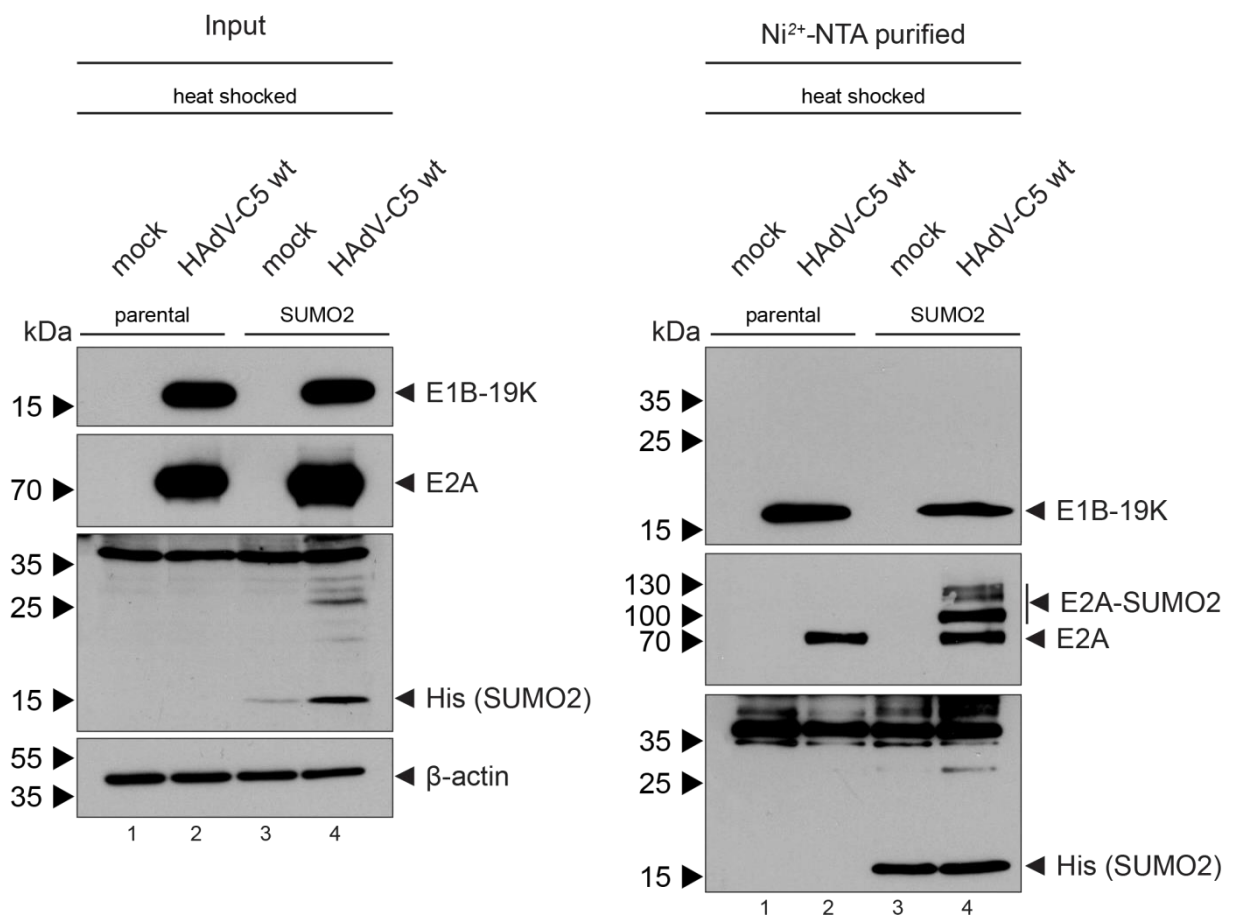


Figure 15: Analysis of E1B-19K SUMO2 modification of HAdV-C5 wt infected HeLa cells after heat shock treatment. Subconfluent parental HeLa cells and HeLa SUMO2 cells were infected with HAdV-C5 wt virus with an MOI of 10. The cells were harvested 72 h p. i. and SUMOylated proteins were enriched by Ni²⁺-NTA purification while the input probes were lysed in RIPA buffer. The proteins were resolved by SDS-PAGE and visualized via immunoblotting, using antibodies specific for E1B-19K (#490), β -actin (#88), His-tag (#551) and E2A (#113).

In addition to the infection experiment shown in Figure 15, a transfection approach was performed in parental HeLa cells and HeLa SUMO2 cells, which were cotransfected with plasmids encoding for

Results

E1B-19K and Ubc9 and additionally heat shocked for 30 min at 42 °C prior to cell harvesting. As a positive control for SUMO2 modification, E1B-55K was transfected in this experimental approach. The input probes showed overexpression of E1B-19K (Figure 16, lanes 4, 5, 8 and 10) and E1B-55K (Figure 16, lanes 2, 3, 7 and 8) upon transient transfection. However, the input levels of Ubc9 are nearly comparable among all probes despite of Ubc9 transfection in lane 3, 5, 8 and 10. E1B-55K staining of the Ni²⁺-NTA purification revealed a strong signal of slower migrating bands in lane 7 and 8 but not in the parental HeLa cells in lanes 2 and 3, indicating intense SUMO2 modification of E1B-55K. The comparable levels of Ubc9 in all probes might explain that the portion of E1B-55K SUMO2 modification was comparable in lanes 7 and 8. Nevertheless, the heat shock treatment did not result in SUMO2 modification of E1B-19K (Figure 16, lane 9 and 10), similar to what was observed in the infection experiment (Figure 15).

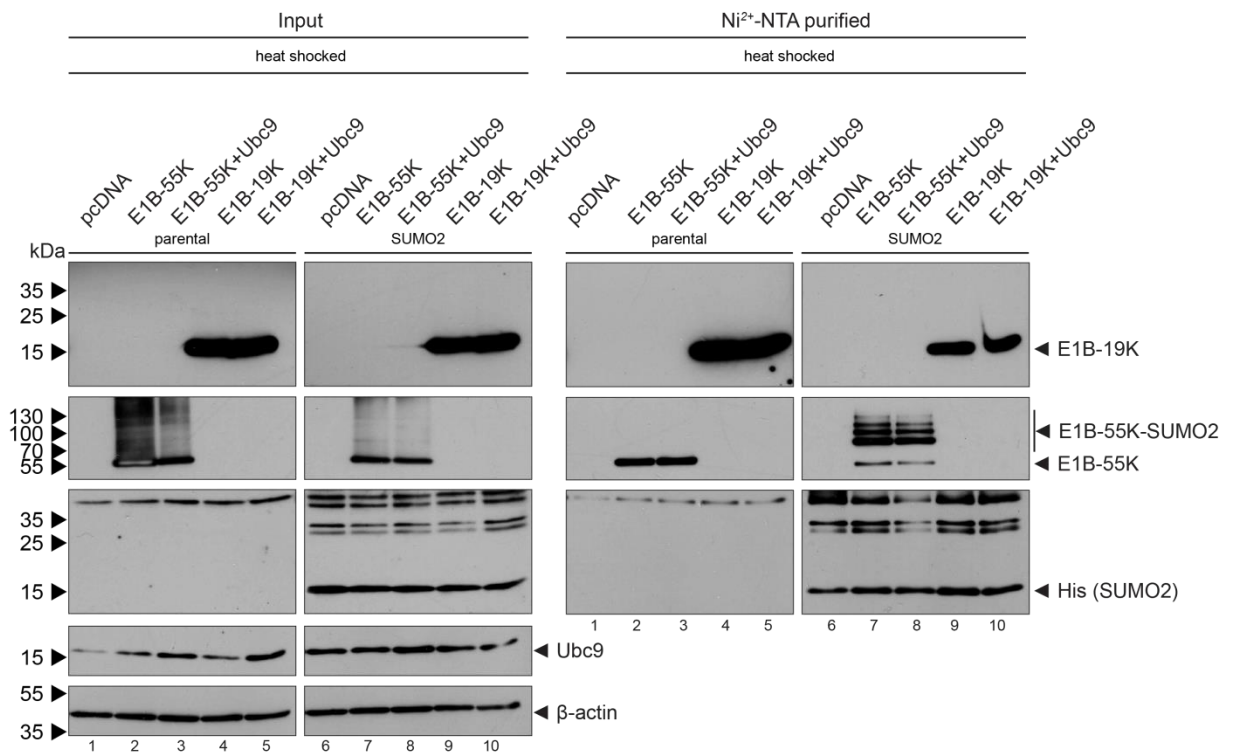


Figure 16: Analysis of E1B-19K SUMO2 modification in the presence of overexpressed SUMO E2 conjugating enzyme Ubc9 combined with heat shock treatment during transient transfection. Subconfluent HeLa SUMO2 cells were transiently transfected with 4 µg of plasmid encoding for E1B-19K (#2870), 5 µg plasmid encoding for E1B-55K (#1319) and 10 µg plasmid encoding for Ubc9 (#3019). Heat shock treated cells were incubated for 30 min at 42 °C prior to cell harvest. All cells were harvested 48 h p. t. SUMOylated proteins were enriched by Ni²⁺-NTA purification, while the input probes were lysed in RIPA buffer. The proteins were resolved by SDS-PAGE and visualized via immunoblotting, using antibodies specific for E1B-19K (#490), E1B-55K (#1), Ubc9 (#57), β-actin (#88) and His-tag (#551).

4.1.5 Nuclear targeting of E1B-19K via Gal4 fusion to enhance its SUMOylation

As a final approach to confirm the results of the SILAC experiment, E1B-19K was fused to the DNA binding domain of the Gal4 transcription factor from the yeast *Saccharomyces cerevisiae*. This domain contains a nuclear localization signal (NLS) in the first 147 N-terminal aa, which was shown to recruit proteins to the nucleus (Silver et al., 1984). The enzymes required for SUMO modification are more abundant in the nucleus than in the cytoplasm, therefore, SUMOylation levels of E1B-19K could be increased by forcing its nuclear localization (Geiss-Friedlander and Melchior, 2007; Melchior et al., 2003). Overexpression of the protein fusion Gal4-E1B-19K was confirmed by the detection of the predicted band at 35 kDa in the input probes (Figure 17, lanes 3 and 6). Besides, a band at 19 kDa was detected in the same probes, corresponding to non-fused E1B-19K (Figure 17, lanes 3 and 6). This was likely due to an internal start codon, which was not removed during the generation of the fusion construct. Along this line, unfused E1B-19K and the Gal4-E1B-19K fusion were detected in the Ni²⁺-NTA purified probes of parental HeLa cells, (Figure 17, lane 3). However, as expected, no slow migrating bands were present. Interestingly, Ni²⁺-NTA purified probes of HeLa SUMO2 cells did show slower migrating bands in the lane corresponding to the Gal4-E1B-19K fusion protein (Figure 17, lane 6). These results point to SUMO2 modification of the protein fusion Gal4-E1B-19K.

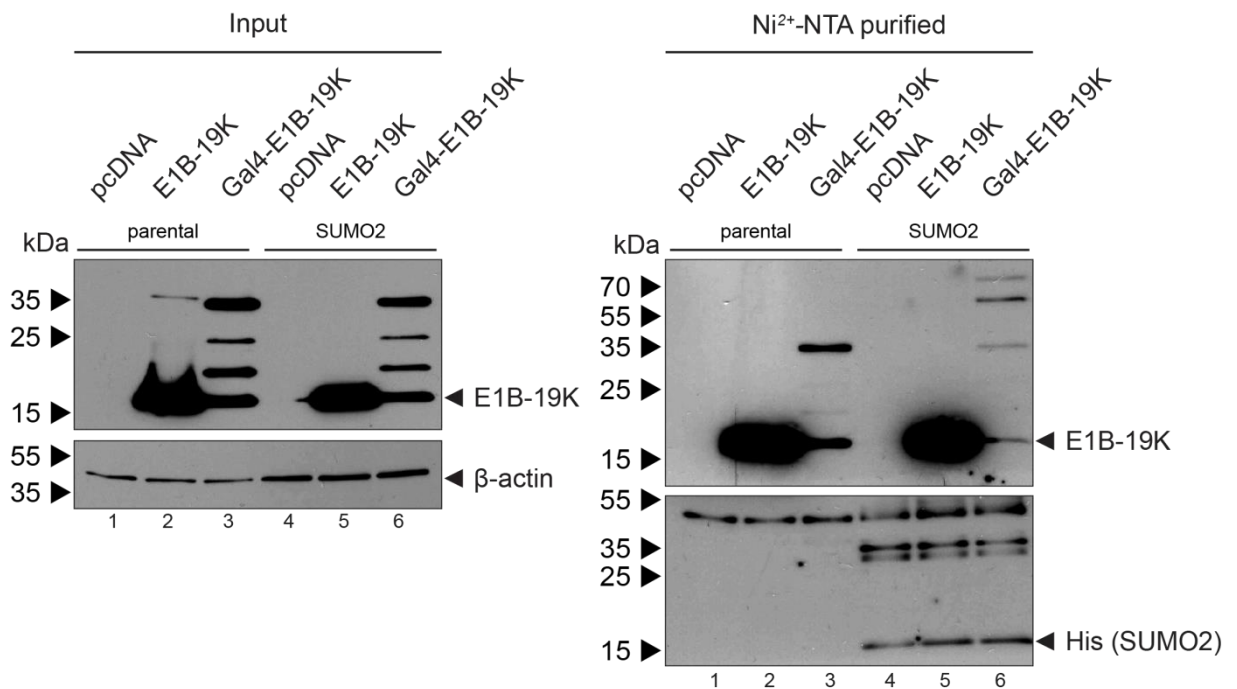


Figure 17: Analysis of the SUMO2 modification of the Gal4-E1B-19K fusion protein. Subconfluent parental HeLa cells and HeLa SUMO2 cells were transiently transfected with 4 μg of plasmid encoding for E1B-19K (#2870), 5 μg plasmid encoding for a Gal4-E1B-19K fusion protein (#3084). Cells were harvested 48 h p. t. SUMOylated proteins were enriched

by Ni²⁺-NTA purification while the input probes were lysed in RIPA buffer. The proteins were resolved by SDS-PAGE and visualized via immunoblotting, using antibodies specific for E1B-19K (#490), β -actin (#88) and His-tag (#551).

In order to elucidate, if the putative SUMOylation of the fusion protein Gal4-E1B-19K was specific to E1B-19K, the aa sequence of the Gal4 domain was analyzed in terms of internal SCMs. *In silico* analysis of the Gal4 region (aa 1-147) revealed a potential SCM at lysine 82 (LKMD), which agrees the classical consensus motif for SUMO conjugation, ψ KxD/E (Rodriguez et al., 2001). Therefore, we could not rule out the possibility that SUMO2 modification of the fusion protein was due SUMOylation of the Gal4 region instead of being specific to nuclear located E1B-19K. To further investigate this observation, one either has to remove the lysine of the Gal4 SCM or fuse E1B-19K to alternative nuclear targeting sequences to determine the specificity of SUMO2 modification.

4.2 Characterization of potential E1B-19K SUMO mutants

4.2.1 Subcellular localization analysis of E1B-19K SUMO mutants

SUMO modification was shown to modulate the stability of its substrate proteins by different means. SUMO-induced masking of the modified lysine can enhance protein stability by preventing poly-ubiquitination and subsequent proteasomal degradation (Bae et al., 2004). However, poly-SUMO chains are recognized by *SUMO targeted ubiquitin ligases* (STUbL), which target SUMOylated proteins for proteasomal degradation by attachment of poly-ubiquitin chains (Perry et al., 2008; Sriramachandran and Dohmen, 2014). Moreover, SUMO modification is described to influence the localization of their target proteins and thus modifies various intracellular processes (Flotho and Melchior, 2013; Hay, 2005; Kerscher, 2007).

The results of the SILAC experiment, which showed E1B-19K SUMOylation for the first time, were strongly supported by *in silico* analysis of the E1B-19K protein in which two potential SCMs were found. One SCM was detected at lysine 44, which was highly conserved among prototypes of all human adenovirus species. The second SCM, which was less conserved among species, was found at lysine 48 in species C and D (Figure 9). In order to characterize the biological relevance of the potential SCMs on E1B-19K protein function, mutant proteins were generated by site-directed mutagenesis, substituting the lysines in these motifs by arginines. In this way, plasmids encoding either E1B-19K K44R, K48R or the corresponding K44/48R double mutant, as well as a mutant virus carrying the E1B-19K K44R mutant were generated. Transient transfection of these plasmids in H1299 cells showed equal expression levels of E1B-19K (Figure 18, lane 2) and its respective SUMO mutants (Figure 18, lane 3-5).

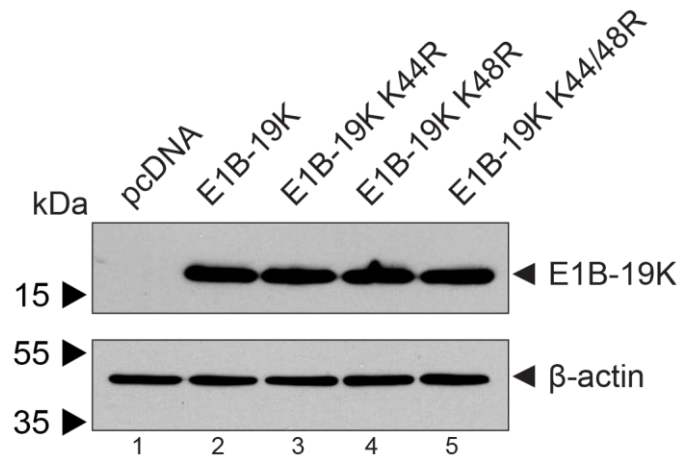


Figure 18: E1B-19K wt and potential SUMO mutants are expressed at similar levels in H1299 cells. Subconfluent H1299 cells were transiently transfected with 4 μ g of plasmid encoding for E1B-19K (#2870) or potential SUMO mutants of E1B-19K containing lysine to arginine substitutions at position 44 (#2874), 48 (#2875) and the double mutant at positions 44 and 48 (#2876). Cells were harvested 48 h p. t. and lysed in RIPA buffer. The proteins were resolved by SDS-PAGE and visualized via immunoblotting, using antibodies specific for E1B-19K (#490) and β -actin (#88).

In order to analyze, if the SCMs of E1B-19K are involved in the regulation of its subcellular localization, immunofluorescence experiments were performed in H1299 cells after transfection with either E1B-19K wt or the SUMO mutants K44R, K48R and K44/48R double mutant. Figure 19 shows E1B-19K wt associated with nuclear membrane structures as well as in intermediate cytosolic filaments and probably membranes of the endoplasmatic reticulum, as described in the literature (Figure 19, e and f) (Persson et al., 1982; Rao et al., 1997; White and Cipriani, 1990; White et al., 1984). All E1B-19K SUMO mutants showed a subcellular localization comparable to the wt protein (Figure 19 K44R h and i; K48R k and l; K44/48R n and o). These observations suggest that the SCMs at lysine 44 and 48 are not involved in the regulation of E1B-19K subcellular localization.

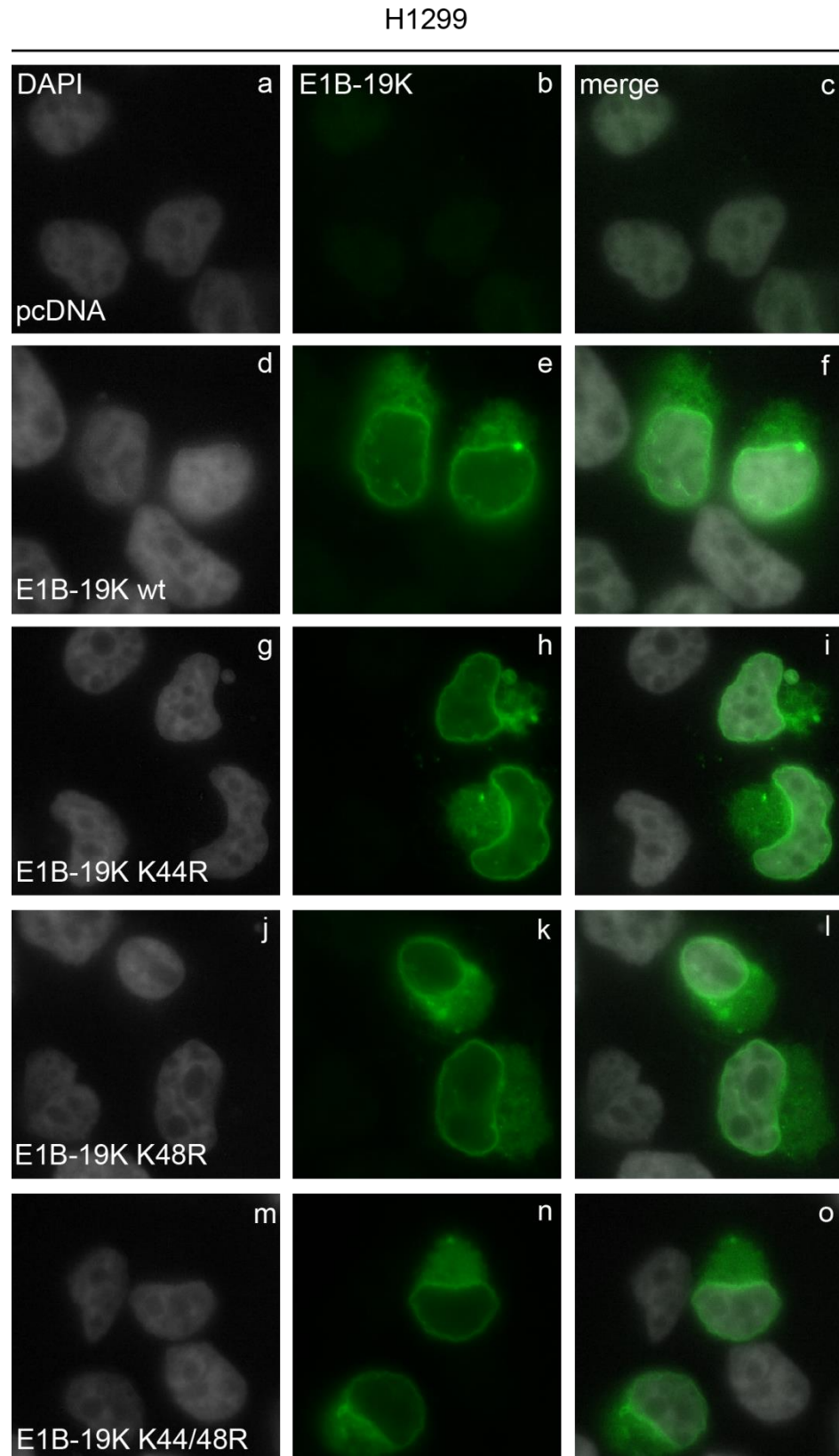


Figure 19: E1B-19K wt and SUMO mutants K44R, K48R and K44/48R localize predominantly in the nuclear lamina and cytosolic filaments. Subconfluent H1299 cells were transiently transfected with 1 μ g plasmid DNA encoding for either E1B-19K wt (#2870, d-f), E1B-19K K44R (#2874, g-i), E1B-19K K48R (#2875, j-l), E1B-19K K44/48R (#2876, m-o) or the empty vector control pcDNA (#136, a-c). The cells were fixed in 4 % PFA 48 h p. t. and the target proteins were visualized with an E1B-19K specific antibody (#490), shown in green, while chromatin was stained with DAPI (grey).

4.2.2 Mutation of potential SCM increases the transforming properties of E1B-19K in primary baby rat kidney (pBRK) cells

Adenoviruses were the first human-pathogenic viruses discovered to be oncogenic and being able to induce malignant tumors when inoculated in newborn rodents (Trentin et al., 1962). Further research showed that the E1A and E1B-regions from various HAdV types are sufficient to induce transformation of primary rodents cells *in vitro* (Endter and Dobner, 2004). Even though HAdVs have not been proven yet to be a causative agent of human cancer development, infiltrating lymphocytes of human sarcomas were found to contain adenoviral genomes (Kosulin et al., 2013). Additionally, there is strong evidence that adenoviral gene products encoded by the E1A and E1B region are able to transform primary human cells *in vitro* pointing to a contribution of adenoviral oncogenes to human carcinogenesis (Speiseder et al., 2017).

During transformation, E1A alone induces cell cycle progression of transfected cells, as well as apoptosis. Complete transformation of primary cells requires the coexpression of E1B-gene products, which repress the E1A-mediated onset of apoptosis by p53-dependent and -independent mechanisms (Debbas and White, 1993; Endter and Dobner, 2004; Gallimore and Turnell, 2001; Querido et al., 1997a). Moreover, SUMOylation of E1B-55K is known to regulate its transforming capacity (Endter et al., 2001). Besides, a publication by White et al. showed that substitution of E1B-19K lysine 44 to glutamic acid dramatically reduces its ability to inhibit TNF α -mediated apoptosis, which is related to a strong decrease of its transforming potential (White et al., 1992). Based on these grounds, we aimed to elucidate whether the transforming potential of E1B-19K could be altered through mutation of its putative SCMs. By using site-directed mutagenesis and plasmids containing the whole E1-gene region (E1A, E1B-55K and E1B-19K) mutations in lysine 44 and 48 of E1B-19K were introduced. The same mutations were introduced into expression plasmids that only encode E1A and E1B-19K in order to determine the transforming potential of E1B-19K in the absence of E1B-55K. For the transformation assay, pBRK cells were transiently transfected with expression vectors encoding either E1A alone or the whole HAdV-C5 E1-gene region containing either E1B-19K wt or its mutant versions with single mutations in lysines 44 and 48, or the double mutant 44/48. After incubation for eight weeks, cells were fixed and stained in order to analyze the number of *foci* formation (Figure 20). Panel A illustrates one representative dish of each condition whereas panel B shows the quantification of *foci* formation in absolute numbers. Mutation of the SCM at lysine 44 showed a significant increase of *foci* formation in the background of the wt E1-gene region, while the mutation of only lysine 48 or the double mutant 44/48 had no effect on transformation. However, in the absence of E1B-55K, all mutant forms of E1B-19K led to a significant increase of *foci* formation when compared to E1B-19K wt, contrary to the literature,

Results

which claimed that an aa exchange at lysine 44 to glutamic acid is a loss of function mutation for the transforming capacities of E1B-19K (White et al., 1992). This indicates that the lysines of E1B-19Ks potential SCMs at position 44 and 48 might be involved in the regulation of its transforming properties.

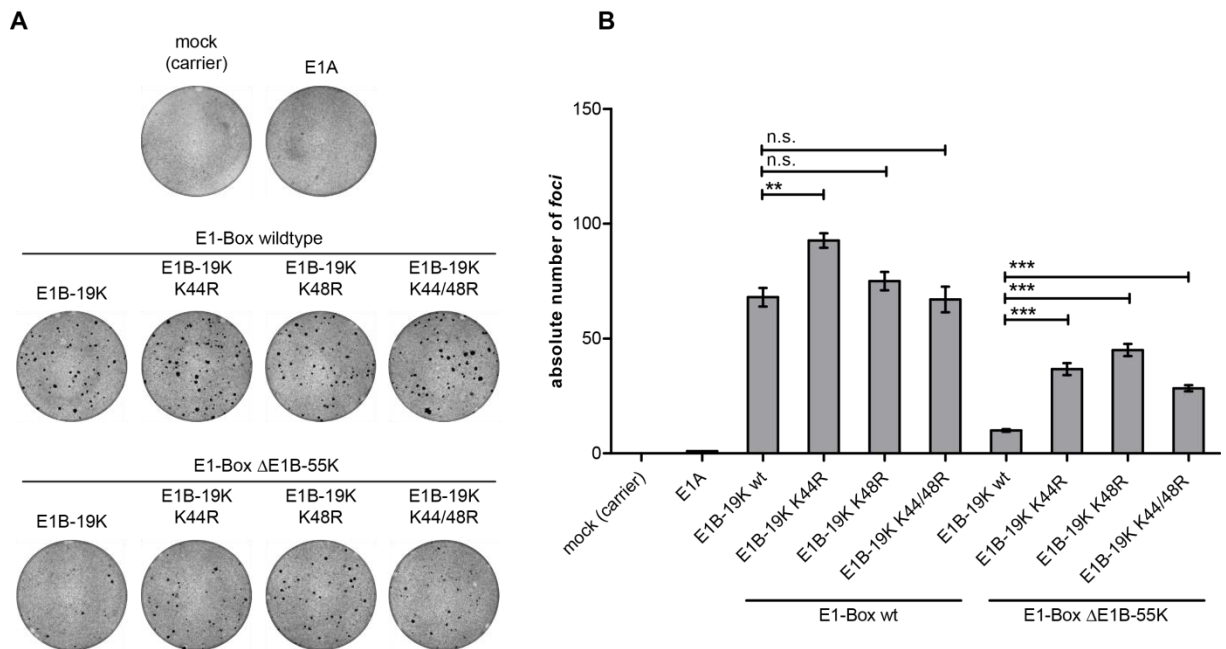


Figure 20: The mutation of potential SCMs in E1B-19K increases its transforming potential. pBRK cells were transfected with plasmids encoding E1A (#737), the E1-Box wt (#1235) or the E1-Box, which lacks E1B-55K (#1680). The E1-Boxes either contained E1B-19K wt or its respective potential SUMO mutants K44R, K48R or K44/48R. Each condition of the experiment was tested in technical triplicates. The cells were propagated for eight weeks, followed by fixation in an aqueous solution containing 25 % MeOH and 1 % crystal violet. Transformed pBRK cells growing in distinct *foci* were visualized and counted. **A:** Representative cell culture dish of each condition upon fixation and staining of the *foci*. **B:** Bar diagram of *foci* quantification in absolute numbers.

4.2.3 Analysis of the impact of the E1B-19K K44R mutation during viral protein expression and viral growth

The findings of the previous experiment demonstrated that removal of lysine 44 leads to an increased transforming potential of E1B-19K. In order to determine, if this gain of function has an effect during virus infection, a HAdV-C5 virus mutant carrying the K44R mutation on E1B-19K was generated. In the next experiment, H1299 cells were either infected with HAdV-C5 wt or the E1B-19K K44R mutant virus and the expression of viral proteins was determined at different time points and compared between the two virus strains (Figure 21). Overall, the viral protein expression seemed to be largely unaffected in the mutant virus, when compared to HAdV-C5 wt. Early viral proteins E1A and E2A could be detected 16 h p. i. in both infections. E1B-19K expression started 24 h p. i. and increased over time to similar concentrations irrespective of the K44R mutation, assuming that the loss of the putative SCM has no effect on protein stability. As described in 4.2.1,

Results

SUMO modification can either increase protein stability or recruit STUbL proteins, which target SUMO substrates for proteasomal degradation. However, this did not seem to be the case for E1B-19K since the wt form and the mutant were equally expressed over time. E1B-55K as well as E4orf6 seemed to be expressed slightly delayed in the K44R mutant virus infection; however, this delay had no effect on MRE11 degradation, which is mediated by the viral ubiquitin E3 ligase complex composed of E1B-55K and E4orf6. In contrast, capsid proteins could be detected earlier in the mutant virus infection, starting to be expressed already at 24 h p. i. (Figure 21, lane 9 and 10). In summary, the levels of viral proteins did not differ significantly between the infections with the two virus strains.

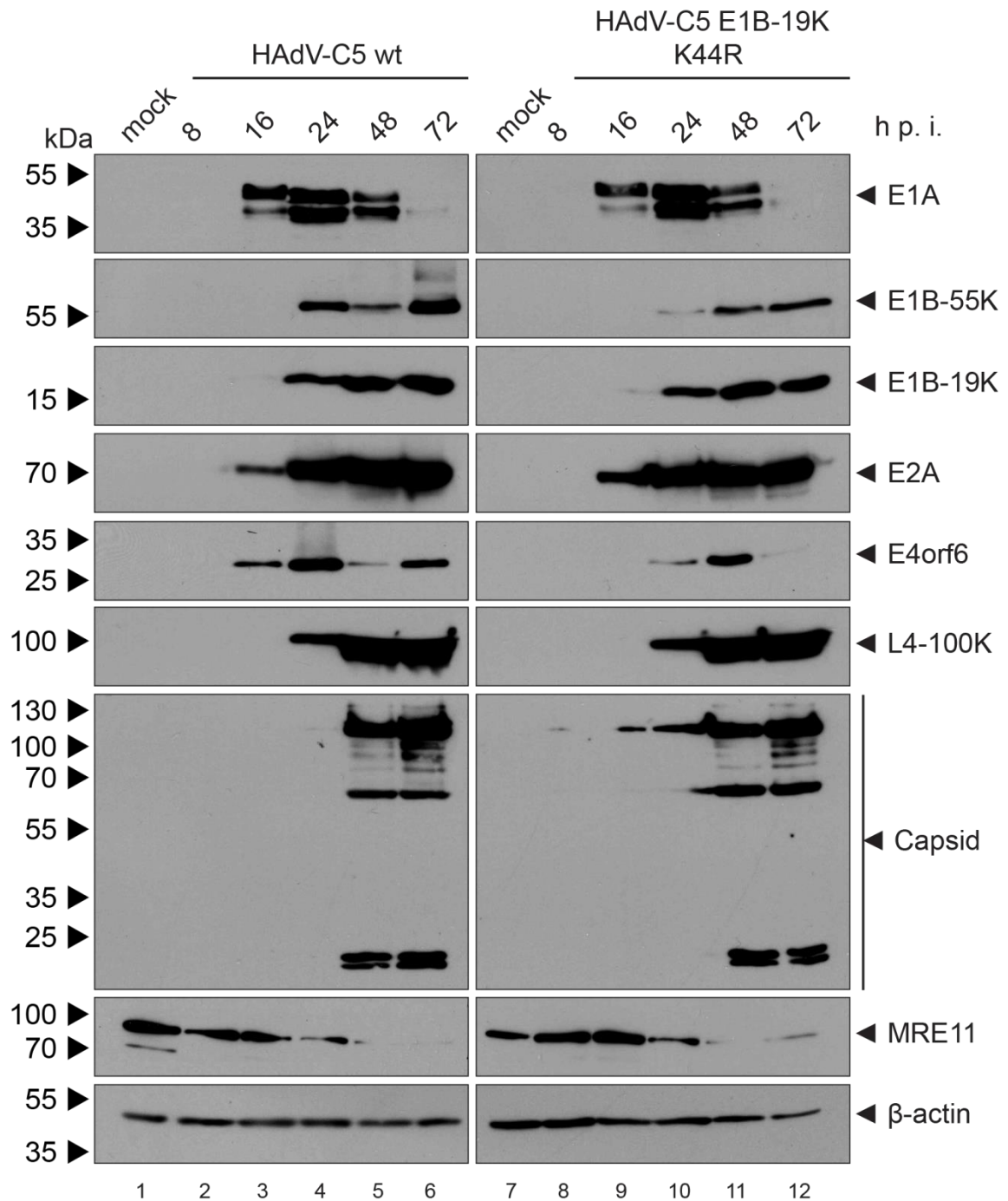


Figure 21: Mutation of lysine 44 within E1B-19K has no effect on virus protein expression. Subconfluent H1299 cells were infected with either HAdV-C5 wt virus or E1B-19K K44R mutant virus with an MOI of 20. The cells were harvested at indicated time points (8, 16, 24, 48 and 72 h p. i.) and lysed in RIPA buffer. The proteins were resolved by SDS-PAGE and visualized via immunoblotting, using antibodies specific for E1A (#131), E1B-55K (#1), E1B-19K (#490) E2A (#113), E4orf6 (#94), L4-100K (#275), Capsid proteins (#452), MRE11 (#477) and β-actin (#88).

In addition to protein expression analysis (Figure 21), the production of newly synthesized infectious particles was determined over 72 h in order to further reveal the effect of the E1B-19K K44R mutation on viral growth (Figure 22). Therefore, HepaRG cells were infected with either HAdV-C5 wt virus or E1B-19K K44R mutant virus and harvested at 24, 48 and 72 h p. i. Titration of newly synthesized virus particles showed no significant difference in viral progeny production

between the wt and the mutant virus at 24 and 48 h p. i. However, after 72 h there is a slight tendency of increased viral progeny production in the mutant virus (Figure 22). In summary, the mutation of the putative SCM at lysine 44 has no effect on viral protein expression and virus progeny production.

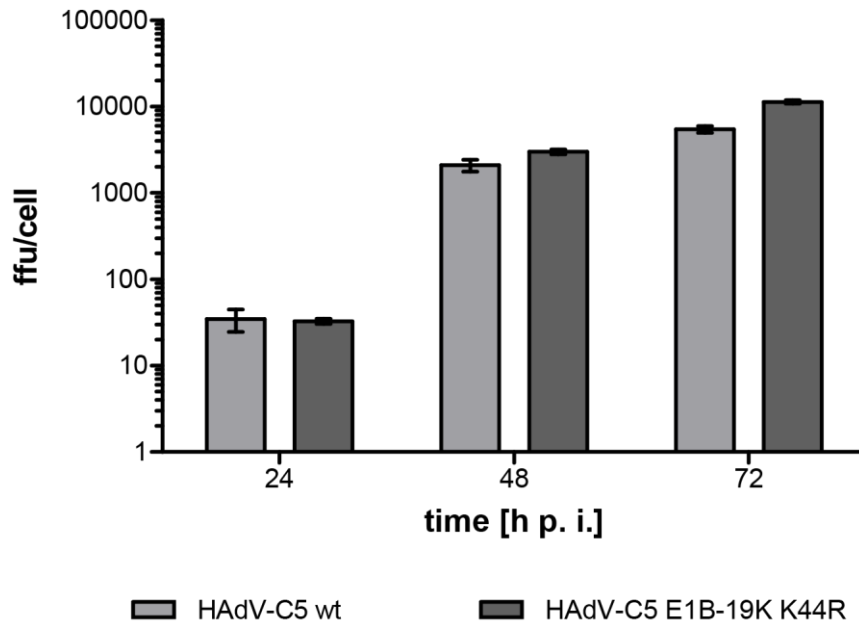


Figure 22: Viral progeny production is slightly enhanced in E1B-19K K44R mutant virus infection in comparison to HAdV-C5 wt virus infection in HepaRG cells. HepaRG cells were infected with either HAdV-C5 wt virus or E1B-19K K44R mutant virus with an MOI of 25 and harvested 24, 48 and 72 h p. i. Infected cells were lysed by three freeze and thaw cycles and HEK 293 cells were reinfected with the virus progeny for titration. Infected HEK 293 cells were visualized by immunofluorescence, using an antibody against E2A (#113), for determination of the virus yield. The experiment was performed in three technical replicates.

4.2.4 Analysis of the subcellular localization of the putative E1B-19K SUMO mutant K44R during infection

As already previously described, SUMO modification often affects the subcellular localization of the modified substrate. Mutation of all potential SCMs did not alter the localization of E1B-19K in transfection experiments (Figure 19). To analyze the importance of lysine 44 for the subcellular localization of E1B-19K during adenoviral infection, H1299 cells were infected with HAdV-C5 wt virus or the E1B-19K K44R mutant virus and analyzed with a Leica DMI 600B microscope. As observed during transfection, E1B-19K associates with nuclear membrane structures as well as with intermediate cytosolic filaments independent of the K44R mutation, suggesting that potential SUMO modification of this particular lysine does not change the typical localization of E1B-19K during infection.

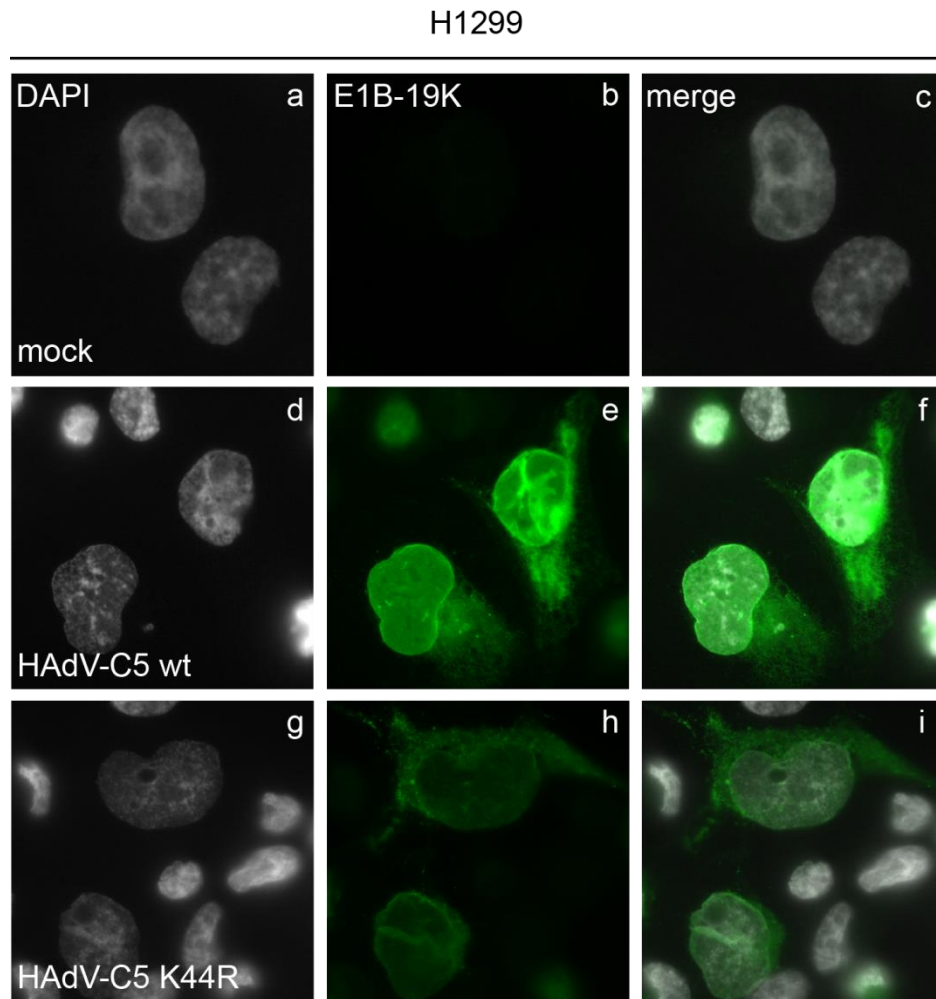


Figure 23: E1B-19K wt and the potential SUMO mutant K44R localize predominantly in the nuclear lamina and cytosolic filaments of infected H1299 cells. Subconfluent H1299 cells were infected with either HAdV-C5 wt virus (d-f) or the E1B-19K K44R mutant virus (g-i) with an MOI of 30. The cells were fixed in 4 % PFA 24 h p. i. and the target protein was visualized with an E1B-19K specific antibody (#490), shown in green, while chromatin was stained with DAPI (grey).

4.3 The role of PIAS4 as a transcriptional regulator of early adenoviral gene products

4.3.1 PIAS4 decreases the steady state level concentration of HAdV-C5 E1B-55K in transient transfection

HAdV-C5 E1B-55K (from here on referred to as E1B-55K) is a multifunctional protein expressed early during adenoviral infection that promotes viral replication and E1-mediated transformation of primary cells. Its pro-viral and oncogenic properties are mediated through an array of functions, which mainly counteract the host intrinsic immune response. In this context, the posttranslational modification (PTM) with *small ubiquitin related modifier* (SUMO) was shown to regulate many of the key functions of E1B-55K. However, little is known about how SUMOylation of this viral protein

is regulated. SUMO E3 ligases mediate the last step of SUMOylation, stabilizing the complex of SUMO-loaded E2 and the substrate protein, and thus accelerating the transfer of SUMO to the substrate (Rytinki et al., 2009). PIAS proteins are potent transcriptional regulators and are described as the largest class of SUMO E3 ligases, involved in the SUMO modification of a vast number of different proteins (Bischof et al., 2006; Liu et al., 2005; Rytinki et al., 2009). In order to elucidate, if one of the PIAS proteins could be the E1B-55K SUMO E3 ligase, regulating its SUMO modification, plasmids encoding different PIAS proteins and E1B-55K were cotransfected in parental HeLa and HeLa SUMO2 cells. Following Ni²⁺-NTA purification, E1B-55K SUMOylation was assayed in the presence of the different PIAS proteins by Western Blot, and compared to empty vector transfection. When cotransfected with the empty vector, E1B-55K SUMOylation could be detected in HeLa SUMO2 cells, as previously described (Figure 24, lane 9). However, the levels of SUMOylated E1B-55K were not altered by overexpression of PIAS1, PIAS2 α and PIAS2 β , although the latter could not be detected in this experiment (Figure 24, lanes 10-14), indicating that these PIAS isoforms are not E1B-55K SUMO E3 ligases. Interestingly, the input levels of E1B-55K were remarkably reduced in the presence of both mouse (mPIAS4) and human PIAS4 (PIAS4) (Figure 24, lanes 11 and 14). As a consequence, SUMOylated E1B-55K could not be detected in the Ni²⁺-NTA purified probes in the presence of both PIAS4 species. The repressive effect seemed to be higher in HeLa SUMO2 cells, although an effect of transfection efficiency between cell lines cannot be ruled out.

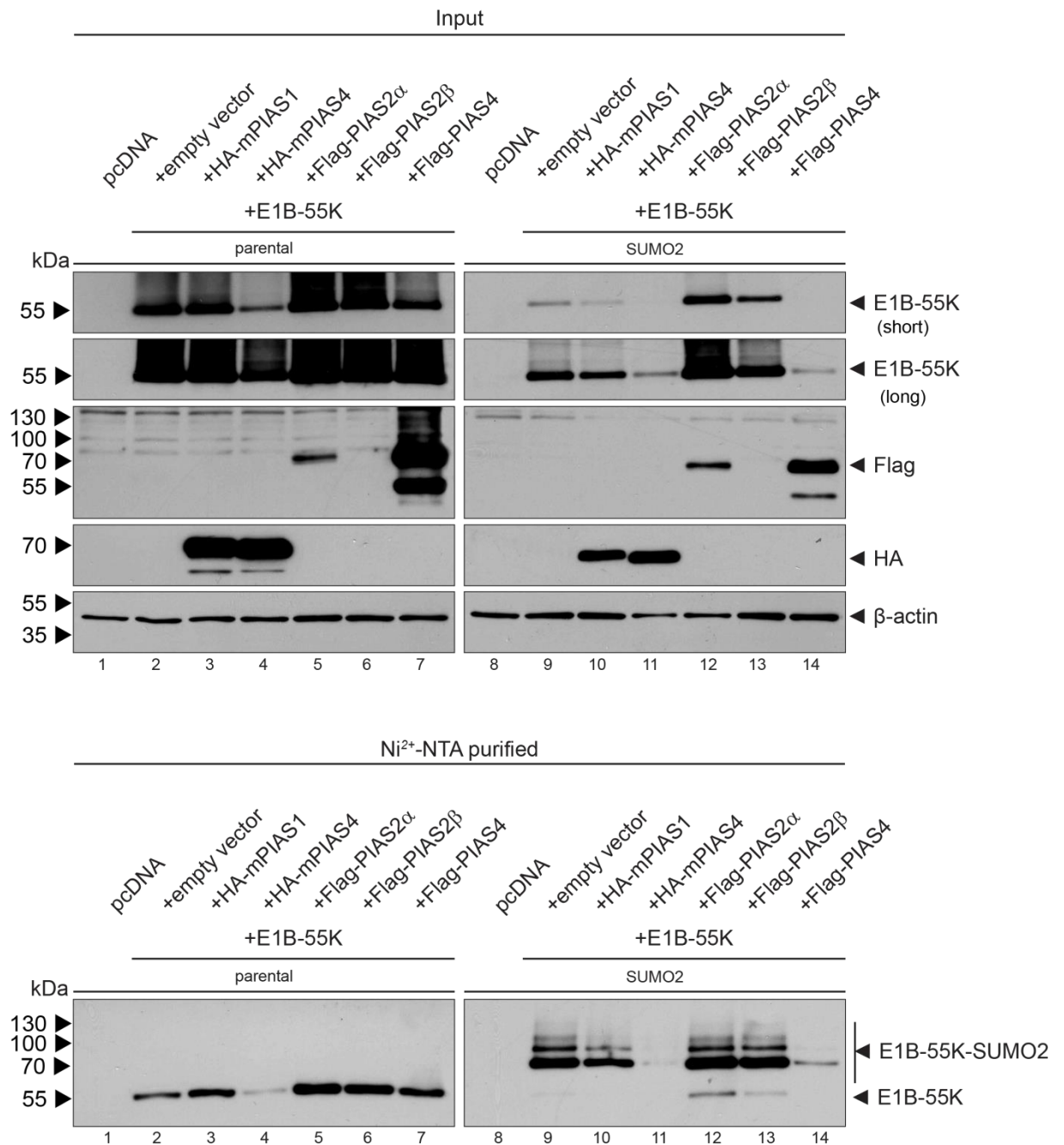


Figure 24: PIAS4 reduces the steady state level concentrations of E1B-55K in transiently transfected HeLa cells. Subconfluent parental HeLa cells and HeLa SUMO2 cells were transiently transfected with 5 μ g of plasmid encoding E1B-55K (#1319) and 10 μ g of plasmid encoding HA-tagged mPIAS1 (#3020), HA-tagged mPIAS4 (#3021), Flag-tagged PIAS2 α (#3022), Flag-tagged PIAS2 β (#3023) or Flag-tagged PIAS4 (#3024) and harvested 48 h p. t. SUMOylated proteins were enriched by Ni²⁺-NTA purification, while the input probes were lysed in RIPA buffer. The proteins were resolved by SDS-PAGE and visualized via immunoblotting, using antibodies specific for E1B-55K (#1), HA-tag (#629), Flag-tag (#196) and β -actin (#88).

4.3.2 PIAS4 specifically represses E1B-55K protein levels

Besides functioning as SUMO E3 ligases, PIAS proteins are known as potent transcriptional regulators and can interact with a vast number of different transcription factors in order to regulate various cellular pathways and molecular processes. To exclude beforehand, that PIAS4

Results

regulates the human Cytomegalovirus (CMV) promoter of the recombinant plasmid, which could result in the observed reduced E1B-55K steady state levels, we tested the expression levels of two alternative recombinant proteins in the presence of PIAS4. The tested plasmids encoded either the early adenoviral protein E4orf6 (Figure 25, panel A) or the non-viral *enhanced green fluorescent protein* (eGFP) (Figure 25, panel B), both expressed under the control of the CMV-promoter and cotransfected with PIAS4 in HeLa SUMO2 cells (Figure 25). The protein concentration of neither E4orf6 (Figure 25, panel A, lane 3), nor eGFP (Figure 25, panel B, lane 3) was reduced in the presence of PIAS4 in comparison to the respective probes without PIAS4 overexpression (Figure 25, panel A and B, lane 2). This indicates, that PIAS4 overexpression is not generally reducing the transcriptional activity of transfected CMV-promoter controlled plasmids and leads to the conclusion that E1B-55K repression is specific. We therefore assumed, that the repression of E1B-55K protein levels in the presence of PIAS4 might be linked to its SUMO E3 ligase function and enhanced E1B-55K SUMO modification.

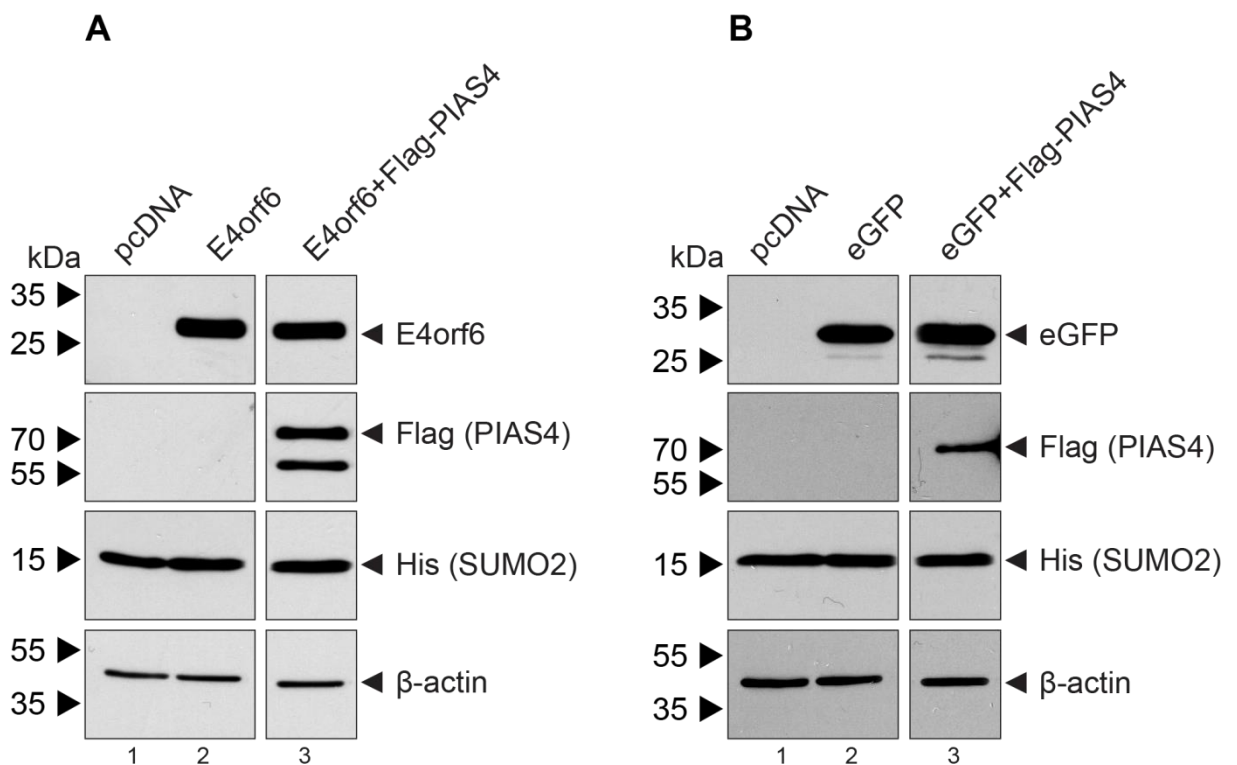


Figure 25: The protein levels of E4orf6 and *enhanced green fluorescent protein* (eGFP) are not reduced in the presence of overexpressed PIAS4. Subconfluent HeLa SUMO2 cells were transiently transfected with 10 μ g of plasmid encoding for either (A) E4orf6 (#1664) or 6 μ g of expression vector encoding for (B) eGFP (#282) and 10 μ g of plasmid encoding Flag-tagged PIAS4 (#3024). 48 h p. t. the cells were harvested and lysed in RIPA buffer. Proteins were resolved by SDS-PAGE and visualized via immunoblotting, using antibodies specific for E4orf6 (#94), eGFP (#622), Flag-tag (#196), His-tag (#551), and β -actin (#88).

4.3.3 E1B-55K is not proteasomal degraded in the presence of overexpressed PIAS4

SUMOylation has very diverse consequences for its modified substrates, ranging from altered subcellular localization and protein stability to modification of protein-protein interactions, which can change the substrate properties remarkably (Geiss-Friedlander and Melchior, 2007; Hay, 2005). Related to protein stability, SUMO chains can also be recognized by *SUMO targeted ubiquitin ligases* (STUbLs), which act by poly-ubiquitination of the initially SUMOylated protein, followed by its proteasomal degradation (Perry et al., 2008; Sriramachandran and Dohmen, 2014). Thus, in order to investigate if the reduction of E1B-55K steady state levels (Figure 24, lanes 4, 7, 11 and 14) was due to the SUMO E3 ligase function of PIAS4 and enriched E1B-55K SUMOylation, an MG132 assay was performed in HeLa SUMO2 cells, transfected with different plasmids encoding for E1B-55K and PIAS4 of murine and human origin. MG132 is a potent cell-permeable inhibitor of the proteasome and reduces the proteasomal degradation of ubiquitinated proteins. When E1B-55K was cotransfected with empty vector plasmid, it could be detected with a strong signal, confirming its overexpression irrespective of the presence of MG132 (Figure 26, lanes 2 and 6). As expected, overexpression of both, mPIAS4 and PIAS4 reduced the steady state levels of E1B-55K in the DMSO controls (Figure 26, lanes 3 and 4). After MG132 treatment, the levels of E1B-55K were reduced to a similar extent when either mPIAS4 or PIAS4 was coexpressed, indicating that E1B-55K is not degraded by the proteasome in the presence of overexpressed PIAS4. To confirm the MG132-mediated inhibition of the proteasome, a positive control was used by staining the p53 protein levels, which showed stabilization in the presence of MG132 (Figure 26, lanes 5-8).

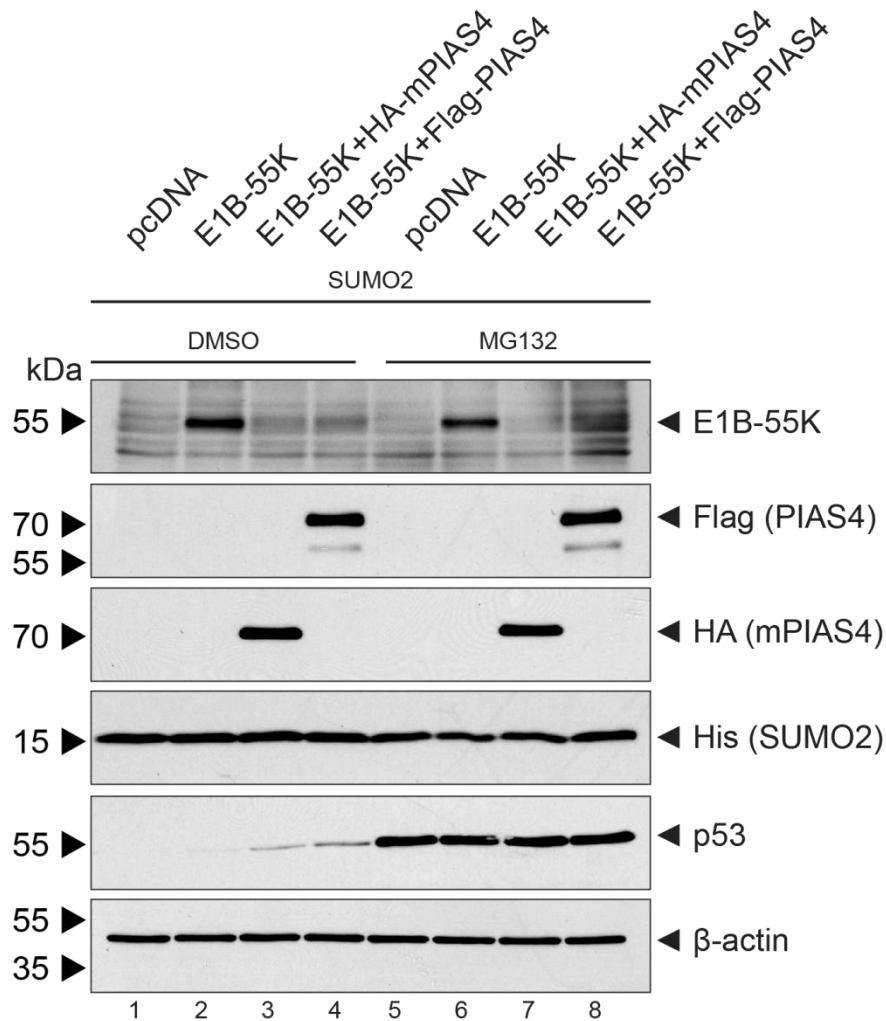


Figure 26: PIAS4 reduces E1B-55K protein concentration in the presence of the proteasome inhibitor MG132. Subconfluent HeLa SUMO2 cells were transiently transfected with 5 μ g of plasmid encoding for E1B-55K (#1319) and 10 μ g of plasmid encoding HA-tagged mPIAS4 (#3021) or Flag-tagged PIAS4 (#3024) and harvested 48 h p. t. 4 h prior to cell harvest, cells were incubated in cell culture medium supplemented with MG132 to a final concentration of 15 μ M or DMSO as a control. Cells were lysed in RIPA buffer and proteins were resolved by SDS-PAGE and visualized via immunoblotting, using antibodies specific for E1B-55K (#1), HA-tag (#629), Flag-tag (#196), His-tag (#551), p53 (#62) β -actin (#88).

4.3.4 Analysis of E1B-55K subcellular localization in the presence of PIAS4

As described previously, SUMOylation often affects the subcellular localization of its substrates and thereby broadens its functions. In the case of E1B-55K, it is already known that SUMOylation regulates its continuous nucleocytoplasmic shuttling, which is crucial for its function and growth-promoting properties (Endter et al., 2005; Kindsmüller et al., 2007). In the assumption, that PIAS4 could be the SUMO E3 ligase of E1B-55K and its reduction is based on enhanced SUMO modification, the next experiments aimed to determine if the subcellular localization of E1B-55K is altered in the presence of PIAS4. HeLa SUMO2 cells were transfected with plasmids encoding for E1B-55K and PIAS4 prior to analysis with a Leica DMI 600B microscope. When E1B-55K was cotransfected with empty vector plasmid it showed a predominant cytosolic accumulation in close

Results

proximity to the nuclear membrane, while only a weak diffuse signal was detected within the nucleus (Figure 27, panel f and j). Coexpression of E1B-55K with PIAS4 did not show any changes on the subcellular localization of this viral protein (Figure 27, panel n and r).

HeLa 6His-SUMO2

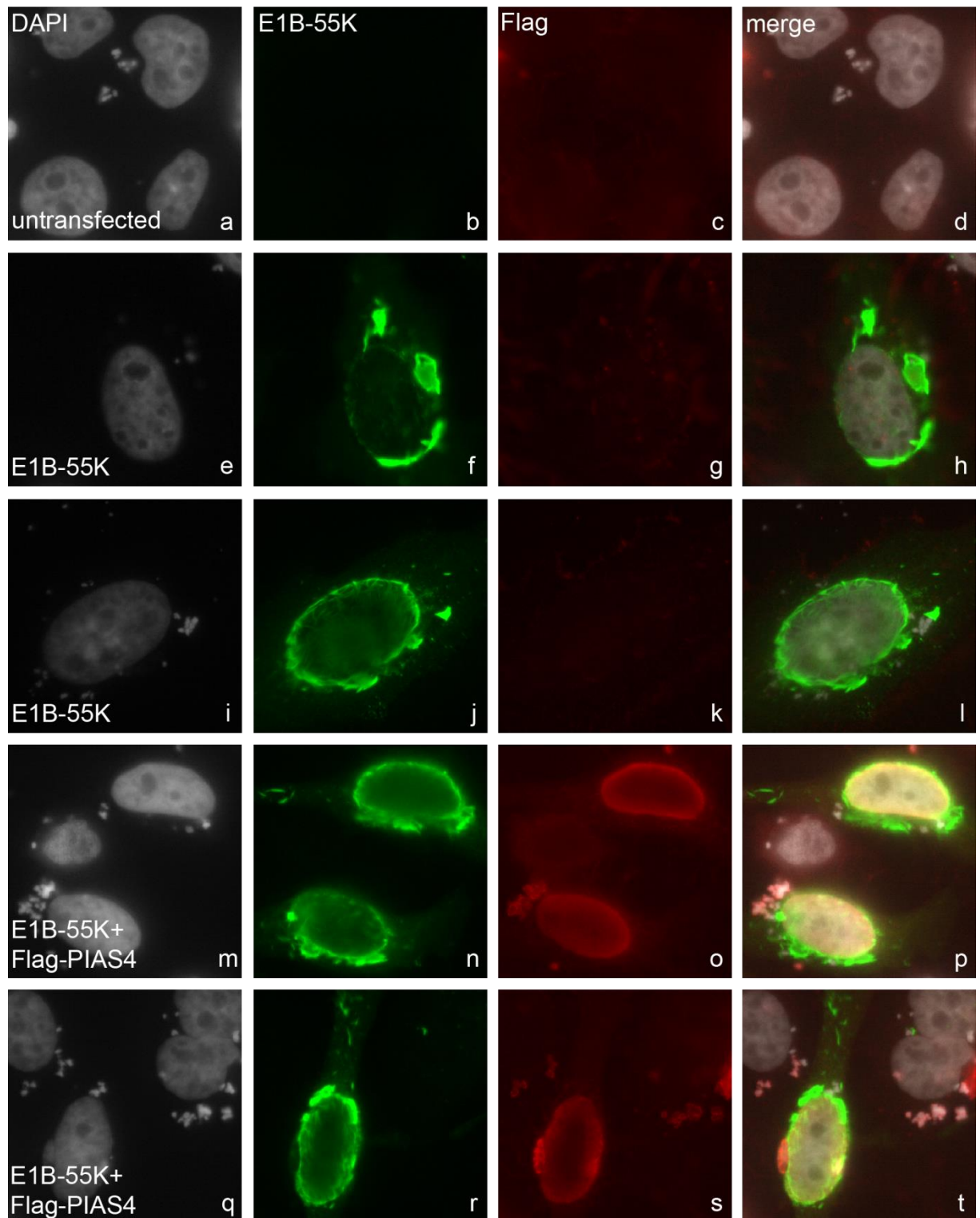


Figure 27: PIAS4 overexpression has no effect on the subcellular localization of E1B-55K. Subconfluent HeLa SUMO2 cells were transiently transfected with 1.5 μ g of each plasmid DNA encoding for E1B-55K (#1319) and Flag-tagged PIAS4

Results

(#3024). The cells were either transfected with E1B-55K alone (e-l) or in combination with PIAS4 (m-t). The cells were fixed in 4 % PFA 48 h p. t. and the target proteins were visualized with an E1B-55K specific antibody (#369), shown in green and a Flag-tag specific antibody (#196) shown in red, while chromatin was stained with DAPI (grey).

It has been shown that PIAS4 recruits its interaction partner LEF-1 to nuclear matrix compartments upon binding, thus repressing its transcription factor activity (Sachdev et al., 2001). In order to test if E1B-55K is relocalized to a specific compartment of the nuclear matrix by PIAS4, HeLa SUMO2 cells transfected with plasmids encoding for E1B-55K and PIAS4 were harvested to perform a subcellular fractionation assay. Subsequently, each fraction was separated by SDS-PAGE and stained for E1B-55K (Figure 28). Staining of histone 3 was used to confirm the proper separation of the nuclear matrix fraction (F5). Fractions F1, F2 and F3 showed a drastic decrease of E1B-55K in the presence of PIAS4, as observed in previous experiments. However, in F4 and F5 the decrease of E1B-55K in the presence of PIAS4 was not as strong as in the other fractions, suggesting a partial relocalization of E1B-55K in these fractions.

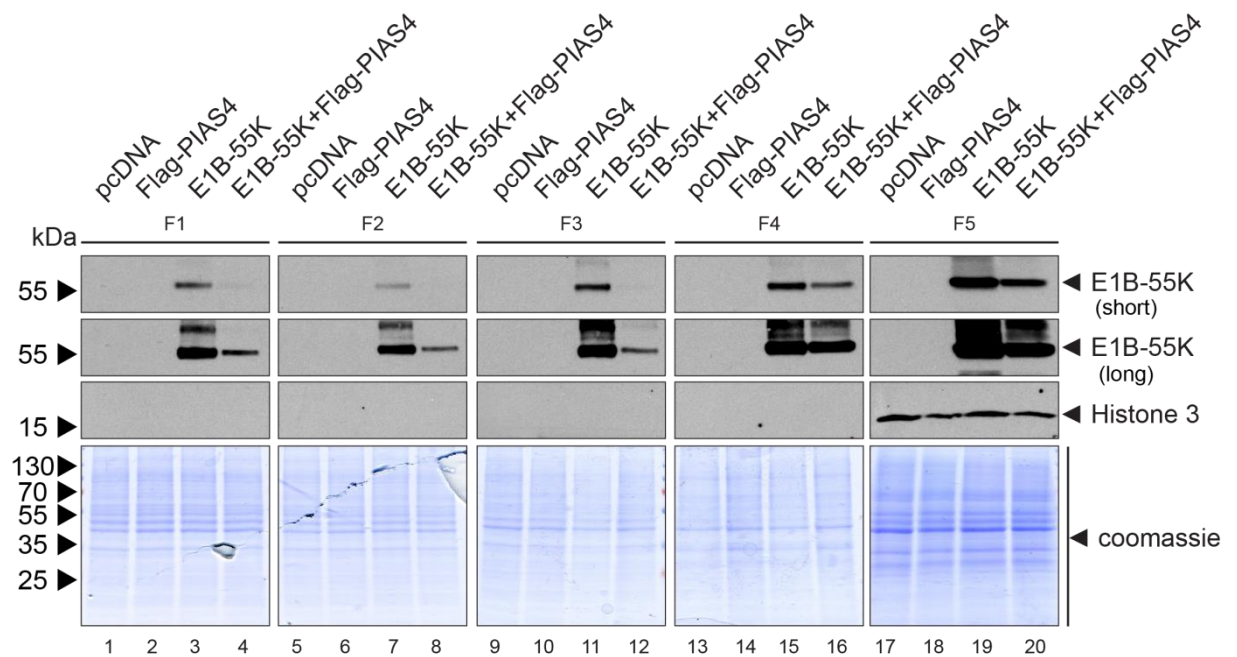


Figure 28: E1B-55K protein is partially relocalized to the chromatin (F4) and insoluble nuclear matrix fraction (F5) in the presence of overexpressed PIAS4. Subconfluent HeLa SUMO2 cells were transiently transfected with 5 μ g of plasmid encoding for E1B-55K (#1319) and 10 μ g of plasmid Flag-tagged PIAS4 (#3024) and harvested 48 h p. t. The cells were lysed fraction-wise using different lysis buffers. F1=cytoplasmic fraction; F2=nuclear membrane fraction, F3=soluble nuclear fraction; F4=chromatin fraction; F5=insoluble nuclear matrix fraction. Proteins were resolved by SDS-PAGE and visualized via immunoblotting, using antibodies specific for E1B-55K (#1) and Flag-tag (#196). The Coomassie gel in the lowest panel served as a loading control and showed equal protein amounts among the probes in each fraction.

4.3.5 PIAS4-mediated reduction of E1B-55K is not dependent on its direct SUMOylation

In previous experiments we could exclude a SUMO-dependent proteasomal degradation as well as complete relocalization of E1B-55K upon SUMOylation, which were the two most likely

explanations for a SUMO-dependent decrease of E1B-55K protein levels. To further investigate whether direct SUMO modification of E1B-55K is involved in its PIAS4-mediated decrease, HeLa SUMO2 cells were transfected with plasmids encoding either E1B-55K wt or its corresponding SUMO mutant carrying a K104R point mutation. Both E1B-55K forms were expressed to similar levels when cotransfected with empty vector plasmid (Figure 29, lane 2 and 3). As expected, E1B-55K wt protein concentration was remarkably reduced upon coexpression of PIAS4 (Figure 29, lane 5). Interestingly, E1B-55K K104R mutant protein levels were repressed to the same extent as E1B-55K wt in the presence of PIAS4. This result demonstrated that PIAS4-mediated reduction of E1B-55K protein concentration is independent of E1B-55K SUMO modification, and therefore, PIAS4 can be excluded as the SUMO E3 ligase of E1B-55K.

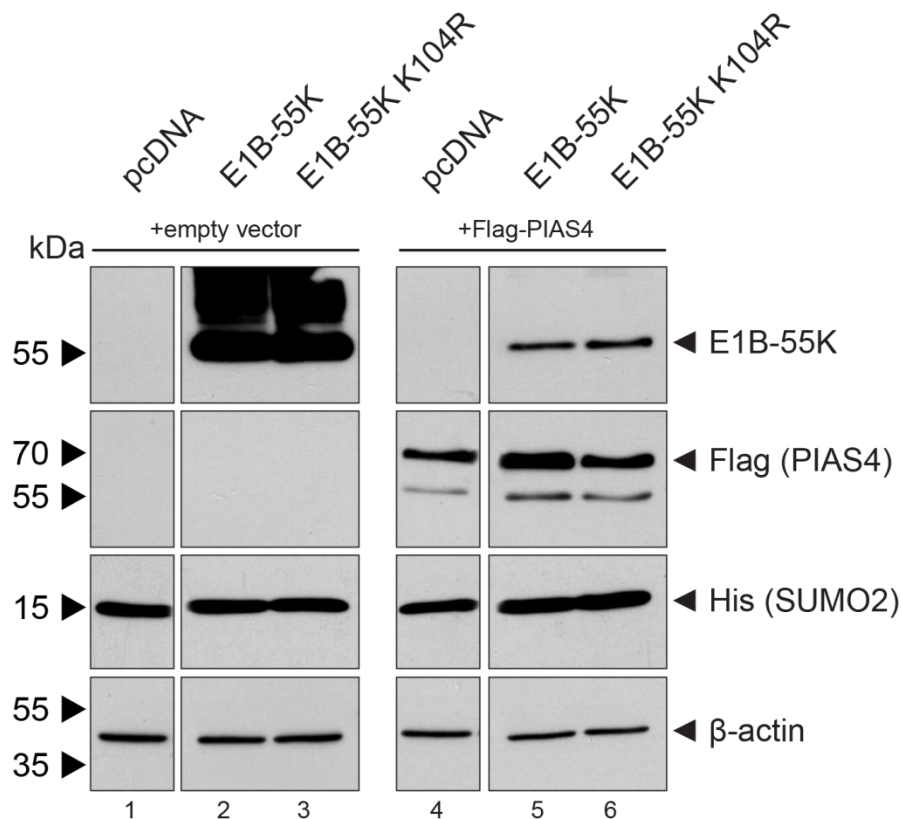


Figure 29: The SUMO mutant E1B-55K K104R is repressed to comparable extents as E1B-55K wt in the presence of overexpressed PIAS4. Subconfluent HeLa SUMO2 cells were transiently transfected with 5 μ g of plasmid encoding for either E1B-55K (#1319) or its SUMO mutant K104R (#1022) and 10 μ g of plasmid encoding Flag-tagged PIAS4 (#3024). Cells were harvested 48 h p. t. and lysed in RIPA buffer. Proteins were resolved by SDS-PAGE and visualized via immunoblotting, using antibodies specific for E1B-55K (#1), Flag-tag (#196), His-tag (#551), and β -actin (#88).

4.3.6 PIAS4 reduces the activity of the E1B-promoter in a dose-dependent manner

Previous experiments could not show PIAS4-mediated repression of E1B-55K protein levels as a consequence of increased SUMOylation, and subsequent SUMO-dependent downstream events,

like STUbL-mediated proteasomal degradation or relocalization. Further, the decrease of E1B-55K protein levels was shown to occur independent of the major SCM at lysine 104, indicating that SUMOylation of E1B-55K is not involved in the decrease of its protein levels. Beside their SUMO E3 ligase function, PIAS proteins are reported to interact with over sixty different transcription factors and thereby, are involved in the regulation of a plethora of cellular pathways by functioning as transcriptional regulators. However, both functions converge to some extents, since many transcription factors are activated upon PIAS-driven SUMOylation. A regulatory connection of PIAS4 to adenovirus infection is new and has not been described yet. However, PIAS4 was clearly linked to repression of Herpes Simplex Virus Type 1 (HSV-1) infection, its SUMO E3 ligase function is repressed by the early protein E6 of human Papillomavirus (HPV) (Bischof et al., 2006; Conn et al., 2016) and the results in Figure 24 pointed to repressive effect of PIAS4 on E1B-55K protein levels. In order to investigate, if PIAS4 represses the E1B-55K protein amount at the level of transcription, we performed a luciferase assay and determined the activity of the adenoviral E1B-promoter in the presence of PIAS4. H1299 cells were transfected with a luciferase reporter plasmid containing the E1B-promoter region fused to the luciferase gene, in combination with a plasmid encoding PIAS4 (Figure 30, panel A). In order to activate the E1B-promoter activity, we cotransfected the adenoviral E1A protein, which is known to stimulate the expression of E1B-transcription unit (reviewed in Berk, 2013). Figure 30, panel A illustrates, that overexpression of PIAS4 remarkably reduced the E1B-promoter activity by almost 5-fold, both, in the presence and in the absence of E1A. It seemed that the E1B-promoter activity was already saturated in the absence of E1A, probably due to E1B-promoter activation by cellular proteins. Thus we did not include E1A in subsequent experiments. To further investigate the specificity of the PIAS4-mediated transcriptional repression of the E1B-promoter, increasing concentrations of plasmids encoding for PIAS4 or PIAS2 α , a PIAS family member that did not show an effect on E1B-55K protein levels (Figure 24), were transfected (Figure 30, panel B). Increasing amounts of PIAS4 resulted in a dose-dependent repression of the E1B-promoter with an approximate 5-fold repression at the highest concentration of PIAS4 (1.0 μ g plasmid DNA). As expected, increasing amounts of PIAS2 α did not show a significant effect on the E1B-promoter activity, indicating that the repression is specific for PIAS4. These results were in line with the reduction of E1B-55K protein concentration observed before (Figure 24) and strongly support the model that PIAS4 acts a transcriptional regulator, which represses the expression of E1B-55K and thus, could have an anti-viral potential as part of the intrinsic immune system of the host cell.

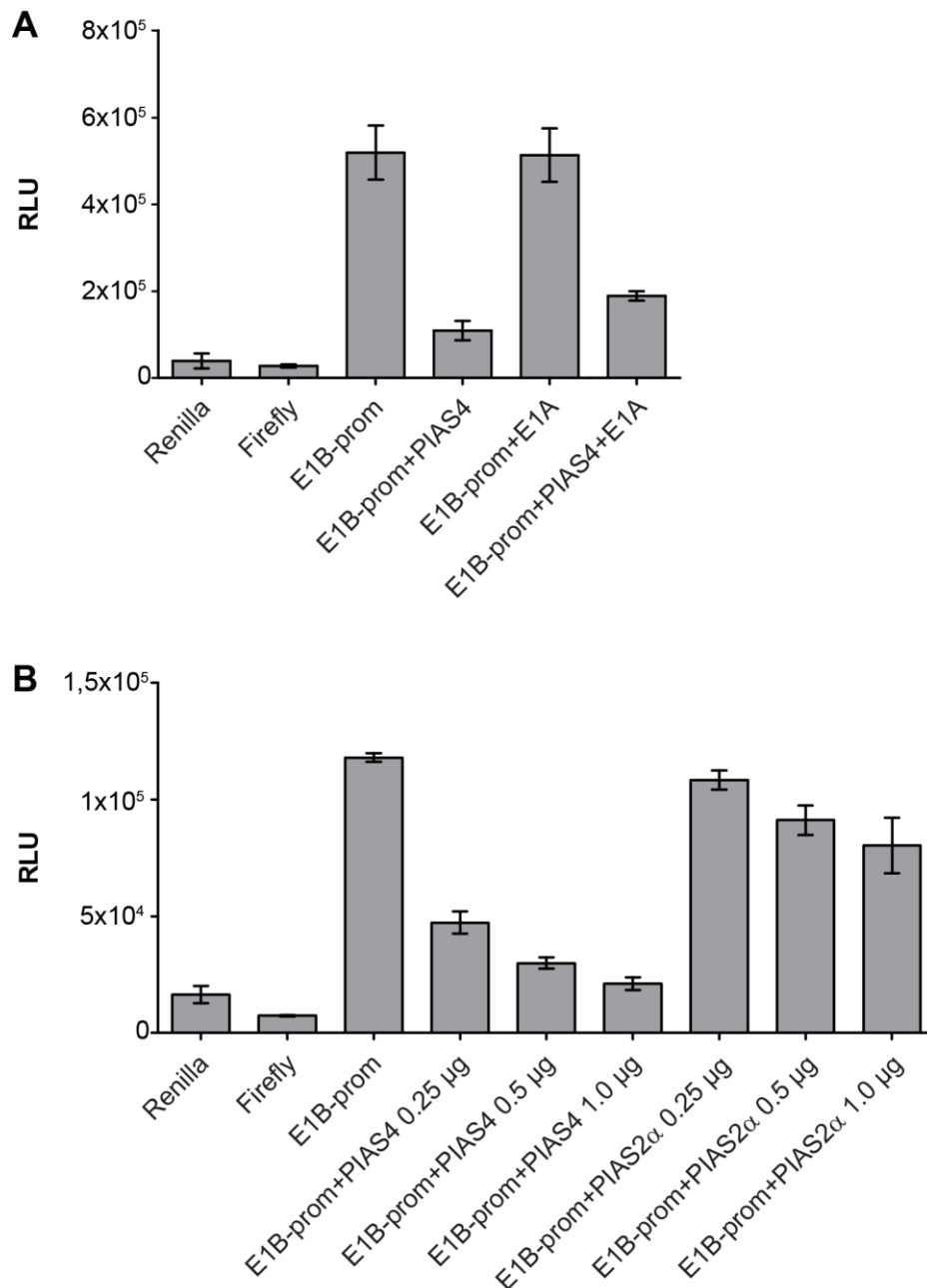


Figure 30: PIAS4 represses the activity of the adenoviral E1B-promoter in a dose-dependent manner. Subconfluent H1299 cells were transfected with 0.5 µg or indicated amounts of plasmid DNA encoding for Flag-tagged PIAS4 (#3024) Flag-tagged PIAS2α (#3022) or E1A (#2476). Additionally, 0.5 µg of a plasmid expressing the *firefly* luciferase gene alone (#138) or under the control of the E1B-promoter (#2421) as well as 0.5 µg of a *renilla* luciferase expression plasmid (#180) were cotransfected. The activity of both luciferases was measured in a dual luciferase assay 24 h p. t. The samples were normalized on the *renilla* activity and the relative light units (RLU) were compared to the empty vector control. The samples were normalized and the relative light units (RLU) compared to the control were calculated. **A:** Analysis of the E1B-promoter activity in the presence of 0.5 µg PIAS4 and E1A. **B:** Analysis of the E1B-promoter activity in the presence of increasing PIAS4 and PIAS2α concentrations.

4.3.7 PIAS4 represses mRNA and protein expression of several genes encoded within the early E1-transcription unit

In order to elucidate if the repressive effect of PIAS4 was exclusive for the E1B-promoter or if it also affects the transcription of other adenoviral early genes, the protein expression of the whole E1-gene region was investigated in the presence of PIAS4. Parental HeLa cells and HeLa SUMO2 cells were transfected with plasmids encoding the whole E1-gene region of HAdV-C5, as well as Flag-tagged PIAS4. The transfected E1-gene region contains the early adenoviral genes E1A and E1B under control of their endogenous adenoviral promoters. When the E1-gene region was cotransfected with empty vector plasmid, high levels of E1A, E1B-55K and E1B-19K could be detected in both cell lines (Figure 31, lanes 2 and 8). As expected, the E1B-55K protein concentration was remarkably reduced in the presence of overexpressed PIAS4, confirming the previous results on E1B-55K protein levels (Figure 24) and E1B-promoter activity (Figure 30). Moreover, E1B-19K protein levels were also reduced in the presence of PIAS4. The primary transcript of the E1B-gene locus is alternatively spliced into two major transcripts, 13S and 22S, encoding E1B-19K and E1B-55K, respectively (Berk and Sharp, 1978; Spector et al., 1978). Hence, repression of the E1B-promoter affects E1B-19K to the same extent as E1B-55K (Figure 31, lane 5 and 11). Interestingly, E1A protein expression was also suppressed in the presence of PIAS4 (Figure 31, lanes 5 and 11). This implicates, that the PIAS4-mediated repression might not be restricted to the E1B-promoter, but seems to affect the E1A-promoter to similar levels.

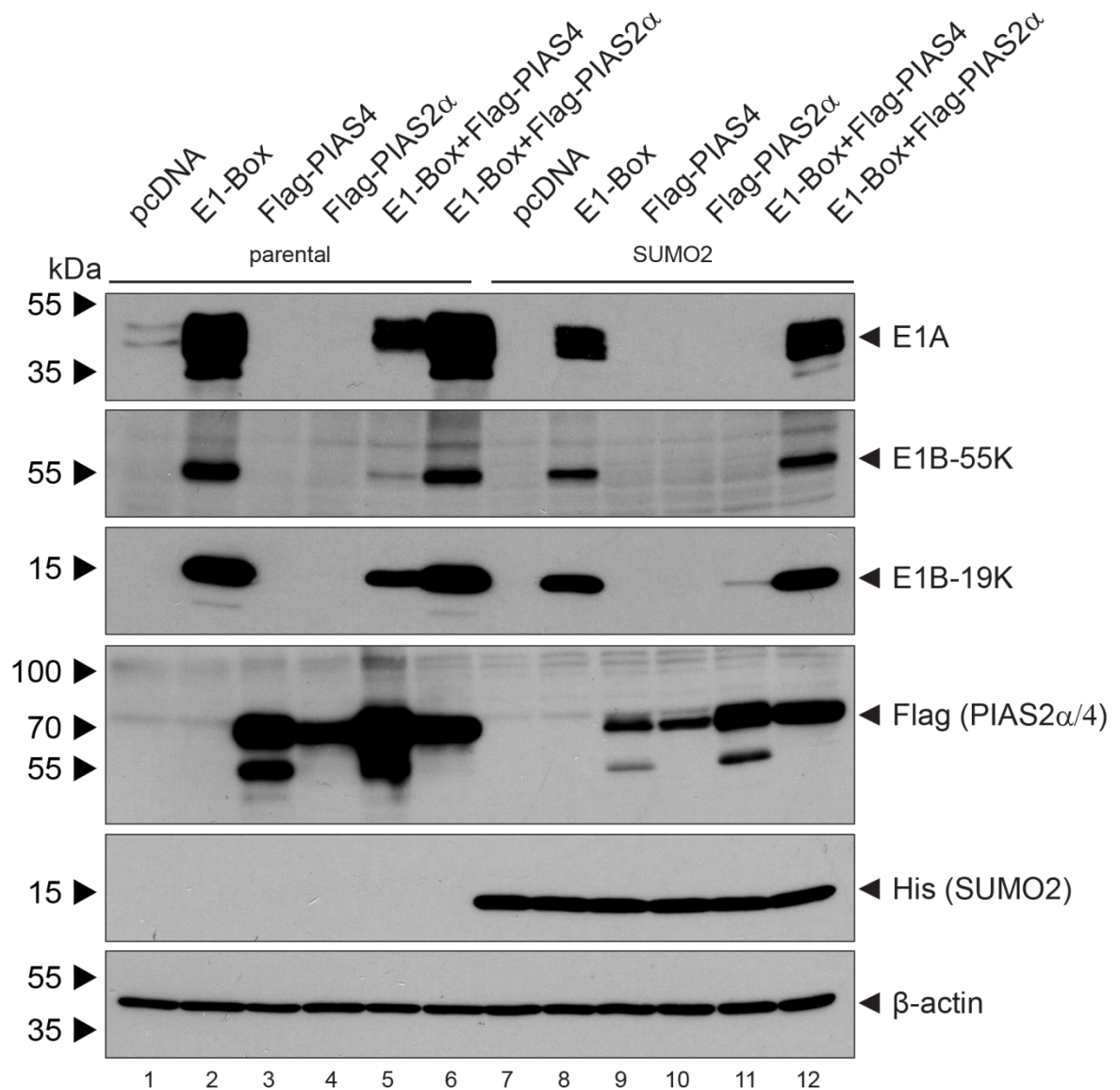


Figure 31: PIAS4 overexpression reduces protein concentration of E1-gene region encoded proteins. Subconfluent parental HeLa cells and HeLa SUMO2 cells were transiently transfected with 5 μ g plasmid DNA encoding for the E1-Box (#608) and 10 μ g of plasmid DNA encoding for either Flag-tagged PIAS4 (#3024) or Flag-tagged PIAS2 α (#3022). 48 h p. t. the cells were harvested and lysed in RIPA buffer. Proteins were resolved by SDS-PAGE and visualized via immunoblotting, using antibodies specific for E1A (#131), E1B-55K (#1), E1B-19K (#490), Flag-tag (#196), His-tag (#551), and β -actin (#88).

In order to confirm, that the reduced protein concentrations of E1A, E1B-55K and E1B-19K were based on reduced mRNA transcription mediated by PIAS4, total RNA was extracted and reverse transcribed followed by determination of E1A and E1B-55K mRNA levels via semi-quantitative real time PCR (Figure 32). In parental HeLa cells the concentration of E1A (panel A) and E1B-55K (panel B) mRNA was remarkably reduced in the presence of PIAS4, by a factor of 71-fold for E1A- and 41-fold for E1B-55K mRNA. In this cell line, the negative control PIAS2 α showed a reduction of 2.3-fold for E1A and 2-fold for E1B-55K mRNA levels (Figure 32, panel A and B). In HeLa SUMO2 cells, E1A levels were repressed by a factor of 50-fold in the presence of PIAS4, while PIAS2 α coexpression reduced the mRNA levels by only 1.5-fold (Figure 32, panel C). E1B-55K mRNA was

Results

repressed 25-fold by PIAS4 and showed even increased levels in the presence of the negative control PIAS2 α (Figure 32, panel D). These data strongly suggested that PIAS4 has a repressive function on both, the E1B- and the E1A-promoter, leading to repressed mRNA levels and thus reduced protein levels of these early viral proteins. The fact that E1A, which is the main transcriptional activator of viral gene expression, is repressed by PIAS4 strengthens the hypothesis that PIAS4 is part of the intrinsic anti-viral immune response, counteracting adenoviral gene expression.

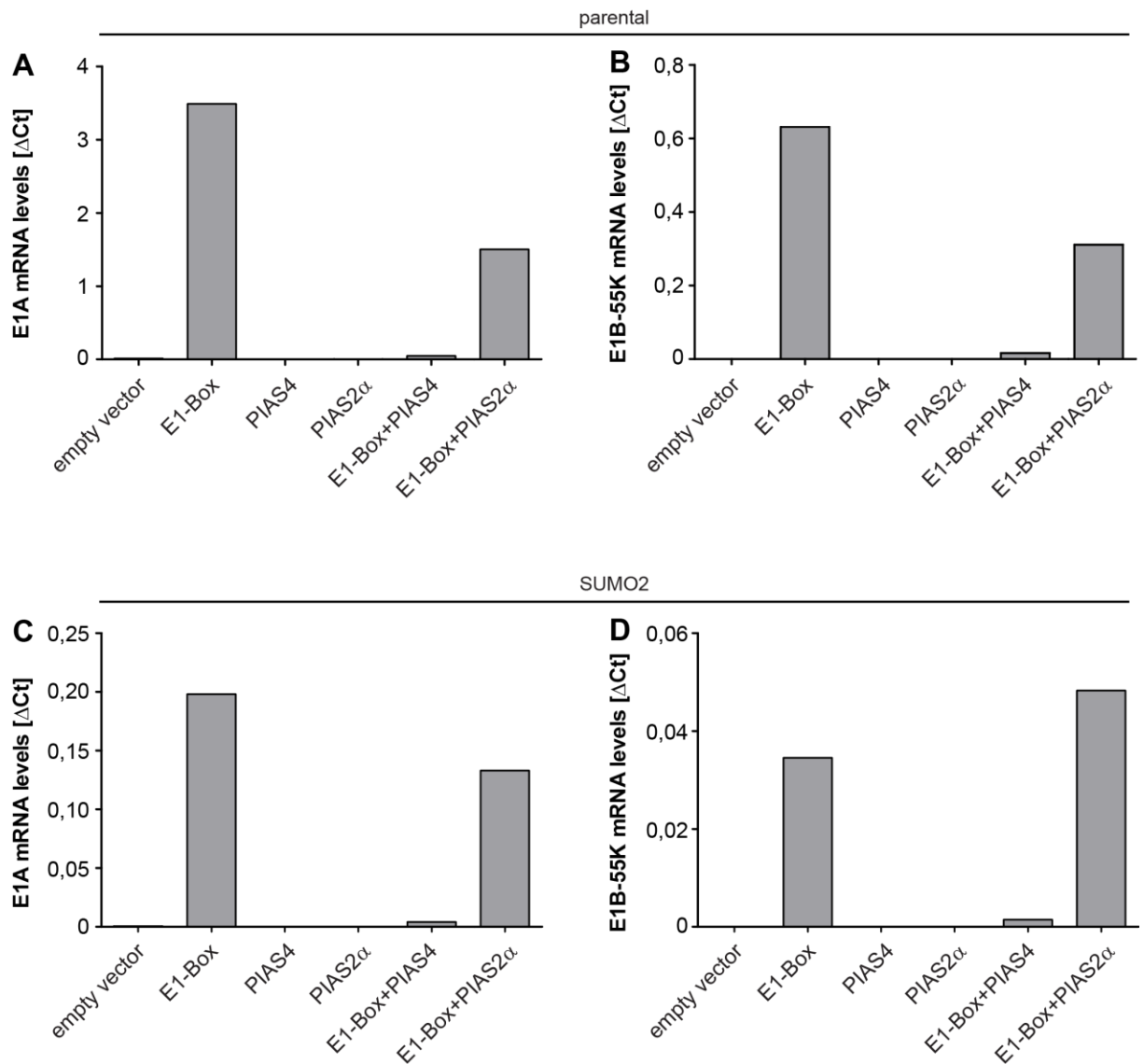


Figure 32: The mRNA levels of E1A and E1B-55K are remarkably reduced in the presence of PIAS4, but not PIAS2 α in HeLa parental and HeLa SUMO2 cells. Subconfluent parental HeLa cells and HeLa SUMO2 cells were transiently transfected with 5 μ g plasmid DNA encoding for the E1-Box (#608) and 10 μ g of plasmid DNA encoding for either Flag-tagged PIAS4 (#3024) or Flag-tagged PIAS2 α (#3022). 48 h p. t. the cells were harvested. Total RNA was isolated and reverse transcribed followed by detection of E1A (panel A and C) and E1B-55K (panel B and D) mRNA levels using specific primers (E1A: #1686, 1687; E1B-55K: #640, 641). The graphs show absolute amounts of E1A and E1B-55K mRNA levels which were normalized to GAPDH (ΔCt).

4.3.8 Overexpression of PIAS4 represses the transforming potential of E1A and E1B-55K in primary baby rat kidney (pBRK) cells

Adenoviral genes encoded by the E1-gene region, namely E1A, E1B-55K and E1B-19K, are known to be sufficient to transform pBRK cells *in vitro*, as already explained in this work in 4.2.2. Due to the observation made that overexpressed PIAS4 considerably represses the levels of all E1-proteins (Figure 31) and viral mRNAs (Figure 32), the next experiment addressed the question, if PIAS4-mediated repression affects the transforming potential of E1-proteins in pBRK cells. Freshly isolated pBRK cells were transfected with plasmids encoding either E1A, the whole E1-gene region, PIAS4 or PIAS2 α alone, or cotransfected with the whole E1-gene region and either PIAS4 or PIAS2 α . After, incubation for six weeks and staining of the formed *foci*, the rate of *foci* formation was determined for each condition (Figure 33). As expected, transfection of E1A alone was not sufficient to induce the formation of *foci*. However, transfection of the whole E1-gene region which encodes E1A, E1B-55K and E1B-19K led to the formation of a significant number of *foci*, as previously described (Endter and Dobner, 2004). Interestingly, cotransfection of PIAS4 remarkably repressed the transforming potential of the E1-gene region by 8.5-fold, while coexpression with the negative control PIAS2 α showed only a slight reduction of 1.8-fold (Figure 33, panel B). These observations phenotypically confirm the previously obtained results regarding the PIAS4-mediated transcriptional repression of E1A, E1B-55K and E1B-19K and implicate a biological effect of PIAS4 on the adenovirus-mediated cell transformation of primary rodent cells.

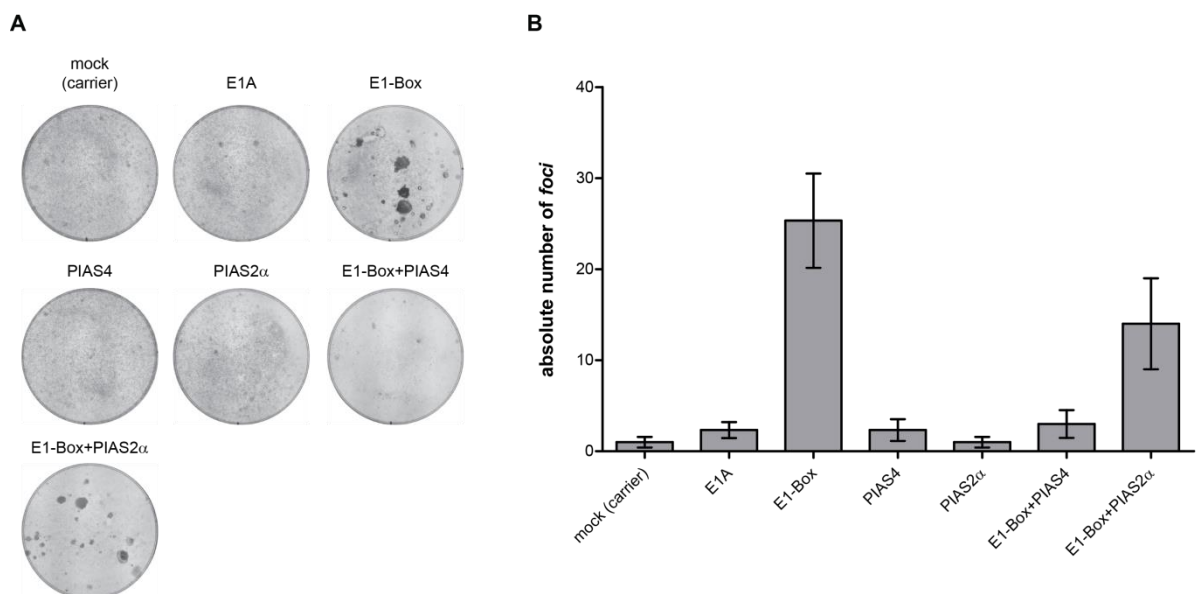


Figure 33: Overexpression of PIAS4 represses the transforming potential of the E1-genes in pBRK cells. Freshly isolated pBRK cells were transfected with 10 μ g DNA plasmid encoding E1A (#737), 10 μ g of the E1-Box (#608), and 10 μ g plasmid encoding for either Flag-tagged PIAS2 α (#3022) or Flag-tagged PIAS4 (#3024). Each condition of the experiment was tested in technical triplicates. The cells were propagated for six weeks, followed by fixation in an aqueous solution

containing 25 % MeOH and 1 % crystal violet. Transformed pBRK cells growing in distinct *foci* were visualized and counted. **A:** Representative cell culture dish of each condition upon fixation and staining of the *foci*. **B:** Bar diagram of *foci* quantification in absolute numbers.

4.3.9 Overexpression of PIAS4 shows mild repressive effects on viral protein expression and mRNA transcription during HAdV-C5 wt infection

The results shown in Figure 30 - Figure 32 confirmed that overexpression of PIAS4 has a dose-dependent repressive effect on the E1B-promoter leading to reduced mRNA and protein levels of E1B-55K and E1B-19K. Moreover, the data suggested that, in addition to the E1B-region, the E1A-gene locus seems to be affected by PIAS4 resulting in reduced mRNA and protein levels not only of the E1B-gene products, but also of E1A. Hence, PIAS4 alters the expression levels of early proteins with key regulatory functions during the early state of adenovirus infection. In order to elucidate the effect of PIAS4 overexpression during HAdV infection, parental HeLa cells and HeLa SUMO2 cells were transfected with Flag-tagged PIAS4 followed by infection with HAdV-C5 wt virus. The levels of viral proteins in the presence and the absence of PIAS4 were determined by Western Blotting at 24 h. p. i. (Figure 34). Overexpression of PIAS4 could be detected and viral proteins confirmed a productive adenoviral infection. In contrast to the transfection experiments (Figure 31) the expression of E1B-55K was not altered in the presence of overexpressed PIAS4 (Figure 34, lanes 3 and 6), showing a protein concentration comparable to the empty vector control (Figure 34, lanes 2 and 5). E1A and E1B-19K showed a slight reduction in protein concentration, when PIAS4 was overexpressed in parental HeLa cells (Figure 34, lane 3). In HeLa SUMO2 cells, only E4orf6 protein levels showed a slight reduction in the presence of PIAS4, compared to the empty vector control (Figure 34, lanes 4-6). Taken together, these results indicate, that the repressive effect of PIAS4 on adenoviral gene expression might be counteracted during adenovirus infection, which would explain the differences between transfection and infection experiments.

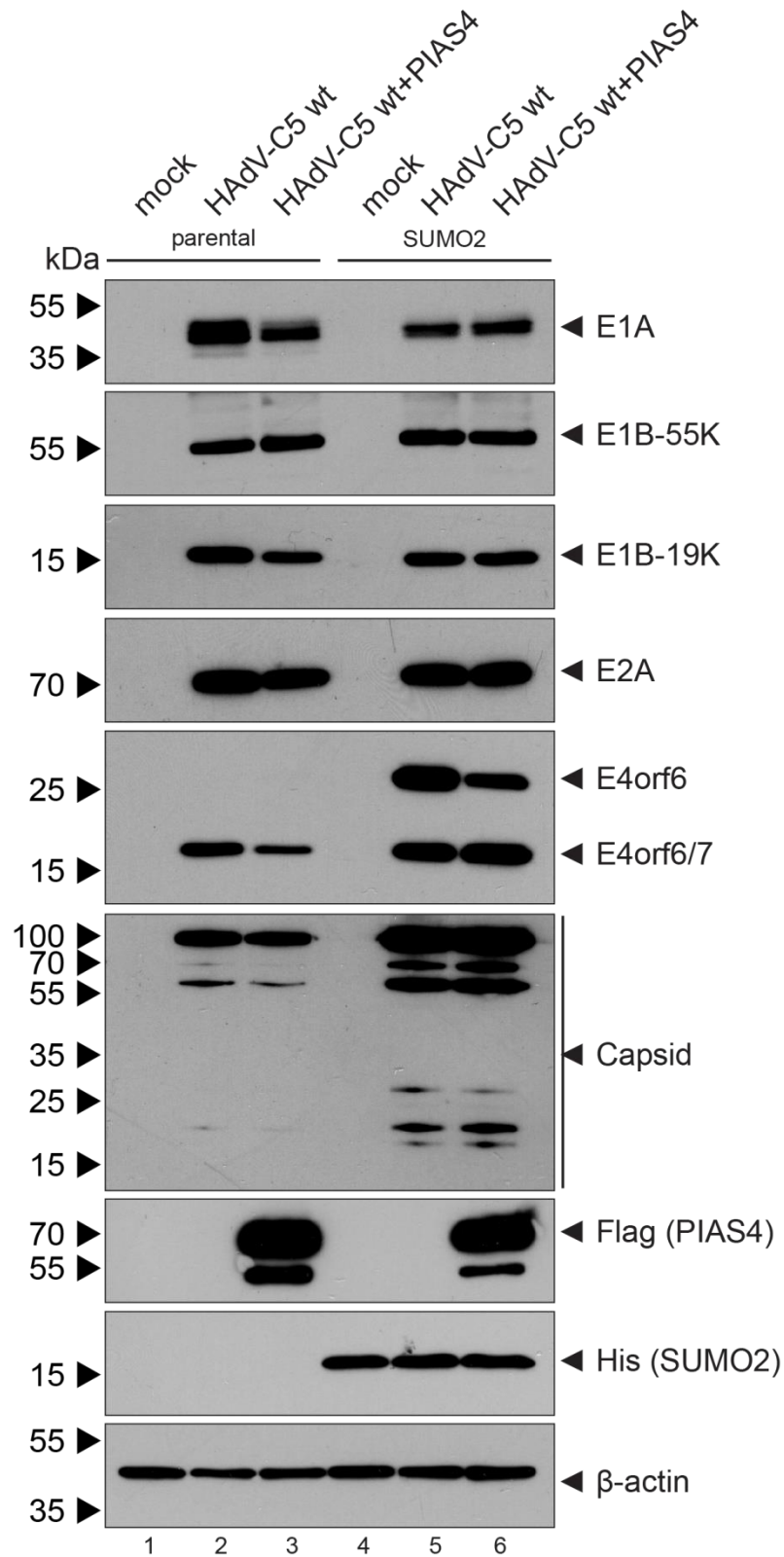


Figure 34: Overexpression of PIAS4 has mild effects on viral gene expression at 24 h p. i. Subconfluent parental HeLa cells and HeLa SUMO2 cells were transfected with 10 μ g of plasmid DNA encoding for either Flag-tagged PIAS4 (#3024) or the empty vector control (#136). 24 h p. t. the cells were infected with HAAdV-C5 wt virus with an MOI of 25. The infected cells were harvested 24 h p. i. and lysed in RIPA buffer. Proteins were resolved by SDS-PAGE and visualized via immunoblotting, using antibodies specific for E1A (#131), E1B-55K (#1), E1B-19K (#490), E2A (#113), E4orf6 and E4orf6/7 (#94), Capsid proteins (#452), Flag-tag (#196), His-tag (#551), and β -actin (#88).

Results

In order to investigate whether the whole viral background compensates the repressive function of PIAS4 on the E1-gene region at certain time points during infection, an infection time course experiment in the presence and the absence of PIAS4 was performed in HeLa cells and analyzed similar to the previous experiment (Figure 34). Infected cells were harvested at 8, 24 and 48 h p. i. and protein expression of viral proteins as well as PIAS4 was determined by Western Blotting (Figure 35). In this experiment, only E4orf6/7 and E1B-55K showed slightly impaired protein expression levels at 24 h p. i. in parental HeLa cells with overexpressed PIAS4 (Figure 35, lane 7). 48 h p. i. the levels of PIAS4 were already decreasing due to the transient transfection, which might explain why viral protein expression is less repressed at this time point. The mock control was harvested together with the 48 h p. i. samples, which explains the low PIAS4 protein levels in these samples. The protein levels of all the other viral proteins analyzed in this experiment were not altered, further supporting the hypothesis, that the whole virus background is able to circumvent PIAS4-mediated transcriptional repression of adenoviral E1-genes.

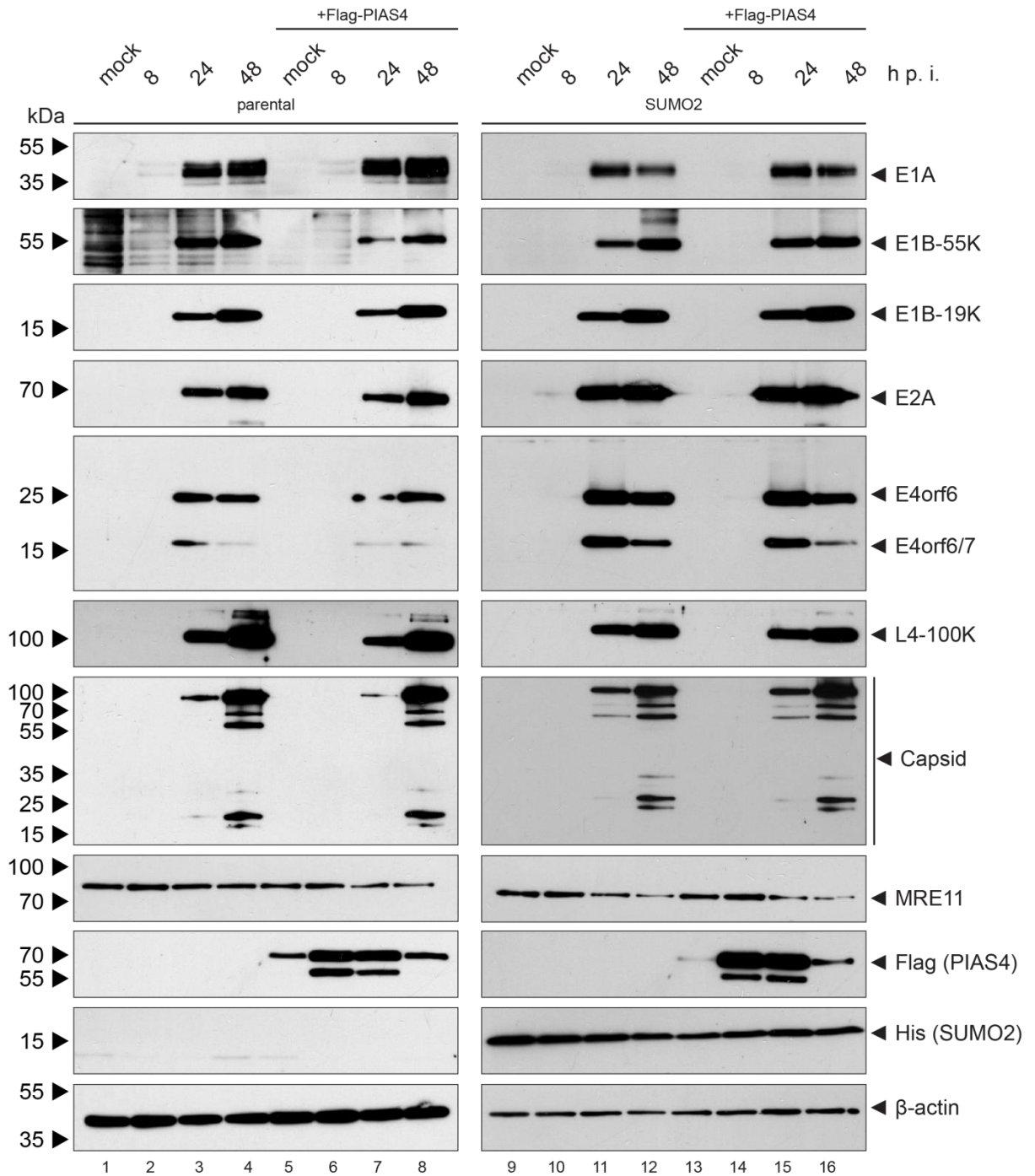


Figure 35: Overexpression of PIAS4 has mild effects on viral protein expression during the course of adenovirus wt infection. Subconfluent parental HeLa cells and HeLa SUMO2 cells were transfected with 10 μ g of plasmid DNA encoding for either Flag-tagged human PIAS4 (#3024) or the empty vector control (#152). 24 h p. t. the cells were infected with HAdV-C5 wt virus with an MOI of 20. The infected cells were harvested at indicated time points (8, 24, 48 h p. i.) and lysed in RIPA buffer. The mock control was harvested together with the 48 h p. i. samples. Proteins were resolved by SDS-PAGE and visualized via immunoblotting, using antibodies specific for HAdV-C5 E1A (#131), HAdV-C5 E1B-55K (#1), HAdV-C5 E1B-19K (#490), HAdV-C5 E2A (#113), HAdV-C5 E4orf6 and E4orf6/7 (#94), HAdV-C5 L4-100K (#275), HAdV-C5 capsid proteins (#452), human MRE11 (#477), Flag-tag (#196), His-tag (#551), and β -actin (#88).

In order to confirm, if the slight reduction of E1B-55K protein in the presence of PIAS4 during infection was based on reduced mRNA levels, total RNA was extracted from the same cells, followed by reverse transcription and determination of E1B-55K mRNA levels via a semi-

Results

quantitative real time PCR (Figure 36). In parental HeLa cells, E1B-55K mRNA levels were not repressed upon PIAS4 overexpression, but showed even enriched levels of E1B-55K mRNA. In contrast, in HeLa SUMO2 cells, a 2.3-fold reduction of E1B-55K mRNA levels was detected at 48 h p. i. Taken together, these results show, that PIAS4 has a mild repressive effect on viral mRNA and protein levels during infection. Intriguingly, this is contrary to the transfection experiments of the adenoviral E1-gene region, where PIAS4 led to remarkably repressed protein (Figure 31) and mRNA levels (Figure 32). This points to an adenoviral factor within the incoming viral particles that might counteract the transcriptional repression induced by PIAS4, either by a direct or an indirect mechanism.

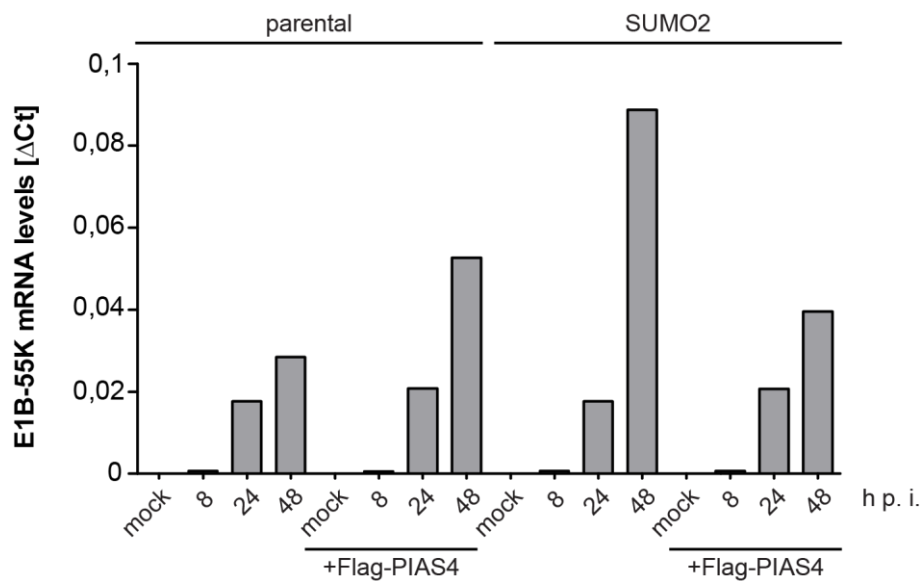


Figure 36: E1B-55K mRNA levels show no or only a slight reduction in the presence of PIAS4 during infection. Subconfluent parental HeLa cells and HeLa SUMO2 cells were transfected with 10 μ g of plasmid DNA encoding for either Flag-tagged PIAS4 (#3024) or the empty vector control (#152). 24 h p. t. the cells were infected with HAdV-C5 wt virus with an MOI of 20. The infected cells were harvested at desired time points (8, 24, 48 h p. i.) and total RNA was isolated and reverse transcribed followed by detection of E1B-55K mRNA using specific primers (#640, 641). The graphs show absolute amounts of E1B-55K mRNA levels which were normalized to GAPDH (Δ Ct).

In several other infection experiments (not shown), comparable results were obtained, showing no or only mild reduction of adenoviral protein concentration in the presence of overexpressed PIAS4. However, some infection experiments did show a reduction of viral protein levels in the presence of overexpressed PIAS4, which is shown in Figure 37. In this infection experiment, the levels of E1B-55K were remarkably reduced 24 and 48 h p. i. in parental HeLa cells, when PIAS4 was overexpressed (Figure 37, lanes 11 and 12). In HeLa SUMO2 cells the levels of E1B-55K were found to be considerably reduced 24 h p. i. in the presence of overexpressed PIAS4 (Figure 37, lane 11) but not at 48 h p. i. Interestingly, at this time point PIAS4 levels are already reduced in this cell line.

Results

This illustrates that during adenovirus infection the repressive properties of PIAS4 on viral gene expression are not that definite, as found in earlier transfection experiments, in which PIAS4-mediated transcriptional repression was detected in every performed experiment.

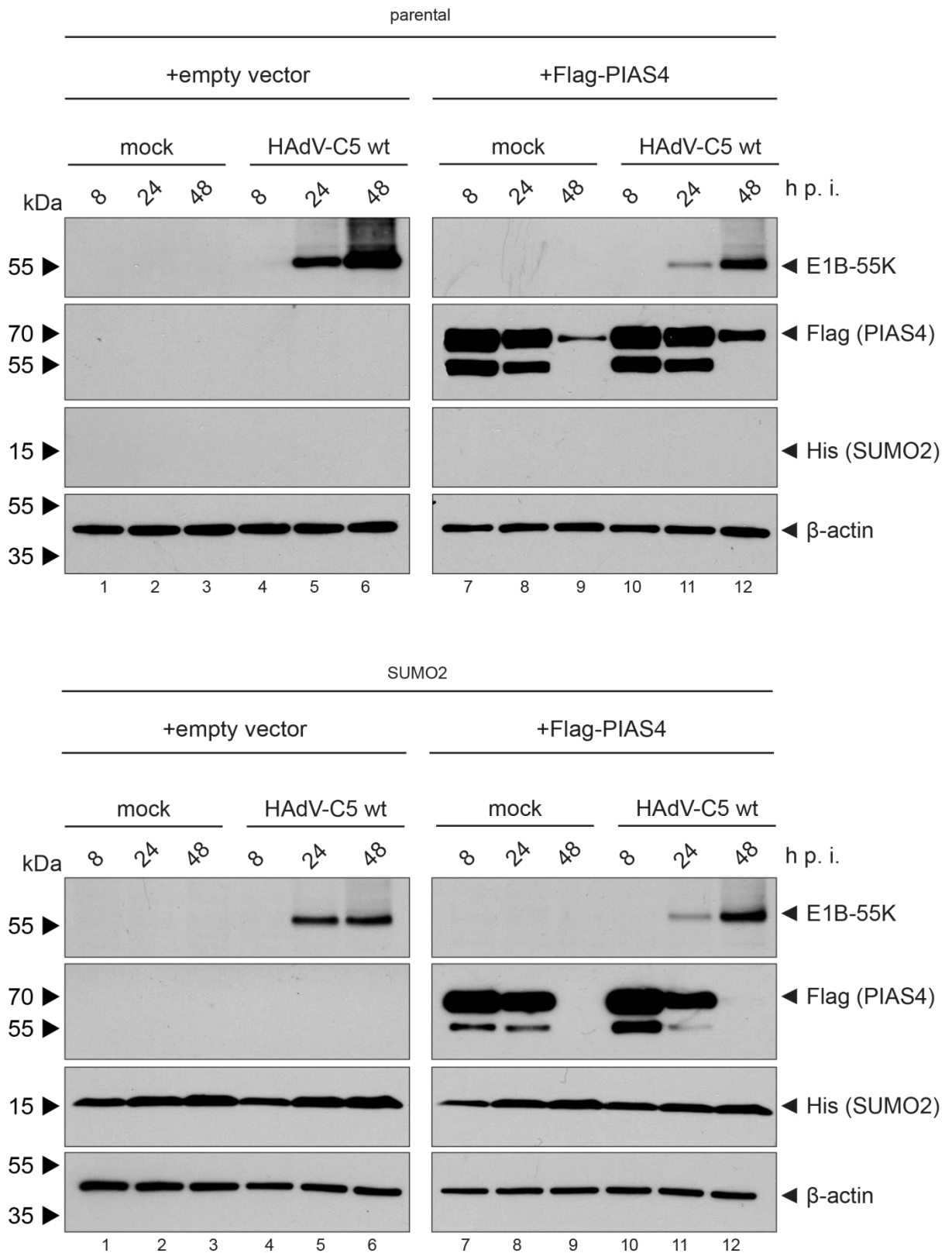


Figure 37: Overexpression of PIAS4 shows repressive effects on E1B-55K expression during the course of adenovirus wt infection. Subconfluent parental HeLa cells and HeLa SUMO2 cells were transfected with 10 µg of plasmid DNA encoding for either Flag-tagged PIAS4 (#3024) or the empty vector control (#136). 24 h p. t. the cells were infected with HAdV-C5 wt virus with an MOI of 20. The infected cells were harvested at indicated time points (8, 24, 48 h p. i.) and lysed in RIPA buffer. Proteins were resolved by SDS-PAGE and visualized via immunoblotting, using antibodies specific for E1B-55K (#1), Flag-tag (#196), His-tag (#551), and β-actin (#88).

4.3.10 Overexpression of PIAS4 has mild effects on adenovirus progeny production

The previous experiments revealed only mild effects of PIAS4 on protein expression and mRNA synthesis during adenoviral infection. In order to further determine whether this has an effect on virus growth, aliquots of the same cells utilized for protein- (Figure 35) and mRNA level measurements (Figure 36) were analyzed in terms of virus progeny production (Figure 38). At 8 h p. i. the titers were too low to be detected in this experiment, which was expected considering that a complete replicative cycle of HAdV takes around 24 h. At 24 h p. i., the levels of newly synthesized virus particles in the absence of PIAS4 were about 22 ffu/cell in HeLa parental cells and more than 200 ffu/cell in HeLa SUMO2 cells. Interestingly, at 24 h. p. i. virus progeny production was completely inhibited by PIAS4 in HeLa parental cells but not in SUMO2 cells. At 48 h p. i., PIAS4 overexpression slightly repressed virus progeny production in both cell lines, whereby this effect was more prominent in HeLa SUMO2 cells. Summarized, these results were in line with previous observations and show a mild effect of PIAS4 on adenovirus progeny production during infection, which seems to be more drastic in the presence of low amount virus particles per cell.

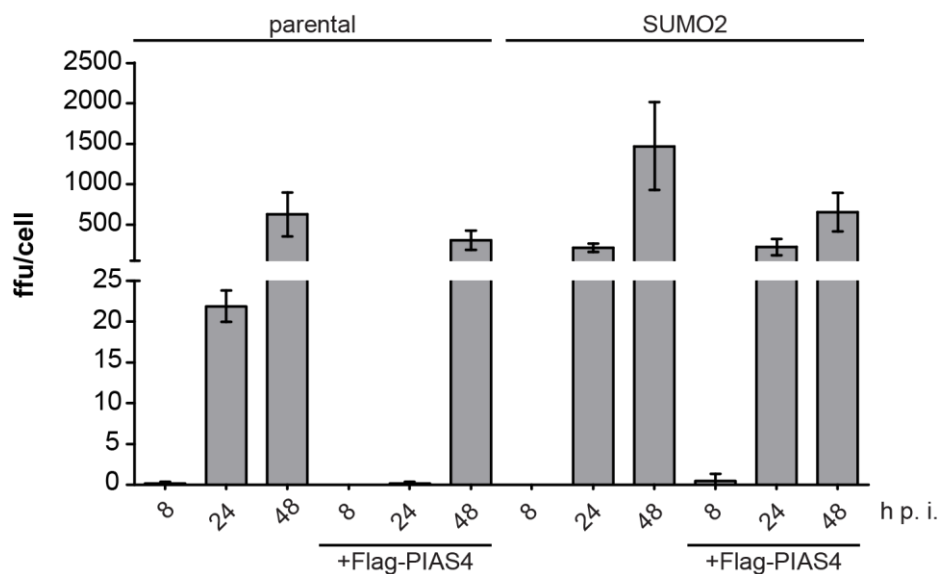


Figure 38: The overexpression of PIAS4 has only mild effects on HAdV-C5 wt virus progeny production. Subconfluent parental HeLa cells and HeLa SUMO2 cells were transfected with 10 µg of plasmid DNA encoding for either Flag-tagged PIAS4 (#3024) or the empty vector control (#152). The cells were infected with HAdV-C5 wt virus with an MOI of 20 at 24 h p. t. The infected cells were harvested at indicated time points (8, 24, 48 h p. i.) and lysed by three freeze and thaw cycles. Subsequently, A549 cells were reinfected with the virus progeny for titration. Reinfected A549 cells were

visualized by immunofluorescence staining of E2A (#113) for determination of the virus yield. The experiment was performed in three technical replicates.

4.3.11 The SUMO E3 ligase function of PIAS4 is partially involved in the transcriptional repression of early adenoviral genes

It is known that viral components from human Papillomavirus (HPV) and Cytomegalovirus (CMV) target PIAS proteins and counteract their SUMO E3 ligase function (Bischof et al., 2006; Kim et al., 2014). After showing only mild repressive effects of overexpressed PIAS4 during HAdV-C5 infection, we aimed to determine if the SUMO E3 ligase function of PIAS4 plays a role in the transcriptional repression of adenoviral genes. PIAS proteins harbor a conserved tryptophan residue in their SP-RING domain, whose mutation to alanine eliminates their SUMO E3 ligase function (Kotaja et al., 2002). In order to compare the repressive function of PIAS4 wt and the SUMO E3 ligase deficient mutant W363A in the context of the E1-gene region, we transfected parental HeLa cells and HeLa SUMO2 cells with the E1-gene region and either PIAS4 wt or its respective mutant W363A (Figure 39). The levels of E1A, E1B-55K and E1B-19K were remarkably repressed in the presence of PIAS4 wt in parental HeLa cells (Figure 38, lanes 2 and 3) and HeLa SUMO2 cells (Figure 38, lanes 6 and 7). However, when we overexpressed the PIAS4 W363A mutant with the E1-gene region, the levels were almost unaffected in parental HeLa cells (Figure 39, lane 4) and less repressed in HeLa SUMO2 cells (Figure 39, lane 8), when compared to PIAS wt overexpression (Figure 39, lane 7). This implicates, that the SUMO E3 ligase function of PIAS4 is at least partially involved in the transcriptional repression of early adenoviral gene expression. Considering this, it is reasonable that the repressive effect of PIAS4 was stronger in HeLa SUMO2 cells, since these cells express the doubled amount of SUMO2.

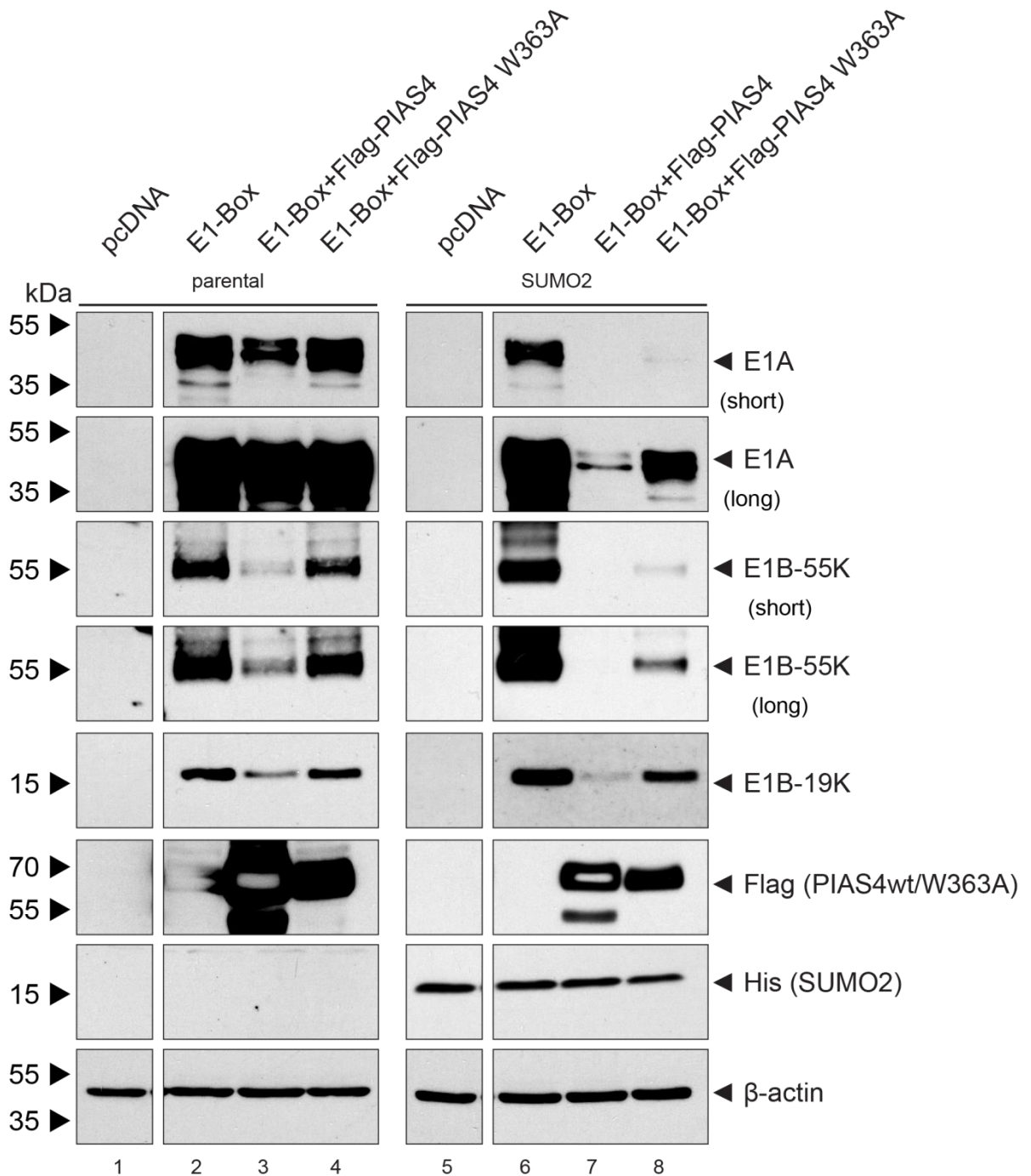


Figure 39: The SUMO E3 ligase function of PIAS4 is partially involved in the transcriptional repression of early adenoviral genes. Subconfluent parental HeLa cells and HeLa SUMO2 cells were transiently transfected with 5 μ g plasmid DNA encoding for the E1-Box (#608) and 10 μ g of plasmid DNA encoding for either Flag-tagged PIAS4 wt (#3024) or Flag-tagged PIAS4 W363A mutant (#3275). 48 h p. t. the cells were harvested and lysed in RIPA buffer. Proteins were resolved by SDS-PAGE and visualized via immunoblotting, using antibodies specific for E1A (#131), E1B-55K (#1), E1B-19K (#490), Flag-tag (#196), His-tag (#551), and β -actin (#88).

4.3.12 The role of adenovirus capsid and core proteins in counteracting PIAS4-mediated transcriptional repression of adenoviral E1-genes

Initial transfection experiments showed, that E1B-55K protein- and mRNA levels were remarkably reduced in the presence of overexpressed PIAS4 and additionally it repressed the E1B-promoter activity in a dose-dependent manner. Transfection of the E1-gene region in the presence of PIAS4 illustrated, that PIAS-mediated repression is not restricted to the E1B-gene locus, but comparably represses E1A protein- and mRNA levels. Since E1A is an essential adenoviral factor, driving cell cycle progression of the host cell and expression of all downstream adenoviral genes, it was promising to determine the role of PIAS4 as a potential anti-viral factor in the whole virus context. Interestingly, different experiments showed that during infection PIAS4 has only mild effects on viral protein expression, as well as on mRNA levels of E1B-55K and virus progeny production, which was in strong contrast to the transfection experiment with the E1-gene region.

Most likely, an unknown viral factor, which is not *de novo* synthesized during infection is able to counteract PIAS4-mediated repression, since low E1A levels would also restrict expression of this particular factor. Hence, it is rather assumed, that the factor is immediately present during infection and starts to counteract PIAS4 at earliest time points during infection. The only adenoviral proteins, which are present before viral protein expression started, are the capsid proteins as part of the incoming viral particles, as well as the core proteins, which are associated to the viral genome. To elucidate their role in the context of PIAS4-mediated repression of transcription, parental HeLa cells and HeLa SUMO2 cells were cotransfected with the E1-gene region and DNA plasmids encoding the HAdV-C5 core proteins pV, pVII and the precursors of p μ and capsid protein pVI in the presence of Flag-tagged PIAS4 or PIAS2 α as a negative control (Figure 40). In both cell lines, the expression of viral proteins was not impaired in the presence of the negative control PIAS2 α (Figure 40, lanes 3 and 11). In parental HeLa cells, the levels of E1A, E1B-55K and E1B-19K were reduced in the presence of PIAS4 but still detectable (Figure 40, lane 4). The repressive effect of PIAS4 was much stronger in the HeLa SUMO2 cells, where viral proteins E1A, E1B-55K and E1B-19K could not be detected anymore (Figure 40, lane 12). All adenoviral core and capsid proteins were expressed at high levels, only p μ expression was weak. Overall, coexpression of the core and capsid proteins did not restore the protein levels of the early adenoviral proteins E1A, E1B-55K and E1B-19K in the presence of PIAS4. However, further experiments are needed to elucidate the role of the adenoviral core and capsid proteins in counteracting PIAS4 in more detail.

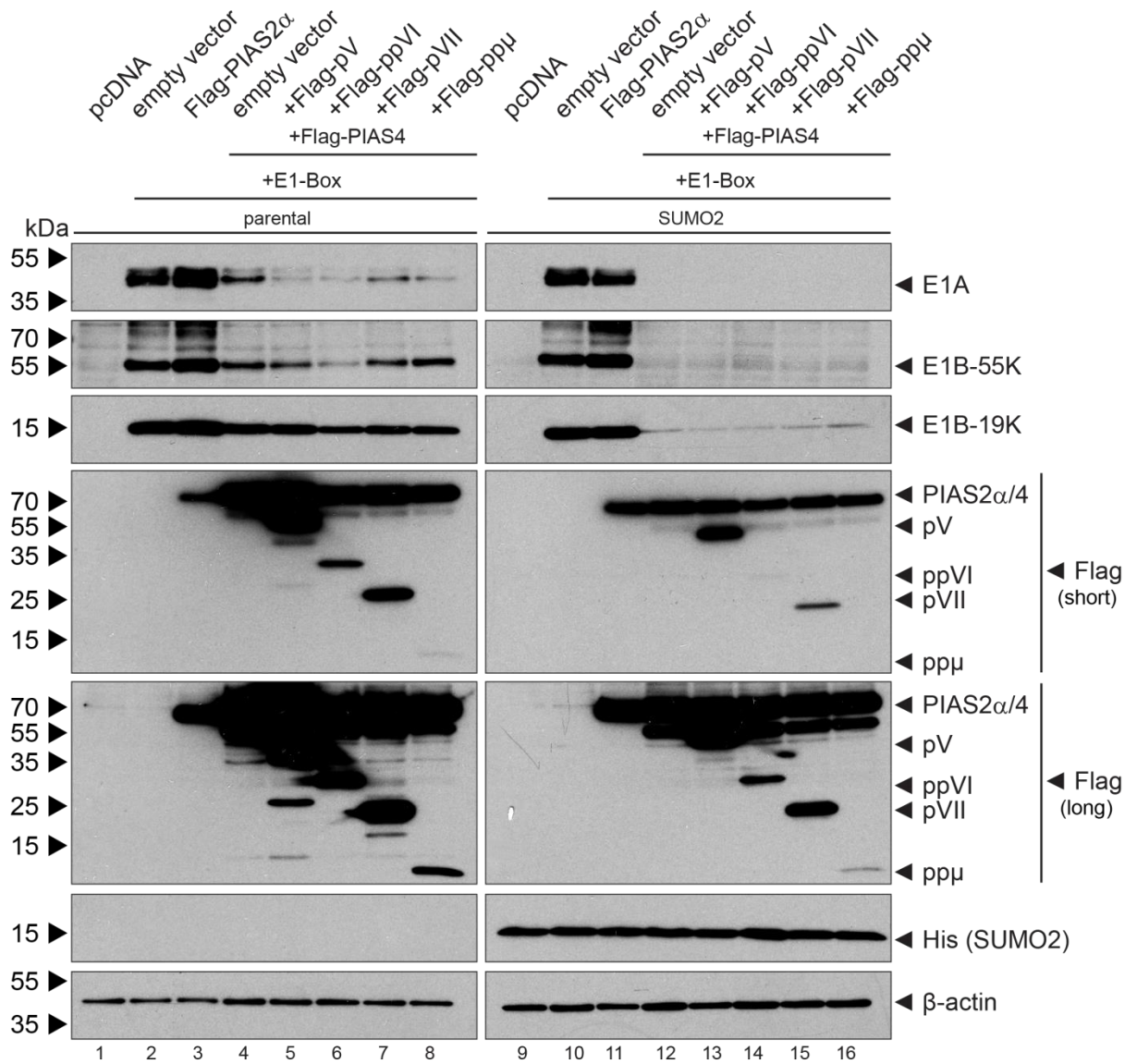


Figure 40: The adenoviral core proteins do not restore the protein levels of early adenoviral proteins encoded by the E1B-Box in the presence of PIAS4. Subconfluent parental HeLa cells and HeLa SUMO2 cells were transfected with 5 μ g plasmid DNA encoding for the E1-Box (#608) and 10 μ g of plasmid DNA encoding for either Flag-tagged PIAS4 (#3024) or Flag-tagged PIAS2 α (#3022). Additionally, 8 μ g of plasmid DNA encoding for either Flag-tagged pV (#2738), Flag-tagged precursor pVI (#2739), Flag-tagged pVII (#2741) or Flag-tagged precursor p μ (#2743) was transfected. 48 h p. t. the cells were harvested and lysed in RIPA buffer. Proteins were resolved by SDS-PAGE and visualized via immunoblotting, using antibodies specific for E1A (#131), E1B-55K (#1), E1B-19K (#490), Flag-tag (#196), His-tag (#551), and β -actin (#88).

5 Discussion

5.1 SUMO2 modification of HAdV-C5 E1B-19K

The PTM with SUMO can influence the subcellular localization as well as the stability of the substrate and provides a vast effect on its global interactome (Geiss-Friedlander and Melchior, 2007; Hay, 2005). Due to its far reaching regulating properties, various human-pathogenic viruses were found to manipulate the host cell SUMO machinery by different mechanisms in order to modulate anti-viral intrinsic immunity and promote viral replication. Infections with Herpes Simplex Virus Type 1 (HSV-1), Epstein Barr virus (EBV) and Influenza A virus (IAV) were recently reported to alter the global levels of SUMO conjugated proteins (Boutell et al., 2002; Domingues et al., 2015; Li et al., 2012; Sloan et al., 2015). Along this line, ICP0 from HSV-1 was found to act as a viral STUbL, inducing the specific degradation of SUMOylated proteins during infection (Boutell et al., 2011). Comparably, EBV protein BRLF1 reduced levels of SUMOylated proteins dependent on the proteasome, but without an ubiquitin ligase activity (De La Cruz-Herrera et al., 2018). In most cases, virus-mediated modulation of the host cells SUMO machinery is based on viral proteins, which directly interact with SUMO enzymes or function as SUMO enzymes themselves (Lowrey et al., 2017). For example, the early protein E6 from high risk human Papillomavirus (HPV) was shown to perturb host cell SUMOylation by interacting with SUMO E2 conjugating enzyme Ubc9 and simultaneously repressing the SUMO E3 ligase function of PIAS4 (Bischof et al., 2006; Heaton et al., 2011). K-bZIP of Kaposi Sarcoma-associated Herpesvirus (KSHV) was shown to function as a SUMO E3 ligase, inducing the SUMOylation of p53 and Rb and thereby promoting the establishment of a pro-viral environment within the host cell (Chang et al., 2010). The avian adenovirus *Chicken Embryonic Lethal Orphan* (CELO) encodes the Gam-1 protein, which decreases the levels of the SUMO E1 activating enzyme complex and SUMO E2 conjugating enzyme Ubc9, thus abolishing the overall SUMOylation (Boggio et al., 2004, 2007). E1A was shown to bind Ubc9, which results in the inhibition of poly-SUMOylation of target proteins early during adenoviral infection while E4orf3 sequesters the SUMO E3 ligase PIAS3 to replication centers, presumably to utilize PIAS3-mediated SUMOylation processes during viral replication (Higginbotham and O'Shea, 2015; Yousef et al., 2010). Additionally, HAdV encodes two viral SUMO E3 ligases, E4orf3 and E1B-55K, which mediate the attachment of SUMO proteins to TIF-1 γ , p53 and probably Sp100A (Muller and Dobner, 2008; Pennella et al., 2010; Sohn and Hearing, 2016). In this context, previous results from a former research unit member showed that adenovirus wildtype infection increased the global levels of SUMO2 modified cellular proteins, which seemed to depend on the presence of E1B-55K.

5.1.1 Initial detection and validation of E1B-19K SUMOylation

Indeed, the presence of the potential SUMO E3 ligase E1B-55K had a strong effect on the cellular and viral SUMO2 proteome. Noteworthy, from 109 cellular proteins with significant upregulation of SUMO2 modification upon HAdV-C5 wt infection, 78 were upregulated dependent on E1B-55K. These results nicely demonstrate that the presence of only one viral factor, which modulates the host cell SUMO machinery, can have a vast effect on the cellular and adenoviral SUMO2 proteome during infection. Indeed, SUMOylation in the absence of SUMO E3 ligases occurs generally rather inefficient and was only observed for RanGAP1, implicating the need of process acceleration by SUMO E3 ligases (Bernier-Villamor et al., 2002). In order to identify so far unknown adenoviral proteins that have not been identified yet to be SUMOylated during infection, the dataset was analyzed with regard to viral proteins. Thus, we identified twenty adenoviral proteins as potential SUMO2 targets, among them the adenoviral Bcl-2 homologue E1B-19K, which plays an important role during infection by inhibiting the p53-independent apoptosis pathway (Figure 8). Bcl-2 proteins are potent regulators in cell death signaling, which necessitate tight regulation, since their dysregulation is a frequent characteristic of human malignancies (Frenzel et al., 2009). In this context, Bcl-2 proteins were frequently described as a target of PTM with ubiquitination and phosphorylation (Kutuk and Letai, 2008). While ubiquitination of Bcl-2 was clearly linked to the induction of apoptosis by inducing Bcl-2 proteasomal degradation, reports of Bcl-2 phosphorylation showed conflictive results with either increased or decreased onset of apoptosis (Chanvorachote et al., 2006; Deng et al., 2004; Geng et al., 2011; Ruvolo et al., 1998; Vantieghem et al., 2002). The adenoviral Bcl-2 homologue E1B-19K was shown to be phosphorylated at serine 164, and removal of this residue led to slightly impaired transforming potential in cooperation with E1A (McGlade et al., 1989). This suggests that E1B-19K phosphorylation of serine 164 is associated with decreased apoptosis. Contrary, the viral Bcl-2 homologue of KSHV, KS-Bcl-2 encoded by orf16 and expressed early during lytic infection, is not regulated by phosphorylation (Ojala et al., 2000). To date, neither human Bcl-2 nor viral Bcl-2 homologues have been found to be directly regulated via SUMOylation. However, recent reports raised evidence for indirect regulation of Bcl-2 protein by SUMOylation or enzymes of the SUMO pathway. Depletion of SUMO1 reduced the levels of β -catenin, which is involved in cell signaling and known to regulate the expression of human Bcl-2 proteins, leading to impaired Bcl-2 expression and increased apoptosis (Huang et al., 2015; Jin et al., 2017; Li et al., 2007). Along this line, SUMO E2 conjugating enzyme Ubc9 seems to upregulate the expression levels of Bcl-2 (Lu et al., 2006; Mo et al., 2005). Our SILAC approach showed, for the first time, direct SUMOylation of E1B-19K and therefore we aimed to investigate, if the anti-apoptotic properties of E1B-19K are regulated by this PTM. One hallmark of SUMOylation is altered protein-

protein interaction of the substrate based on binding of SUMOylated proteins to SUMO interacting motifs (SIM) of potential binding partners. The E1B-19K-mediated apoptosis perturbation strongly relies on interaction with Bax and Bak proteins, which are inactivated upon E1B-19K complex formation (Figure 4). However, these interactions seem to depend on a highly conserved region of E1B-19K, which shares sequence homology to Bcl-2 (Chiou et al., 1994a; Rao et al., 1992; White et al., 1992). *In silico* analysis of Bak and Bax revealed no SIM, thus SUMOylation of E1B-19K is most likely not involved in the interaction to Bax and Bak proteins. However, E1B-19K was recently reported to associate with the caspase-8-binding protein FLICE-associated huge protein (FLASH), thereby inhibiting caspase 8 activation and the onset of apoptosis (Milovic-Holm et al., 2007). Intriguingly, FLASH contains various SIMs, which were shown to interact with SUMO1 and SUMO2, hence SUMOylation of E1B-19K could be involved in the interaction to FLASH and thus catalyzes the subsequent inhibition of caspase 8 activation (Sun and Hunter, 2012). Along this line, E1B-19K was reported to interact with lamins, which are intermediate filaments found in the cytosol and the nuclear lamina. This interaction is not dependent on Bcl-2 homology, since it was not found for Bcl-2. However, binding of E1B-19K to lamins is thought to mediate proper subcellular localization of E1B-19K and was shown to be intimately linked to its anti-apoptotic properties (Rao et al., 1997). It was recently shown that lamin contains a SIM, which mediates binding to SUMO2 modified proteins and is involved in the regulation of lamin assembly (Moriuchi et al., 2016). Hence, lamin interaction and functional localization of E1B-19K could potentially be regulated by E1B-19K SUMO2 modification and SIM-dependent binding to lamins. Finally, E1B-19K was recently reported to be involved in cell lysis of adenovirus infected cells via autophagy. In this context, E1B-19K binds to beclin B, which is the key regulator of autophagy (Jiang et al., 2011; Piya et al., 2011). *In silico* analysis revealed one SIM within the beclin B sequence, which might be involved in binding to E1B-19K.

To cross-validate the SUMO modification of the SILAC approach, we performed various transfection and infection experiments in HeLa cells overexpressing 6His-tagged SUMO2 (HeLa SUMO2), followed by Ni²⁺-NTA purification and Western Blot detection of SUMO2 modified proteins (Figure 10-Figure 17). However, SUMO2 modification of E1B-19K could not be confirmed in these approaches. The SILAC screen, which initially detected SUMOylated E1B-19K, was performed during infection, indicating that the virus background might be important for its PTM with SUMO2 (Figure 8).

A putative explanation for not detecting SUMOylated forms of E1B-19K could be drawn from the following circumstances. Even though SUMOylation was intensively studied in the recent years, there are still many open questions concerning this PTM that have not been properly answered

yet. SUMOylation is a reversible and highly dynamic process that allows a rapid course of substrate modification and deconjugation. Of different known SUMO substrates, only an exiguous portion is actually SUMOylated, while the main proportion of the protein remains unmodified. Nevertheless, the SUMOylation-induced effect of the particular substrate is maximal and affects the overall properties of the substrate protein pool (Hay, 2005). In line with this “SUMO enigma” a model was postulated, which suggested that once a substrate experiences SUMO modification, the PTM leaves a remaining imprint continuously altering the long-term fate of the substrate, even though the SUMO protein is deconjugated again. This model provides a possible explanation for the maximal efficacy of a low substrate pool of SUMOylated proteins (Hay, 2004). Hence, it might be possible that only a small amount of E1B-19K is SUMOylated so that it is below Western Blot detection limits, even though we used high affinity antibodies and CMV-promoter driven overexpression (Figure 10). Considering the methodical differences of the two proteomic methods used, we cannot rule out that the sensitivity of the mass spectrometry-based SILAC approach was higher, compared to the Western Blotting we utilized for validation. Mass spectrometry encompasses several independent peptide measurements of the quantified protein, whereas Western Blotting results are based on a single signal per protein species derived from only one antibody (Aebersold et al., 2013). Taken together, we have to consider that based on the “SUMO enigma” only a very small portion of E1B-19K was SUMO modified, which was detectable using mass spectrometry. However, the results of the SILAC approach could not be validated by Western Blotting due to methodical and sensitivity differences.

Due to the frequently observed low level modification of SUMO substrates, various strategies are described in the literature, which efficiently increase the levels of SUMO conjugation. The induction of cellular stress response in a hypoxic environment leads to elevated SUMO1 conjugation due to increased SUMO1 mRNA transcription and protein levels, and additionally reduced activity of sentrin specific proteases (SENPs) (Jiang et al., 2015; Kunz et al., 2016). Alternatively, heat shocked cells are reported to globally induce the conjugation of SUMO2 moieties (Golebiowski et al., 2009). In 2004, the SUMO4 isoform was discovered, which in contrast to SUMO1-3 harbors a proline instead of a glutamine in close proximity to the di-glycine motif at its C-terminus. This proline was shown to abrogate SUMO-SENPs interaction and prevents both, SUMO maturation and deconjugation (Bohren et al., 2004; Owerbach et al., 2005). Interestingly, the recombinant expression of matured SUMO2/3 with a proline insertion at the respective glutamine led to elevated levels of SUMOylated proteins, since these SUMO mutants were not deconjugated by SENPs (Békés et al., 2011; Mukherjee et al., 2009). By modulating the levels of SUMO enzymes, the levels of SUMOylated proteins can be increased. Overexpression of Ubc9 and, if known, the corresponding SUMO E3 ligase can increase the SUMO conjugation of a particular protein. In

addition, the global concentration of SUMO conjugates can be increased by knockdown of sentrin specific protease 5 (SEN5), which abrogates the removal of conjugated SUMO moieties (Di Bacco et al., 2006). With the goal to enhance global SUMO2 conjugation induced by stress stimuli, we applied heat shock prior to cell harvesting and overexpressed the SUMO E2 conjugating enzyme Ubc9 in our approaches (Figure 14-Figure 16). However, we could not detect E1B-19K SUMO modification in these alternative experiments.

In a final approach, we aimed to target E1B-19K to the nucleus by fusion to a Gal4 DNA binding domain, in order to enforce and therefore detect SUMOylation of E1B-19K (Silver et al., 1984). All enzymes required for SUMO modification are predominantly expressed in the nucleus, suggesting that SUMOylation mainly occurs in this particular cellular compartment (Geiss-Friedlander and Melchior, 2007; Melchior et al., 2003). Indeed, Ni²⁺-NTA purification of the Gal4-E1B-19K fusion protein showed slower migrating bands in the HeLa SUMO2 cells, indicative for SUMO modification (Figure 17). The plasmid encoding for the Gal4-E1B-19K fusion protein harbors two start codons, one upstream of the Gal4 DNA binding domain, and an additional one upstream of E1B-19K. *In silico* analysis of Gal4-E1B-19K revealed an internal SCM in the Gal4 DNA binding domain which might be SUMO modified itself. This, and not the nuclear localization, could be the reason for detecting a higher SUMOylation of the fusion protein. Mutation of the SCM at lysine 82 within Gal4-DNA binding domain should be utilized to prove that the detected SUMO2 modification is based on nuclear localization. However, in the context of this work, the potential cause of SUMO2 modification of Gal4-E1B-19K remains elusive.

5.1.2 Characterization of E1B-19K SUMO mutants

In silico analysis of E1B-19K revealed two potential SUMO conjugating motifs (SCM) at lysine 44 and 48, which followed the classical consensus motif ψ KxD/E (Figure 9) (Rodriguez et al., 2001). Both potential SCMs are integrated in a highly conserved region, which shares limited sequence homology to Bcl-2 and is essential for the anti-apoptotic function of E1B-19K (Chiou et al., 1994a; Rao et al., 1992; White et al., 1992). Intriguingly, the SCM at lysine 44 was shown to be conserved among different HAdV species. Hence, we generated various expression plasmids encoding for E1B-19K SUMO mutants K44R, K48R and the corresponding double mutant K44/48R and characterized the mutation by different means. In addition, a E1B-19K K44R mutant virus was characterized in order to determine the biological relevance of this mutation during adenoviral infection. However, no significant alterations in protein stability (Figure 18) and subcellular localization during transfection (Figure 19) were detectable for the SUMO mutants. Likewise, the HAdV-C5 E1B-19K K44R mutant virus showed no phenotype in terms of E1B-19K stability and viral protein expression

(Figure 21) as well as localization (Figure 23) and production of new infectious particles (Figure 22). Bcl-2 and E1B-19K are functional homologues, which inhibit the onset of p53-independent apoptosis by identical modes. In this context, it could be shown that overexpression of human Bcl-2 compensates the enhanced apoptotic phenotype of a HAdV-C5 E1B-19K minus mutant virus infection and inhibits the degradation of viral and host DNA (Chiou et al., 1994a; Tarodi et al., 1993). Functional interchangeability of Bcl-2 and E1B-19K is a reasonable explanation for not detecting a phenotype of the K44R mutation during infection, since Bcl-2 possibly compensates the lack of fully functional E1B-19K. In contrast to other PTMs, which are specific for selected protein species, SUMOylation seems to be preferentially attached global to whole functionally related protein groups in order to modulate a cellular process, also referred to as a “SUMO-spray” effect (Psakhye and Jentsch, 2012; Tammsalu et al., 2014). It is well accepted that SUMOylation is involved in the regulation of apoptosis (Gostissa et al., 1999; Rodriguez et al., 1999). Hence, the apoptotic regulator E1B-19K might be SUMOylated during infection, which has no particular effect on E1B-19K itself, but occurs globally to regulate a larger group of proteins involved in apoptosis regulation. Further, system-wide identification of SUMO2 conjugation sites revealed that SUMOylation occurs preferentially at classical SCMs. However, a considerable number of modified lysines were detected without following a certain motif (Hendriks et al., 2015; Tammsalu et al., 2014). Beside the two lysines at position 44 and 48, HAdV-C5 E1B-19K contains seven additional lysines, which do not follow the classical SCM. Therefore, it is possible that E1B-19K is SUMO2 modified at these residual lysines, explaining why E1B-19K K44R and K48R mutations showed no significant phenotype in transfection and infection.

5.1.2.1 SUMO mutants of E1B-19K show increased transforming potential

In order to elucidate the role of E1B-19K SUMO2 modification during E1-mediated transformation, we transfected primary baby rat kidney (pBRK) cells with our E1B-19K SUMO mutants in the context of the whole E1-gene region or exclusively with E1A (Figure 20). Intriguingly, we detected an enhanced transforming potential of the K44R mutation, when coexpressed with E1A and E1B-55K. Upon expression with E1A alone, all SUMO mutants were increased in transforming pBRKs. Both SCMs of E1B-19K (K44 and K48) are located in a highly conserved central region of E1B-19K, ranging from aa 44 to 113, and displaying limited sequence homology to the apoptosis regulating Bcl-2 protein. Mutational analysis showed that these conserved region is essential for the anti-apoptotic function of E1B-19K and very sensitive to mutations (Chiou et al., 1994a; Rao et al., 1992; White et al., 1992). Intriguingly, it was reported that mutation of lysine 44 to arginine, which reflects our mutation, exhibits no phenotype during transformation in pBRKs when coexpressed

with E1A (Chiou et al., 1994a). Conversely, mutation of lysine 44 to glutamic acid (K44E) resulted in an E1B-19K mutant unable to inhibit TNF α -mediated induction of apoptosis and showing impaired transforming potential (Chiou et al., 1994a; White et al., 1992). However, E1B-19K K44E was shown to be expressed at very low levels. Therefore, the impaired apoptosis inhibition of this mutant is probably attributed to altered protein structure or stability, rather than a loss of function of the conserved region (Chiou et al., 1994a). If both mutations of lysine 44 would show the same phenotype, it would be tempting to speculate that the absence of SUMOylation determines the observed phenotype. Based on the contradictory observations for the mutation of the very same residue, it is most likely that the phenotype during transformation is not based on the destroyed SCM, but depends on chemical characteristics of the replacing aa. In this context, glutamic acid contains a carboxyl group, which can be deprotonated leading to a negatively-charged residue, while mutation to arginine restores the positive charge of lysine. Obviously, the charge of residue 44 is a functional determinant for apoptosis inhibition, and not potential SUMO2 modification of E1B-19K. Alternatively, it has to be considered that the transforming potential of E1B-19K seems to be, at least in part, regulated by phosphorylation of serine 164 (McGlade et al., 1989). The introduction of an acidic residue in close proximity to a potential phospho-acceptor site can lead to a phospho-mimetic mutant, which in the case of E1B-19K might exhibit impaired apoptosis inhibition. HAdV-C5 harbors a tyrosine at position 47, which could be potentially phosphorylated although it has not been described in the literature to date. It might be possible that the potential phospho-mimicry of the K44E mutation represses the transforming potential of E1B-19K, additionally to the low-level protein expression.

Contrary to the literature, we saw an increased transforming potential of E1B-19K K44R in the presence of E1B-55K and enhanced transformation for all E1B-19K SUMO mutants (K44R, K48R and K44/48R) when expressed with E1A alone (Figure 20). Since we were not able to confirm SUMOylation of E1B-19K by Western Blotting, and thus far saw no other phenotype for the E1B-19K SUMO mutants, we assumed that the increased transforming potential observed in our transformation assays is based on alternative molecular consequences of the K44R mutation. In the case of E1B-19K, increased transforming properties might rise from abrogated potential ubiquitination at lysine 44 and/or 48 in the SUMO mutants, which could promote cell transformation due to a prolonged half-life and E1B-19K-mediated inhibition of apoptosis. It is also conceivable that the lysines 44 and 48 of E1B-19K are substrates of acetylation, which could positively alter the pro-apoptotic functions of the E1B-19K mutants.

5.2 PIAS4 as an intrinsic anti-viral factor during adenovirus infection

Protein inhibitor of activated STAT (PIAS) proteins function as SUMO E3 ligases and were shown to interact with over sixty different transcription factors, thus they are involved in the regulation of vast cellular pathways and processes (Rytinki et al., 2009; Schmidt and Müller, 2003). PIAS proteins seem to have a dual role during virus infection. Different publications showed a virus-mediated alteration of various PIAS proteins, suggesting a partial anti-viral function of PIAS proteins. The SUMO E3 Ligase function of PIAS4 is counteracted by the human Papillomavirus (HPV) immediate early protein E6, hence abrogating p53 SUMOylation and cellular growth arrest (Bischof et al., 2006). In the same context, PIAS4 depletion allowed a productive infection of an ICP0 deletion mutant, which is normally highly susceptible to restriction of the anti-viral intrinsic immunity (Conn et al., 2016). Similar to what has been described for HPV protein E6 and PIAS4, the human Cytomegalovirus (CMV) protein IE2 blocks the SUMO E3 enzymatic activity of PIAS1 during infection (Kim et al., 2014). Furthermore, PIAS1 was found associated with HSV-1 replication compartments, restricting HSV-1 infection. The early protein ICP0 abrogates the recruitment of PIAS1 to HSV-1 replication compartments and thereby counteracts its restricting effect (Brown et al., 2016). The early adenoviral protein E4orf3 was shown to specifically bind and sequester PIAS3 to nuclear scaffolds, being linked to viral genome replication. The outcome of PIAS3 sequestration has to be determined, but likely influences its ability to regulate transcriptional activity and promotes viral replication (Higginbotham and O'Shea, 2015). Conversely, other reports revealed data that point to a pro-viral function of PIAS proteins, based on their ability to repress STAT transcription factors and their association to IFN signaling. Infection with Ebola Zaire Virus increases the SUMO E3 ligase function of PIAS1, thus enhancing the SUMO-dependent repression of interferon regulatory factors (IRF) 3 and 7 (Chang et al., 2009). The NS1 protein of Parvovirus B19 was shown to transactivate cellular promoters, leading to enhanced expression of PIAS3 and subsequent modulation of inflammatory signaling (Duechting et al., 2008). Further, PIAS4 knockout cells were reported to exhibit enhanced anti-viral properties during Vesicular Stomatitis Virus (VSV), Encephalomyocarditis Virus (EMCV) and Sendai Virus infection, due to absent repression of STAT in the virus-induced interferon response (Kubota et al., 2011). For the first time we identified PIAS4 as a direct transcriptional repressor of early adenoviral genes.

5.2.1 PIAS4 during transfection of the E1-gene region

Initially, we observed decreased protein levels of E1B-55K specifically in the presence of overexpressed mouse and human PIAS4, but not in the presence of other PIAS isoforms (Figure 24). In follow up experiments, we could exclude that PIAS4 has SUMO E3 ligase function for E1B-55K and that enhanced SUMOylation caused the repression of E1B-55K protein levels. Subsequent luciferase assays showed a dose-dependent repression of the E1B-promoter activity specific for PIAS4, resulting in reduced mRNA and protein levels of E1B-55K and E1B-19K in the context of the transfected E1-gene region (Figure 30-Figure 32). PIAS-mediated transcriptional regulation is molecularly based on blockage of DNA binding of transcription factors and recruitment of transcriptional coactivators/-repressors. Additionally, the SUMO E3 ligase function of PIAS proteins is often associated with their ability to regulate transcription due to SUMO-mediated activation or recruitment of transcription factors (Johnson and Gupta, 2001; Takahashi et al., 2001a). Therefore, we generated the PIAS4 mutant W363A with a mutation in the SP-RING domain, unable to induce SUMOylation (Kotaja et al., 2002). With this mutant we showed that the transcriptional repression of early adenoviral genes partially depends on the PIAS4 SUMO E3 ligase function, by detecting decreased repression compared to wildtype PIAS4 (Figure 39). Considering this, it is reasonable that the repressive effect of PIAS4 showed the tendency to be stronger in HeLa SUMO2 cells in most of the conducted experiments. Even though, HeLa SUMO2 cells express the 6His-tagged SUMO2 in amounts comparable to endogenous SUMO2, these cells still contain the doubled pool of SUMO2 as the expression of endogenous SUMO2 is still present.

E1A mRNA and protein levels are repressed in the presence of PIAS4. Therefore, the viral E1A-promoter is affected by the PIAS4-mediated transcriptional repression. Transformation assays in the presence of overexpressed PIAS4 confirmed this observation and showed a considerable reduction of E1-mediated *foci* formation (Figure 33). Hence, the decreased mRNA and protein levels of E1A indicate that PIAS4 targets factors involved in the very initial expression of E1A. Furthermore, the observed transcriptional repression of E1-genes could result from PIAS4-mediated increased SUMOylation of transcriptional regulators, like the acetyl transferases p300, PCAF as well as CBP, which facilitate the E1A transactivation activity on downstream adenoviral promoters (Pelka et al., 2009a, 2009b). It was shown that the transcriptional activity and the intranuclear shuttling of CBP is tightly regulated upon SUMO modification (Kuo et al., 2005; Ryan et al., 2010). In addition, the function of p300 seems to be repressed by SUMOylation through subsequent recruitment of histone deacetylases (HDACs) (Girdwood et al., 2003). We could show that PIAS4 still represses the levels of early adenoviral genes E1A, E1B-19K and E1B-55K after abrogating its SUMO E3 ligase function (W363A mutant), although the repression was less

compared to PIAS4 wt (Figure 39). These results suggest that additional SUMO-independent mechanisms of PIAS4-mediated transcriptional repression of adenoviral E1-genes exist. Indeed it has been shown, that PIAS4 recruits potent transcriptional corepressors like HDAC 1 and 2, independent of its SUMO E3 ligase function (Gross et al., 2004; Long et al., 2003). Beside the SP-RING domain, the SAP domain of PIAS proteins is frequently reported to be involved in the regulation of various transcription factors. This domain of PIAS confers DNA binding capacity to a PIAS bound transcription factor or relocalization into scaffolds of the nuclear matrix, which serve as an environment of transcriptional regulation (Van Den Akker et al., 2005; Lee et al., 2006; Shuai and Liu, 2005; Zhou et al., 2008). PIAS4 is known to bind to LEF-1 and thereby relocalizes it into the nuclear matrix. There, the transcriptional activity of LEF-1 is repressed independent of the integrity of the PIAS4 SUMO E3 ligase function (Sachdev et al., 2001). Similarly, PIAS4 could impair the transactivation properties of E1A through either inactivating transcription factors that control E1A transcription or inactivating E1A-associated cofactors. Additionally, PIAS4 might directly associate with sections of the viral DNA via its SAP domain followed by sequestration to regions of repressed transcriptional activity.

5.2.2 PIAS4 during adenovirus infection

Since the transcription of the essential E1-gene region was repressed by PIAS4, we assumed a strong anti-viral effect of PIAS4 during HAdV infection. Surprisingly, PIAS4 overexpression exhibited only mild repressive effects on protein expression of all adenoviral proteins and mRNA levels of E1B-55K (Figure 34-Figure 36). Further, overexpression of PIAS4 did not impair the productive adenovirus infection and showed rather mild effects on the production of newly synthesized virus progeny (Figure 38). Based on these observations, we assume that the whole adenovirus background was able to circumvent PIAS4-mediated repression in order to ensure a productive infection. We observed a reduced transcriptional repression of E1-genes after transfection with PIAS4 W363A mutant compared to PIAS4 wt. One adenoviral strategy of partially counteracting PIAS4 could be the inhibition of the PIAS4 E3 SUMO ligase function, thereby abrogating SUMO-dependent modulations of transcription factors. Virus-mediated inhibition of PIAS SUMO E3 ligase functions is already described for the HPV E6 protein and HCMV IE2 in the context of PIAS4 and PIAS1, respectively (Bischof et al., 2006; Kim et al., 2014). However, PIAS4 W363 still repressed the expression of E1-genes during transfection, indicating that HAdV counteracts PIAS4 not solely through inhibition of the SUMO E3 ligase function, but probably by other mechanisms. Indeed, in few infection experiments, we have found that E1B-55K levels were remarkably reduced, showing that the effect of PIAS4 in the context of infection varies (Figure 37). Adenoviral inhibition of PIAS4

might be a sensitive interplay of various factors, which deviates in its efficiency between different experiments. At this point, it is very important to consider that PIAS proteins were also described to exhibit pro-viral properties, due to the negative regulation of key transcription factors of the innate immune system. PIAS1^(-/-) cells showed increased IFN- γ and IFN- β signaling due to STAT1 activation, which resulted in high anti-viral activity of these cells (Liu et al., 2004). Contrary, PIAS1 overexpression can considerably repress STAT and NF κ B responsive genes, which leads to decreased IFN signaling (Liu et al., 2004; Shuai, 2006; Shuai and Liu, 2005). Similarly, PIAS4 was shown to efficiently repress both, STAT1 and NF κ B signaling, and its deletion led to enhanced immune responses in dendritic cells (Liu et al., 2001; Tahk et al., 2007). Depletion of PIAS4 enhanced the replication of a HSV-1 ICPO null mutant, which is normally highly susceptible to repression by the innate immunity (Conn et al., 2016). In this context, PIAS4 knockout mice have been described to show moderate, but significant defects in IFN and Wnt signaling (Roth et al., 2004). The adenoviral E1A protein is able to repress IFN signaling by inhibiting the binding of transcriptional activators to interferon response elements, so the virus *per se* is able to circumvent anti-viral IFN responses (Gutch and Reich, 1991; Leonard and Sen, 1996). However, additional IFN repression induced by high levels of PIAS4 could function synergistic to E1A, providing a highly pro-viral environment. This, in part, could compensate the transcriptional repression of PIAS4, leading to a less distinct phenotype of PIAS4 during infection. However, it is more likely that PIAS4-mediated transcriptional repression is counteracted by viral components during infection, which are not encoded within the E1-gene region. Upon virion disassembly during early adenovirus infection, the viral genome is translocated into the nucleus, followed by expression of the immediate early genes. Throughout the nuclear translocation, the adenoviral genome remains associated to the highly abundant core protein VII (pVII) and probably associates with core protein V (pV) in the nucleus (Chatterjee et al., 1985, 1986b; Kremer and Nemerow, 2015; Matthews and Russell, 1998a, 1998b). Generally, all adenoviral core proteins, pVII, pV and p μ are highly basic and tightly associated unspecifically to the adenoviral genome (Chatterjee et al., 1985, 1986a). In addition to the core proteins, also capsid components are immediately present at the earliest stages of infection and do not require *de novo* synthesis. Our research unit identified SPOC-1 as an intrinsic host restriction factor that efficiently represses adenoviral promoter activity during infection. The adenoviral core protein pVII was shown to interact with SPOC-1 prior to the onset of viral gene expression and hence, likely protects the viral genome from SPOC-1-mediated repression. Subsequently, SPOC-1 is targeted for proteasomal degradation by the HAdV-C5 ubiquitin E3 ligase complex (Karen and Hearing, 2011; Schreiner et al., 2013a). Along this line, the chromatin remodeling factor Daxx complexes with ATRX and represses adenoviral transcription by mediating histone deacetylation. To evade the Daxx/ATRX-mediated repression, the adenoviral

capsid protein pVI initially interacts with Daxx and mediates its cytosolic translocation, where E1B-55K mediates its proteasomal degradation independent of E4orf6 (Schreiner et al., 2010, 2012a, 2013b). Thus, viral core and capsid proteins provide the potential to counteract PIAS4 prior to the onset of viral gene expression, e.g. by shielding the viral genome or through interaction with PIAS4. Based on our results, we assume that PIAS4-mediated transcriptional repression of HAdV-C5 early genes can be counteracted by comparable molecular mechanisms, as found for the inhibition of Daxx, ATRX and SPOC-1. We cotransfected the E1-gene region and PIAS4, and introduced either the core protein pVII, pV, (precursor) p μ or (precursor) capsid protein pVI in order to elucidate their role in the context of PIAS4. However, the levels of E1A, E1B-55K and E1B-19K were remarkably repressed by PIAS4 and not restored by any of the cotransfected proteins (Figure 40). We have to consider that this initial approach did not properly resemble the situation during adenoviral infection, which would explain the results obtained after introduction of pVII, pV, p μ as well as pVI. For example, the protein levels during transfection exceed the common protein level during adenoviral infection by many times, which might disturb the orchestration of PIAS4 repression. Hence, it would be worth to transfect different amounts of plasmid DNA in follow up experiments to determine if the proteins show an effect when expressed at lower levels, which more resembles the situation during adenovirus infection. Further, it could be possible that the adenoviral core proteins circumvent PIAS4-mediated transcriptional repression synergistically, but not if expressed individually. To adapt the core protein levels to physiological levels in follow up experiments, they could be induced into the experimental system by infection adenovirus-like particles. This approach delivers protein ratios similar to what is found during infection and might show alternative results to the individual overexpression.

5.2.3 Summary of PIAS4 transcriptional repression of adenoviral early genes

We found for the first time, that PIAS4 possesses potential intrinsic anti-adenoviral properties by remarkably repressing the transcription of essential early adenoviral genes in the context of the transfected E1-gene region. Immediate detection of viral components and subsequent restriction of virus infection and replication is the hallmark of the host's intrinsic immunity, which represents the first molecular barrier the virus has to conquer. Intriguingly, PIAS4 overexpression has only a mild repressive effect during HAdV wt infection, pointing to a viral factor that counteracts the intrinsic anti-viral properties of PIAS4 prior to the onset of gene expression. In this context, it is an attractive possibility that immediately present capsid and/or core proteins are involved in the counteraction of PIAS4. As discussed before, alternative experimental approaches have to be performed to investigate the role of these factors more in detail.

Our findings and potential molecular mechanisms behind the observation are summarized in a simplified model, shown in Figure 41. PIAS4 represses the activity of the E1B-promoter during transfection and we propose that the E1A-promoter is similarly affected by PIAS4, resulting in repressed protein and mRNA levels. Repression of viral transcription could occur by two different mechanisms, which might overlap to some extent. SAP domain-mediated interaction of PIAS4 and adenovirus DNA recruits transcriptional repressors like HDAC 1 and 2 leading to repressed transcriptional activity for juxtaposed DNA (Figure 41, panel A, 1). Additionally, PIAS4 might either modulate transcriptional regulators through PTM with SUMO or relocalization, which in turn represses the activity of early adenoviral promoters (Figure 41, panel A, 2 and 3). During infection, we detected rather mild repressive effects of PIAS4 and we hypothesize three potential modes of how an adenoviral factor counteracts PIAS4 restriction prior to the onset of adenoviral gene expression. First, the viral factor might be associated with the viral genome, thus shielding the genome from interaction with PIAS4 (Figure 41, panel B, 1). Second, we could show that the SUMO E3 ligase function of PIAS4 is partly involved in the transcriptional repression. Therefore, partial counteraction of PIAS4 could be achieved by repressing its SUMO E3 ligase function. As a consequence, SUMO-dependent activation of corepressors is abrogated and viral transcription can occur (Figure 41, panel B, 2). However, this mode of action would only partially restrict PIAS4, since the SUMO ligase mutant W363A showed residual restriction. Third, similar to the transcriptional repressors Daxx and SPOC-1, the viral factor sequesters PIAS4 to the cytoplasm where it is subsequently degraded by the adenoviral ubiquitin E3 ligase complex (Figure 41, panel B, 3).

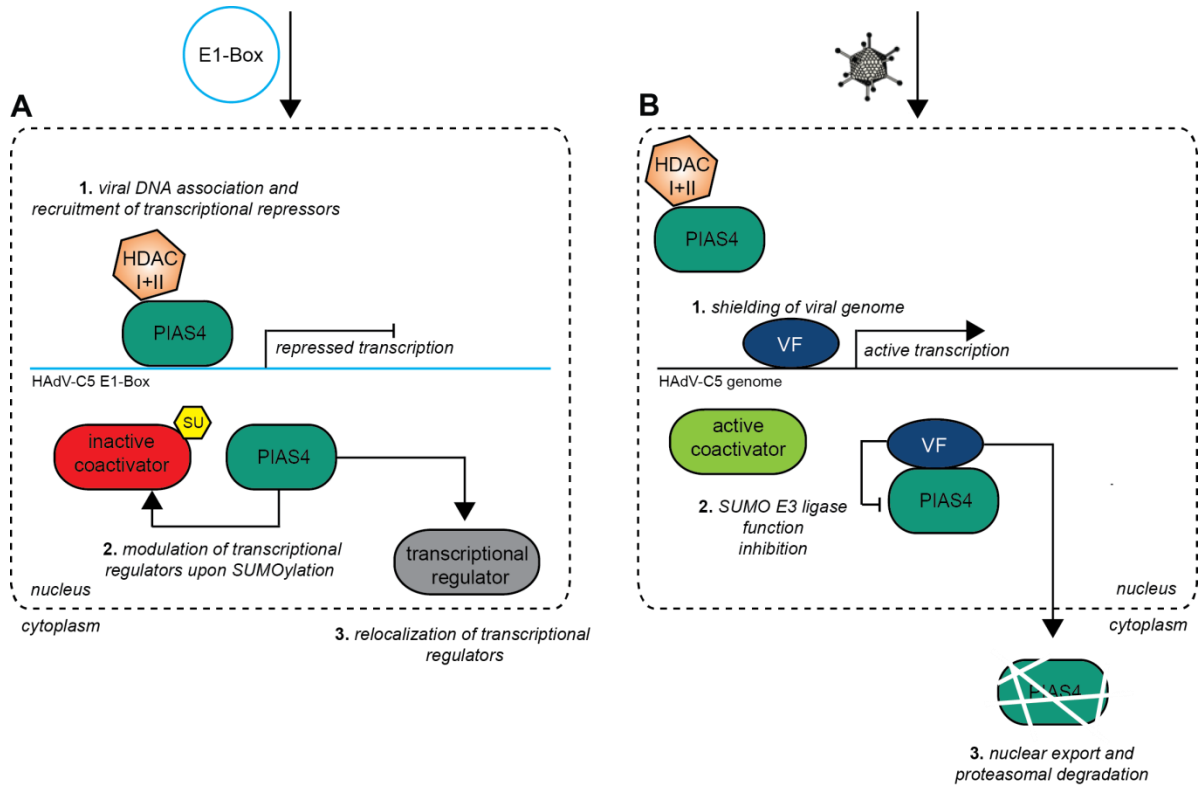


Figure 41: Molecular mechanisms of PIAS4-mediated transcriptional repression during transient transfection and potential counteracting modes of the virus during infection. (A) During transient transfection of the E1-Box, overexpressed PIAS4 might associate with viral DNA and recruits transcriptional repressors (1). Additionally, PIAS4 can modulate transcriptional regulators upon SUMOylation, which represses viral transcription (2). Inhibition of transcriptional regulators through subnuclear relocalization (3). **(B)** During infection, an unknown viral factor (VF), might shield the viral genome from interaction with PIAS4 (1). Alternatively, the VF might repress the SUMO E3 ligase function of PIAS4, therefore transcriptional coactivators remain active (2). As known for Daxx and SPOC-1, PIAS4 can be sequestered to the cytoplasm, where it is targeted for proteasomal degradation by the adenoviral ubiquitin E3 ligase complex (3).

Literature

- Adams, J.M., and Cory, S. (1998). The Bcl-2 protein family: Arbiters of cell survival. *Science* (80-.). *281*, 1322–1326.
- Aebersold, R., Burlingame, A.L., and Bradshaw, R.A. (2013). Western blots versus selected reaction monitoring assays: time to turn the tables? *Mol. Cell. Proteomics* *12*, 2381–2382.
- Van Den Akker, E., Ano, S., Shih, H.M., Wang, L.C., Pironin, M., Palvimo, J.J., Kotaja, N., Kirsh, O., Dejean, A., and Ghysdael, J. (2005). FLI-1 functionally interacts with PIASx α , a member of the PIAS E3 SUMO ligase family. *J. Biol. Chem.* *280*, 38035–38046.
- Alimonti, J.B., Shi, L., Baijal, P.K., and Greenberg, a H. (2001). Granzyme B induces BID-mediated cytochrome c release and mitochondrial permeability transition. *J. Biol. Chem.* *276*, 6974–6982.
- Andersson, M., Pääbo, S., Nilsson, T., and Peterson, P.A. (1985). Impaired intracellular transport of class I MHC antigens as a possible means for adenoviruses to evade immune surveillance. *Cell* *43*, 215–222.
- Aravind, L., and Koonin, E. V. (2000). SAP - A putative DNA-binding motif involved in chromosomal organization. *Trends Biochem. Sci.* *25*, 112–114.
- Di Bacco, A., Ouyang, J., Lee, H.-Y., Catic, A., Ploegh, H., and Gill, G. (2006). The SUMO-Specific Protease SENP5 Is Required for Cell Division. *Mol. Cell. Biol.* *26*, 4489–4498.
- Bae, S.H., Jeong, J.W., Park, J.A., Kim, S.H., Bae, M.K., Choi, S.J., and Kim, K.W. (2004). Sumoylation increases HIF-1 α stability and its transcriptional activity. *Biochem. Biophys. Res. Commun.* *324*, 394–400.
- Békés, M., Prudden, J., Srikumar, T., Raught, B., Boddy, M.N., and Salvesen, G.S. (2011). The dynamics and mechanism of SUMO chain deconjugation by SUMO-specific proteases. *J. Biol. Chem.* *286*, 10238–10247.
- Benhamed, M., Ye, T., Gras, L., Cossec, J., Lapaquette, P., Bischof, O., Ouspenskaia, M., Dasso, M., Seeler, J., Davidson, I., et al. (2013). Sumoylation at chromatin governs coordinated repression of a transcriptional program essential for cell growth and proliferation. *1563–1579*.
- Bergelson, J.M., Cunningham, J.A., Droguett, G., Kurt-Jones, E.A., Krithivas, A., Hong, J.S., Horwitz, M.S., Crowell, R.L., and Finberg, R.W. (1997). Isolation of a common receptor for coxsackie B viruses and adenoviruses 2 and 5. *Science* (80-.). *275*, 1320–1323.
- Berget, S.M., Moore, C., and Sharp, P.A. (1977). Spliced segments at the 5' terminus of adenovirus 2 late mRNA. *Proc. Natl. Acad. Sci.* *74*, 3171–3175.
- Berk, A.J. (2013). *Fields Virology - Chapter 55 Adenoviridae* (Lippincott Williams & Wilkins).
- Berk, A.J., and Sharp, P.A. (1978). Structure of the adenovirus 2 early mRNAs. *Cell* *14*, 695–711.
- Bernier-Villamor, V., Sampson, D.A., Matunis, M.J., and Lima, C.D. (2002). Structural basis for E2-mediated SUMO conjugation revealed by a complex between ubiquitin-conjugating enzyme Ubc9 and RanGAP1. *Cell* *108*, 345–356.
- Bischof, O., Schwamborn, K., Martin, N., Werner, A., Sustmann, C., Grosschedl, R., and Dejean, A. (2006). The E3 SUMO Ligase PIASy Is a Regulator of Cellular Senescence and Apoptosis. *Mol. Cell* *22*, 783–794.

- Blanchette, P., Cheng, C.Y., Yan, Q., Ketner, G., Ornelles, D.A., Dobner, T., Conaway, R.C., Conaway, J.W., and Branton, P.E. (2004). Both BC-Box Motifs of Adenovirus Protein E4orf6 Are Required To Efficiently Assemble an E3 Ligase Complex That Degrades p53. *Mol. Cell. Biol.* *24*, 9619–9629.
- Boggio, R., Colombo, R., Hay, R.T., Draetta, G.F., and Chiocca, S. (2004). A mechanism for inhibiting the SUMO pathway. *Mol. Cell* *16*, 549–561.
- Boggio, R., Passafaro, A., and Chiocca, S. (2007). Targeting SUMO E1 to ubiquitin ligases: A viral strategy to counteract sumoylation. *J. Biol. Chem.* *282*, 15376–15382.
- Bohren, K.M., Nadkarni, V., Song, J.H., Gabbay, K.H., and Owerbach, D. (2004). A M55V polymorphism in a novel SUMO gene (SUMO-4) differentially activates heat shock transcription factors and is associated with susceptibility to type I diabetes mellitus. *J. Biol. Chem.* *279*, 27233–27238.
- Boutell, C., Sadis, S., and Everett, R.D. (2002). Herpes simplex virus type 1 immediate-early protein ICPO and its isolated RING finger domain act as ubiquitin E3 ligases in vitro. *J. Virol.*
- Boutell, C., Cuchet-Lourenço, D., Vanni, E., Orr, A., Glass, M., McFarlane, S., and Everett, R.D. (2011). A viral ubiquitin ligase has substrate preferential sumo targeted ubiquitin ligase activity that counteracts intrinsic antiviral defence. *PLoS Pathog.* *7*.
- Boyd, J.M., Malstrom, S., Subramanian, T., Venkatesh, L.K., Schaeper, U., Elangovan, B., D'Sa-Eipper, C., and Chinnadurai, G. (1994). Adenovirus E1B 19 kDa and Bcl-2 proteins interact with a common set of cellular proteins. *Cell* *79*, 341–351.
- Boyer, J., Rohleder, K., and Ketner, G. (1999a). Adenovirus E4 34k and E4 11k inhibit double strand break repair and are physically associated with the cellular DNA-dependent protein kinase. *Virology* *263*, 307–312.
- Boyer, T.G., Martin, M.E.D., Lees, E., Ricciardi, R.P., and Berk, A.J. (1999b). Mammalian Srb/mediator complex is targeted by adenovirus E1A protein. *Nature* *399*, 276–279.
- BOYER, G.S., DENNY, F.W., and GINSBERG, H.S. (1959). Sequential cellular changes produced by types 5 and 7 adenoviruses in HeLa cells and in human amniotic cells; cytological studies aided by fluorescein-labelled antibody. *J. Exp. Med.* *110*, 827–844.
- Bradford, M.M. (1976). A rapid and sensitive method for the quantitation of microgram quantities of protein utilizing the principle of protein-dye binding. *Anal. Biochem.* *72*, 248–254.
- Brady, C.A., and Attardi, L.D. (2010). p53 at a glance. *J. Cell Sci.* *123*, 2527–2532.
- Bratton, D.L., Fadok, V.A., Richter, D.A., Kailey, J.M., Guthrie, L.A., and Henson, P.M. (1997). Appearance of phosphatidylserine on apoptotic cells requires calcium-mediated nonspecific flip-flop and is enhanced by loss of the aminophospholipid translocase. *J. Biol. Chem.* *272*, 26159–26165.
- Brown, J.R., Conn, K.L., Wasson, P., Charman, M., Tong, L., Grant, K., Mcfarlane, S., and Boutell, C. (2016). Constituent Promyelocytic Leukemia Nuclear Body Protein That Contributes to the Intrinsic Antiviral Immune Response to Herpes Simplex Virus 1. *90*, 5939–5952.
- Burgert, H.G., and Kvist, S. (1985). An adenovirus type 2 glycoprotein blocks cell surface expression of human histocompatibility class I antigens. *Cell* *41*, 987–997.
- Cantin, G.T., Stevens, J.L., and Berk, A.J. (2003). Activation domain-mediator interactions promote transcription preinitiation complex assembly on promoter DNA. *Proc. Natl. Acad. Sci.* *100*, 12003–

12008.

Carmichael, G.P., Zahradnik, J.M., Moyer, G.H., and Porter, D.D. (1979). Adenovirus hepatitis in an immunosuppressed adult patient. *Am. J. Clin. Pathol.* **71**, 352–355.

Carvalho, T., Seeler, J.S., Öhman, K., Jordan, P., Pettersson, U., Akusjärvi, G., Carmo-Fonseca, M., and Dejean, A. (1995). Targeting of adenovirus E1A and E4-ORF3 proteins to nuclear matrix-associated PML bodies. *J. Cell Biol.* **131**, 45–56.

Cassany, A., Ragues, J., Guan, T., Bégu, D., Wodrich, H., Kann, M., Nemerow, G.R., and Gerace, L. (2015). Nuclear Import of Adenovirus DNA Involves Direct Interaction of Hexon with an N-Terminal Domain of the Nucleoporin Nup214. *J. Virol.* **89**, 1719–1730.

Catalucci, D., Sporeno, E., Cirillo, A., Ciliberto, G., Nicosia, A., and Colloca, S. (2005). An Adenovirus Type 5 (Ad5) Amplicon-Based Packaging Cell Line for Production of High-Capacity Helper-Independent E1-E2-E3-E4 Ad5 Vectors. *J. Virol.* **79**, 6400–6409.

Cerami, E., Gao, J., Dogrusoz, U., Gross, B.E., Sumer, S.O., Aksoy, B.A., Jacobsen, A., Byrne, C.J., Heuer, M.L., Larsson, E., et al. (2012). The cBio Cancer Genomics Portal: An open platform for exploring multidimensional cancer genomics data. *Cancer Discov.* **2**, 401–404.

Chang, P.C., Izumiya, Y., Wu, C.Y., Fitzgerald, L.D., Campbell, M., Ellison, T.J., Lam, K.S., Luciw, P.A., and Kung, H.J. (2010). Kaposi's Sarcoma-associated Herpesvirus (KSHV) encodes a SUMO E3 ligase that is SIM-dependent and SUMO-2/3-specific. *J. Biol. Chem.*

Chang, T.H., Kubota, T., Matsuoka, M., Jones, S., Bradfute, S.B., Bray, M., and Ozato, K. (2009). Ebola Zaire virus blocks type I interferon production by exploiting the host SUMO modification machinery. *PLoS Pathog.*

Chanvorachote, P., Nimmannit, U., Stehlik, C., Wang, L., Jiang, B.H., Ongpipatanakul, B., and Rojanasakul, Y. (2006). Nitric oxide regulates cell sensitivity to cisplatin-induced apoptosis through S-nitrosylation and inhibition of Bcl-2 ubiquitination. *Cancer Res.*

Chatterjee, P.K., Vayda, M.E., and Flint, S.J. (1985). Interactions among the three adenovirus core proteins. *J. Virol.* **55**, 379–386.

Chatterjee, P.K., Vayda, M.E., and Flint, S.J. (1986a). Identification of proteins and protein domains that contact DNA within adenovirus nucleoprotein cores by ultraviolet light crosslinking of oligonucleotides ³²P-labelled in vivo. *J. Mol. Biol.* **188**, 23–37.

Chatterjee, P.K., Vayda, M.E., and Flint, S.J. (1986b). Adenoviral protein VII packages intracellular viral DNA throughout the early phase of infection. *EMBO J.* **5**, 1633–1644.

Chinnaiyan, A.M. (1999). The Apoptosome: Heart and Soul of the Cell Death Machine. *Neoplasia* **1**, 5–15.

Chiocca, S., Baker, a, and Cotten, M. (1997). Identification of a novel antiapoptotic protein, GAM-1, encoded by the CELO adenovirus. *J. Virol.* **71**, 3168–3177.

Chiou, S.K., Tseng, C.C., Rao, L., and White, E. (1994a). Functional complementation of the adenovirus E1B 19-kilodalton protein with Bcl-2 in the inhibition of apoptosis in infected cells. *J. Virol.* **68**, 6553–6566.

Chiou, S.K., Rao, L., and White, E. (1994b). Bcl-2 blocks p53-dependent apoptosis. *Mol. Cell. Biol.* **14**, 2556–2563.

- Chittenden, T., Flemington, C., Houghton, a B., Ebb, R.G., Gallo, G.J., Elangovan, B., Chinnadurai, G., and Lutz, R.J. (1995). A conserved domain in Bak, distinct from BH1 and BH2, mediates cell death and protein binding functions. *EMBO J.* *14*, 5589–5596.
- Chmielewicz, B., Benzler, J., Pauli, G., Krause, G., Bergmann, F., and Schweiger, B. (2005). Respiratory disease caused by a species B2 Adenovirus in a military camp in Turkey. *J. Med. Virol.* *77*, 232–237.
- Chow, L.T., Gelinas, R.E., Broker, T.R., and Roberts, R.J. (1977). An amazing sequence arrangement at the 5' ends of adenovirus 2 messenger RNA. *Cell* *12*, 1–8.
- Christensen, J.B., Byrd, S.A., Walker, A.K., Strahler, J.R., Andrews, P.C., and Imperiale, M.J. (2008). Presence of the Adenovirus IVa2 Protein at a Single Vertex of the Mature Virion. *J. Virol.* *82*, 9086–9093.
- Chung, C.D., Liao, J., Liu, B., Rao, X., Jay, P., Berta, P., and Shuai, K. (1997). Specific inhibition of Stat3 signal transduction by PIAS3. *Science (80-)*. *278*, 1803–1805.
- Colombo, R., Boggio, R., Seiser, C., Draetta, G.F., and Chiocca, S. (2002). The adenovirus protein Gam1 interferes with sumoylation of histone deacetylase 1. *EMBO Rep.* *3*, 1062–1068.
- Conn, K.L., Wasson, P., Mcfarlane, S., Tong, L., Brown, J.R., Grant, K.G., Domingues, P., and Boutell, C. (2016). Novel Role for Protein Inhibitor of Activated STAT 4 (PIAS4) in the Restriction of Herpes Simplex Virus 1 by the Cellular Intrinsic Antiviral Immune Response. *90*, 4807–4826.
- Conradt, B., and Horvitz, H.R. (1998). The *C. elegans* Protein EGL-1 is required for programmed cell death and interacts with the Bcl-2-like protein CED-9. *Cell* *93*, 519–529.
- Cuconati, A., and White, E. (2002). Viral homologs of BCL-2: Role of apoptosis in the regulation of virus infection. *Genes Dev.* *16*, 2465–2478.
- Dahiya, A., Gavin, M.R., Luo, R.X., and Dean, D.C. (2000). Role of the LXCXE Binding Site in Rb Function. *Mol. Cell. Biol.* *20*, 6799–6805.
- Dales, S., and Chardonnet, Y. (1973). Early events in the interaction of adenoviruses with HeLa cells. IV. Association with microtubules and the nuclear pore complex during vectorial movement of the inoculum. *Virology* *56*, 465–483.
- van Damme, E., Laukens, K., Dang, T.H., and van Ostade, X. (2010). A manually curated network of the pml nuclear body interactome reveals an important role for PML-NBs in SUMOylation dynamics. *Int. J. Biol. Sci.* *6*, 51–67.
- Darmon, A.J., Nicholson, D.W., and Bleackley, R.C. (1995). Activation of the apoptotic protease CPP32 by cytotoxic T-cell-derived granzyme B. *Nature* *377*, 446–448.
- Davison, A.J., Benko, M., and Harrach, B. (2003). Genetic content and evolution of adenoviruses. *J. Gen. Virol.* *84*, 2895–2908.
- Debbas, M., and White, E. (1993). Wild-type p53 mediates apoptosis by E1A, which is inhibited by E1B. *Genes Dev.* *7*, 546–554.
- Dellaire, G., and Bazett-Jones, D.P. (2004). PML nuclear bodies: Dynamic sensors of DNA damage and cellular stress. *BioEssays* *26*, 963–977.
- Deng, X., Gao, F., Flagg, T., and May, W.S. (2004). Mono- and multisite phosphorylation enhances Bcl2's antiapoptotic function and inhibition of cell cycle entry functions. *Proc. Natl. Acad. Sci.*

- Desterro, J.M.P., Thomson, J., and Hay, R.T. (1997). Ubch9 conjugates SUMO but not ubiquitin. *FEBS Lett.* *417*, 297–300.
- Dobbelstein, M., Roth, J., Kimberly, W.T., Levine, A.J., and Shenk, T. (1997). Nuclear export of the E1B 55-kDa and E4 34-kDa adenoviral oncoproteins mediated by a rev-like signal sequence. *EMBO J.* *16*, 4276–4284.
- Domingues, P., Golebiowski, F., Tatham, M.H., Lopes, A.M., Taggart, A., Hay, R.T., and Hale, B.G. (2015). Global Reprogramming of Host SUMOylation during Influenza Virus Infection. *Cell Rep.*
- Doszpoly, A., Wellehan, J.F.X., Childress, A.L., Tarján, Z.L., Kovács, E.R., Harrach, B., and Benko, M. (2013). Partial characterization of a new adenovirus lineage discovered in testudinoid turtles. *Infect. Genet. Evol.* *17*, 106–112.
- Doucas, V., Ishov, A.M., Romo, A., Juguilon, H., Weitzman, M.D., Evans, R.M., and Maul, G.G. (1996). Adenovirus replication is coupled with the dynamic properties of the PML nuclear structure. *Genes Dev.* *10*, 196–207.
- Driscoll, J.J., Pelluru, D., Lefkimmatis, K., Fulciniti, M., Prabhala, R.H., Greipp, P.R., Barlogie, B., Tai, Y.T., Anderson, K.C., Shaughnessy, J.D., et al. (2010). The sumoylation pathway is dysregulated in multiple myeloma and is associated with adverse patient outcome. *Blood* *115*, 2827–2834.
- Du, C., Fang, M., Li, Y., Li, L., and Wang, X. (2000). Smac, a mitochondrial protein that promotes cytochrome c-dependent caspase activation by eliminating IAP inhibition. *Cell* *102*, 33–42.
- Duechting, A., Tschöpe, C., Kaiser, H., Lamkemeyer, T., Tanaka, N., Aberle, S., Lang, F., Torresi, J., Kandolf, R., and Bock, C.-T. (2008). Human parvovirus B19 NS1 protein modulates inflammatory signaling by activation of STAT3/PIAS3 in human endothelial cells. *J. Virol.*
- Duval, D., Duval, G., Kedinger, C., Poch, O., and Boeuf, H. (2003). The “PINIT” motif, of a newly identified conserved domain of the PIAS protein family, is essential for nuclear retention of PIAS3L. *FEBS Lett.* *554*, 111–118.
- Van Eekelen, C.A.G., and Van Venrooij, W.J. (1981). hnRNA and its attachment to a nuclear protein matrix. *J. Cell Biol.* *88*, 554–563.
- Eguchi, Y., Shimizu, S., and Tsujimoto, Y. (1997). Intracellular ATP levels determine cell death fate by apoptosis or necrosis. *Cancer Res.* *57*, 1835–1840.
- El-Deiry, W.S. (1998). Regulation of p53 downstream genes. *Semin. Cancer Biol.* *8*, 345–357.
- Elmore, S. (2007). Apoptosis: a review of programmed cell death. *Toxicol. Pathol.* *35*, 495–516.
- ENDERS, J.F., BELL, J.A., DINGLE, J.H., FRANCIS, T., HILLEMANN, M.R., HUEBNER, R.J., and PAYNE, A.M. (1956). Adenoviruses: group name proposed for new respiratory-tract viruses. *Science* *124*, 119–120.
- Endter, C., and Dobner, T. (2004). Cell transformation by human adenoviruses. *Curr. Top. Microbiol. Immunol.* *273*, 163–214.
- Endter, C., Kzhyshkowska, J., Stauber, R., and Dobner, T. (2001). SUMO-1 modification required for transformation by adenovirus type 5 early region 1B 55-kDa oncoprotein. *Proc. Natl. Acad. Sci. U. S. A.* *98*, 11312–11317.
- Endter, C., Härtl, B., Spruss, T., Hauber, J., and Dobner, T. (2005). Blockage of CRM1-dependent nuclear export of the adenovirus type 5 early region 1B 55-kDa protein augments oncogenic

transformation of primary rat cells. *Oncogene* 24, 55–64.

Everett, R.D. (2001). DNA viruses and viral proteins that interact with PML nuclear bodies. *Oncogene* 20, 7266–7273.

Farrow, S.N., White, J.H.M., Martinou, I., Raven, T., Pun, K.-T., Grinham, C.J., Martinou, J.-C., and Brown, R. (1995). Cloning of a bcl-2 homologue by interaction with adenovirus E1B 19K. *Nature* 374, 731–733.

Fattaey, A.R., Harlow, E., and Helin, K. (1993). Independent regions of adenovirus E1A are required for binding to and dissociation of E2F-protein complexes. *Mol. Cell. Biol.* 13, 7267–7277.

Ferrari, R., Pellegrini, M., Horwitz, G.A., Xie, W., Berk, A.J., and Kurdistani, S.K. (2008). Epigenetic reprogramming by adenovirus e1a. *Science* 321, 1086–1088.

Fields, B.N., Knipe, D.M., and Howley, P.M. (2013). *Fields Virology*, 6th Edition.

Flotho, A., and Melchior, F. (2013). Sumoylation: A Regulatory Protein Modification in Health and Disease. *Annu. Rev. Biochem.* 82, 357–385.

Fowler, C.J., Dunlap, J., Troyer, D., Stenzel, P., Epner, E., and Maziarz, R.T. (2010). Life-threatening adenovirus infections in the setting of the immunocompromised allogeneic stem cell transplant patients. *Adv. Hematol.* 2010.

Freemont, P.S. (1993). The RING finger. A novel protein sequence motif related to the zinc finger. *Ann. N. Y. Acad. Sci.* 684, 174–192.

Freemont, P.S., Hanson, I.M., and Trowsdale, J. (1991). A novel cysteine-rich sequence motif. *Cell* 64, 483–484.

Frenzel, A., Grespi, F., Chmelewskij, W., and Villunger, A. (2009). Bcl2 family proteins in carcinogenesis and the treatment of cancer. *Apoptosis*.

Gaggar, A., Shayakhmetov, D.M., and Lieber, A. (2003). CD46 is a cellular receptor for group B adenoviruses. *Nat. Med.* 9, 1408–1412.

Galanty, Y., Belotserkovskaya, R., Coates, J., Polo, S., Miller, K.M., and Jackson, S.P. (2009). Mammalian SUMO E3-ligases PIAS1 and PIAS4 promote responses to DNA double-strand breaks. *Nature* 462, 935–939.

Gallimore, P.H., and Turnell, A.S. (2001). Adenovirus E1A: remodelling the host cell, a life or death experience. *Oncogene* 20, 7824–7835.

Gavin, P.J., and Katz, B.Z. (2002). Intravenous Ribavirin Treatment for Severe Adenovirus Disease in Immunocompromised Children. *Pediatrics* 110, e9–e9.

Geiss-Friedlander, R., and Melchior, F. (2007). Concepts in sumoylation: A decade on. *Nat. Rev. Mol. Cell Biol.* 8, 947–956.

Geng, F., Tang, L., Li, Y., Yang, L., Choi, K.S., Kazim, A.L., and Zhang, Y. (2011). Allyl isothiocyanate arrests cancer cells in mitosis, and mitotic arrest in turn leads to apoptosis via Bcl-2 protein phosphorylation. *J. Biol. Chem.*

Gey, G.O., Coffmann, W.D., and Kubicek, M.T. (1952). Tissue culture studies of the proliferative capacity of cervical carcinoma and normal epithelium. *Cancer Res.* 12, 264–265.

Ghosh, M.K., and Harter, M.L. (2003). A viral mechanism for remodeling chromatin structure in G0

cells. *Mol. Cell* 12, 255–260.

Giard, D.J., Aaronson, S. a, Todaro, G.J., Arnstein, P., Kersey, J.H., Dosik, H., and Parks, W.P. (1973). In vitro cultivation of human tumors: establishment of cell lines derived from a series of solid tumors. *J. Natl. Cancer Inst.* 51, 1417–1423.

Girdwood, D., Bumpass, D., Vaughan, O.A., Thain, A., Anderson, L.A., Snowden, A.W., Garcia-Wilson, E., Perkins, N.D., and Hay, R.T. (2003). p300 transcriptional repression is mediated by SUMO modification. *Mol. Cell*.

Golebiowski, F., Matic, I., Tatham, M.H., Cole, C., Yin, Y., Nakamura, A., Cox, J., Barton, G.J., Mann, M., and Hay, R.T. (2009). System-wide changes to SUMO modifications in response to heat shock. *Sci. Signal.* 2, ra24.

Gooding, L.R., Elmore, L.W., Tollefson, A.E., Brady, H.A., and Wold, W.S.M. (1988). A 14,700 MW protein from the E3 region of adenovirus inhibits cytolysis by tumor necrosis factor. *Cell* 53, 341–346.

Gooding, L.R., Aquino, L., Duerksen-Hughes, P.J., Day, D., Horton, T.M., Yei, S.P., and Wold, W.S. (1991). The E1B 19,000-molecular-weight protein of group C adenoviruses prevents tumor necrosis factor cytolysis of human cells but not of mouse cells. *J. Virol.* 65, 3083–3094.

Gostissa, M., Hengstermann, A., Fogal, V., Sandy, P., Schwarz, S.E., Scheffner, M., and Del Sal, G. (1999). Activation of p53 by conjugation to the ubiquitin-like protein SUMO-1. *EMBO J.*

Graham, F.L., Smiley, J., Russell, W.C., and Nairn, R. (1977). Characteristics of a human cell line transformed by DNA from human adenovirus type 5. *J. Gen. Virol.* 36, 59–74.

Gripon, P., Rumin, S., Urban, S., Le Seyec, J., Glaise, D., Cannie, I., Guyomard, C., Lucas, J., Trepo, C., and Guguen-Guillouzo, C. (2002). Infection of a human hepatoma cell line by hepatitis B virus. *Proc. Natl. Acad. Sci. U. S. A.* 99, 15655–15660.

Gross, M., Yang, R., Top, I., Gasper, C., and Shuai, K. (2004). PIASy-mediated repression of the androgen receptor is independent of sumoylation. *Oncogene* 23, 3059–3066.

Gutch, M.J., and Reich, N.C. (1991). Repression of the interferon signal transduction pathway by the adenovirus E1A oncogene. *Proc. Natl. Acad. Sci. U. S. A.*

Hage, E., Liebert, U.G., Bergs, S., Ganzenmueller, T., and Heim, A. (2015). Human mastadenovirus type 70: A novel, multiple recombinant species D mastadenovirus isolated from diarrhoeal faeces of a haematopoietic stem cell transplantation recipient. *J. Gen. Virol.* 96, 2734–2742.

Han, J., Sabbatini, P., Perez, D., Rao, L., Modha, D., and White, E. (1996). The E1B 19K protein blocks apoptosis by interacting with and inhibiting the p53-inducible and death-promoting Bax protein. *Genes Dev.* 10, 461–477.

Hanahan, D., and Meselson, M. (1983). [24] Plasmid Screening at High Colony Density. *Methods Enzymol.* 100, 333–342.

Hari, K.L., Cook, K.R., and Karpen, G.H. (2001). The *Drosophila* Su(var)2-10 locus regulates chromosome structure and function and encodes a member of the PIAS protein family. *Genes Dev.* 15, 1334–1348.

Harlow, E., Franza, B.R., and Schley, C. (1985). Monoclonal antibodies specific for adenovirus early region 1A proteins: extensive heterogeneity in early region 1A products. *J. Virol.* 55, 533–546.

- Harrach, B., Benkő, M., Both, G., Brown, M., Davison, A., Echavarria, M., Hess, M., Jones, M., Kajon, A., Lehmkuhl, H., et al. (2012). Adenoviridae - ninth report of the International Committee on Taxonomy of Viruses. In *Virus Taxonomy*, pp. 125–141.
- Hashimoto, S., Ishii, A., and Yonehara, S. (1991). The E1b oncogene of adenovirus confers cellular resistance to cytotoxicity of tumor necrosis factor and monoclonal anti-Fas antibody. *Int. Immunol.* *3*, 343–351.
- Hateboer, G., Hijmans, E.M., Nooij, J.B.D., Schlenker, S., Jentsch, S., and Bernards, R. (1996). mUBC9, a novel adenovirus E1A-interacting protein that complements a yeast cell cycle defect. *J. Biol. Chem.* *271*, 25906–25911.
- Hay, R.T. (2004). Modifying NEMO. *Nat. Cell Biol.*
- Hay, R.T. (2005). SUMO: A history of modification. *Mol. Cell* *18*, 1–12.
- Hay, R.T. (2007). SUMO-specific proteases: a twist in the tail. *Trends Cell Biol.* *17*, 370–376.
- Hearing, P., and Shenk, T. (1983). The adenovirus type 5 E1A transcriptional control region contains a duplicated enhancer element. *Cell* *33*, 695–703.
- Heaton, P.R., Deyrieux, A.F., Bian, X.L., and Wilson, V.G. (2011). HPV E6 proteins target Ubc9, the SUMO conjugating enzyme. *Virus Res.*
- Heery, D.M., Kalkhoven, E., Hoare, S., and Parker, M.G. (1997). A signature motif in transcriptional co-activators mediates binding to nuclear receptors. *Nature* *387*, 733–736.
- Hendriks, I.A., D'Souza, R.C., Chang, J.G., Mann, M., and Vertegaal, A.C.O. (2015). System-wide identification of wild-type SUMO-2 conjugation sites. *Nat. Commun.*
- Hershko, A., and Ciechanover, A. (1998). The ubiquitin system. *Annu. Rev. Biochem.* *67*, 425–479.
- Van Den Heuvel, S., and Dyson, N.J. (2008). Conserved functions of the pRB and E2F families. *Nat. Rev. Mol. Cell Biol.* *9*, 713–724.
- Hietakangas, V., Anckar, J., Blomster, H.A., Fujimoto, M., Palvimo, J.J., Nakai, A., and Sistonen, L. (2006). PDSM, a motif for phosphorylation-dependent SUMO modification. *Proc. Natl. Acad. Sci. U. S. A.* *103*, 45–50.
- Higginbotham, J.M., and O'Shea, C.C. (2015). Adenovirus E4-ORF3 Targets PIAS3 and Together with E1B-55K Remodels SUMO Interactions in the Nucleus and at Virus Genome Replication Domains. *J. Virol.* *89*, 10260–10272.
- Hilleman, M.R. (1957). EPIDEMIOLOGY OF ADENOVIRUS RESPIRATORY INFECTIONS IN MILITARY RECRUIT POPULATIONS. *Ann. N. Y. Acad. Sci.* *67*, 262–272.
- Hochstrasser, M. (2001). SP-RING for SUMO. *Cell* *107*, 5–8.
- Hodge, L.D., Mancini, P., Davis, F.M., and Heywood, P. (1977). Nuclear matrix of HeLa S3 cells. Polypeptide composition during adenovirus infection and in phases of the cell cycle. *J. Cell Biol.* *72*, 194–208.
- Hofer, J., Schfer, G., Klocker, H., Erb, H.H.H., Mills, I.G., Hengst, L., Puhr, M., and Culig, Z. (2012). PIAS1 is increased in human prostate cancer and enhances proliferation through inhibition of p21. *Am. J. Pathol.* *180*, 2097–2107.
- Horwitz, G.A., Zhang, K., McBrien, M.A., Grunstein, M., Kurdiani, S.K., and Berk, A.J. (2008).

- Adenovirus small e1a alters global patterns of histone modification. *Science* (80-.). *321*, 1084–1085.
- Hsu, H., Xiong, J., and Goeddel, D. V. (1995). The TNF receptor 1-associated protein TRADD signals cell death and NF- κ B activation. *Cell* *81*, 495–504.
- Huang, H.-J., Zhou, L.-L., Fu, W.-J., Zhang, C.-Y., Jiang, H., Du, J., and Hou, J. (2015). β -catenin SUMOylation is involved in the dysregulated proliferation of myeloma cells. *Am. J. Cancer Res.*
- Huang, S., Kamata, T., Takada, Y., Ruggeri, Z.M., Nemerow, G.R., and Nemerow, G.R. (1996). Adenovirus interaction with distinct integrins mediates separate events in cell entry and gene delivery to hematopoietic cells. *J Virol* *70*, 4502–4508.
- Ishov, A.M., Sotnikov, A.G., Negorev, D., Vladimirova, O. V., Neff, N., Kamitani, T., Yeh, E.T.H., Strauss, J.F., and Maul, G.G. (1999). PML is critical for ND10 formation and recruits the PML-interacting protein Daxx to this nuclear structure when modified by SUMO-1. *J. Cell Biol.* *147*, 221–233.
- Itoh, N., and Nagata, S. (1993). A Novel Protein Domain Required for Apoptosis. Mutational analysis of human Fas antigen. *J. Biol. Chem.* *268*, 10932–10937.
- J. F. R. KERR*, A.H.W.A.A.R.Currie. (1972). APOPTOSIS: A BASIC BIOLOGICAL PHENOMENON WITH WIDE-RANGING IMPLICATIONS IN TISSUE KINETICS. *J. Intern. Med.* *258*, 479–517.
- Jawetz, E. (1959). The story of shipyard eye. *Br. Med. J.* *1*, 873–876.
- Jiang, H., White, E.J., Ríos-Vicil, C.I., Xu, J., Gomez-Manzano, C., and Fueyo, J. (2011). Human adenovirus type 5 induces cell lysis through autophagy and autophagy-triggered caspase activity. *J. Virol.* *85*, 4720–4729.
- Jiang, Y., Wang, J., Tian, H., Li, G., Zhu, H., Liu, L., Hu, R., and Dai, A. (2015). Increased SUMO-1 expression in response to hypoxia: Interaction with HIF-1 α in hypoxic pulmonary hypertension. *Int. J. Mol. Med.*
- Jin, L., Shen, K., Chen, T., Yu, W., and Zhang, H. (2017). SUMO-1 Gene Silencing Inhibits Proliferation and Promotes Apoptosis of Human Gastric Cancer SGC-7901 Cells. *Cell. Physiol. Biochem.* *41*, 987–998.
- Johnson, E.S., and Blobel, G. (1997). Ubc9p is the conjugating enzyme for the ubiquitin-like protein Smt3p. *J. Biol. Chem.* *272*, 26799–26802.
- Johnson, E.S., and Gupta, A.A. (2001). An E3-like Factor that Promotes SUMO Conjugation to the Yeast Septins. *106*, 735–744.
- Joza, N., Susin, S. a, Daugas, E., Stanford, W.L., Cho, S.K., Li, C.Y., Sasaki, T., Elia, a J., Cheng, H.Y., Ravagnan, L., et al. (2001). Essential role of the mitochondrial apoptosis-inducing factor in programmed cell death. *Nature* *410*, 549–554.
- Kagey, M.H., Melhuish, T.A., and Wotton, D. (2003). The polycomb protein Pc2 is a SUMO E3. *Cell* *113*, 127–137.
- Kalin, S., Amstutz, B., Gastaldelli, M., Wolfrum, N., Boucke, K., Havenga, M., DiGennaro, F., Liska, N., Hemmi, S., and Greber, U.F. (2010). Macropinocytotic Uptake and Infection of Human Epithelial Cells with Species B2 Adenovirus Type 35. *J. Virol.* *84*, 5336–5350.
- Kamitani, T., Kito, K., Nguyen, H.P., Wada, H., Fukuda-Kamitani, T., and Yeh, E.T.H. (1998).

Identification of three major sentrinization sites in PML. *J. Biol. Chem.* *273*, 26675–26682.

Karen, K.A., and Hearing, P. (2011). Adenovirus Core Protein VII Protects the Viral Genome from a DNA Damage Response at Early Times after Infection. *J. Virol.*

Kerscher, O. (2007). SUMO junction—what's your function? New insights through SUMO-interacting motifs. *EMBO Rep.* *8*, 550–555.

Kim, E.T., Kim, Y.E., Kim, Y.J., Lee, M.K., Hayward, G.S., and Ahn, J.H. (2014). Analysis of human cytomegalovirus-encoded SUMO targets and temporal regulation of SUMOylation of the immediate-early proteins IE1 and IE2 during infection. *PLoS One* *9*.

Kimelman, D., Miller, J.S., Porter, D., and Roberts, B.E. (1985). E1a regions of the human adenoviruses and of the highly oncogenic simian adenovirus 7 are closely related. *J. Virol.* *53*, 399–409.

Kindsmüller, K., Groitl, P., Härtl, B., Blanchette, P., Hauber, J., and Dobner, T. (2007). Intranuclear targeting and nuclear export of the adenovirus E1B-55K protein are regulated by SUMO1 conjugation. *Proc. Natl. Acad. Sci. U. S. A.* *104*, 6684–6689.

Kindsmüller, K., Schreiner, S., Leinenkugel, F., Groitl, P., Kremmer, E., and Dobner, T. (2009). A 49 kDa isoform of the adenovirus type 5 early region 1B 55K protein is sufficient to support virus replication. *J. Virol.*

Kischkel, F.C., Hellbardt, S., Behrmann, I., Germer, M., Pawlita, M., Krammer, P.H., and Peter, M.E. (1995). Cytotoxicity-dependent APO-1 (Fas/CD95)-associated proteins form a death-inducing signaling complex (DISC) with the receptor. *EMBO J.* *14*, 5579–5588.

Kosulin, K., Hoffmann, F., Clauditz, T.S., Wilczak, W., and Dobner, T. (2013). Presence of Adenovirus Species C in Infiltrating Lymphocytes of Human Sarcoma. *PLoS One* *8*.

Kotaja, N., Karvonen, U., Janne, O.A., and Palvimo, J.J. (2002). PIAS Proteins Modulate Transcription Factors by Functioning as SUMO-1 Ligases. *Mol. Cell. Biol.* *22*, 5222–5234.

Krätzer, F., Rosorius, O., Heger, P., Hirschmann, N., Dobner, T., Hauber, J., and Stauber, R.H. (2000). The adenovirus type 5 E1B-55K oncoprotein is a highly active shuttle protein and shuttling is independent of E4orf6, p53 and Mdm2. *Oncogene* *19*, 850–857.

Kremer, E.J., and Nemerow, G.R. (2015). Adenovirus Tales: From the Cell Surface to the Nuclear Pore Complex. *PLoS Pathog.* *11*.

Kubota, T., Matsuoka, M., Xu, S., Otsuki, N., Takeda, M., Kato, A., and Ozato, K. (2011). PIASy inhibits virus-induced and interferon-stimulated transcription through distinct mechanisms. *J. Biol. Chem.*

Kunz, K., Wagner, K., Mendler, L., Hölper, S., Dehne, N., and Müller, S. (2016). SUMO Signaling by Hypoxic Inactivation of SUMO-Specific Isopeptidases. *Cell Rep.*

Kuo, H.-Y., Chang, C.-C., Jeng, J.-C., Hu, H.-M., Lin, D.-Y., Maul, G.G., Kwok, R.P.S., and Shih, H.-M. (2005). SUMO modification negatively modulates the transcriptional activity of CREB-binding protein via the recruitment of Daxx. *Proc. Natl. Acad. Sci. U. S. A.*

Kutuk, O., and Letai, A. (2008). Regulation of Bcl-2 family proteins by posttranslational modifications. *Curr. Mol. Med.*

Kzhyshkowska, J., Kremmer, E., Hofmann, M., Wolf, H., and Dobner, T. (2004). Protein arginine

methylation during lytic adenovirus infection. *Biochem. J.* **383**, 259–265.

De La Cruz-Herrera, C.F., Shire, K., Siddiqi, U.Z., and Frappier, L. (2018). A genome-wide screen of Epstein-Barr virus proteins that modulate host SUMOylation identifies a SUMO E3 ligase conserved in herpesviruses. *PLOS Pathog.*

Laemmli, U.K. (1970). Cleavage of structural proteins during the assembly of the head of bacteriophage T4. *Nature* **227**, 680–685.

Lee, H., Quinn, J.C., Prasanth, K. V., Swiss, V.A., Economides, K.D., Camacho, M.M., Spector, D.L., and Abate-Shen, C. (2006). PIAS1 confers DNA-binding specificity on the Msx1 homeoprotein. *Genes Dev.* **20**, 784–794.

Leonard, G.T., and Sen, G.C. (1996). Effects of adenovirus E1A protein on interferon-signaling. *Virology*.

Leopold, P., Kreitzer, G., Miyazawa, N., Rempel, S., and Pfister, K. (2000). Dynein- and microtubule-mediated translocation of adenovirus serotype 5 occurs after endosomal lysis. *Hum. Gene Ther.* **11**, 151–165.

Li, H., Zhu, H., Xu, C.J., and Yuan, J. (1998). Cleavage of BID by caspase 8 mediates the mitochondrial damage in the Fas pathway of apoptosis. *Cell* **94**, 491–501.

Li, L., Chapman, K., Hu, X., Wong, A., and Pasdar, M. (2007). Modulation of the oncogenic potential of beta-catenin by the subcellular distribution of plakoglobin. *Mol Carcinog.*

Li, R., Wang, L., Liao, G., Guzzo, C.M., Matunis, M.J., Zhu, H., and Hayward, S.D. (2012). SUMO Binding by the Epstein-Barr Virus Protein Kinase BGLF4 Is Crucial for BGLF4 Function. *J. Virol.*

Liang, Y.C., Lee, C.C., Yao, Y.L., Lai, C.C., Schmitz, M.L., and Yang, W.M. (2016). SUMO5, a novel poly-SUMO isoform, regulates PML nuclear bodies. *Sci. Rep.* **6**.

Lin, D., Tatham, M.H., Yu, B., Kim, S., Hay, R.T., and Chen, Y. (2002). Identification of a substrate recognition site on Ubc9. *J. Biol. Chem.* **277**, 21740–21748.

Lion, T. (2014). Adenovirus infections in immunocompetent and immunocompromised patients. *Clin. Microbiol. Rev.* **27**, 441–462.

Liu, X., and Marmorstein, R. (2007). Structure of the retinoblastoma protein bound to adenovirus E1A reveals the molecular basis for viral oncoprotein inactivation of a tumor suppressor. *Genes Dev.* **21**, 2711–2716.

Liu, B., Liao, J., Rao, X., Kushner, S.A., Chung, C.D., Chang, D.D., and Shuai, K. (1998). Inhibition of Stat1-mediated gene activation by PIAS1. *Proc. Natl. Acad. Sci.* **95**, 10626–10631.

Liu, B., Gross, M., ten Hoeve, J., and Shuai, K. (2001). A transcriptional corepressor of Stat1 with an essential LXXLL signature motif. *Proc. Natl. Acad. Sci.* **98**, 3203–3207.

Liu, B., Mink, S., Wong, K.A., Stein, N., Getman, C., Dempsey, P.W., Wu, H., and Shuai, K. (2004). PIAS1 selectively inhibits interferon-inducible genes and is important in innate immunity. *Nat. Immunol.* **5**, 891–898.

Liu, B., Yang, R., Wong, K.A., Getman, C., Stein, N., Teitell, M.A., Cheng, G., Wu, H., and Shuai, K. (2005). Negative regulation of NF-kappaB signaling by PIAS1. *Mol. Cell. Biol.* **25**, 1113–1123.

Liu, B., Yang, Y., Chernishof, V., Loo, R.R.O., Jang, H., Tahk, S., Yang, R., Mink, S., Shultz, D., Bellone, C.J., et al. (2007). Proinflammatory Stimuli Induce IKK α -Mediated Phosphorylation of PIAS1 to

Restrict Inflammation and Immunity. *Cell* 129, 903–914.

Liu, H., Jin, L., Koh, S.B.S., Atanasov, I., Schein, S., Wu, L., and Zhou, Z.H. (2010). Atomic structure of human adenovirus by cryo-EM reveals interactions among protein networks. *Science* 329, 1038–1043.

Liu, X., Kim, C.N., Yang, J., Jemmerson, R., and Wang, X. (1996). Induction of apoptotic program in cell-free extracts: Requirement for dATP and cytochrome c. *Cell* 86, 147–157.

Liu, Y., Colosimo, A.L., Yang, X.J., and Liao, D. (2000). Adenovirus E1B 55-kilodalton oncoprotein inhibits p53 acetylation by PCAF. *Mol. Cell. Biol.* 20, 5540–5553.

Lomonosova, E., Subramanian, T., and Chinnadurai, G. (2005). Mitochondrial localization of p53 during adenovirus infection and regulation of its activity by E1B-19K. *Oncogene* 24, 6796–6808.

Long, B.H., Huang, C.Y., and Pogo, a O. (1979). Isolation and characterization of the nuclear matrix in Friend erythroleukemia cells: chromatin and hnRNA interactions with the nuclear matrix. *Cell* 18, 1079–1090.

Long, J., Matsuura, I., He, D., Wang, G., Shuai, K., and Liu, F. (2003). Repression of Smad transcriptional activity by PIASy, an inhibitor of activated STAT. *Proc. Natl. Acad. Sci.* 100, 9791–9796.

Lowrey, A.J., Cramblet, W., and Bentz, G.L. (2017). Viral manipulation of the cellular sumoylation machinery. *Cell Commun. Signal.* 15.

Lu, Z., Wu, H., and Mo, Y.Y. (2006). Regulation of bcl-2 expression by Ubc9. *Exp. Cell Res.*

Mabit, H., Nakano, M.Y., Prank, U., Saam, B., Döhner, K., Sodeik, B., and Greber, U.F. (2002). Intact microtubules support adenovirus and herpes simplex virus infections. *J. Virol.* 76, 9962–9971.

Mahajan, R., Delphin, C., Guan, T., Gerace, L., and Melchior, F. (1997). A small ubiquitin-related polypeptide involved in targeting RanGAP1 to nuclear pore complex protein RanBP2. *Cell* 88, 97–107.

Martin, M.E., and Berk, a J. (1998). Adenovirus E1B 55K represses p53 activation in vitro. *J. Virol.* 72, 3146–3154.

Marton, M.J., Baim, S.B., Ornelles, D. a, and Shenk, T. (1990). The adenovirus E4 17-kilodalton protein complexes with the cellular transcription factor E2F, altering its DNA-binding properties and stimulating E1A-independent accumulation of E2 mRNA. *J. Virol.* 64, 2345–2359.

Mast, T.C., Kierstead, L., Gupta, S.B., Nikas, A.A., Kallas, E.G., Novitsky, V., Mbewe, B., Pitisuttithum, P., Schechter, M., Vardas, E., et al. (2010). International epidemiology of human pre-existing adenovirus (Ad) type-5, type-6, type-26 and type-36 neutralizing antibodies: Correlates of high Ad5 titers and implications for potential HIV vaccine trials. *Vaccine* 28, 950–957.

Matthews, D.A., and Russell, W.C. (1998a). Adenovirus core protein V interacts with p32 - a protein which is associated with both the mitochondria and the nucleus. *J. Gen. Virol.* 79, 1677–1685.

Matthews, D.A., and Russell, W.C. (1998b). Adenovirus core protein V is delivered by the invading virus to the nucleus of the infected cell and later in infection is associated with nucleoli. *J. Gen. Virol.* 79 (Pt 7), 1671–1675.

Matunis, M.J., Coutavas, E., and Blobel, G. (1996). A novel ubiquitin-like modification modulates the partitioning of the Ran-GTPase-activating protein RanGAP1 between the cytosol and the

nuclear pore complex. *J. Cell Biol.* *135*, 1457–1470.

Matunis, M.J., Wu, J., and Blobel, G. (1998). SUMO-1 modification and its role in targeting the Ran GTPase-activating protein, RanGAP1, to the nuclear pore complex. *J. Cell Biol.* *140*, 499–509.

McGlade, C.J., Tremblay, M.L., and Branton, P.E. (1989). Mapping of a phosphorylation site in the 176R (19 kDa) early region 1B protein of human adenovirus type 5. *Virology* *168*, 119–127.

McNeill, K.M., Benton, F.R., Monteith, S.C., Tuchscherer, M.A., and Gaydos, J.C. (2000). Epidemic spread of adenovirus type 4-associated acute respiratory disease between U.S. Army installations. *Emerg. Infect. Dis.* *6*, 415–419.

Meier, O., and Greber, U.F. (2003). Adenovirus endocytosis. *J. Gene Med.* *5*, 451–462.

Melchior, F., Schergaut, M., and Pichler, A. (2003). SUMO: Ligases, isopeptidases and nuclear pores. *Trends Biochem. Sci.* *28*, 612–618.

Milovic-Holm, K., Kriehoff, E., Jensen, K., Will, H., and Hofmann, T.G. (2007). FLASH links the CD95 signaling pathway to the cell nucleus and nuclear bodies. *EMBO J.* *26*, 391–401.

Mitsudomi, T., Steinberg, S.M., Nau, M.M., Carbone, D., D’Amico, D., Bodner, S., Oie, H.K., Linnoila, R.I., Mulshine, J.L., Minna, J.D., et al. (1992). p53 gene mutations in non-small-cell lung cancer cell lines and their correlation with the presence of ras mutations and clinical features. *Oncogene* *7*, 171–180.

Miura, K., Rus, A., Sharkhuu, A., Yokoi, S., Karthikeyan, A.S., Raghothama, K.G., Baek, D., Koo, Y.D., Jin, J.B., Bressan, R.A., et al. (2005). The Arabidopsis SUMO E3 ligase SIZ1 controls phosphate deficiency responses. *Proc. Natl. Acad. Sci.* *102*, 7760–7765.

Mo, Y.Y., Yu, Y., Theodosiou, E., Ee, P.L.R., and Beck, W.T. (2005). A role for Ubc9 in tumorigenesis. *Oncogene*.

Moriuchi, T., Kuroda, M., Kusumoto, F., Osumi, T., and Hirose, F. (2016). Lamin A reassembly at the end of mitosis is regulated by its SUMO-interacting motif. *Exp. Cell Res.*

Mueller, A.J., and Klauss, V. (1993). Main sources of infection in 145 cases of epidemic keratoconjunctivitis. *Ger J Ophthalmol* *2*, 224–227.

Mukherjee, S., Thomas, M., Dadgar, N., Lieberman, A.P., and Iñiguez-Lluhi, J.A. (2009). Small ubiquitin-like modifier (SUMO) modification of the androgen receptor attenuates polyglutamine-mediated aggregation. *J. Biol. Chem.* *284*, 21296–21306.

Muller, S., and Dobner, T. (2008). The adenovirus E1B-55K oncoprotein induces SUMO modification of p53. *Cell Cycle* *7*, 754–758.

Müller, S., Matunis, M.J., and Dejean, A. (1998). Conjugation with the ubiquitin-related modifier SUMO-1 regulates the partitioning of PML within the nucleus. *EMBO J.* *17*, 61–70.

Munarriz, E., Barcaroli, D., Stephanou, A., Townsend, P.A., Maisse, C., Terrinoni, A., Neale, M.H., Martin, S.J., Latchman, D.S., Knight, R.A., et al. (2004). PIAS-1 Is a Checkpoint Regulator Which Affects Exit from G1 and G2 by Sumoylation of p73. *Mol. Cell. Biol.* *24*, 10593–10610.

Nakano, M.Y., Boucke, K., Suomalainen, M., Stidwill, R.P., and Greber, U.F. (2000). The first step of adenovirus type 2 disassembly occurs at the cell surface, independently of endocytosis and escape to the cytosol. *J. Virol.* *74*, 7085–7095.

Negorev, D., and Maul, G.G. (2001). Cellular proteins localized at and interacting within ND10/PML

- nuclear bodies/PODs suggest functions of a nuclear depot. *Oncogene* 20, 7234–7242.
- Nemerow, G.R., Pache, L., Reddy, V., and Stewart, P.L. (2009). Insights into adenovirus host cell interactions from structural studies. *Virology* 384, 380–388.
- Nevins, J.R., and Darnell, J.E. (1978). Groups of adenovirus type 2 mRNA's derived from a large primary transcript: probable nuclear origin and possible common 3' ends. *J Virol* 25, 811–823.
- Nevins, J.R., Ginsberg, H.S., Blanchard, J.M., Wilson, M.C., and Darnell, J.E. (1979). Regulation of the primary expression of the early adenovirus transcription units. *J. Virol.* 32, 727–733.
- Ojala, P.M., Yamamoto, K., Castãos-Vélez, E., Biberfeld, P., Korsmeyer, S.J., and Mäkelä, T.P. (2000). The apoptotic v-cyclin-CDK6 complex phosphorylates and inactivates Bcl-2. *Nat. Cell Biol.*
- Olsen, S.K., Capili, A.D., Lu, X., Tan, D.S., and Lima, C.D. (2010). Active site remodelling accompanies thioester bond formation in the SUMO E1. *Nature* 463, 906–912.
- van Oostrum, J., and Burnett, R.M. (1985). Molecular composition of the adenovirus type 2 virion. *J. Virol.* 56, 439–448.
- De Ory, F., Avellón, A., Echevarría, J.E., Sánchez-Seco, M.P., Trallero, G., Cabrerizo, M., Casas, I., Pozo, F., Fedele, G., Vicente, D., et al. (2013). Viral infections of the central nervous system in Spain: A prospective study. *J. Med. Virol.* 85, 554–562.
- Ou, H.D., Kwiatkowski, W., Deerinck, T.J., Noske, A., Blain, K.Y., Land, H.S., Soria, C., Powers, C.J., May, A.P., Shu, X., et al. (2012). A structural basis for the assembly and functions of a viral polymer that inactivates multiple tumor suppressors. *Cell* 151, 304–319.
- Owerbach, D., McKay, E.M., Yeh, E.T.H., Gabbay, K.H., and Bohren, K.M. (2005). A proline-90 residue unique to SUMO-4 prevents maturation and sumoylation. *Biochem. Biophys. Res. Commun.* 337, 517–520.
- Pelka, P., Ablack, J.N.G., Shuen, M., Yousef, A.F., Rasti, M., Grand, R.J., Turnell, A.S., and Mymryk, J.S. (2009a). Identification of a second independent binding site for the pCAF acetyltransferase in adenovirus E1A. *Virology* 391, 90–98.
- Pelka, P., Ablack, J.N.G., Torchia, J., Turnell, A.S., Grand, R.J.A., and Mymryk, J.S. (2009b). Transcriptional control by adenovirus E1A conserved region 3 via p300/CBP. *Nucleic Acids Res.* 37, 1095–1106.
- Pennella, M.A., Liu, Y., Woo, J.L., Kim, C.A., and Berk, A.J. (2010). Adenovirus E1B 55-Kilodalton Protein Is a p53-SUMO1 E3 Ligase That Represses p53 and Stimulates Its Nuclear Export through Interactions with Promyelocytic Leukemia Nuclear Bodies. *J. Biol. Chem.* 285, 12210–12225.
- Peraro, M.D., and Van Der Goot, F.G. (2016). Pore-forming toxins: Ancient, but never really out of fashion. *Nat. Rev. Microbiol.* 14, 77–92.
- Perez, D., and White, E. (2000). TNF-alpha signals apoptosis through a bid-dependent conformational change in Bax that is inhibited by E1B 19K. *Mol. Cell* 6, 53–63.
- Perry, J.J.P., Tainer, J.A., and Boddy, M.N. (2008). A SIM-ultaneous role for SUMO and ubiquitin. *Trends Biochem. Sci.* 33, 201–208.
- Persson, H., Katze, M.G., and Philipson, L. (1982). Purification of a native membrane-associated adenovirus tumor antigen. *J Virol* 42, 905–917.
- Pichler, A., Gast, A., Seeler, J.S., Dejean, A., and Melchior, F. (2002). The nucleoporin RanBP2 has

SUMO1 E3 ligase activity. *Cell* *108*, 109–120.

Piya, S., White, E.J., Klein, S.R., Jiang, H., McDonnell, T.J., Gomez-Manzano, C., and Fueyo, J. (2011). The E1B19K oncoprotein complexes with beclin 1 to regulate autophagy in adenovirus-infected cells. *PLoS One* *6*, 1–7.

Plevin, M.J., Mills, M.M., and Ikura, M. (2005). The LxxLL motif: A multifunctional binding sequence in transcriptional regulation. *Trends Biochem. Sci.* *30*, 66–69.

Pronk, R., and van der Vliet, P.C. (1993). The adenovirus terminal protein influences binding of replication proteins and changes the origin structure. *Nucleic Acids Res.* *21*, 2293–2300.

Psakhye, I., and Jentsch, S. (2012). Protein Group Modification and Synergy in the SUMO Pathway as Exemplified in DNA Repair. *Cell* *151*, 807–820.

Puhr, M., Hoefler, J., Eigentler, A., Dietrich, D., Van Leenders, G., Uhl, B., Hoogland, M., Handle, F., Schlick, B., Neuwirt, H., et al. (2016). PIAS1 is a determinant of poor survival and acts as a positive feedback regulator of AR signaling through enhanced AR stabilization in prostate cancer. *Oncogene* *35*, 2322–2332.

Querido, E., Teodoro, J.G., and Branton, P.E. (1997a). Accumulation of p53 induced by the adenovirus E1A protein requires regions involved in the stimulation of DNA synthesis. *J. Virol.* *71*, 3526–3533.

Querido, E., Marcellus, R.C., Lai, A., Charbonneau, R., Teodoro, J.G., Ketner, G., and Branton, P.E. (1997b). Regulation of p53 levels by the E1B 55-kilodalton protein and E4orf6 in adenovirus-infected cells. *J Virol* *71*, 3788–3798.

Querido, E., Blanchette, P., Yan, Q., Kamura, T., Morrison, M., Boivin, D., Kaelin, W.G., Conaway, R.C., Conaway, J.W., and Branton, P.E. (2001). Degradation of p53 by adenovirus E4orf6 and E1B55K proteins occurs via a novel mechanism involving a Cullin-containing complex. *1*, 3104–3117.

Rabellino, A., Carter, B., Konstantinidou, G., Wu, S.Y., Rimessi, A., Byers, L.A., Heymach, J. V., Girard, L., Chiang, C.M., Teruya-Feldstein, J., et al. (2012). The SUMO E3-ligase PIAS1 regulates the tumor suppressor PML and its oncogenic counterpart PML-RARA. *Cancer Res.* *72*, 2275–2284.

Rabellino, A., Andreani, C., and Scaglioni, P.P. (2017). The Role of PIAS SUMO E3-Ligases in Cancer. *Cancer Res.* *77*, 1542–1547.

Rao, L., Debbas, M., Sabbatini, P., Hockenbery, D., Korsmeyer, S., and White, E. (1992). The adenovirus E1A proteins induce apoptosis, which is inhibited by the E1B 19-kDa and Bcl-2 proteins. *Proc. Natl. Acad. Sci. U. S. A.* *89*, 7742–7746.

Rao, L., Modha, D., and White, E. (1997). The E1b 19k Protein Associates With Lamins In Vivo and Its Proper Localization Is Required For Inhibition Of Apoptosis. *Oncogene* *15*, 1587–1597.

Reddy, V.S., and Nemerow, G.R. (2014). Structures and organization of adenovirus cement proteins provide insights into the role of capsid maturation in virus entry and infection. *Proc. Natl. Acad. Sci.* *111*, 11715–11720.

Reddy, V.S., Natchiar, S.K., Stewart, P.L., and Nemerow, G.R. (2010). Crystal structure of human adenovirus at 3.5 Å resolution. *Science* *329*, 1071–1075.

Reich, N.C., Sarnow, P., Duprey, E., and Levine, A.J. (1983). Monoclonal antibodies which recognize native and denatured forms of the adenovirus DNA-binding protein. *Virology* *128*, 480–484.

- Reindle, A., Belichenko, I., Bylebyl, G.R., Chen, X.L., Gandhi, N., and Johnson, E.S. (2006). Multiple domains in Siz SUMO ligases contribute to substrate selectivity. *J. Cell Sci.* *119*, 4749–4757.
- Robertson, A.M., Bird, C.C., Waddell, A.W., and Currie, A.R. (1978). Morphological aspects of glucocorticoid-induced cell death in human lymphoblastoid cells. *J. Pathol.* *126*, 181–187.
- Rock, K.L., and Kono, H. (2008). The inflammatory response to cell death. *Annu. Rev. Pathol.* *3*, 99–126.
- Rodriguez, M.S., Desterro, J.M.P., Lain, S., Midgley, C.A., Lane, D.P., and Hay, R.T. (1999). SUMO-1 modification activates the transcriptional response of p53. *EMBO J.*
- Rodriguez, M.S., Dargemont, C., and Hay, R.T. (2001). SUMO-1 conjugation in vivo requires both a consensus modification motif and nuclear targeting. *J. Biol. Chem.* *276*, 12654–12659.
- Rogers, R.S., Horvath, C.M., and Matunis, M.J. (2003). SUMO modification of STAT1 and its role in PIAS-mediated inhibition of gene activation. *J. Biol. Chem.* *278*, 30091–30097.
- ROSEN, L. (1960). A hemagglutination-inhibition technique for typing adenoviruses. *Am. J. Hyg.* *71*, 120–128.
- Roth, W., Sustmann, C., Kieslinger, M., Gilmozzi, A., Irmer, D., Kremmer, E., Turck, C., and Grosschedl, R. (2004). PIASy-deficient mice display modest defects in IFN and Wnt signaling. *J. Immunol.* *173*, 6189–6199.
- Rowe, W.P., Huebner, R.J., Gilmore, L.K., Parrott, R.H., and Ward, T.G. (1953). Isolation of a Cytopathogenic Agent from Human Adenoids Undergoing Spontaneous Degeneration in Tissue Culture. *Exp. Biol. Med.* *84*, 570–573.
- Ruvolo, P.P., Deng, X., Carr, B.K., and May, W.S. (1998). A functional role for mitochondrial protein kinase Calpha in Bcl2 phosphorylation and suppression of apoptosis. *J. Biol. Chem.*
- Ryan, C.M., Kindle, K.B., Collins, H.M., and Heery, D.M. (2010). SUMOylation regulates the nuclear mobility of CREB binding protein and its association with nuclear bodies in live cells. *Biochem. Biophys. Res. Commun.*
- Rytinki, M.M., Kaikkonen, S., Pehkonen, P., Jääskeläinen, T., and Palvimo, J.J. (2009). PIAS proteins: Pleiotropic interactors associated with SUMO. *Cell. Mol. Life Sci.* *66*, 3029–3041.
- Sabbatini, P., Chiou, S.K., Rao, L., White, E., P., S., S.-K., C., L., R., and E., W. (1995). Modulation of p53-mediated transcriptional repression and apoptosis by the adenovirus E1B 19K protein. *Mol. Cell. Biol.* *15*, 1060–1070.
- Sachdev, S., Bruhn, L., Sieber, H., Pichler, A., Melchior, F., and Grosschedl, R. (2001). PIASy, a nuclear matrix-associated SUMO E3 ligase, represses LEF1 activity by sequestration into nuclear bodies. *Genes Dev.* *15*, 3088–3103.
- Saelens, X., Festjens, N., Vande Walle, L., Van Gurp, M., Van Loo, G., and Vandenabeele, P. (2004). Toxic proteins released from mitochondria in cell death. *Oncogene* *23*, 2861–2874.
- Saiki, R., Gelfand, D., Stoffel, S., Scharf, S., Higuchi, R., Horn, G., Mullis, K., and Erlich, H. (1988). Primer-directed enzymatic amplification of DNA with a thermostable DNA polymerase. *Science* (80-). *239*, 487–491.
- Saitoh, H., and Hinchey, J. (2000). Functional heterogeneity of small ubiquitin-related protein modifiers SUMO-1 versus SUMO-2/3. *J. Biol. Chem.* *275*, 6252–6258.

- Sakahira, H., Enari, M., and Nagata, S. (1998). Cleavage of CAD inhibitor in CAD activation and DNA degradation during apoptosis. *Nature* 391, 96–99.
- Salomoni, P., and Pandolfi, P.P. (2002). The role of PML in tumor suppression. *Cell* 108, 165–170.
- Sampson, D.A., Wang, M., and Matunis, M.J. (2001). The small ubiquitin-like modifier-1 (SUMO-1) consensus sequence mediates Ubc9 binding and is essential for SUMO-1 modification. *J. Biol. Chem.* 276, 21664–21669.
- Saphire, A.C.S., Guan, T., Schirmer, E.C., Nemerow, G.R., and Gerace, L. (2000). Nuclear import of adenovirus DNA in vitro involves the nuclear protein import pathway and hsc70. *J. Biol. Chem.* 275, 4298–4304.
- Sarnow, P., Hearing, P., Anderson, C.W., Reich, N., and Levine, A.J. (1982). Identification and characterization of an immunologically conserved adenovirus early region 11,000 Mr protein and its association with the nuclear matrix. *J. Mol. Biol.* 162, 565–583.
- Scaffidi, P., Misteli, T., and Bianchi, M.E. (2002). Release of chromatin protein HMGB1 by necrotic cells triggers inflammation. *Nature* 418, 191–195.
- Schindelin, J., Arganda-Carreras, I., Frise, E., Kaynig, V., Longair, M., Pietzsch, T., Preibisch, S., Rueden, C., Saalfeld, S., Schmid, B., et al. (2012). Fiji: An open-source platform for biological-image analysis. *Nat. Methods*.
- Schmidt, D., and Müller, S. (2003). PIAS/SUMO: New partners in transcriptional regulation. *Cell. Mol. Life Sci.* 60, 2561–2574.
- Schonland, M., Strong, M.L., and Wesley, a (1976). Fatal adenovirus pneumonia: Clinical and pathological features. *S. Afr. Med. J.* 50, 1748–1751.
- Schreiner, S., Wimmer, P., Sirma, H., Everett, R.D., Blanchette, P., Groitl, P., and Dobner, T. (2010). Proteasome-Dependent Degradation of Daxx by the Viral E1B-55K Protein in Human Adenovirus-Infected Cells. *J. Virol.* 84, 7029–7038.
- Schreiner, S., Martinez, R., Groitl, P., Rayne, F., Vaillant, R., Wimmer, P., Bossis, G., Sternsdorf, T., Marcinowski, L., Ruzsics, Z., et al. (2012a). Transcriptional activation of the adenoviral genome is mediated by capsid protein VI. *PLoS Pathog.* 8.
- Schreiner, S., Wimmer, P., and Dobner, T. (2012b). Adenovirus degradation of cellular proteins. *Future Microbiol.* 7, 211–225.
- Schreiner, S., Kinkley, S., Bürck, C., Mund, A., Wimmer, P., Schubert, T., Groitl, P., Will, H., and Dobner, T. (2013a). SPOC1-Mediated Antiviral Host Cell Response Is Antagonized Early in Human Adenovirus Type 5 Infection. *PLoS Pathog.* 9.
- Schreiner, S., Bürck, C., Glass, M., Groitl, P., Wimmer, P., Kinkley, S., Mund, A., Everett, R.D., and Dobner, T. (2013b). Control of human adenovirus type 5 gene expression by cellular Daxx/ATR chromatin-associated complexes. *Nucleic Acids Res.* 41, 3532–3550.
- Scott, F.L., Stec, B., Pop, C., Dobaczewska, M.K., Lee, J.J., Monosov, E., Robinson, H., Salvesen, G.S., Schwarzenbacher, R., and Riedl, S.J. (2009). The Fas-FADD death domain complex structure unravels signalling by receptor clustering. *Nature* 457, 1019–1022.
- Shen, T.H., Lin, H.K., Scaglioni, P.P., Yung, T.M., and Pandolfi, P.P. (2006). The Mechanisms of PML-Nuclear Body Formation. *Mol. Cell* 24, 331–339.

- Shenk, T., and Flint, J. (1991). Transcriptional and transforming activities of the adenovirus e1a proteins. *Adv. Cancer Res.* *57*, 47–85.
- Shi, L., Kraut, R.P., Aebersold, R., and Greenberg, A.H. (1992). A natural killer cell granule protein that induces DNA fragmentation and apoptosis. *J. Exp. Med.* *175*, 553–566.
- Shindo K, Kitayama T, Ura T, Matsuya F, Kusaba Y, Kanetake H, S.Y. (1986). Acute Hemorrhagic Cystitis Caused by Adenovirus type 11 After Renal Transplantation. *Urol. Int.* *41*, 152–155.
- Shuai, K. (2006). Regulation of cytokine signaling pathways by PIAS proteins. In *Cell Research*, pp. 196–202.
- Shuai, K., and Liu, B. (2005). Regulation of gene-activation pathways by pias proteins in the immune system. *Nat. Rev. Immunol.*
- Silver, P. a, Keegan, L.P., and Ptashne, M. (1984). Amino terminus of the yeast GAL4 gene product is sufficient for nuclear localization. *Proc. Natl. Acad. Sci. U. S. A.* *81*, 5951–5955.
- Sloan, E., Tatham, M.H., Gros Lambert, M., Glass, M., Orr, A., Hay, R.T., and Everett, R.D. (2015). Analysis of the SUMO2 Proteome during HSV-1 Infection. *PLoS Pathog.* *11*, 1–34.
- Sohn, S.-Y., and Hearing, P. (2016). The adenovirus E4-ORF3 protein functions as a SUMO E3 ligase for TIF-1 γ sumoylation and poly-SUMO chain elongation. *Proc. Natl. Acad. Sci.* *113*, 6725–6730.
- Spector, D.J., McGrogan, M., and Raskas, H.J. (1978). Regulation of the appearance of cytoplasmic RNAs from region 1 of the adenovirus 2 genome. *J. Mol. Biol.* *126*, 395–414.
- Speiseder, T., Hofmann-Sieber, H., Rodríguez, E., Schellenberg, A., Akyüz, N., Dierlamm, J., Spruss, T., Lange, C., and Dobner, T. (2017). Efficient Transformation of Primary Human Mesenchymal Stromal Cells by Adenovirus Early Region 1 Oncogenes. *J. Virol.* *91*, e01782-16.
- Sriramachandran, A.M., and Dohmen, R.J. (2014). SUMO-targeted ubiquitin ligases. *Biochim. Biophys. Acta - Mol. Cell Res.* *1843*, 75–85.
- Stennicke, H.R., and Salvesen, G.S. (1998). Properties of the caspases. *Biochim. Biophys. Acta - Protein Struct. Mol. Enzymol.* *1387*, 17–31.
- Stennicke, H.R., Jürgensmeier, J.M., Shin, H., Deveraux, Q., Wolf, B.B., Yang, X., Zhou, Q., Ellerby, H.M., Ellerby, L.M., Bredesen, D., et al. (1998). Pro-caspase-3 is a major physiologic target of caspase-8. *J. Biol. Chem.* *273*, 27084–27090.
- Stevens, J.L., Cantin, G.T., Wang, G., Shevchenko, A., Shevchenko, A., and Berk, A.J. (2002). Transcription control by E1A and MAP kinase pathway via Sur2 Mediator subunit. *Science (80-)*. *296*, 755–758.
- Stracker, T.H., Carson, C.T., and Weitzman, M.D. (2002). Adenovirus oncoproteins inactivate the Mre11 Rad50 NBS1 DNA repair complex. *Nature* *418*, 348.
- Straussberg, R., Harel, L., Levy, Y., and Amir, J. (2001). A Syndrome of Transient Encephalopathy Associated With Adenovirus Infection. *Pediatrics* *107*, e69–e69.
- Su, H.L., and Li, S.S.L. (2002). Molecular features of human ubiquitin-like SUMO genes and their encoded proteins. *Gene* *296*, 65–73.
- Sun, H., and Hunter, T. (2012). Poly-small ubiquitin-like modifier (PolySUMO)-binding proteins identified through a string search. *J. Biol. Chem.*

- Sundararajan, R., and White, E. (2001). E1B 19K blocks Bax oligomerization and tumor necrosis factor alpha-mediated apoptosis. *J. Virol.* *75*, 7506–7516.
- Sundararajan, R., Cuconati, A., Nelson, D., and White, E. (2001). Tumor Necrosis Factor- α Induces Bax-Bak Interaction and Apoptosis, Which Is Inhibited by Adenovirus E1B 19K. *J. Biol. Chem.* *276*, 45120–45127.
- Tahk, S., Liu, B., Chernishof, V., Wong, K. a, Wu, H., and Shuai, K. (2007). Control of specificity and magnitude of NF-kappa B and STAT1-mediated gene activation through PIASy and PIAS1 cooperation. *Proc. Natl. Acad. Sci. U. S. A.* *104*, 11643–11648.
- Takahashi, Y., and Kikuchi, Y. (2005). Yeast PIAS-type Ull1/Siz1 is composed of SUMO ligase and regulatory domains. *J. Biol. Chem.* *280*, 35822–35828.
- Takahashi, Y., Toh-e, A., and Kikuchi, Y. (2001a). A novel factor required for the SUMO1 / Smt3 conjugation of yeast septins. *275*, 223–231.
- Takahashi, Y., Kahyo, T., Toh-e, A., Yasuda, H., and Kikuchi, Y. (2001b). Yeast Ull1 / Siz1 Is a Novel SUMO1 / Smt3 Ligase for Septin Components and Functions as an Adaptor between Conjugating Enzyme and Substrates *. *276*, 48973–48977.
- Takahashi, Y., Lallemand-Breitenbach, V., Zhu, J., and De Thé, H. (2004). PML nuclear bodies and apoptosis. *Oncogene* *23*, 2819–2824.
- Tammsalu, T., Matic, I., Jaffray, E.G., Ibrahim, A.F.M., Tatham, M.H., and Hay, R.T. (2014). Proteome-wide identification of SUMO2 modification sites. *Sci. Signal.* *7*, rs2.
- Tarodi, B., Subramanian, T., and Chinnadurai, G. (1993). Functional similarity between adenovirus e1b 19k gene and bcl2 oncogene - mutant complementation and suppression of cell-death induced by DNA-damaging agents. *Int. J. Oncol.* *3*, 467–472.
- Tartaglia, L.A., Ayres, T.M., Wong, G.H.W., and Goeddel, D. V. (1993). A novel domain within the 55 kd TNF receptor signals cell death. *Cell* *74*, 845–853.
- Tatham, M.H., Jaffray, E., Vaughan, O.A., Desterro, J.M., Botting, C.H., Naismith, J.H., and Hay, R.T. (2001). Polymeric chains of SUMO-2 and SUMO-3 are conjugated to protein substrates by SAE1/SAE2 and Ubc9. *J. Biol. Chem.* *276*, 35368–35374.
- Tatham, M.H., Kim, S., Jaffray, E., Song, J., Chen, Y., and Hay, R.T. (2005). Unique binding interactions among Ubc9, SUMO and RanBP2 reveal a mechanism for SUMO paralog selection. *Nat. Struct. Mol. Biol.* *12*, 67–74.
- Tatham, M.H., Rodriguez, M.S., Xirodimas, D.P., and Hay, R.T. (2009). Detection of protein SUMOylation in vivo. *Nat. Protoc.* *4*, 1363–1371.
- Täuber, B., and Dobner, T. (2001a). Adenovirus early E4 genes in viral oncogenesis. *Oncogene* *20*, 7847–7854.
- Täuber, B., and Dobner, T. (2001b). Molecular regulation and biological function of adenovirus early genes: The E4 ORFs. *Gene* *278*, 1–23.
- Tavalai, N., and Stamminger, T. (2008). New insights into the role of the subnuclear structure ND10 for viral infection. *Biochim. Biophys. Acta - Mol. Cell Res.* *1783*, 2207–2221.
- Taylor, R.C., Cullen, S.P., and Martin, S.J. (2008). Apoptosis: Controlled demolition at the cellular level. *Nat. Rev. Mol. Cell Biol.* *9*, 231–241.

- Thomas, D.A., Du, C., Xu, M., Wang, X., and Ley, T.J. (2000). DFF45/ICAD can be directly processed by granzyme B during the induction of apoptosis. *Immunity* 12, 621–632.
- Thomson, B.J. (2001). Viruses and apoptosis. *Int. J. Exp. Pathol.* 82, 65–76.
- Trapani, J.A., and Smyth, M.J. (2002). Functional significance of the perforin/granzyme cell death pathway. *Nat. Rev. Immunol.* 2, 735–747.
- TRENTIN, J.J., YABE, Y., and TAYLOR, G. (1962). The quest for human cancer viruses. *Science* 137, 835–841.
- Trotman, L.C., Mosberger, N., Fornerod, M., Stidwill, R.P., and Greber, U.F. (2001). Import of adenovirus DNA involves the nuclear pore complex receptor CAN/Nup214 and histone H1. *Nat. Cell Biol.* 3, 1092–1100.
- Vantieghem, A., Xu, Y., Assefa, Z., Piette, J., Vandenheede, J.R., Merlevede, W., De Witte, P.A.M., and Agostinis, P. (2002). Phosphorylation of Bcl-2 in G 2/M phase-arrested cells following photodynamic therapy with hypericin involves a CDK1-mediated signal and delays the onset of apoptosis. *J. Biol. Chem.*
- Vento, T.J., Prakash, V., Murray, C.K., Brosch, L.C., Tchandja, J.B., Cogburn, C., and Yun, H.C. (2011). Pneumonia in military trainees: A comparison study based on adenovirus serotype 14 infection. *J. Infect. Dis.* 203, 1388–1395.
- Virtanen, A., Gilardi, P., Naslund, A., LeMoullec, J.M., Pettersson, U., and Perricaudet, M. (1984). mRNAs from human adenovirus 2 early region 4. *J Virol* 51, 822–831.
- Vojtěšek, B., Bártek, J., Midgley, C. a, and Lane, D.P. (1992). An immunochemical analysis of the human nuclear phosphoprotein p53. New monoclonal antibodies and epitope mapping using recombinant p53. *J. Immunol. Methods* 151, 237–244.
- Wajant, H. (2002). The Fas signaling pathway: More than a paradigm. *Science* (80-). 296, 1635–1636.
- Weber, J.M. (2007). Synthesis and assay of recombinant adenovirus protease. *Methods Mol. Med.* 131, 251–255.
- Weinmann, R., Raskas, H.J., and Roeder, R.G. (1974). Role of DNA-dependent RNA polymerases II and III in transcription of the adenovirus genome late in productive infection. *Proc. Natl. Acad. Sci. U. S. A.* 71, 3426–3439.
- White, E. (2001). Regulation of the cell cycle and apoptosis by the oncogenes of adenovirus. *Oncogene* 20, 7836–7846.
- White, E., and Cipriani, R. (1990). Role of adenovirus E1B proteins in transformation: altered organization of intermediate filaments in transformed cells that express the 19-kilodalton protein. *Mol. Cell. Biol.* 10, 120–130.
- White, E., Blose, S.H., and Stillman, B.W. (1984). Nuclear envelope localization of an adenovirus tumor antigen maintains the integrity of cellular DNA. *Mol. Cell Biol.* 4, 2865–2875.
- White, E., Sabbatini, P., Debbas, M., Wold, W.S.M., Kusher, D.I., and Gooding, L.R. (1992). The 19-Kilodalton Adenovirus E1B Transforming Protein Inhibits Programmed Cell Death and Prevents Cytolysis by Tumor Necrosis Factor alpha. *Mol. Cell. Biol.* 12, 2570–2580.
- Wickham, T. (1993). Integrins $\alpha\beta 3$ and $\alpha\beta 5$ promote adenovirus internalization but not virus

attachment. *Cell* 73, 309–319.

Wiethoff, C.M., Wodrich, H., Gerace, L., and Nemerow, G.R. (2005). Adenovirus Protein VI Mediates Membrane Disruption following Capsid Disassembly. *J. Virol.* 79, 1992–2000.

Wimmer, P., Schreiner, S., Everett, R.D., Sirma, H., Groitl, P., and Dobner, T. (2010). SUMO modification of E1B-55K oncoprotein regulates isoform-specific binding to the tumour suppressor protein PML. *Oncogene* 29, 5511–5522.

Wimmer, P., Schreiner, S., and Dobner, T. (2012). Human Pathogens and the Host Cell SUMOylation System. *J. Virol.* 86, 642–654.

Winberg, G., and Shenk, T. (1984). Dissection of overlapping functions within the adenovirus type 5 E1A gene. *EMBO J.* 3, 1907–1912.

Wood, D.J. (1988). Adenovirus gastroenteritis. *Br. Med. J. (Clin. Res. Ed.)* 296, 229–230.

Wu, E., Pache, L., Von Seggern, D.J., Mullen, T.M., Mikyas, Y., Stewart, P.L., and Nemerow, G.R. (2003). Flexibility of the Adenovirus Fiber Is Required for Efficient Receptor Interaction. *J. Virol* 77, 7225–7235.

Wyllie, A.H., Kerr, J.F.R., and Currie, A.R. (1980). Cell Death: The Significance of Apoptosis. *Int. Rev. Cytol.* 68, 251–306.

Yang, Q.H., Church-Hajduk, R., Ren, J., Newton, M.L., and Du, C. (2003). Omi/HtrA2 catalytic cleavage of inhibitor of apoptosis (IAP) irreversibly inactivates IAPs and facilitates caspase activity in apoptosis. *Genes Dev.* 17, 1487–1496.

Yang, S.-H., Galanis, A., Witty, J., and Sharrocks, A.D. (2006). An extended consensus motif enhances the specificity of substrate modification by SUMO. *EMBO J.* 25, 5083–5093.

Yeh, E.T.H., Gong, L., and Kamitani, T. (2000). Ubiquitin-like proteins: New wines in new bottles. *Gene* 248, 1–14.

Yousef, a F., Fonseca, G.J., Pelka, P., Ablack, J.N.G., Walsh, C., Dick, F. a, Bazett-Jones, D.P., Shaw, G.S., and Mymryk, J.S. (2010). Identification of a molecular recognition feature in the E1A oncoprotein that binds the SUMO conjugase UBC9 and likely interferes with polySUMOylation. *Oncogene* 29, 4693–4704.

Zhou, S., Si, J., Liu, T., and DeWille, J.W. (2008). PIASy represses CCAAT/enhancer-binding protein δ (C/EBP δ) transcriptional activity by sequestering C/EBP δ to the nuclear periphery. *J. Biol. Chem.* 283, 20137–20148.

Zou, H., Li, Y., Liu, X., and Wang, X. (1999). An APAf-1 · cytochrome C multimeric complex is a functional apoptosome that activates procaspase-9. *J. Biol. Chem.* 274, 11549–11556.

Acknowledgements

First, I want to sincerely thank my doctor father and first supervisor Prof. Dr. Thomas Dobner for offering me the opportunity to work on these two interesting project in his department, and for his steady interest in my research, his guidance, trust and support.

I would like to thank the members of my examining board; Prof. Wolfram Brune for being my second supervisor and for evaluation of my dissertation and Prof. Dr. Julia Kehr for chairing my disputation. In addition I thank Prof. Dr. Joachim Hauber for being part of the disputation evaluation committee.

I owe thanks to the whole research department of *Viral Transformation* for the nice time throughout my whole PhD thesis. It was great fun to work with all of you. Especially I thank my direct lab members Thomas Speiseder, Michael Melling, Konstantin von Stromberg, Vicky Kolbe and Marie Fiedler, for uncountable laughter, helpful scientific discussions and the nice atmosphere in the lab.

I am exceptionally grateful to Wing Hang Ip for her helpful comments and corrections and to Estefania Rodriguez, for her tireless personal support during the last years, valuable scientific exchange and the development of new ideas.

Further I would like to acknowledge the Universität Hamburg for funding my participation of scientific meetings.

Finally, I want to thank my wife and my mother for their never ending support at any time, Thank you!